PHILOSOPHICAL MAGAZINE

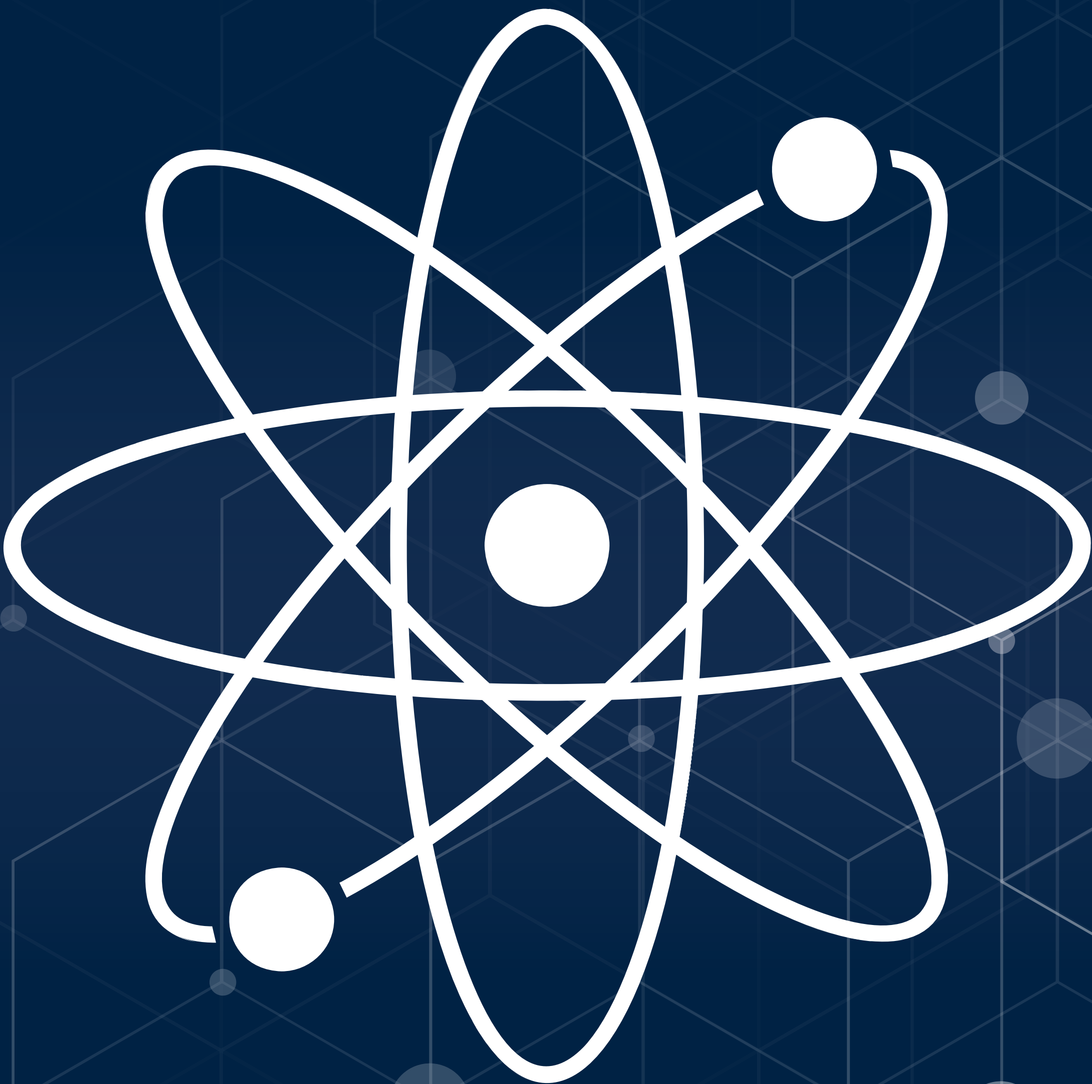

eBook

Quantum questions: qubits, optics and the time of arrival problem

Taylor & Francis
by informa

eBook

Quantum questions: qubits, optics and the time of arrival problem

Contents

Taylor & Francis
by informa

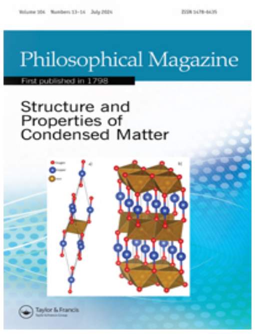

Philosophical Magazine

ISSN: 1478-6435 (Print) 1478-6443 (Online) Journal homepage: www.tandfonline.com/journals/tphm20

Correlated noise enhancement of coherence and fidelity in coupled qubits

Eric R. Bittner, Hao Li, S. A. Shah, Carlos Silva-Acuña & Andrei Piryatinski

To cite this article: Eric R. Bittner, Hao Li, S. A. Shah, Carlos Silva-Acuña & Andrei Piryatinski (2024) Correlated noise enhancement of coherence and fidelity in coupled qubits, Philosophical Magazine, 104:13-14, 630-646, DOI: 10.1080/14786435.2024.2341011

To link to this article: https://doi.org/10.1080/14786435.2024.2341011

Published online: 17 Apr 2024.

PHILOSOPHICAL MAGAZINE
2024, VOL. 104, NOS. 13–14, 630–646
https://doi.org/10.1080/14786435.2024.2341011

Correlated noise enhancement of coherence and fidelity in coupled qubits

Eric R. Bittner [a,b], Hao Li [a], S. A. Shah [b,c], Carlos Silva-Acuña [d] and Andrei Piryatinski [c]

[a]Department of Chemistry, University of Houston, Houston, TX, USA; [b]Center for Nonlinear Studies, Los Alamos National Laboratory, Los Alamos, NM, USA; [c]Theoretical Division, Los Alamos National Laboratory, Los Alamos, NM, USA; [d]Institut Courtois & Département de physique, Université de Montréal, Montréal, Québec, Canada

ABSTRACT

It is generally assumed that environmental noise arising from thermal fluctuations are detrimental to preserving coherence and entanglement in a quantum system. In the simplest sense, dephasing and decoherence are tied to energy fluctuations driven by coupling between the system and the normal modes of the bath. Here, we explore the role of noise correlation in an open-loop model quantum communication system whereby the 'sender' and the 'receiver' are subject to local environments with various degrees of correlation or anti-correlation. We introduce correlation within the spectral density by solving multidimensional stochastic differential equations and introduce these into the Redfield equations of motion for the system density matrix. We find that correlation can enhance both the fidelity and purity of a maximally entangled (Bell) state. Moreover, by comparing the evolution of different initial Bell states, we show that one can effectively probe the correlation between two local environments. These observations may be useful in the design of high-fidelity quantum gates and communication protocols.

ARTICLE HISTORY
Received 2 August 2023
Accepted 22 March 2024

KEYWORDS
Quantum information processing; quantum mechanical calculation; correlated systems

1. Introduction

Noise and environmental fluctuations are detrimental to preserving coherence and entanglement in an open quantum system. Correlations between individual quantum systems represent the basic resources in quantum information and quantum computing, and one of the major technological tasks is to protect and control these correlations and entanglements. Entanglement expresses the non-separability of the quantum state of a compound system. However, the coupling to the environment leads to dissipation and

CONTACT Eric R. Bittner ebittner@central.uh.edu Department of Chemistry, University of Houston, Houston, TX77204, USA; Center for Nonlinear Studies, Los Alamos National Laboratory, Los Alamos, NM 87545, USA

loss of the quantum correlations, often on time scales much shorter than those needed for implementing quantum information tasks. Such fluctuations can arise from nuclear and electronic motions of the surrounding environment and induce a noisy driving field that can modulate the energy gaps of individual qubit states, as well as the couplings between separated qubits. This idea is encapsulated in the well-known Anderson-Kubo model for the spectral lineshape [1–4].

Actively preventing decoherence from affecting quantum entanglement holds theoretical and practical significance in quantum information processing technologies. Several recent studies suggest that decoherence can be suppressed by carefully engineering the system-bath coupling [5–7]. For example, Mouloudakis and Lambropoulos, extending previous work by Yang *et al.* [8], studied the steady-state entanglement between two qubits that interacted asymmetrically with a common non-Markovian environment. The study found that depending on the initial two-qubit state, the asymmetry in the couplings between each qubit and the non-Markovian environment could lead to enhanced entanglement in the steady state of the system [9,10].

However, it is possible, especially in a condensed phase environment, that multiple modes of the environment can contribute to the frequency fluctuations, and it is possible that these contributions can be correlated, anti-correlated, or uncorrelated. To set the stage for our subsequent analysis, let us consider a single stochastic process, E_t, described by a generalisation of the Itô stochastic differential equation (SDE) [11],

$$\mathrm{d}E(t) = -\gamma E(t)\,\mathrm{d}t + B \cdot \,\mathrm{d}W(t), \tag{1}$$

where B is a vector of variances $B = \{s_{11}, s_2\}$, and $\mathrm{d}W = \{\mathrm{d}W_1, \mathrm{d}W_2\}$ are correlated Wiener processes with $\mathrm{d}W_1(t)\,\mathrm{d}W_2(t') = \delta(t-t')\xi\,\mathrm{d}t$ and $\mathrm{d}W_i(t)\,\mathrm{d}W_i(t') = \delta(t-t')\,\mathrm{d}t$, where $-1 \leq \xi \leq 1$ is the correlation parameter between the two Wiener processes. We can rewrite the SDE in Equation (1) in terms of two uncorrelated processes by defining the variances $B' = \{s_{11} + s_2\xi, s_2(1-\xi^2)^{1/2}\}$ such that Equation (1) becomes

$$\mathrm{d}E(t) = -\gamma E(t)\,\mathrm{d}t + (s_1 + s_2\xi)\,\mathrm{d}W_1' + s_2(1-\xi^2)^{1/2}\,\mathrm{d}W_2' \tag{2}$$

and W_1' and W_2' are now uncorrelated Wiener processes. If we work out the covariance of $E(t)$ one finds that

$$Cov[E_t, E_{t'}] = \frac{e^{-\gamma(t'+t)}}{2\gamma}(e^{2\gamma\min(t',t)} - 1)s_{\mathrm{eff}}^2 \tag{3}$$

where we can define an effective covariance parameter

$$s_{\mathrm{eff}}^2 = s_1^2 + s_1 s_2 \xi + s_2^2. \tag{4}$$

We see from this that anticorrelation ($\xi < 0$) leads to a net decrease in the covariance function for a given stochastic process. This implies that a system coupled to an anticorrelated environment will have a longer dephasing time than one coupled to uncorrelated or completely correlated baths.

2. Theory

Our theory is initialised by assuming that the total system can be separated into system and reservoir variables such that

$$H = H_o + \sum_k \hat{A}_k E_k(t) = H_o + H_r(t) \tag{5}$$

where H_o describes the system independent of reservoir with eigenstates $H_o|\alpha\rangle = \hbar\,\omega_\alpha|\alpha\rangle$, $\hat{A}_k$ are a set of quantum operators acting on the system subspace, and $E_k(t)$ are stochastic variables representing the dynamics of the environment. Formally, we write these in terms of an Itô stochastic differential equation of the form

$$\mathrm{d}\mathbf{E} = \mathbf{A}(t, \mathbf{E}(t))\,\mathrm{d}t + \mathbf{B}(t, \mathbf{E}(t)) \cdot \mathrm{d}\mathbf{W} \tag{6}$$

where $\mathbf{W}$ is a vector of Wiener processes and $\mathbf{A}(t, \mathbf{E})$ and $\mathbf{B}(t, \mathbf{E})$ define the the drift and the diffusion. This general form allows for both nonlinear and geometric processes to be incorporated into our model on an even footing. The process $\mathbf{E}(t)$ is in general, multidimensional and driven by a multidimensional Wiener process with a correlation matrix Σ. The process itself can be written in integral form as

$$\begin{aligned}\mathbf{E}(t) - \mathbf{E}(t_o) = &\int_{t_o}^{t} \mathrm{d}\tau \mathbf{A}(\tau, \mathbf{E}(\tau)) \\ &+ \int_{t_o}^{t} \mathrm{d}\tau \mathbf{B}(\tau, \mathbf{E}(\tau)) \cdot \mathrm{d}\mathbf{W}(t)\end{aligned} \tag{7}$$

with $\mathrm{d}W_i(t)\,\mathrm{d}W_j(t') = \delta(t - t')\Sigma_{ij}\,\mathrm{d}t$ as the generalised statement of Itô's lemma. If we take the noise terms to be correlated Ornstein-Uhlenbeck processes with

$$\mathrm{d}\mathbf{E} = -\mathbf{A} \cdot \mathbf{E}\,\mathrm{d}t + \mathbf{B} \cdot \mathrm{d}\mathbf{W} \tag{8}$$

with $\boldsymbol{\Sigma}\,\mathrm{d}t\delta(t - t') = \mathrm{d}\mathbf{W} \otimes \mathrm{d}\mathbf{W}$ as the correlation matrix, the general spectral density matrix takes the form

$$J(\omega) = \frac{1}{2\pi}(\mathbf{A} + i\omega)^{-1} \cdot \mathbf{B} \cdot \boldsymbol{\Sigma} \cdot \mathbf{B}^T \cdot (\mathbf{A} - i\omega)^{-1}, \tag{9}$$

as derived in Appendix 2 (c.f. Equation (A27)). These terms enter into the quantum dynamics of the reduced density matrix for the system variables via the Bloch Redfield equations

$$d_t\rho_{\alpha\alpha'} = -i(\omega_\alpha - \omega'_\alpha)\rho_{\alpha\alpha'} - \sum_{\beta\beta'} \mathcal{R}_{\alpha\alpha',\beta\beta'}(\rho_{\beta\beta'} - \rho^{eq}_{\beta\beta'}) \tag{10}$$

where ρ^{eq} is the equilibrium reduced density matrix and $\mathcal{R}$ is the Bloch-Redfield tensor

$$\begin{aligned}\mathcal{R}_{\alpha\alpha',\beta\beta'} = \sum_{nm}\Bigg\{ & \delta_{\alpha'\beta'}\sum_{\gamma} J_{nm}(\omega_\beta - \omega_\gamma)(A_n)_{\gamma\beta}(A_m)_{\alpha\gamma}0 \\ & -(J_{nm}(\omega'_\alpha - \omega'_\beta) + J_{nm}(\omega_\beta - \omega_\alpha))(A_n)_{\beta'\alpha'}(A_m)_{\alpha\beta} \\ & + \delta_{\alpha\beta}\sum_{\gamma} J_{nm}(\omega_\gamma - \omega'_\beta)(A_n)_{\beta'\gamma}(A_m)_{\gamma\alpha'}\Bigg\}\end{aligned} \tag{11}$$

where $(A_n)_{\alpha\beta} = \langle\alpha|\hat{A}_n|\beta\rangle$ are the matrix elements of the $\hat{A}_n$ operator in the eigenbasis of H_o and $J_{nm}(\omega)$ are elements of the generalised spectral matrix characterising the coupling between the system and its environment [12–15].

Under the secular approximation in which the time evolution of the system is slow compared to the characteristic correlation time of the environment $|\omega_{\alpha\beta} - \omega_{\gamma\delta}| \ll 1/\tau_c$, the population terms on the diagonal can be decoupled from the off-diagonal coherence terms via

$$\mathcal{R}^{sec}_{ij;kl} = \delta_{ij}\delta_{kl} + \delta_{ik}\delta_{jl}(1 - \delta_{ij}\delta_{kl}). \tag{12}$$

The time evolution of the reduced density matrix is strictly unitary under the secular approximation, which guarantees that the $\mathrm{tr}(\rho) = 1$ and all diagonal elements representing the populations are positive.

Table A1 gives a list of Redfield tensor elements for a single $SU(2)$ qubit driven by correlated noise in both longitudinal (σ^z) and spin-lattice (σ^x) terms. Within the secular approximation, the longitudinal terms contribute to the pure dephasing (T_2) time, while the spin-lattice term contributes to the relaxation and dephasing. Even when the diffusion matrix **B** is diagonal, cross-correlation enters the Redfield tensor via non-vanishing terms involving the cross-spectral densities; however, these terms only contribute to the non-secular terms of the tensor.

2.1. Coherence transfer between two qubits

We can easily generalise this model to accompany any number of states to explore how correlated noise affects the relaxation dynamics of the system. Here we consider a system of two spatially separated qubits (Figure 1), each driven by locally correlated fields, coupled together by a static tunnelling interaction τ,

$$H_o = \sum_{i=1,2} \frac{\epsilon_i}{2}\hat{\sigma}^k_i + \tau(\hat{\sigma}^+_1\hat{\sigma}^-_2 + \hat{\sigma}^+_2\hat{\sigma}^-_1) \tag{13}$$

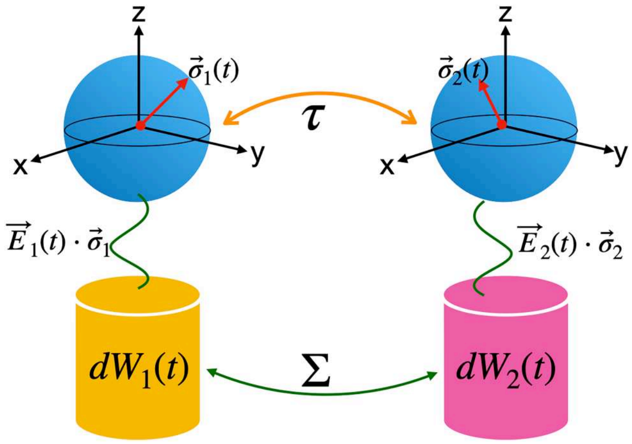

Figure 1. Sketch of the 2-site model with correlated noise interactions. Here, each site is taken as a 2-state qubit and is coupled to its neighbour via J (c.f. Equation (13)) and to its local environment via $\vec{E}_i \cdot \vec{\sigma}_i$ as per Equation (15). However, the local environments are correlated via Σ.

Here, we adopt the notation that the operators σ_i^k are $SU(2)$ Pauli matrices with $k = 0, 1, 2, 3$ associated with qubit i. Any system operators in the state space $SU(2) \otimes SU(2)$ can be constructed by taking the tensor products of $SU(2)$ Pauli matrices. If the energy gaps of the uncoupled qubits are identical, $\epsilon_1 = \epsilon_2$, then the two tunnelling states are obtained by taking symmetric and antisymmetric combinations of singly excited configurations $|10\rangle$ and $|01\rangle$, that is,

$$|\psi_\pm\rangle = \frac{1}{\sqrt{2}}(|01\rangle \pm |10\rangle) \tag{14}$$

and dipole transitions from the ground state $|00\rangle$ are only to the symmetric linear combination. If $\tau > 0$, the symmetric state lies higher in energy than the antisymmetric state and vice versa when $\tau < 0$. For $\epsilon_1 \neq \epsilon_2$ both states are optically coupled to the ground state, producing a pair of optical transitions, one of which is more intense than the other (superradiant vs. subradiant). The coupling to the environment is given by

$$H_r = \sum_j \hat{A}_j E_j(t) \tag{15}$$

where $E_j(t)$ is a stochastic process and $\hat{A}_j$ are operators in $SU(2) \otimes SU(2)$.

Physically, this model could be achieved in systems in which the energy of the local sites are strongly modulated by the local phonon modes, as in the case of Jahn-Teller distortions of high-spin octahedral d^4 coordination compounds where axial or equatorial distortions split the otherwise degenerate d_{z^2} and $d_{x^2-y^2}$ orbitals. Consequently, for a pair of octahedral sites, one can have symmetric and antisymmetric combinations of normal modes that drive the Jahn-Teller distortions of each site, giving rise to various degrees of correlation of the thermal noise experienced at each metal site. Furthermore, it may be possible through chemical or external stimulation to selectively enhance these modes.

We examine the effect of cross-correlation by computing the linear absorption spectrum of the system for a suitable choice of parameters. From time-dependent perturbation theory, the linear absorption spectrum is given by

$$S(\omega) \propto \left| \frac{1}{i\hbar} \int_{-\infty}^{\infty} e^{i\omega t} \langle \mu(t)[\mu(0), \rho(-\infty)]] \rangle \right|^2 \tag{16}$$

where $\hat{\mu}(t)$ is the transition dipole operator in the Heisenberg representation at time t and $\rho(-\infty)$ is the system density matrix at $t \to -\infty$.

Figure 2(a–d) shows the linear absorption spectra and the corresponding relative line widths for a pair of qubits with interaction $J/\epsilon = -0.2$ and with correlation between *either* the two transverse ($\sigma_z\sigma_z$) or the two longitudinal ($\sigma_x\sigma_x$) noise terms. Since only two noise terms are correlated, the spectral density matrix is given by

$$J(z) = \frac{1}{2\pi} \begin{pmatrix} \frac{2\xi s_{12}s_{11} + s_{11}^2 + s_{12}^2}{\gamma_1^2 + z^2} & \frac{\xi s_{11}s_{22} + \xi s_{12}s_{21} + s_{12}s_{22} + s_{11}s_{21}}{(z - i\gamma_1)(z + i\gamma_2)} \\ \frac{\xi s_{11}s_{22} + \xi s_{12}s_{21} + s_{12}s_{22} + s_{11}s_{21}}{(z + i\gamma_1)(z - i\gamma_2)} & \frac{2\xi s_{21}s_{22} + s_{22}^2 + s_{21}^2}{\gamma_2^2 + z^2} \end{pmatrix} \tag{17}$$

to denote whether the term is local to site 1 or 2 or involves explicit correlation between the two. Again, ξ denotes whether or not the terms are correlated or anticorrelated. In the transverse-transverse case, the spectral density $J(z)$ is evaluated at the transition frequency since this coupling involves the inelastic coupling to the environment; whereas in the longitudinal-longitudinal case, $J(z)$ is evaluated at $z = 0$ since this corresponds to a purely elastic coupling between the system and the environment.

Here, we see that correlations between transverse components have little effect on the spectral line shape. We can understand this since the spectral density terms are all evaluated at the transition frequency and are always smaller than their longitudinal counterparts.

On the other hand, the correlations between longitudinal components have a much more dramatic effect on both the transition intensity and line width, with anti-correlated noise giving much sharper and more intense transitions. We can understand this in the following way. According to the Kubo-Anderson model, the spectral lineshape is determined by fluctuations in the transition frequency. In the anticorrelated case, the local fluctuations are perfectly synchronised but in opposite ways. That is, as the local site energy of one increases, the other site energy always decreases. Therefore, the two local fluctuations cancel each other out. In the fully correlated case, the fluctuations are also perfectly synchronised, but both site energies increase or decrease, which results in a broader spectral transition.

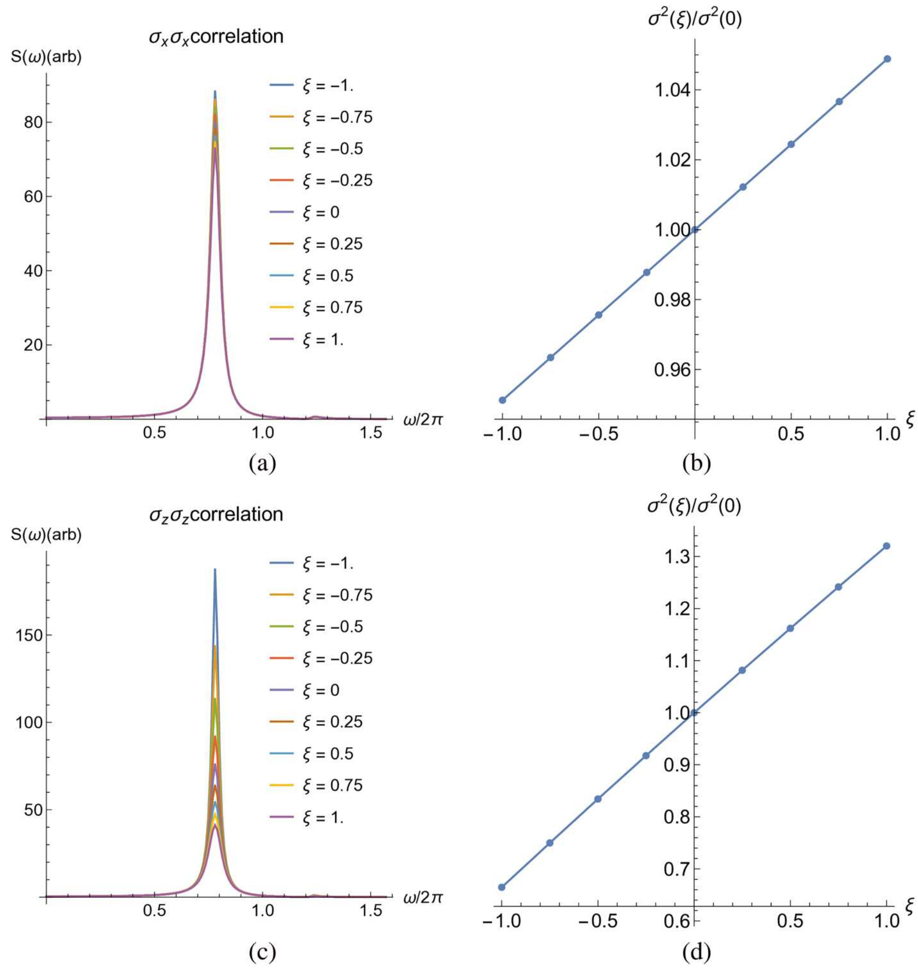

Figure 2. Linear response absorption spectra and associated line-width for a pair of qubits subject to transverse (a,b) and longitudinal (c,d) noise terms with various degrees of correlation.

We next consider the effect of initial-state preparation on the quantum dynamics of the entangled qubits. For this, we introduce the following four Bell-states

$$|\Phi^{\pm}\rangle = \frac{1}{2}(|00\rangle \pm |11\rangle) \tag{18}$$

$$|\Psi^{\pm}\rangle = \frac{1}{2}(|01\rangle \pm |10\rangle) \tag{19}$$

which correspond to the four maximally entangled quantum states of two qubits. From the previous discussion, longitudinal correlations appear to have the most profound effect on the dynamics, so we shall consider only that sort of coupling in this example.

The purity, $\gamma = \mathrm{tr}(\rho^2)$, provides a useful measure of the degree to which a quantum state is mixed. Mathematically, $\gamma = 1$ for a pure state since $\rho = \rho^2$

and takes a lower bound of $\gamma = 1/4$ corresponding to the case where all 4 states of the system are equally probable. Initially, the system is in a pure state with $\gamma = 1$ and evolves toward a mixed state as it evolves. At long time and low temperature, the system will relax completely to the ground state $|00\rangle$ with $\gamma = 1$.

Figure 3(a,b) shows the purity of a composite $SU(2) \otimes SU(2)$ qubit pair vs time for systems prepared in a maximally entangled (Bell) state and subject to longitudinal (σ_z) noise with various degrees of correlation or anti-correlation. In Figure 3(a), we take the initial state as a coherence between the doubly excited state $|11\rangle$ and the ground state $|00\rangle$, corresponding to the Φ_+ Bell state. Here, anticorrelation leads to a profound increase in the system's ability to retain its purity for nearly two orders of magnitude in time longer than the fully correlated case. In contrast, if the initial state is prepared in one of the $\Psi_\pm$ Bell states, corresponding to a linear combination within the singly excited manifold of states, correlation *enhances* the system's ability to retain purity. The only difference between the two results are in the preparation of the initial state. This provides a potentially useful experimental means for determining the correlation or anti-correlation between local environments.

However, the fidelity

$$F(\rho, \rho') = \left(\mathrm{tr}\left(\sqrt{\sqrt{\rho}\rho'\sqrt{\rho}}\right)\right)^2 \tag{20}$$

is also an important consideration for whether or not a given Bell state is suitable for an shared key. Fidelity provides a measure of the 'closeness' of two quantum states. It expresses the probability that one state will pass a test to identify itself as the other. By symmetry, $F(\rho, \sigma) = F(\sigma, \rho)$. In Figure 3(c,d), we compute the time-evolved fidelity $F(\rho_0, \rho_t)$ starting from the Φ^+(c) or Ψ^+(d) Bell states, versus various degrees of correlation between the baths. For Φ^+, the system loses fidelity rapidly and undergoes Rabi oscillation within the double excitation manifold spanned by Φ^+ and Φ^-. The fidelity eventually relaxes to $F = 1/2$ for a long time, corresponding to complete relaxation into the ground state $|00\rangle$. As with purity, the envelope of fidelity is enhanced by anti-correlated noise.

In contrast, the *correlated* noise helps to maintain both the purity and fidelity of the Ψ^+ Bell state. This state is an eigenstate of the bare system Hamiltonian can be prepared by direct photoexcitation from the ground state. Curiously, the above results suggest that correlated noise suppresses the optical response. However, the optical response is a measure of the coherence between the ground state and Ψ^+ and not a measure of the purity or fidelity of a given state. While we focus on purity and fidelity, one can easily extend the results and approach for computing the coherence between the two spins, entanglement entropy, and similar measures of quantum entanglement.

We can straightforwardly understand these results by considering that in the correlated case, the local energy gaps are being modulated in the same way. In essence, if energy gap 1 increases then energy gap 2 is also likely to increase and

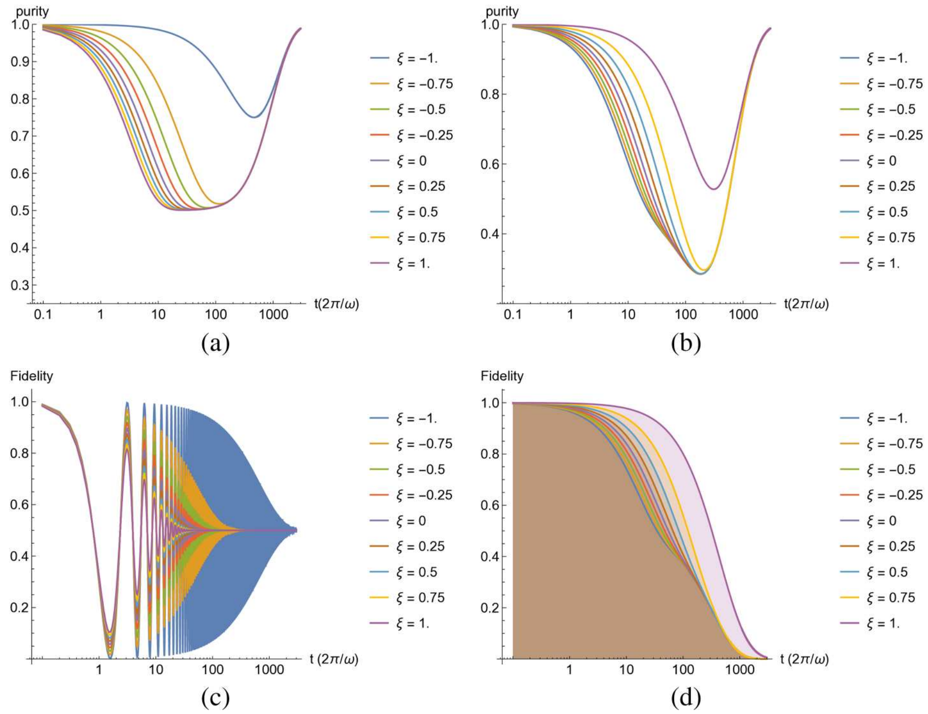

Figure 3. Purity(a,b) and fidelity (c,d) of composite $SU(2) \otimes SU(2)$ qubit pair vs time for systems prepared in a maximally entangled (Bell) state corresponding to (a,c)$|\Phi^+\rangle$ or (b,d) Ψ^+.

vice verse if the two are correlated ($\xi > 0$). This means that any entanglement that is sensitive to the sum of the two energies will experience a greater degree of environmental noise. Consequently, since the $\Phi^\pm$ state corresponds to a superposition of the $|00\rangle$ ground state and $|11\rangle$ doubly excited state is expected to be more sensitive to correlated noise than anti-correlated noise. On the other hand, it should be insensitive to anti-correlated noise since the two gaps are increasing and decreasing in opposite ways on average. Similarly, the other two Bell states represent the tunnelling exchange between $|01\rangle$ and $|10\rangle$ and will be more sensitive to anti-correlated noise ($\xi < 0$) since it leads to a greater average energetic mismatch between the two spins. On the other hand, it is less sensitive to correlated noise since both energy gaps are increasing and decreasing the same way on average.

3. Discussion

In this paper, we explored the role of noise correlation on a model open quantum system consisting of one and two coupled $SU(2)$ qubits and showed how the dynamics and spectroscopy of the system can be profoundly affected by environmental correlations. This has deep implications for searching materials suitable for quantum communications and computation applications in which long coherence times and retention of are required. In the case of super-dense coding, a sender (A) and a receiver (B) can communicate several classical bits of information by only transmitting a smaller number of qubits, provided that A and B share an entangled resource [16]. Since this resource is subject to environmental noise, the ability of A and B to perform super-dense coding hinges on their ability to maintain the fidelity of the state of the shared resource. Similarly, quantum teleportation requires the sender and receiver to share a maximally entangled state [17]. Our results suggest that by knowing whether the state is subject to correlated or anticorrelated noise, A and B can be ensured that their shared resource state can maintain its purity long enough for the information to be communicated. We also suggest that the local noise correlation can be tuned by manipulating the local environment around the two qubits and that the approach can be extended for multiple spin-qubit systems. Indeed, it has been suggested that physical processes such as photosynthetic light-harvesting [18] and charge-separation in organic photovoltaics [19] may take advantage of environmental noise correlation in which the system acts much like a quantum heat engine [20,21].

Author Contributions

Eric Bittner: Supervision, Funding acquisition, Conceptualisation, Methodology, Formal analysis, Validation, Writing; **Hao Li:** Formal analysis, Methodology, Validation; **Syad A Shah:** Conceptualisation; **Carlos Silva:** Conceptualisation Funding acquisition; **Andrei Piryatinski:** Conceptualisation, Validation, Funding acquisition. All authors contributed to the final draft and editing of this manuscript.

Disclosure statement

No potential conflict of interest was reported by the author(s).

Funding

The work at the University of Houston funded by the National Science Foundation (CHE-2102506) and the Robert A. Welch Foundation (E-1337). The work at Los Alamos National Laboratory was funded by the Laboratory Directed Research and Development (LDRD) program, 20220047DR. The National Science Foundation (DMR-1904293) funded the work at Georgia Tech.

ORCID

Eric R. Bittner http://orcid.org/0000-0002-0775-9664

Data availability

Data supporting the findings of this study are available from the corresponding author on a reasonable request.

References

[1] R. Kubo, *Note on the stochastic theory of resonance absorption*, J. Phys. Soc. Jpn 9 (1954), pp. 935–944. https://doi.org/10.1143/JPSJ.9.935.

[2] P.W. Anderson, *A mathematical model for the narrowing of spectral lines by exchange or motion*, J. Phys. Soc. Jpn 9 (1954), pp. 316–339. https://doi.org/10.1143/JPSJ.9.316.

[3] R. Kubo, *A Stochastic Theory of Line Shape*, in Advances in Chemical Physics, K.E. Shuler (Ed.), 1969, pp. 101–127.

[4] S. Mukamel, *Stochastic theory of resonance Raman line shapes of polyatomic molecules in condensed phases*, J. Chem. Phys. 82 (1984), pp. 5398–5408. https://doi.org/10.1063/1.448623.

[5] A.Y. Smirnov and M.H. Amin, *Theory of open quantum dynamics with hybrid noise*, New. J. Phys. 20 (2018), p. 103037.

[6] S. Golkar and M.K. Tavassoly, *Dynamics of entanglement protection of two qubits using a driven laser field and detunings: Independent and common, markovian and/or non-markovian regimes*, Chinese Phys. B 27 (2018), pp. 040303.

[7] J.-T. Hsiang, O. Arisoy, and B.-L. Hu, *Entanglement dynamics of coupled quantum oscillators in independent nonmarkovian baths*, Entropy 24(12) (2022), pp. 1814.

[8] Y. Li, J. Zhou, and H. Guo, *Effect of the dipole-dipole interaction for two atoms with different couplings in a non-markovian environment*, Phys. Rev. A 79 (2009), p. 012309.

[9] G. Mouloudakis and P. Lambropoulos, *Coalescence of non-markovian dissipation, quantum zeno effect, and non-hermitian physics in a simple realistic quantum system*, Phys. Rev. A. 106 (2022), pp. 053709.

[10] G. Mouloudakis and P. Lambropoulos, *Entanglement instability in the interaction of two qubits with a common non-markovian environment*, Quantum Information Processing 20 (2021), pp. 331.

[11] C. Gardner, *Stochastic Methods-A Handbook for the Natural and Social Sciences*, 4th ed., Springer Series in Synergetics, Springer, Berlin, Heidelberg, 2009.

[12] R. Konrat and H. Sterk, *Cross-correlation effects in the transverse relaxation of multiple-quantum transitions of heteronuclear spin systems*, Chem. Phys. Lett. 203 (1993), pp. 75–80.

[13] A.G. Redfield, *On the theory of relaxation processes*, IBM J. Res. Dev. 1 (1957), pp. 19–31.

[14] I. Solomon, *Relaxation processes in a system of two spins*, Phys. Rev. 99 (1955), pp. 559–565. cited by: 2808.

[15] P.N. Argyres and P.L. Kelley, *Theory of spin resonance and relaxation*, Phys. Rev. 134 (1964), pp. 98–111.

[16] C.H. Bennett and S.J. Wiesner, *Communication via one- and two-particle operators on einstein-podolsky-rosen states*, Phys. Rev. Lett. 69 (1992), pp. 2881–2884.

[17] C.H. Bennett, G. Brassard, C. Crépeau, R. Jozsa, A. Peres, and W.K. Wootters, *Teleporting an unknown quantum state via dual classical and einstein-podolsky-rosen channels*, Phys. Rev. Lett. 70 (1993), pp. 1895–1899.

[18] G.S. Engel, T.R. Calhoun, E.L. Read, T.-K. Ahn, T. Mančal, Y.-C. Cheng, R.E. Blankenship, and G.R. Fleming, *Evidence for wavelike energy transfer through quantum coherence in photosynthetic systems*, Nature 446 (2007), pp. 782–786.

[19] E.R. Bittner and C. Silva, *Noise-induced quantum coherence drives photo-carrier generation dynamics at polymeric semiconductor heterojunctions*, Nat. Commun. 5 (2014), p. 3119.

[20] K.E. Dorfman, D.V. Voronine, S. Mukamel, and M.O. Scully, *Photosynthetic reaction center as a quantum heat engine*, Proc. Nat. Acad. Sci. 110 (2013), pp. 2746–2751. REFDOI https://www.pnas.org/doi/pdf/10.1073/pnas.1212666110.

[21] M.O. Scully, K.R. Chapin, K.E. Dorfman, M.B. Kim, and A. Svidzinsky, *Quantum heat engine power can be increased by noise-induced coherence*, Proc. Nat. Acad. Sci. 108 (2011), pp. 15097–15100. REFDOI https://www.pnas.org/doi/pdf/10.1073/pnas.1110234108.
[22] H. Li, A.R. Srimath Kandada, C. Silva, and E.R. Bittner, *Stochastic scattering theory for excitation-induced dephasing: Comparison to the Anderson–Kubo lineshape*, J. Chem. Phys. 153 (2020), p. 154115. https://doi.org/10.1063/5.0026467.
[23] A.R. Srimath Kandada, H. Li, F. Thouin, E.R. Bittner, and C. Silva, *Stochastic scattering theory for excitation-induced dephasing: Time-dependent nonlinear coherent exciton lineshapes*, J. Chem. Phys. 153 (2020), p. 164706. https://doi.org/10.1063/5.0026351.

Appendix 1. A brief review of the Anderson-Kubo model for spectral lineshapes

A simple theory for spectral line-shapes was developed independently by Anderson and Kubo (AK) in the 1950s as a way to understand spectral line-broadening in magnetic resonance experiments [1–4]. We briefly recap the model as it pertains to the discussion in our paper.

Within the model, the transition frequency $\omega(t)$ of a two-state system is modulated about its average by (unspecified) fluctuations in the environment with

$$H/\hbar = \omega(t)\hat{\sigma}(3) \tag{A1}$$

where $\hat{\sigma}(i)$ is a Pauli matrix and $\omega(t) = \omega_o + \delta\omega(t)$ with

$$\mathrm{d}\delta\omega(t) = -\gamma\delta\omega(t)\,\mathrm{d}t + s\,\mathrm{d}W(t) \tag{A2}$$

with $\langle\delta\omega(t)\rangle = 0$ where $W(t)$ is a Wiener process with

$$\langle\delta\omega(t)\delta\omega(0)\rangle = \frac{s^2}{2\gamma}e^{-\gamma|t|}. \tag{A3}$$

We also define $\Delta^2 = \frac{s^2}{2\gamma}$ as the fluctuation amplitude (which is proportional to the temperature of the environment, and $1/\gamma = \tau_c$ as the correlation time for the environment.

It is straightforward, then, to show using time-dependent perturbation theory that the optical response of the system can be given as

$$S(t) = \frac{1}{i\hbar}\langle\mu_{01}(t)\mu_{10}(0)\rho(-\infty)\rangle \tag{A4}$$

were $\mu_{01}(t)$ is the matrix element coupling state 0 to 1 written in the Heisenberg representation with

$$\mu_{01}(t) = e^{-i\int_0^t \omega(\tau)\,\mathrm{d}\tau}\mu_{01}(0). \tag{A5}$$

Thus,

$$S(t) = \frac{|\mu_{01}|^2}{i\hbar}e^{i\omega t}\langle e^{-i\int_0^t \delta\omega(\tau)\,\mathrm{d}\tau}\rangle, \tag{A6}$$

where the angle brackets denote the ensemble average. The bracketed expression can be evaluated using the cumulant expansion technique

$$\langle e^{-i\int_0^t \delta\omega(\tau)\,\mathrm{d}\tau}\rangle = e^{-g(t)} \tag{A7}$$

$$= 1 - g(t) + \frac{1}{2}g^2(t) + \cdots \tag{A8}$$

and we expand $g(t)$ in terms of powers of $\delta\omega(t)$

$$g(t) = g_1(t) + g_2(t) + \cdots \tag{A9}$$

where each g_n is on the order of $\mathcal{O}^n(\delta\omega)$. Since $g_1(t) = \langle\delta\omega(t)\rangle = 0$ and all terms with $n > 2$ vanish under the Ito identity, only the g_2 term contributes to the cumulant summation. Thus, we obtain

$$g(t) = g_2(t) = \frac{1}{2}\int_0^t \int_0^t \mathrm{d}\tau \mathrm{d}\tau' \langle\delta\omega(\tau')\delta\omega(\tau)\rangle. \tag{A10}$$

Finally, since we assume the fluctuations are about a stationary value, the correlation function can only depend on the time interval $\tau - \tau'$ so that

$$\langle\delta\omega(\tau')\delta\omega(\tau)\rangle = \langle\delta\omega(\tau' - \tau)\delta\omega(0) = \Delta^2 e^{-|\tau'-\tau|/\tau_c} \tag{A11}$$

where $\Delta^2 = \frac{\sigma^2}{2\gamma}$ and $\tau_c = 1/\gamma$ is the correlation time as given above. Performing the double-time integration,

$$g(t) = \Delta^2 \tau_c^2 \left[e^{-t/\tau_c} + \frac{t}{\tau_c} - 1 \right] \tag{A12}$$

which is the *Kubo-lineshape* function.

There are two important limits to this model. First, in which $\Delta\tau_c \ll 1$ corresponds to the case of fast modulation. This results in a purely Lorentzian spectral line shape and a pure dephasing time of $T_2 = (\Delta^2\tau_c)^{-1}$. Similarly, $\Delta\tau_c \gg 1$ represents a slow modulation regime. Here, the spectral lineshape takes a purely Gaussian form, reflecting the inhomogeneities of the environment. Note that we recently extended this approach to account for non-stationary/non-equilibrium environments encountered in semiconducting systems [22,23].

Appendix 2. Correlations amongst random variables

The Ornstein-Uhlenbeck process is a very useful method to account for many Markovian stochastic processes. Its multivariate representation is even more practical for physical processes. Here we discuss the multivariate Ornstein-Uhlenbeck process, including correlated Wiener processes, for the purpose of tackling realistic physical problems such as chromorphores coupled to their respective phonon environments but interacting with a common bath.

We write the multivariate Ornstein-Uhlenbeck process as a vector $\boldsymbol{E}(t)$ composed of individual processes $X_i(t)$. The stochastic differential equation reads

$$\mathrm{d}\boldsymbol{E}(t) = A\left[\boldsymbol{\mu} - \boldsymbol{E}(t)\right]\mathrm{d}t + B\,\mathrm{d}\boldsymbol{W}(t), \tag{A13}$$

in which A and B are coefficient matrices, $\boldsymbol{\mu}$ is the vector of the Wiener process drift μ_i corresponding to W_i. $\boldsymbol{W}(t)$ is the vector of Wiener processes $W_i(t)$ which are correlated through the correlation matrix

$$\xi(t, t') \equiv \delta_{tt'}\mathrm{d}\boldsymbol{W}(t)\mathrm{d}\boldsymbol{W}(t')^{\mathrm{T}}/\mathrm{d}t, \tag{A14}$$

where the angular brackets represent the ensemble average. The matrix elements $\xi_{ij} = \mathrm{d}W_i(t)\mathrm{d}W_j(t)/\mathrm{d}t$ are defined through the Itô isometry in higher dimensions. Obviously $\xi_{ii} = 1$ according to the quadratic variation $(\mathrm{d}W_t)^2 = \mathrm{d}t$. ξ_{ij} varies from -1 to 1, respectively, corresponding to the fully anticorrelated and fully correlated cases. $\xi_{ij} = 0$ means that the two Wiener processes are completely uncorrelated.

According to the Itô's lemma, one finds the solution

$$\boldsymbol{E}(t) = e^{-At}\boldsymbol{E}(0) + (1 - e^{-At})\boldsymbol{\mu} + \int_0^t e^{-A(t-t')} B\, \mathrm{d}\boldsymbol{W}(t'), \tag{A15}$$

where $\boldsymbol{E}(0)$ is the initial condition of the process $\boldsymbol{E}(t)$, the mean value

$$\langle \boldsymbol{E}(t) \rangle = e^{-At}\langle \boldsymbol{E}(0) \rangle + (1 - e^{-At})\boldsymbol{\mu}, \tag{A16}$$

and the correlation function

$$\begin{aligned} \left\langle \boldsymbol{E}(t), \boldsymbol{E}^{\mathrm{T}}(s) \right\rangle &\equiv \left\langle [\boldsymbol{E}(t) - \langle \boldsymbol{E}(t) \rangle][\boldsymbol{E}(s) - \langle \boldsymbol{E}(s) \rangle]^{\mathrm{T}} \right\rangle \\ &= e^{-At}\left\langle \boldsymbol{E}(0), \boldsymbol{E}^{\mathrm{T}}(0) \right\rangle e^{-A^{\mathrm{T}}s} + \int_0^{\min(s,t)} e^{-A(t-t')} B\xi B^{\mathrm{T}} e^{-A^{\mathrm{T}}(s-t')} \mathrm{d}t' \end{aligned} \tag{A17}$$

following the Itô isometry in higher dimensions.

If $AA^{\mathrm{T}} = A^{\mathrm{T}}A$, one can find a unitary matrix S to diagonalise the coefficient matrix $SAS^{\dagger} = SA^{\mathrm{T}}S^{\dagger} = \mathrm{diag}(\gamma_1, \gamma_2, \ldots, \gamma_n)$. For deterministic initial condition $\left\langle \boldsymbol{E}(0), \boldsymbol{E}^{\mathrm{T}}(0) \right\rangle = 0$, so does the correlation function $\left\langle \boldsymbol{E}(t), \boldsymbol{E}^{\mathrm{T}}(s) \right\rangle = S^{\dagger}G(t, s)S$, in which

$$\begin{aligned} [G(t, s)]_{ij} &= \frac{\left(B\xi B^{\mathrm{T}}\right)_{ij}}{\gamma_i + \gamma_j}\left[e^{-\gamma_i|t-s|} - e^{-\gamma_i t - \gamma_j s}\right] \ (t \geq s), \\ [G(t, s)]_{ij} &= \frac{\left(B\xi B^{\mathrm{T}}\right)_{ij}}{\gamma_i + \gamma_j}\left[e^{-\gamma_j|t-s|} - e^{-\gamma_i t - \gamma_j s}\right] \ (t \leq s). \end{aligned} \tag{A18}$$

If the real parts of all A's eigenvalues are positive, one finds the stationary solution

$$\boldsymbol{E}_{\mathrm{s}}(t) = \boldsymbol{\mu} + \int_{-\infty}^t e^{-A(t-t')} B \mathrm{d}\boldsymbol{W}(t'), \tag{A19}$$

with the stationary correlation matrix

$$\left\langle \boldsymbol{E}_{\mathrm{s}}(t), \boldsymbol{E}_{\mathrm{s}}^{\mathrm{T}}(t') \right\rangle = \int_{-\infty}^{\min(t',t)} e^{-A(t-\tau)} B\xi B^{\mathrm{T}} e^{-A^{\mathrm{T}}(t'-\tau)} \mathrm{d}\tau \tag{A20}$$

We define the stationary covariance matrix

$$\Sigma = \left\langle \boldsymbol{E}_{\mathrm{s}}(t), \boldsymbol{E}_{\mathrm{s}}^{\mathrm{T}}(t) \right\rangle, \tag{A21}$$

then find a useful algebraic equation for stationary covariance matrix

$$A\sigma + \sigma A^{\mathrm{T}} = B\xi B^{\mathrm{T}}. \tag{A22}$$

For $s < t$ the stationary correlation function Equation (A20) can be written as

$$\begin{aligned} \left\langle \boldsymbol{E}_{\mathrm{s}}(t), \boldsymbol{E}_{\mathrm{s}}^{\mathrm{T}}(s) \right\rangle &= e^{-A(t-s)} \int_{-\infty}^{s} e^{-A(s-t')} B\xi B^{\mathrm{T}} e^{-A^{\mathrm{T}}(s-t')} \mathrm{d}t' \\ &= e^{-A(t-s)}\sigma \quad s < t, \end{aligned} \tag{A23}$$

and

$$= \sigma e^{-A^{\mathrm{T}}(s-t)} \quad s > t. \tag{A24}$$

The correlation function only depends on the time difference $|t - s|$ as expected for the stationary solution. We define the stationary correlation matrix $G_{\mathrm{s}}(\tau) = \left\langle \boldsymbol{E}_{\mathrm{s}}(t), \boldsymbol{E}_{\mathrm{s}}^{\mathrm{T}}(t - \tau) \right\rangle$, obviously $G_{\mathrm{s}}(0) = \sigma$. Then the above relation can be written in the form of the regression theorem

$$\frac{\mathrm{d}}{\mathrm{d}\tau}[G_s(\tau)] = \frac{\mathrm{d}}{\mathrm{d}\tau}\left\langle \boldsymbol{E}_s(\tau), \boldsymbol{E}_s^{\mathrm{T}}(0)\right\rangle = -AG_s(\tau). \tag{A25}$$

Noting that $G_s(0) = \sigma$, one can compute the stationary correlation matrix.

Since $\sigma^{\mathrm{T}} = \sigma$, we have

$$G_s(\tau) = [G_s(-\tau)]^{\mathrm{T}}. \tag{A26}$$

Therefore, one can find the spectrum matrix as the Fourier transform of the autocorrelation matrix $G_s(\tau)$

$$\begin{aligned} J(\omega) &= \frac{1}{2\pi}\int_{-\infty}^{\infty} e^{-i\omega\tau}G_s(\tau)\mathrm{d}\tau \\ &= \frac{1}{2\pi}(A+i\omega)^{-1}B\xi B^{\mathrm{T}}(A-i\omega)^{-1}. \end{aligned} \tag{A27}$$

As an example, we consider the case of the case of two correlated modes, in which we define the 2D Ornstein-Uhlenbeck process sby the SDEs

$$\begin{aligned} \mathrm{d}E_1(t) &= -\gamma_1 E_1(t)\mathrm{d}t + s_{11}\mathrm{d}B_1(t) + s_{12}\mathrm{d}B_2(t), \\ \mathrm{d}E_2(t) &= -\gamma_2 E_2(t)\mathrm{d}t + s_{21}\mathrm{d}B_1(t) + s_{22}\mathrm{d}B_2(t). \end{aligned}$$

The two Wiener processes $B_1(t)$ and $B_2(t)$ are coupled through the correlation parameter $\xi = \mathrm{d}B_1(t)\mathrm{d}B_2(t)/\mathrm{d}t$. The range of ξ is between -1 to 1 corresponding to the cases of complete anti-correlation and correlation, respectively. $\xi = 0$ means that the two Wiener processes are completely decoupled. The solutions of the OU processes are

$$\begin{aligned} E_1(t) &= e^{-\gamma_1 t}E_1(0) + s_{11}\int_0^t e^{-\gamma_1(t-s)}\mathrm{d}B_1(s) + s_{12}\int_0^t e^{-\gamma_1(t-s)}\mathrm{d}B_2(s), \\ E_2(t) &= e^{-\gamma_2 t}E_2(0) + s_{21}\int_0^t e^{-\gamma_2(t-s)}\mathrm{d}B_1(s) + s_{22}\int_0^t e^{-\gamma_2(t-s)}\mathrm{d}B_2(s). \end{aligned}$$

From this we compute the mean values

$$\begin{aligned} \langle E_1(t)\rangle &= \langle E_1(0)\rangle e^{-\gamma_1 t}, \\ \langle E_2(t)\rangle &= \langle E_2(0)\rangle e^{-\gamma_2 t}, \end{aligned}$$

as well as the correlation functions

$$\begin{aligned} \mathrm{Cov}[E_1(t), E_1(s)] &= \left\langle E_1(0)^2\right\rangle e^{-\gamma_1(t+s)} + \frac{s_{11}^2 + s_{12}^2 + 2\xi s_{11}s_{12}}{2\gamma_1}\left[e^{-\gamma_1|t-s|} - e^{-\gamma_1(t+s)}\right], \\ \mathrm{Cov}[E_2(t), E_2(s)] &= \left\langle E_2(0)^2\right\rangle e^{-\gamma_2(t+s)} + \frac{s_{21}^2 + s_{22}^2 + 2\xi s_{21}s_{22}}{2\gamma_2}\left[e^{-\gamma_2|t-s|} - e^{-\gamma_2(t+s)}\right], \\ \mathrm{Cov}[E_1(t), E_2(s)] &= \langle E_1(0), E_2(0)\rangle e^{-\gamma_1 t-\gamma_2 s} + \frac{s_{11}s_{21} + s_{12}s_{22} + \xi s_{11}s_{22} + \xi s_{12}s_{21}}{\gamma_1+\gamma_2}e^{-\gamma_1 t-\gamma_2 s} \\ &\quad \left[e^{(\gamma_1+\gamma_2)\min(s,t)} - 1\right], \\ \mathrm{Cov}[E_2(t), E_1(s)] &= \langle E_1(0), E_2(0)\rangle e^{-\gamma_2 t-\gamma_1 s} + \frac{s_{11}s_{21} + s_{12}s_{22} + \xi s_{11}s_{22} + \xi s_{12}s_{21}}{\gamma_1+\gamma_2}e^{-\gamma_2 t-\gamma_1 s} \\ &\quad \left[e^{(\gamma_1+\gamma_2)\min(s,t)} - 1\right]. \end{aligned}$$

Using these we find the spectral density matrix for the correlated processes as

$$J(\omega) = \frac{1}{2\pi}\begin{bmatrix} \frac{s_{11}^2+2\xi s_{11}s_{22}+s_{12}^2}{\gamma_1^2+\omega^2} & \frac{s_{12}s_{22}+s_{11}s_{21}+\xi(s_{12}s_{21}+s_{11}s_{22})}{(\gamma_1+i\omega)(\gamma_2-i\omega)} \\ \frac{s_{12}s_{22}+s_{11}s_{21}+\xi(s_{12}s_{21}+s_{11}s_{22})}{(\gamma_1-i\omega)(\gamma_2+i\omega)} & \frac{s_{11}^2+2\xi s_{21}s_{22}+s_{22}^2}{\gamma_2^2+\omega^2} \end{bmatrix}. \tag{A28}$$

Appendix 3. Redfield tensor elements for cross correlation between *x* and *z* for a single *SU*(2) qubit

The Bloch-Redfield equations give the quantum dynamics of the reduced density matrix according to

$$d_t\rho_{\alpha\alpha'} = -i(\omega_\alpha - \omega'_\alpha)\rho_{\alpha\alpha'} - \sum_{\beta\beta'}\mathcal{R}_{\alpha\alpha';\beta\beta'}(\rho_{\beta\beta'} - \rho^{eq}_{\beta\beta'}) \tag{A29}$$

where ρ^{eq} is the equilibrium reduced density matrix and $\mathcal{R}$ is the Bloch-Redfield tensor with elements [12–15]

$$\begin{aligned}\mathcal{R}_{\alpha\alpha';\beta\beta'} = \sum_{nm}\Bigg\{&\delta_{\alpha'\beta'}\sum_{\gamma}J_{nm}(\omega_\beta - \omega_\gamma)(A_n)_{\gamma\beta}(A_m)_{\alpha\gamma} \\ &- (J_{nm}(\omega'_\alpha - \omega'_\beta) + J_{nm}(\omega_\beta - \omega_\alpha))(A_n)_{\beta'\alpha'}(A_m)_{\alpha\beta} \\ &+ \delta_{\alpha\beta}\sum_{\gamma}J_{nm}(\omega_\gamma - \omega'_\beta)(A_n)_{\beta'\gamma}(A_m)_{\gamma\alpha'}\Bigg\}\end{aligned} \tag{A30}$$

where $(A_n)_{\alpha\beta} = \langle\alpha|\hat{A}_n|\beta\rangle$ are the matrix elements of the $\hat{A}_n$ operator in the eigenbasis of H_o and $J_{nm}(\omega)$ are elements of the generalised spectral matrix characterising the coupling between the system and its environment. Table A1 gives the tensor elements for the case of a single qubit with transition frequency ε coupled to a noisy environment through both longitudinal (through $\hat{\sigma}_z$) and transverse (through $\hat{\sigma}_x$ or $\hat{\sigma}_y$). $J_{ij}(\omega)$ to denote the spectral density associated with the correlation function $\langle E_i(t)E_j(t')\rangle$.

The second column indicates whether or not R_{ijkl} is non-vanishing within the secular approximation.

$$R^{sec}_{ij;kl} = \big(\delta_{ij}\delta_{kl} + \delta_{ik}\delta_{jl}(1 - \delta_{ij}\delta_{kl})\big)R_{ij;kl} \tag{A31}$$

When operating under this limit, the system populations are decoupled from the coherences, following a regular Pauli Master equation with the population rate matrix R_{iikk}. This ensures population conservation and achieves the correct thermal equilibrium over extended periods. Under this approximation, the density matrix exhibits the appropriate physical behaviour with $\mathrm{Tr}[\rho] = 1$. The population rate matrix, being real, facilitates exponential relaxation of the populations. Coherences are also fully separated from the population and experience attenuation by the dephasing rates $R_{ij;ij}$. Generally, $R_{ij;ij}$ is complex, with its imaginary component representing bath-induced energy shifts. For example, under the secular approximation, we expect that $R_{11;11} + R_{22;11} = R_{22;22} + R_{11;22} = 0$ and $R_{12;12} = R^*_{21;21}$ for the coherence terms. The presence of the cross-correlation terms does not lead to a violation of these conditions.

Table A1. Redfield tensor elements for $SU(2)$ qubit with cross-correlation between $\hat{\sigma}^x$ and $\hat{\sigma}^z$ noise terms.

i	j	k	l	Secular	$\mathcal{R}_{ij;kl}$	Ornstein-Uhlenbeck
1	1	1	1	Secular	$J_{xx}(-\epsilon)+J_{xx}(\epsilon)$	$\frac{2s_x(s_x+2\xi s_{xz})}{\gamma_x^2+\epsilon^2}$
1	1	1	2	Non-Secular	$-J_{xz}(0)-J_{zx}(0)$	$-\frac{2(s_x(s_{xz}+\xi s_z)+\xi s_{xz}^2)}{\gamma_x\gamma_z}$
1	1	2	1	Non-Secular	$J_{xz}(-\epsilon)-J_{zx}(-\epsilon)-2J_{zx}(0)$	$-\frac{2(\gamma_x^2(i\epsilon\gamma_z+\gamma_z^2+\epsilon^2)-i\epsilon\gamma_x\gamma_z^2+\epsilon^2(\gamma_z^2+\epsilon^2))(s_x(s_{xz}+\xi s_z)+\xi s_{xz}^2)}{\gamma_x\gamma_z(\gamma_x^2+\epsilon^2)(\gamma_z^2+\epsilon^2)}$
1	1	2	2	Secular	$-J_{xx}(-\epsilon)-J_{xx}(\epsilon)$	$-\frac{2s_x(s_x+2\xi s_{xz})}{\gamma_x^2+\epsilon^2}$
1	2	1	1	Non-Secular	$-2J_{xz}(-\epsilon)-J_{xz}(0)+J_{zx}(0)$	$-\frac{2(s_x(s_{xz}+\xi s_z)+\xi s_{xz}^2)}{(\epsilon+i\gamma_x)(\epsilon-i\gamma_z)}$
1	2	1	2	Secular	$2(J_{xx}(\epsilon)+2J_{zz}(0))$	$\frac{4s_{xz}^2(\gamma_x^2+\epsilon^2)+4\xi s_{xz}(2s_z(\gamma_x^2+\epsilon^2)+s_x\gamma_z^2)+2s_x^2\gamma_z^2}{\gamma_z^2(\gamma_x^2+\epsilon^2)}$
1	2	2	1	Non-Secular	$-2J_{xx}(-\epsilon)$	$-\frac{2s_x(s_x+2\xi s_{xz})}{\gamma_x^2+\epsilon^2}$
1	2	2	2	Non-Secular	$J_{xz}(-\epsilon)+J_{zx}(-\epsilon)$	$\frac{2(\gamma_x\gamma_z+\epsilon^2)(s_x(s_{xz}+\xi s_z)+\xi s_{xz}^2)}{(\gamma_x^2+\epsilon^2)(\gamma_z^2+\epsilon^2)}$
2	1	1	1	Non-Secular	$-J_{xz}(\epsilon)-J_{zx}(\epsilon)$	$-\frac{2(\gamma_x\gamma_z+\epsilon^2)(s_x(s_{xz}+\xi s_z)+\xi s_{xz}^2)}{(\gamma_x^2+\epsilon^2)(\gamma_z^2+\epsilon^2)}$
2	1	1	2	Non-Secular	$-2J_{xx}(\epsilon)$	$-\frac{2s_x(s_x+2\xi s_{xz})}{\gamma_x^2+\epsilon^2}$
2	1	2	1	Secular	$2(J_{xx}(-\epsilon)+2J_{zz}(0))$	$\frac{4s_{xz}^2(\gamma_x^2+\epsilon^2)+4\xi s_{xz}(2s_z(\gamma_x^2+\epsilon^2)+s_x\gamma_z^2)+2s_x^2\gamma_z^2}{\gamma_z^2(\gamma_x^2+\epsilon^2)}$
2	1	2	2	Non-Secular	$2J_{xz}(\epsilon)+J_{xz}(0)-J_{zx}(0)$	$\frac{2(s_x(s_{xz}+\xi s_z)+\xi s_{xz}^2)}{(\epsilon-i\gamma_x)(\epsilon+i\gamma_z)}$
2	2	1	1	Secular	$-J_{xx}(-\epsilon)-J_{xx}(\epsilon)$	$-\frac{2s_x(s_x+2\xi s_{xz})}{\gamma_x^2+\epsilon^2}$
2	2	1	2	Non-Secular	$-J_{xz}(\epsilon)+J_{zx}(\epsilon)+2J_{zx}(0)$	$\frac{2(\gamma_x^2(-i\epsilon\gamma_z+\gamma_z^2+\epsilon^2)+i\epsilon\gamma_x\gamma_z^2+\epsilon^2(\gamma_z^2+\epsilon^2))(s_x(s_{xz}+\xi s_z)+\xi s_{xz}^2)}{\gamma_x\gamma_z(\gamma_x^2+\epsilon^2)(\gamma_z^2+\epsilon^2)}$
2	2	2	1	Non-Secular	$J_{xz}(0)+J_{zx}(0)$	$\frac{2(s_x(s_{xz}+\xi s_z)+\xi s_{xz}^2)}{\gamma_x\gamma_z}$
2	2	2	2	Secular	$J_{xx}(-\epsilon)+J_{xx}(\epsilon)$	$\frac{2s_x(s_x+2\xi s_{xz})}{\gamma_x^2+\epsilon^2}$

Notes: The second column indicates whether the term survives under the secular approximation, which separates the evolution of the population and the coherence terms. The last column gives the tensor element within the correlated Ornstein-Uhlenbeck model.

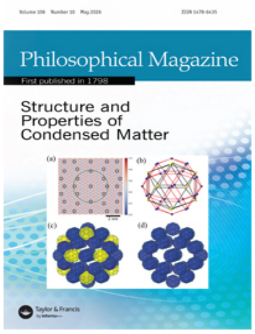

Philosophical Magazine

ISSN: 1478-6435 (Print) 1478-6443 (Online) Journal homepage: www.tandfonline.com/journals/tphm20

Quantum aspects of spacetime: a quantum optics view of acceleration radiation and black holes

C. R. Ordóñez, A. Chakraborty, H. E. Camblong, Marlan O. Scully & William G. Unruh

PHILOSOPHICAL MAGAZINE
https://doi.org/10.1080/14786435.2025.2605361

Taylor & Francis
Taylor & Francis Group

Check for updates

Quantum aspects of spacetime: a quantum optics view of acceleration radiation and black holes

C. R. Ordóñez [a], A. Chakraborty [b], H. E. Camblong [c], Marlan O. Scully [d] and William G. Unruh [d,e]

[a]Department of Physics, University of Houston, Houston, TX, USA; [b]Institute for Quantum Computing, Department of Physics and Astronomy, University of Waterloo, Waterloo, ON, Canada; [c]Department of Physics and Astronomy, University of San Francisco, San Francisco, CA, USA; [d]Institute for Quantum Science and Engineering, Department of Physics and Astronomy, Texas A&M University, College Station, TX, USA; [e]Department of Physics and Astronomy, University of British Columbia, Vancouver, BC, Canada

ABSTRACT
For the *centennial of quantum mechanics*, we offer an overview of the central role played by quantum information and thermalisation in problems involving fundamental properties of spacetime and gravitational physics. This is an open area of research still a century after the initial development of formal quantum mechanics, highlighting the effectiveness of quantum physics in the description of all natural phenomena. These remarkable connections can be highlighted with the tools of modern quantum optics, which effectively addresses the three-fold interplay of interacting atoms, fields, and spacetime backgrounds describing gravitational fields and noninertial systems. In this review article, we select aspects of these phenomena centred on quantum features of the acceleration radiation of particles in the presence of black holes. The ensuing horizon-brightened radiation (HBAR) provides a case study of the role played by quantum physics in nontrivial spacetime behaviour, and also shows a fundamental correspondence with black hole thermodynamics.

ARTICLE HISTORY
Received 25 August 2025
Accepted 12 December 2025

KEYWORDS
Quantum fields in curved spacetime; Unruh effect; quantum aspects of black holes

1. Quantum physics: introduction and historical overview

A century of developments in *quantum mechanics*, following the successful establishment of the matrix and wave mechanics frameworks in 1925 and 1926 [1–4], has provided the foundations for most areas of science and technology, leading to a vast range of theoretical and practical applications, and a complete redesign of our view of nature [5]. This radical transformation offers a unified view of a universal *quantum dynamics governing all particles and fields* [5,6].

1.1. Quantum framework

One fundamental approach to quantum dynamics is the matrix mechanics framework of Heisenberg, Born, and Jordan, developed in 1925 [7–9], where physical observables are

CONTACT C. R. Ordóñez ordonez@uh.edu Department of Physics, University of Houston, Houston, TX 77024-5005, USA

described by matrices subject to a set of time evolution equations. An alternative framework was discovered in late 1925 [10,11]: the Schrödinger picture, in which the evolution of a quantum state $|\Psi\rangle$ with respect to the given time t is governed by the Schrödinger equation

$$i\hbar\frac{\mathrm{d}}{\mathrm{d}t}|\Psi(t)\rangle = \hat{H}|\Psi(t)\rangle, \tag{1}$$

driven by a Hamiltonian operator $\hat{H}$ (using the modern notation developed by Dirac [12,13]), and with a physical scale in terms of the reduced Planck or Dirac constant $\hbar = h/2\pi$ (where h is the ordinary Planck constant). Correspondingly, the physical observables are represented by operators or matrices $\hat{A}$ satisfying commutation relations, with the primary canonical commutators,

$$[\hat{q}, \hat{p}] \equiv \hat{q}\hat{p} - \hat{p}\hat{q} = i\hbar, \tag{2}$$

between pairs of conjugate position-momentum variables $\hat{q}$ and $\hat{p}$. In this quantum context, the commutator between two operators or matrices $\hat{A}$ and $\hat{B}$ is generally defined by $[\hat{A}, \hat{B}] = \hat{A}\hat{B} - \hat{B}\hat{A}$, and the hats denote the operator nature of these quantities. The primary relation (2) is introduced to accommodate the Heisenberg uncertainty principle [14], describing the incompatibility of simultaneous measurements of position and momentum, as well as of any pair of canonically conjugate variables.

In terms of a distinct but equivalent approach, the observables of matrix mechanics are subject to a set of time evolution equations that give the same physical outcome as Equation (1), as first shown in Ref. [15]. The complete equivalence of these two dynamical approaches was further established in a generalised transformation theory by Dirac [16], in what became the modern framework of quantum mechanics [12]. In this setting, the original matrix mechanics can be displayed in the Heisenberg picture by starting with the evolution of states given by the dynamical Equation (1) of the Schrödinger picture and recasting the operator dynamics (representable as matrices) in terms of the Heisenberg equation

$$\frac{\mathrm{d}}{\mathrm{d}t}\hat{A}_{\mathrm{H}}(t) = \frac{i}{\hbar}[H_{\mathrm{H}}(t), \hat{A}_{\mathrm{H}}(t)] + \left(\frac{\partial \hat{A}_{\mathrm{S}}}{\partial t}\right)_{\mathrm{H}}, \tag{3}$$

which highlights that the Hamiltonian governs the time evolution via quantum-mechanical commutators. The Schrödinger and Heisenberg picture quantities are labelled with subscripts S and H. The relation between the quantities $\hat{A}_{\mathrm{H}}$ and $\hat{A}_{\mathrm{S}}$ in the two pictures is defined by a similarity transformation with respect to the time evolution of Equation (1) – this guarantees identical outcomes for the predicted values of any observable quantities. In what follows, we will omit the hats for the notation of operators.

The underlying formal mathematical structure of quantum mechanics was fully spelled out in two groundbreaking treatises, by Dirac [12] and by von Neumann [17], both based on their earlier series of seminal papers from 1927 [16,18–20]. These also included an alternative and more general description of *quantum states as statistical mixtures* in terms of a density matrix or density operator ρ [19,21], subject to the von

Neumann equation [19]

$$i\hbar \frac{\mathrm{d}\rho}{\mathrm{d}t} = [H, \rho], \tag{4}$$

which generalises Equation (1). In addition, the quantum-information measure of states can be expressed in terms of the von Neumann entropy [20]

$$S = -k_B \mathrm{Tr}\big[\rho \ln \rho\big], \tag{5}$$

which, as the quantum-mechanical counterpart of the Gibbs entropy, physically scales in terms of Boltzmann's constant k_B; in Equation (5), Tr stands for the operator trace. The ensuing comprehensive, information-based framework, centred on Equations (4) and (5), has become central to the ongoing developments in *quantum information and quantum computing* [22,23]. These revolutionary beginnings, including the establishment of a consistent universal framework and its initial success in atomic physics and chemistry [1–3], were followed by an impressive sequence of transcendental discoveries and applications of the quantum principles to an ever expanding set of systems over the next one hundred years [5].

1.2. Quantum field theory

One of the most consequential applications was the development of *quantum field theory*, which also followed naturally by 1927, in a formulation of the quantisation of the ubiquitous electromagnetic fields [24]. This approach, the canonical quantisation of fields, became a paradigm for all field theories, generalising the dynamics of Equations (1) and (3) for field operators Φ using a Hamiltonian framework, with conjugate field momenta and commutation relations [6]. The simplest realisation of this framework is provided by the quantisation of a real scalar (spin-zero) field, to be used in this review for the sake of simplicity. This can be expressed in terms of a complete set of orthonormal modes: $\{\phi_{\boldsymbol{s}}(t, \mathbf{r}), \phi^*_{\boldsymbol{s}}(t, \mathbf{r})\}$ (including the complex-conjugate modes $\phi^*_{\boldsymbol{s}}$), via the expansion [6,25]

$$\Phi(t, \mathbf{r}) = \sum_{\boldsymbol{s}} [a_{\boldsymbol{s}} \phi_{\boldsymbol{s}}(t, \mathbf{r}) + a^\dagger_{\boldsymbol{s}} \phi^*_{\boldsymbol{s}}(t, \mathbf{r})], \tag{6}$$

where $(t, \mathbf{r})$ stand for the spacetime coordinates, and the field modes $\phi_{\boldsymbol{s}}$ are identified by the mode frequency ω and a set of quantum numbers (collectively labelled by the symbol $\boldsymbol{s}$). For example, in flat spacetime, there is a natural choice of Fourier modes $\phi_{\boldsymbol{s}}(t, \mathbf{r}) \propto e^{-i\omega_s t}\, \phi_{\boldsymbol{s}}(\mathbf{r})$ associated with the time t of a given inertial frame; this is the common procedure used in ordinary quantum field theory, dating back to the seminal paper [24] on the quantisation of the electromagnetic field. (An elaboration of this procedure is shown in Section 2.1 and in Appendix 1). In addition, the operator coefficients $a_{\boldsymbol{s}}$ and $a^\dagger_{\boldsymbol{s}}$ in Equation (6), known as mode operators, are associated with particle annihilation and creation (where $a^\dagger_{\boldsymbol{s}}$ is the adjoint of $a_{\boldsymbol{s}}$), and satisfy the canonical commutator relations of the field-operator algebra (generalising $[q, p] = i\hbar$):

$$[a_{\boldsymbol{s}}, a^\dagger_{\boldsymbol{s}'}] = \delta_{\boldsymbol{s},\boldsymbol{s}'}, \quad [a_{\boldsymbol{s}}, a_{\boldsymbol{s}'}] = 0, \quad [a^\dagger_{\boldsymbol{s}}, a^\dagger_{\boldsymbol{s}'}] = 0. \tag{7}$$

Similar expressions involving anticommutators are applicable to fermion fields. The quantum-field mode expansion is ordinarily written as in Equation (6) for a field $\Phi(t, \mathbf{r})$ in the Heisenberg picture, with time dependence such that the dynamics satisfies the Heisenberg Equation (3). This choice has several advantages, including an intuitive correspondence with the classical regime, where the dynamics is similarly described in terms of Poisson brackets – this played an important role in the early development of quantum field theory [6,26]. Moreover, this general technique can be appropriately generalised to all quantum fields [6], though a complete understanding of the subtleties of quantum field theory and associated technical tools took decades of development [26], culminating with the successful Standard Model of particle physics by the 1970s, and leading the way to the current frontiers of particle physics [27]. In addition, the canonical approach, based on Equations (6)–(7) has been shown to be equally valid in curved spacetime [25], as emphasised in the next paragraph and throughout this review article. Specifically, a similar procedure applies with modes $\phi_s(t, \mathbf{r}) \propto e^{-i\omega_s t}\, \phi_s(\mathbf{r})$, provided that the given spacetime is endowed with time-translation symmetry, i.e. for stationary spacetimes; in such cases, Equation (6) effectively separates the expansion into positive-frequency and negative-frequency modes [$\phi_s(t, \mathbf{r})$ and $\phi_s^*(t, \mathbf{r})$ respectively]. One can still use Equation (6) with more general modes in other instances, though additional subtleties need to be considered [25]. The technical details of quantum field theory, including how to define an inner product for orthonormality, are introduced in Section 2. Parenthetically, in all the applications of quantum physics, there is an alternative and powerful path-integral or functional formulation due to Dirac [28] and Feynman [29], based on the classical Lagrangian, and equivalent to the canonical quantisation described above. Even though we do not further elaborate on the path-integral formalism in this review article, it is noteworthy that it provides both deep insight and computational efficiency for a variety of problems [6,30,31].

1.3. Quantum information and quantum field theory in curved spacetime

Even in recent decades, profoundly surprising implications in its foundations and technological applications have been discovered, most notably in terms of its relation to *quantum information theory and quantum computing* [22,23], and their interplay with spacetime behaviour [32]. In its more general context, now known as *relativistic quantum information* [32,33], the concepts of vacuum, particles, and particle detectors have been reexamined, and a wealth of surprising phenomena related to thermodynamic properties have been uncovered. The basic framework to tackle spacetime quantum behaviour has been *quantum field theory in curved spacetime* [25], where the canonical quantisation is enforced as in Equations (6)–(7) with an appropriate definition of orthonormality and choice of a complete set of modes adapted to the given spacetime geometry. In this framework, the role of horizons in governing quantum effects via information properties is instrumental in altering the nature of physical states and generating thermal behaviour. An outstanding manifestation of these concepts is the thermodynamics of black holes [34,35], where a network of relations linking quantum theory with gravitation and thermodynamics include: (i) the Hawking effect [36,37], with thermal radiation at the Hawking temperature

$$T_H = \frac{1}{2\pi}\frac{\hbar}{k_B c}\kappa, \tag{8}$$

proportional to the surface gravity κ [38]; and the Bekenstein-Hawking entropy S_{BH} of the black hole [39,40],

$$S_{\mathrm{BH}} = \frac{1}{4}\frac{k_B c^3}{\hbar G}A, \tag{9}$$

proportional to its event horizon area A, along with a generalised second law of thermodynamics (GSL) [39,40] and the four laws of black hole mechanics [41]. This thermodynamic behaviour suggests a quantum-information interpretation of the entropy as encoded on the black hole event horizon, in units of the Planck area ℓ_P^2, with the Planck length $\ell_P = \sqrt{\hbar G/(k_B c^3)}$, as depicted in Figure 1. Similar thermodynamic behaviour is displayed by accelerated particles, leading to Unruh effect [42–45], with acceleration radiation, and an associated Unruh temperature [42–45],

$$T_U = \frac{1}{2\pi}\frac{\hbar}{k_B c}a, \tag{10}$$

proportional to the acceleration a; in this case, the apparent horizon emergent in the noninertial frame of the accelerated observer also encodes nontrivial quantum-information properties. These nontrivial spacetime effects are quantum-

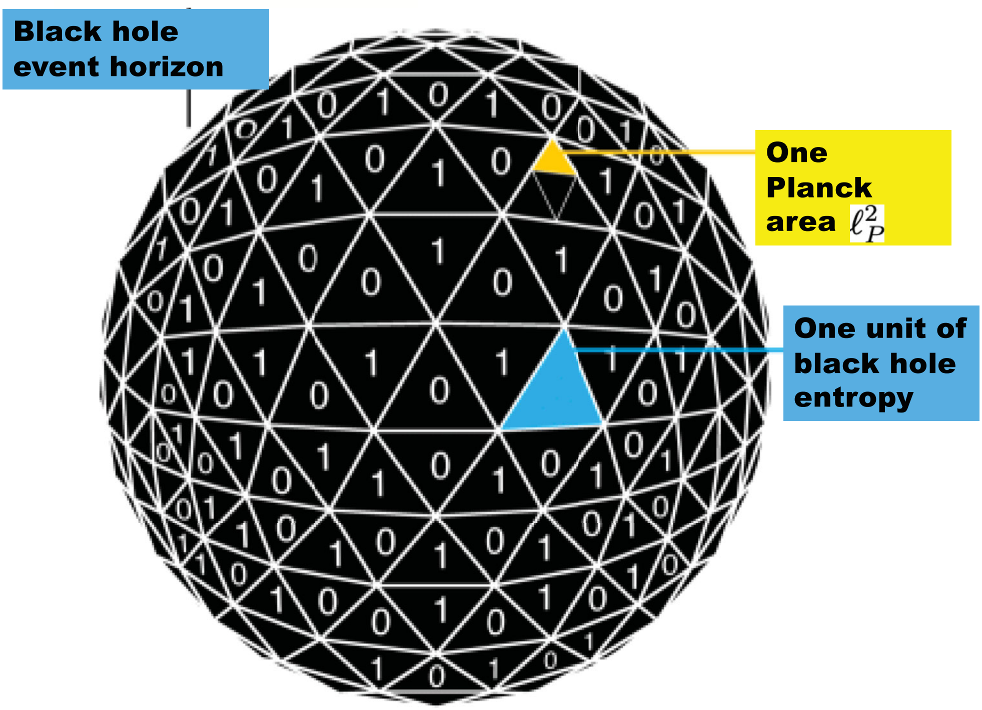

Figure 1. A quantum information representation of the event horizon as a quantum computer, in units proportional to the Planck area $\ell_P^2 = \hbar G/(k_B c^3)$.

relativistic in nature, a fact that which is highlighted in Equations (9)–(10) via the Planck constant $\hbar$ and the speed of light c; and they are also thermal, as revealed by the Boltzmann constant k_B. In addition, they provide further realisations of the quantum nature of all physical systems in a manner that points to a transition towards a *theory of quantum gravity* [46].

1.4. Quantum optics

In parallel with the development of quantum information and curved spacetime field theory, the discipline of *quantum optics* [47,48], with its foundations on *quantum electrodynamics (QED)* [49], has revealed a remarkable effectiveness in explaining the same phenomena. Arguably, the great experimental success of quantum optics is intertwined with the development of laser physics and other applications in atomic physics [47,48]. However, its domain of applicability has been greatly expanded as a theoretical tool, adding insights from the *quantum theory of matter-field interactions* [50], which has been the trademark of quantum physics since its early beginnings [5]. Specifically, a direct use of quantum optics techniques in the context of relativistic spacetime, with applications to various configurations dealing with accelerated systems, can be traced back to Refs. [51,52], where the relevance of the conversion of virtual to real atomic transitions is highlighted. In these spacetime quantum developments, the 'physical reality' of acceleration radiation was theoretically confirmed [53] from first principles, extending earlier results on the excitation of accelerated particle detectors of Ref. [54]. Recently, these ideas were further extended to study the acceleration radiation in the presence of black holes, which has been called 'horizon-brightened acceleration radiation' (HBAR); see below [55]. These techniques have verified and further developed the extensive earlier literature on moving mirror models [56–60]. In particular, important conceptual problems – including the interpretation of various configurations of detectors and mirrors as well as the equivalence principle – have been easily tackled with related quantum-optics treatments [61,62], which are applicable to a variety of spacetime configurations [63] and further discussed in this review article. Other closely related developments involve the Casimir [64,65] and dynamical Casimir [66,67] effects – with *quantum virtual processes* and particle creation in a vacuum as a common denominator. Several aspects of most of these phenomena are comprehensively summarised in recent reviews [67–70] that have a significant overlap with this article.

For our current purposes, in this review article, we select a subset of concepts of relativistic quantum information and highlight the effectiveness of quantum optics techniques to shed light on the nature of spacetime and surprising *spacetime and gravitational quantum effects*. Specifically, our focus will be on the *quantum effects associated with the motion of particles in black hole backgrounds*, summarising and extending the work of Ref. [55].

1.5. Organisation of this article

This article is organised as follows. An extensive discussion of the quantum optics description of interactions and particle detectors is given in Section 2, including general overviews of *quantum field theory* in curved spacetime (for scalar fields) and the two-level atom in the form of the *quantum Rabi model* (QRM) and generalisations. In Section 3, we offer an introduction to the *quantum-optics density matrix* approach. In addition, in Section 4 we discuss the setup of quantum aspects of spacetime geometry, as well as the quantum-mechanical framework known as *conformal quantum mechanics* (CQM) [71,72], which is governed by an inverse square potential [73], and generically offers a versatile description of scale-invariant physics applications [74–76], including its central role in all near-horizon black hole geometries [77–84]. With this comprehensive background, in Section 5 we derive the most important results of acceleration radiation (HBAR) [55,81–84], leading to an HBAR-black hole thermodynamics correspondence in Section 6. After some concluding remarks on the implications of these nontrivial quantum effects in Section 7, we supplement the article with two appendices dealing with (i) additional technical and historical background on quantum optics, and (ii) other aspects of spacetime physics and black holes.

Some remarks on conventions and units are in order. First, in this introductory section, standard general units have been useful to highlight the interplay of scales across physics. By contrast, for the remainder of this article (starting with Sections 2 and 3), we will switch to units with $c = 1$, so that spatial and temporal measurements have the same dimensions, and the relativity formulas are easier to read. Moreover, throughout the paper, the notation $x^\mu = (t, \mathbf{r})$ is being used to denote an arbitrary set of spacetime coordinates adapted to the geometry, with a splitting into temporal and spatial components. Subsequently, in the technical presentations of the geometry of spacetime and conformal quantum mechanics in Section 4, and for quantum thermodynamics in Sections 5 and 6, we will mostly switch to a full-fledged set of natural units, with all of the universal constants c, $\hbar$, k_B, and G equal to one (except where stated otherwise). Finally, for the spacetime geometry, we will use a ‘mostly plus metric’ with signature $(-, +, +, \dots)$, having only one negative sign for time, along with the other metric spacetime conventions of Refs. [38,85].

2. Quantum field theory and quantum optics of atom-field interactions and particle detectors

In this section, we review the quantum behaviour of matter and fields, and their interactions. It is for these interactions that the techniques of quantum optics become most insightful. While the natural setting of quantum optics is usually for systems in the lab in flat spacetime [47,48], the same concepts apply more generally to arbitrary spacetime configurations. Thus, for our current purposes, we will consider the interaction between atoms (representing an atomic cloud) and a quantum field, in a generic gravitational spacetime background. Specific spacetime geometries are described in Section 4 and Appendix 2 for generalised Schwarzschild and Kerr metrics [38], respectively.

In a particular experimental setup, an initial state should be specified. For the HBAR model [55] of acceleration radiation in black hole backgrounds, a thought experiment consists of atoms that are randomly injected, following free-fall paths in the given gravitational background around a black hole, as shown in Figure 2. And the quantum field is set up in a Boulware-like vacuum, which is defined with modes adapted to stationary coordinates [25,86]. The experimental arrangement of Figure 2 corresponds to the

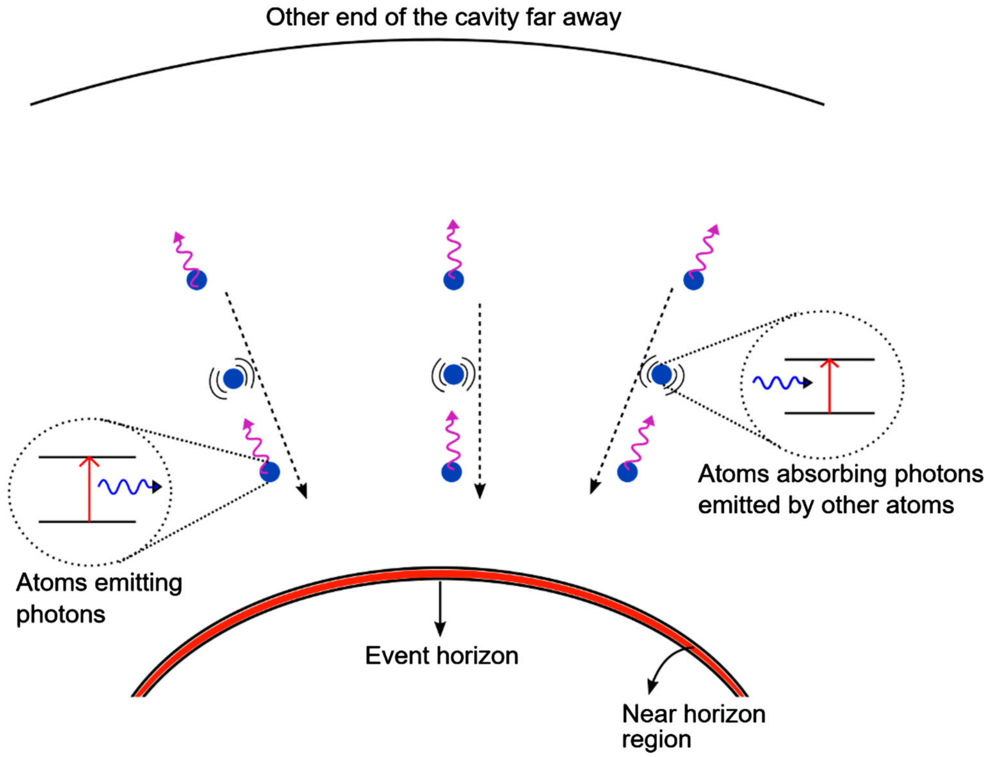

Figure 2. The thought experiment for the HBAR model, where atoms freely fall into a black hole in a Boulware vacuum, simulating an analog quantum-optics system with boundary mirrors. This 'optical cavity model' is only a conceptual device to represent the vacuum setup. The dashed lines show the direction of the free-fall motion of the atoms, which radiate in all directions (but only the outgoing radiation, to be measured far away, is shown for clarity). As the radiation goes up the gravity well, gravitational redshift makes its wavelength increase.

way in which quantum optics experiments with fixed mirrors are used in the laboratory. In that sense, it is an 'optical cavity model' that simulates the Boulware-like vacuum most naturally. Unlike ordinary lab experiments, the presence of a gravitational background has nontrivial effects; for example, the top and bottom of the cavity are accelerating in a general relativistic sense, and the radiation emitted near the black hole's horizon has a wavelength that increases as it travels in the outgoing direction due to the gravitational redshift.

However, cautionary remarks on the cavity model are in order. First, the setup involves an appropriate boundary condition at the event horizon, which can be enforced with a mirror, as displayed in Figure 3.

Now, a physical model of a mirror an infinitesimal distance above the horizon would be probably be unstable under reasonable assumptions of causal sound wave propagation. Second, as a result, the cavity should only be viewed as an auxiliary construction within a thought experiment that simulates a cavityless black hole with a Boulware state. Third, even the Boulware vacuum would not be the physically reasonable assumption if one considered an ordinary black hole formed from the usual processes of gravitational

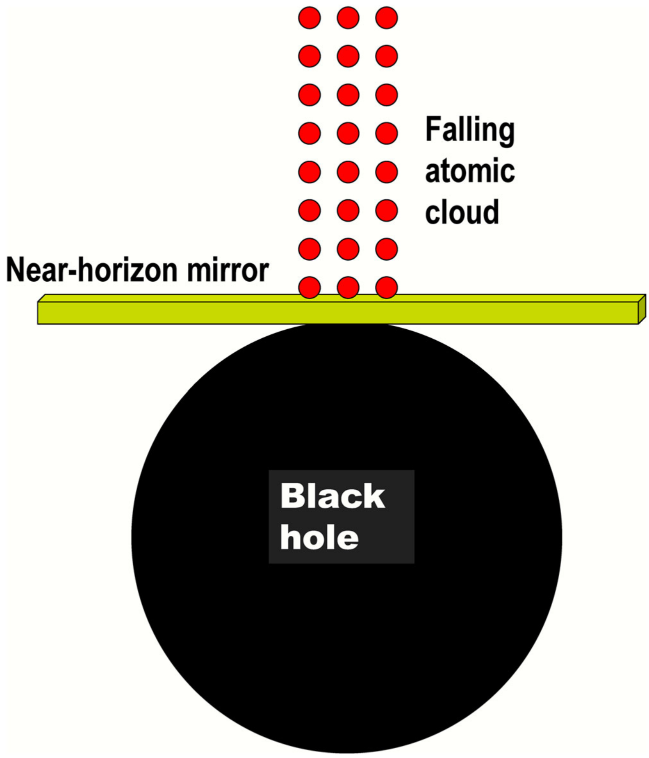

Figure 3. In the thought experiment for the HBAR model, a mirror is an operational quantum-optics type device that enforces a boundary condition to guarantee the presence of a Boulware vacuum.

collapse, as this system would normally end up with an Unruh vacuum instead [87,88]. Despite these limitations, if caution is exercised in its interpretation, the proposed HBAR thought experiment remains a powerful device to probe the interplay between fundamental quantum effects and strong gravitational fields, and provides an alternative probe of black hole thermodynamics.

2.1. Quantum field theory: scalar field in curved spacetime

For the sake of simplicity, a scalar (spin-zero) field Φ provides the essential ingredients of the relevant physics for a variety of fundamental questions. Moreover, the results can be easily generalised to fields with nonzero spin. In fact, quantum optics was originally developed for and is most commonly applied to spin-one electromagnetic fields [47–49] (see Appendix 1), but its methodology generically works in a similar manner for scalar and other fields. In other words, ordinary vector, spin-one photons can be replaced in this model by scalar, spin-zero 'photons'. Likewise, we can consider a simplified treatment with a two-level atom capturing the essential features of atomic electron transitions. When the field is described by a Boulware vacuum, which corresponds to stationary coordinates [25,86], there exits a relative acceleration between the atoms and the field, which is the physical source of the ensuing acceleration radiation [55,81–84].

2.1.1. Field action and quantisation

A real scalar field Φ, with mass μ_Φ, in the geometric background of a spacetime metric $g_{\mu\nu}$, is defined by an action [25,86]

$$S[\Phi] = -\frac{1}{2}\int d^D x \sqrt{-g}\left[g^{\mu\nu}\nabla_\mu\Phi\nabla_\nu\Phi + \mu_\Phi^2\Phi^2 + \xi R\Phi^2\right] \tag{11}$$

(with spacetime dimensions $D \geq 4$), where g is the determinant of the metric and the coupling of Φ to the metric $g_{\mu\nu}$ is via its covariant derivatives $\nabla_\mu\Phi$ and with the curvature scalar R via the nonminimal coupling constant ξ. At the classical level, the action principle $\delta S[\Phi]/\delta\Phi = 0$ gives the Euler-Lagrange equations for the action (11), which govern the dynamics in a spacetime background and take the form of the Klein-Gordon equation

$$\left[\Box - \left(\mu_\Phi^2 + \xi R\right)\right]\Phi \equiv \frac{1}{\sqrt{-g}}\partial_\mu\left(\sqrt{-g}\, g^{\mu\nu}\,\partial_\nu\Phi\right) - (\mu_\Phi^2 + \xi R)\Phi = 0. \tag{12}$$

Here, we will use the spacetime conventions of Refs. [38,85], including units with $c = 1$ [as stated at the end of Sec. (1)]; and the field theory conventions of Refs. [68,89]. Additional details, related to the metric and near-horizon behaviour, are described in Section 4 and Appendix 2.

The quantisation of the theory is established by the usual canonical Hamiltonian rules. The canonical quantisation procedure involves promoting the classical field and its conjugate momentum to quantum operators satisfying the canonical commutation relations similar to the primary commutators of Equation (2). Given the Lagrangian density $\mathcal{L}$ as the integrand of the action integral (11),

$$\mathcal{L} = -\sqrt{-g}\left[g^{\mu\nu}\nabla_\mu\Phi\nabla_\nu\Phi + \mu_\Phi^2\Phi^2 + \xi R\Phi^2\right], \tag{13}$$

the conjugate momentum is

$$\Pi = \frac{\partial\mathcal{L}}{\partial(\nabla_0\Phi)} = -\sqrt{-g}\,\nabla^0\Phi. \tag{14}$$

Upon quantisation, the field $\Phi(t, \mathbf{r})$ and its canonical momentum $\Pi(t, \mathbf{r})$ are operators that satisfy the equal-time canonical commutation relations similar to Equation (2),

$$\begin{gathered}[\Phi(t, \mathbf{r}), \Phi(t, \mathbf{r}')] = 0, \quad [\Pi(t, \mathbf{r}), \Pi(t, \mathbf{r}')] = 0 \\ [\Phi(t, \mathbf{r}), \Pi(t, \mathbf{r}')] = i\hbar\delta^{(D-1)}(\mathbf{r} - \mathbf{r}'),\end{gathered} \tag{15}$$

with a delta-function distribution defined via $\int_\Sigma d^{D-1}x'\, w(\mathbf{r}')\,\delta^{(D-1)}(\mathbf{r} - \mathbf{r}') = w(\mathbf{r})$, for all Schwartz test functions $w(\mathbf{r})$ (density of weight one in the second argument) on the $(D-1)$-dimensional spacelike hypersurface Σ, which is essentially a slice in spacetime usually described as 'space'.

2.1.2. Field modes

Formally, the quantisation is reduced to the problem of finding a complete set of solutions $\{\phi_s(t, \mathbf{r}), \phi_s^*(t, \mathbf{r})\}$ of the classical Equation (12) and expanding the quantum field theory operator Φ as in Equation (6), which reads

$$\Phi(t, \mathbf{r}) = \sum_s [a_s \phi_s(t, \mathbf{r}) + \text{H.c.}], \tag{16}$$

where H.c. is the Hermitian conjugate. The modes are labelled with the subscript $\boldsymbol{s}$, specifying a complete set of quantum numbers and the mode frequency ω. In addition, the modes are assumed to satisfy the orthonormality conditions

$$(\phi_s, \phi_{s'}) = -(\phi_s^*, \phi_{s'}^*) = \delta_{s,s'}, \quad (\phi_s^*, \phi_{s'}) = (\phi_s, \phi_{s'}^*) = 0, \tag{17}$$

where the standard inner product in the given geometry [68,89],

$$(\Phi_1, \Phi_2) = i \int_\Sigma \left(\Phi_1^* \partial_\mu \Phi_2 - \Phi_1 \partial_\mu \Phi_2^*\right) \mathrm{d}\Sigma^\mu, \tag{18}$$

is consistent with the Klein-Gordon equation. In Equation (18), the integral is performed on a $(D-1)$-dimensional spacelike hypersurface Σ, with 'volume' element $d\Sigma^\mu = n^\mu \sqrt{\gamma}\, d^{D-1}x$ is along the normal, future-directed 'time direction' n^μ (with a corresponding induced metric γ_{ij}). This product is independent of the chosen hypersurface Σ, thus it is applicable to any spatial slice, as follows from Gauss's divergence theorem. For example, in flat (Minkowski) spacetime, the inner product is simply: $(\Phi_1, \Phi_2) = i \int (\Phi_1^* \partial_t \Phi_2 - \Phi_1 \partial_t \Phi_2^*) d^{D-1}x$ integrated over ordinary space.

In the quantisation of the theory, for the interpretation of particle excitations of the field, the functions $\{\phi_s(t, \mathbf{r}), \phi_s^*(t, \mathbf{r})\}$ are identified as positive/negative frequency modes. This classification is naturally suggested by the form it takes in the simplest geometry: flat (Minkowski) spacetime, where the condition $\partial_t \phi_s = -i\omega\phi_s$ (with $\omega > 0$) gives the familiar time dependence $e^{-i\omega t}$, with a frequency ω such that $\hbar\omega$ is the positive energy of the corresponding quantum particle excitation. This relation can be generalised to spacetimes that have time-translation symmetry, so that a timelike vector field $\boldsymbol{\xi}$ akin to ∂_t is available, where the positive frequency can be similarly identified with the energy. Such a generalisation involves a Killing vector field [38,85,90], which is an infinitesimal generator of a symmetry of the metric, so that the distances between points on the manifold are invariant along the Killing-field direction; see Section 4. In such spacetimes, the positive frequency modes ϕ_s can be identified in a coordinate-independent manner by the equation

$$\xi^\mu \partial_\mu \phi_s = -i\omega\phi_s \tag{19}$$

($\omega > 0$), where the left-hand side is an example of a Lie derivative [38,85,90] along the flow of the Killing vector field $\boldsymbol{\xi}$. Moreover, the condition $\xi^\mu \partial_\mu t = 1$ formally defines the Killing time as the preferred time associated with the symmetry. The corresponding conjugate modes ϕ_s^* satisfy the negative-frequency geometric condition

$$\xi^\mu \partial_\mu \phi_s^* = i\omega\phi_s^*, \tag{20}$$

confirming the frequency-sign classification. Operationally, the particle interpretation can be probed considering a detector following orbits of the Killing vector field; then, the Killing time and the proper time τ are proportional, so that the positive and negative frequencies correspond to what the detector actually registers, with $\partial_\tau \phi_s = -i\omega\phi_s$, and the modes can be used to compute the number of particles.

2.1.3. Fock space and Hamiltonian

The field canonical commutators (15) are equivalent to a set of the commutation relations for the annihilation/creation operators. These are the canonical commutator relations of the field-operator algebra (7), i.e. $[a_s, a^\dagger_{s'}] = \delta_{s,s'}$, $[a_s, a_{s'}] = 0$, and $[a^\dagger_s, a^\dagger_{s'}] = 0$. The proof of this statement involves a straightforward substitution of the field expansion (16) in Equation (15), along with the use of the Klein-Gordon inner product (18). These operator-algebra commutators have the same form as for a simple one-dimensional problem in quantum mechanics, with the interpretation that Equation (16) represents an expansion in a set of quantum harmonic oscillators corresponding to all the modes with configuration labels $\boldsymbol{s}$. Once this is established, with the annihilation/creation canonical commutators, one can build the states of the quantum theory as follows. The lowest energy state, known as the vacuum $|0\rangle$, is defined by the set of annihilation conditions

$$a_s|0\rangle = 0, \quad \text{for all } \boldsymbol{s}. \tag{21}$$

The vacuum state can then be used to generate all other states by repeated action with the creation operators. Thus, starting with a single mode labelled by $\boldsymbol{s}$,

$$|n_s\rangle = \frac{1}{\sqrt{n_s!}} \left(a^\dagger_s\right)^{n_s} |0\rangle \tag{22}$$

gives a state with n_s excitations or 'photons'. From the commutator relations, this excitation number or 'occupation number' is the eigenvalue of the number operator $N_s = a^\dagger_s a_s$. Repeating the procedure for all modes, a basis for the states of the quantum-field system can be established with the tensor products of single-particle Hilbert spaces, displaying all excitation numbers in the form

$$\left| n_{s_1}, n_{s_2} \ldots n_{s_j} \ldots \right\rangle = \left| n_{s_1} \right\rangle \otimes \left| n_{s_2} \right\rangle \otimes \ldots \otimes \left| n_{s_j} \right\rangle \ldots . \tag{23}$$

This is often called the occupation number representation and the general framework is the so-called 'second quantisation'. An alternative shorthand notation for the occupation number representation, which we use and extend in Section 3.4 is $\{n\} \equiv \{n_1, n_2, \ldots, n_j, \ldots\}$, where n refers to the collection of excitation numbers. Finally, with this basis, and considering all possible states with different numbers of excitations for all modes, this procedure amounts to the construction of the Fock space of states as the direct sum of tensor products of single-particle Hilbert spaces [6]. A simple example of this construction is given in Appendix 1 for a spin-one electromagnetic field in Minkowski spacetime. In conclusion, Fock space and the occupation number representation provide the framework to describe quantum states with a variable number of particles, thus forming the foundation for quantum field theory and many-body physics [91]. These powerful tools were also developed in Dirac's 1927 seminal paper [24], and were subsequently extended by Jordan and Wigner [92], and Fock [93].

In order to describe the dynamics, the Hamiltonian density

$$\mathcal{H} = \Pi\,\nabla_0\Phi - \mathcal{L} \tag{24}$$

is needed, leading to a field Hamiltonian $H = \int d^D x\,\mathcal{H}$. For the free scalar field Lagrangian (13), this gives $\mathcal{H} = \frac{1}{2}(-\nabla^0\Phi\nabla_0\Phi + \nabla^j\Phi\nabla_j\Phi + \mu_\Phi^2\Phi^2 + \xi R\Phi^2)$, where the index j (with implicit summation of derivatives) refers to the spatial coordinates; and this can be restated as a generic Hamiltonian quadratic in the canonical variables. Any such Hamiltonian has the following mode decomposition, which can be derived using the field expansion (16), the orthonormality relations (17), and the classical Equation (12) for the modes:

$$H_{\text{field}} = \sum_s \hbar\omega_s\left(a_s^\dagger a_s + a_s a_s^\dagger\right) = \sum_s \hbar\omega_s(a_s^\dagger a_s + \frac{1}{2}), \tag{25a}$$

$$H_{\text{field}} \approx \hbar\omega_s\, a_s^\dagger a_s, \tag{25b}$$

where the notation H_{field} will be used to distinguish this physical system from the other parts of the Hamiltonian of an interacting system of fields and atoms. In its final form, the field Hamiltonian (25) is identical to the sum of mode-specific quantum harmonic oscillator Hamiltonians. Here, the symbol ω_s is used redundantly for the sake of clarity (as, in the notation used here, ω is part of the mode label $\boldsymbol{s}$). For computational convenience, the expression (25b) is written with the $\approx$ symbol to implement the subtraction of the zero-point energy, i.e. the energy of quantum fluctuations in the vacuum, which has no direct impact on the relevant physics, excluding questions of gravitational interactions via a cosmological constant [5], or for the Casimir effect in systems with finite boundaries [64,65,70]. This is the expression to be used in practical calculations for the great majority of experimental realisations. Additional details on the physics of quantum fields, when the system is modelled by the usual spin-one electromagnetic fields, are discussed in Appendix 1.

2.1.4. Subtleties of quantum field theory in curved spacetime

Finally, it should be highlighted that the equations outlined in this section are applicable to any state of the quantum field. However, the interpretation of mode functions and the associated definition of 'positive frequency' modes encounter significant challenges in curved spacetime, due to the absence of global time-translation invariance [25]. Unlike flat spacetime, where the Poincaré group provides a unique vacuum state, general curved spacetimes lack such a preferred definition. Thus, as the definition of vacuum and the number of particle excitations relies on a chosen set of mode functions with a specific positive-frequency characterisation, this means that the different different choices of time slicing can lead to different, observer-dependent results. Nonetheless, there is a well-defined procedure for comparison of particle measurements among observers: Bogoliubov transformations [25,38,68]. In this framework, two different sets of modes, $\{f_s(x), f_s^*(x)\}$ and $\{g_s(x), g_s^*(x)\}$, with their corresponding operator algebras $\{a_s, a_s^\dagger\}$ and $\{b_s, b_s^\dagger\}$ respectively, are linearly related by

$$g_s = \sum_{s'}\left(\alpha_{ss'}f_{s'} + \beta_{ss'}f_{s'}^*\right), \tag{26}$$

as follows by their linear completeness. Then, Equation (27) can be used to fully predict all well-posed questions on particle excitations. This can be done by establishing the whole network of linear relations: (i) the inverse of the transformation (27); (ii) the Bogoliubov coefficients in terms of inner-product projections: $\alpha_{ss'} = (f_{s'}, g_s)$ and $\beta_{ss'} = -(f^*_{s'}, g_s)$; and (iii) f the corresponding operator-algebra relations: $b_s = \sum_{s'} (\alpha^*_{ss'} a_{s'} - \beta^*_{ss'} a^\dagger_{s'})$ and their inverses. For example, the excitation number of g-mode particles is the expectation value of the number operator $N_{(g),s} = b^\dagger_s b_s$; now, if this is computed for the vacuum state $|0_f\rangle$ of the other f-mode set, then straightforward algebra yields

$$\langle 0_f | N_{(g),s} | 0_f \rangle = \sum_{s'} |\beta_{ss'}|^2. \tag{27}$$

Thus, an empty vacuum in one set of modes appears populated with $\langle 0_f | N_{(g),s} | 0_f \rangle \neq 0$ particle excitations in another set when at least some of the $\beta_{ss'}$ coefficients are nonzero, i.e, $\beta_{ss'}$ measures the non-overlap between the two sets of positive-frequency modes, yielding an observable nontrivial mismatch. These properties highlight the observer-dependent nature of the vacuum and particle concepts in curved spacetime. Extraordinary predictions from this framework include the Unruh and Hawking effects, and other phenomena [25].

For our purposes, in the HBAR setup, we will use modes adapted to stationary coordinates in a black hole geometry, thus defining a Boulware vacuum [25,86].

2.2. Particle-field interactions: atom Hamiltonian, field coupling, and allowed transitions

In the previous section, we discussed the formulation of quantum field theory in generic spacetime backgrounds, centred on the details of the quantisation of a scalar field. Aside from some subtle technical issues, such framework is straightforward. By contrast, the physics of atoms and their interactions with the field can be considerably more complex. Thus, we will consider a simplified framework for the atom-field interactions.

2.2.1. Generalised quantum Rabi model

In our analysis of the HBAR problem, we will treat the atom-field interactions by using a simplified model of the atom as a two-level system. This model does capture the essence of the relevant physics and is of widespread use in quantum optics and quantum information science.

As a two-state system, the relevant model is a generalisation of the quantum Rabi model (QRM), whose semiclassical version was established by Rabi in the seminal Refs. [94,95], and further extended with a coupling of the atom to a single quantised electromagnetic or bosonic field mode in the 1960s [96]. A particular case of the quantum Rabi model is the celebrated Jaynes-Cummings model (JCM) [96], which can be solved analytically in a closed form. (For details on the quantum optics related to these models, see Refs. [47,48]; also, Refs. [97–99] for extensive reviews and discussions of the JCM and applications; and Ref. [100] for a recent review of the more general QRM.) The standard QRM, which is of widespread use in quantum optics, condensed matter physics, quantum information science, and other fields, consists of: (i) a two-level atom described by the Hamiltonian $H_{\rm at}$ as a two-state system; (ii) a field mode of the form $\hbar\omega_0 a^\dagger a$ [cf. $H_{\rm int}$ in Equation (25b)]; (iii) an interaction $H_{\rm int}$ as a linear monopole or dipole coupling of the two-level atom with the bosonic field. Despite its apparent simplicity, it continues to be an active area of theoretical and applied research. In fact, a completely general solution of the QRM has eluded researchers for decades, but it is now regarded as a quasi-exactly-solvable model [100], following a series of partial solutions found in the past decade [101–105]. However, this solution is complex, and most of the applications rely on numerical approximations [106–110] and approximate analytical solutions [111–113]. In addition to the well-known quantum optics applications [47], this model also appears in similar formats in a variety of problems: the Holstein model for the electron-phonon interaction in crystal lattice [114], in superconducting qubits [115–118], in quantum dots [119], and in coupled nanomechanical oscillators oscillators [120], and other more recent applications [100], including growing interest within quantum information science and circuit QED [121]. For the problems under the discussion in this article, and for similar studies of atom-field interactions in nontrivial spacetime configurations, a multimode form of the QRM is used, adapted to a specific spacetime background with field modes that solve the classical Equation (12), as in Section 2.1. The two-level atom of the QRM and its generalisations has an energy spectrum with a ground state and an excited state: $|b\rangle \equiv |E_-\rangle$ and $|a\rangle \equiv \left|E_+\right\rangle$ respectively. These are orthonormal energy eigenstates $\left|E_\mp\right\rangle$, with

$$E_a \equiv E_+ > E_b \equiv E_-, \quad E_+ - E_- = \hbar\nu, \quad E_+ + E_- = 2\overline{E}, \tag{28}$$

such that $\left\langle E_\pm \middle| E_\pm \right\rangle = 1$ and $\left\langle E_\pm \middle| E_\mp \right\rangle = 0$. Then, the atom Hamiltonian is given by

$$H_{\rm at} = E_b|b\rangle\langle b| + E_a|a\rangle\langle a| = \overline{E}\,\mathbb{1}_2 + \frac{1}{2}\hbar\nu\sigma_z, \tag{29}$$

where $\sigma_z = \mathrm{diag}(1, -1)$ is the diagonal Pauli matrix operator of a two-state system; and the first term proportional to the identity matrix $\mathbb{1}_2$ (with the average energy $\overline{E}$) can be dropped by choosing the energy reference level. Then, the total Hamiltonian of the field-atom system is

$$H = H_{\rm at} + H_{\rm field} + H_{\rm int}, \tag{30}$$

where the field Hamiltonian of the full-fledged quantum field version takes the form of Equation (25b). Correspondingly, for the atom-field interaction $H_{\rm int} \equiv V_{\rm int}$, as shown in Appendix 1, this is the monopole analog of a dipole coupling for a spin-one photon field. The scale of this simplified model can be adjusted by considering a coupling $g = \mu E/\hbar$, where μ is the atomic dipole moment and E is the electric field. With a given coupling strength g, which we will assume to be weak, this interaction yields the Hamiltonian $H_{\rm int} \equiv V_I$ given by

$$H_{\rm int} = g\,\Phi(\boldsymbol{r}(\tau), t(\tau))\,\sigma(\tau), \tag{31}$$

where σ is the atomic-state transition operator defined below, and both the field operator Φ and σ are evaluated at the proper time τ of the atom. The atomic state transitions are described by the evolving linear-combination operators

$$\sigma(\tau) = \sigma_- e^{-i\nu\tau} + \sigma_+ e^{i\nu\tau} = \sigma_- e^{-i\nu\tau} + \mathrm{H.c.}, \tag{32}$$

where H.c. is the Hermitian conjugate and $\sigma_{\mp}$ are the atomic lowering and raising operators

$$\sigma_{-} \equiv \sigma_{ba} = |b\rangle\langle a|, \quad \sigma_{+} \equiv \sigma_{ab} = |a\rangle\langle b| \tag{33}$$

(as lowering/raising Pauli matrices); notice that these can be defined via $\sigma(0)\left|E_{\pm}\right\rangle = \left|E_{\mp}\right\rangle$.

2.2.2. Perturbation theory and the interaction picture

The expressions above for the Hamiltonian (31) are written in the interaction picture, where the operators acquire an extra time dependence from the free Hamiltonians of the field and atom. More generally, in the interaction picture, of widespread use for perturbative calculations in quantum field theory, the action and the Hamiltonian are separated into a free part ('unperturbed') associated with the free fields and a part associated with the interactions (both self-interactions or interactions among the different fields). As a result, this picture involves: (i) operators evolving in time according to the Heisenberg Equation (3) associated with only the free part of the Hamiltonian; and (ii) states evolving in time according to Equation (1) associated with the interaction terms. In this hybrid interaction-picture form, the expressions in Equation (33) are ideally suited for standard quantum field theory calculations. Instead, in atomic physics, quantum optics, condensed matter physics, quantum information science and other fields, the QRM interaction Hamiltonian is written in the Schrödinger picture, without the time dependence and for a single mode, i.e. as $H_{\text{int}} = g(a + a^{\dagger})(\sigma_{-} + \sigma_{+})$, with the Hamiltonian being $H = \frac{1}{2}\hbar\nu\sigma_z + \hbar\omega_0 a^{\dagger}a + 2g(a + a^{\dagger})\sigma_x$. For our applications, we will use the Hamiltonian expressions (25b) and (29)–(33) as the anticipated multimode generalisation of the QRM. Moreover, the product $\hat{m} = g\sigma$ acts as a monopole operator implementing the coupling with the field Φ, and can also be used as the basis for a model detector.

With the expansions (6) and (32) of the field and atomic operators, the interaction Hamiltonian (31) in the interaction picture takes the explicit form

$$\begin{aligned} V_I &\equiv H_{\text{int, I}} \\ &= \sum_s g_s\left[a_s\sigma_{+}e^{-i(\omega_s t-\nu\tau)} + a_s^{\dagger}\ \sigma_{-}e^{i(\omega_s t-\nu\tau)} + a_s^{\dagger}\sigma_{+}e^{i(\omega_s t+\nu\tau)} + a_s\sigma_{-}e^{-i(\omega_s t+\nu\tau)}\right], \end{aligned} \tag{34}$$

in the notation we will use in subsequent sections. (Here, the symbol I stands for interaction picture.) Incidentally, the products of field and atomic transition operators in Equations (31) and (34) denote tensor products of factors in separate spaces (e.g. the term $a_s\sigma_{+}$ stands for $a_s \otimes \sigma_{+}$ affecting two distinct systems).

2.2.3. Interpretation of the interaction terms

For each frequency, Equation (34) involves four terms, with each one representing a particular photon creation/annihilation process with atomic excitation/de-excitation, as shown in Figure 4.

The interaction terms in Equation (34) are usually classified in two pairs: (i) rotating terms, labelled I and II in Figure 4; and (ii) counter-rotating terms, labelled III and IV. The rotating terms are $a_s\sigma_{+}$, where the field loses a photon with atom excitation, and $a_s^{\dagger}\sigma_{-}$, where the field gains a photon with atom de-excitation. By contrast, the

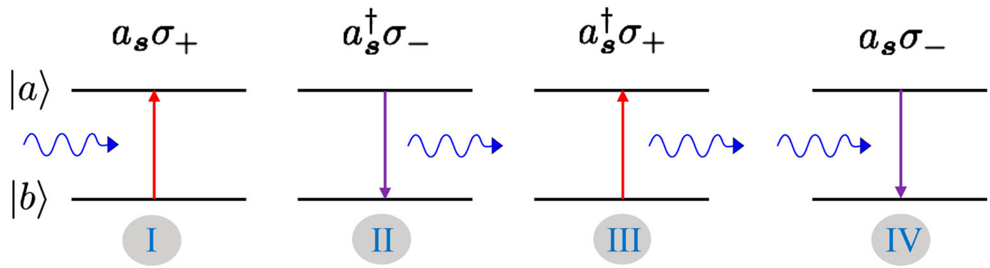

Figure 4. Schematics of the emission and absorption processes corresponding to the four terms in the interaction Hamiltonian of Equation (34). Here, $\sigma_\pm$ are the atomic raising and lowering operators defined in Equation (33). The specific couplings of I and II give the rotating terms, while those of III and IV give the counter-rotating terms. The latter can be neglected as the rotating-wave approximation (RWA) under a broad range of ordinary lab conditions (near resonance and in the weak-coupling regime), but they are critically important in relativistic setups with accelerated particles and/or horizons.

counter-rotating terms are $a_s^\dagger\sigma_+$, where the field gains a photon with atom excitation, and $a_s\sigma_-$, where the field loses a photon with atom de-excitation. The rotating interaction terms are so called because of their oscillatory phases with respect to time, whereas the faster time oscillations of the counter-rotating terms tend to have them suppressed near resonance. Thus, the rotating terms are considered the dominant building blocks for the resonant energy exchange with weak coupling between the atom and the field; as such, they are the ones that appear in the Jaynes-Cummings model – this selective use of terms is called the rotating-wave approximation (RWA) [47,48]. In that context, the counter-rotating terms are usually considered virtual processes, but this only means that their effects less are significant in specific regimes under ordinary lab conditions. However, in the strong coupling regime and far from resonance, the counter-rotating terms do become important and the full-fledged QRM is mandatory. The remarks made about the interaction terms so far apply to the usual discussions of the physics of inertial observers in flat spacetime. However, in the presence of acceleration or nontrivial spacetime backgrounds, there is no physical rationale to consider regimes where processes III and IV would be neglected, and they do become instrumental in nontrivial effects associated with radiation acceleration. This is often described intuitively as virtual processes turning to real ones under special conditions, e.g. with accelerated particles. We will see how this is physically realised for acceleration radiation, starting in Section 2.4.

2.3. Particle detectors in quantum field theory

The use of simple models to describe photon detectors has a long tradition in quantum optics [122]. More generally, a particle detector is a controllable quantum system locally coupled to quantum fields. In this generalised sense, detector models can be used as probes for a large variety of effects in the presence of a nontrivial spacetime structure, including various relativistic quantum information properties. Thus, they have become standard tools in modern quantum field theory. The first type of such models, by Unruh [44], involves a small-box detector with a particle transitioning from the ground state to an excited state. DeWitt [123] introduced the point-source two-level detector, commonly known as the Unruh-DeWitt (UDW) detector in the literature [68]. The UDW detector is based on the point-like two-level atom discussed in the previous section, with monopole coupling (31); essentially, it couples a qubit to a quantum field via a monopole interaction. Specifically, in this form, the UDW detector was originally conceived as a basic probe of the thermal nature of the vacuum in accelerated frames, where it can be used to identify a mixed, thermal state [124] at the Unruh temperature (10). Additional varieties of this concept have been extensively studied in the literature; for example, particle detectors with finite spatial extent [125], and more recently, harmonic-oscillator detectors [126–128], which are ideally suited for nonperturbative calculations. The study and applications of particle detectors is an ongoing area of research, where quantum correlations can be studied in detail [129,130].

For an UDW monopole detector, the detector-field interaction is described by the Hamiltonian of Equations (31) and (34). As discussed in Section 2.2, the terms in Equation (34), which are depicted in Figure 4, correspond to the four combinations of photon absorption/emission and atomic excitation/deexcitation allowed by the physics. Ordinarily, only the terms I and II are consistent with conservation of energy, but the virtual processes III and IV can be realised in nontrivial spacetime configurations with acceleration and/or gravitational fields. For the current purposes, the initial state of the detector-field system is a tensor product state $|0_M, b\rangle \equiv |0_M\rangle \otimes |b\rangle$, where $|b\rangle$ is the ground state of the detector. Thus, when the detector clicks ('detects a particle'), this signifies its transition to the excited state $|a\rangle$ via the interaction (31) with the field; and the field goes to an excited state $|\psi\rangle$.

2.4. Particle-field interactions: transition probabilities of HBAR radiation

The horizon-brightened acceleration radiation (HBAR) discussed in this paper is one of the most interesting applications of the conversion of virtual into real processes via the counter-rotating terms in Equation (34) and Figure 4. In HBAR radiation [55,81–84], a black hole provides a nontrivial spacetime background, where one can consider a field Φ prepared with a configuration corresponding to stationary coordinates, in what is known as a Boulware-like state. One simple operational approach to set up this configuration is the introduction of mirrors at specific boundaries, with one boundary right outside the event horizon – see Appendix 2. This setup amounts to a thought experiment involving an atom or atoms interacting with a field, as in Sections 2.2 and 2.3. In essence, this is *a scaled-up version of an optical cavity in a lab, but with the ability to probe near-horizon black hole behaviour*. See the qualifying remarks on the 'optical cavity model' in the introductory part of Section 2.

The atoms are initially in their ground state $|b\rangle$: each one acts as an UDW detector, but collectively they produce a radiation field. The calculations outlined below refer to this radiation field. The basic description of the field Φ follows the theory reviewed in Section 2.1, with the field states labelled by their occupation numbers $n_{\boldsymbol{s}}$. In particular, the state with no scalar photons is the vacuum or ground state $|0\rangle$, such that $a_{\boldsymbol{s}}|0\rangle = 0$ for all modes $\boldsymbol{s}$; and the state $|1_{\boldsymbol{s}}\rangle$ has only one photon in mode $\boldsymbol{s}$. Then, the coupling (32) allows for: (i) the emission of a scalar photon with the simultaneous transition of the atom to its excited state $|a\rangle$; and (ii) the absorption of a scalar photon with the atom also transitioning to its excited state $|a\rangle$. These correspond to the counter-rotating term III and the rotating term I, respectively, as illustrated in Figure 4. For the term III, the field is in the vacuum configuration, and the first-order perturbation probability amplitude is $-(i/\hbar)\, I_{\mathrm{e},\mathbf{s}}$, where $I_{\mathrm{e},\mathbf{s}} = \int \mathrm{d}\tau\, \langle 1_{\mathbf{s}}, a|V_I(\tau)|0, b\rangle$. Similarly, for the term I, the field is in the one-photon mode configuration $|1_{\mathbf{s}}\rangle$, with the absorption probability amplitude being $-(i/\hbar)\, I_{\mathrm{a},\mathbf{s}}$, where $I_{\mathrm{a},\mathbf{s}} = \int \mathrm{d}\tau\, \langle 0, a|V_I(\tau)|1_{\mathbf{s}}, b\rangle$.

Therefore, up to first order in perturbation theory, and using the operators (33), the emission probability $P_{\mathrm{e},\mathbf{s}}$ for the field mode $\mathbf{s}$, is given by

$$P_{\mathrm{e},\mathbf{s}} = \left| \int \mathrm{d}\tau \langle 1_{\mathbf{s}}, a|V_I(\tau)|0, b\rangle \right|^2 = g^2 \left| \int \mathrm{d}\tau\, \phi^*_{\mathbf{s}}(\mathbf{r}(\tau), t(\tau))\, e^{i\nu\tau} \right|^2; \tag{35}$$

and the absorption probability is

$$P_{\mathrm{a},\mathbf{s}} = \left| \int \mathrm{d}\tau \langle 0, a|V_I(\tau)|1_{\mathbf{s}}, b\rangle \right|^2 = g^2 \left| \int \mathrm{d}\tau \phi_{\mathbf{s}}(\mathbf{r}(\tau), t(\tau))\, e^{i\nu\tau} \right|^2. \tag{36}$$

The expressions in Equations (35) and (36) are critical in finding the field configuration generated by the falling atomic cloud in the HBAR thought experiment. With the reasonable assumption that the coupling is weak, they are dominant first-order approximations; as such, this involves no serious physical restrictions. Otherwise, the spacetime background can be completely general. But, as we will see below, a near-horizon black hole background leads to a universal outcome for HBAR radiation. In order to assess this effect, we have to specify the spacetime configuration and evaluate the probabilities (35) and (36) for the corresponding field modes and spacetime geodesic worldlines (with proper time τ). As we will see in the next section, the field density matrix will characterise the thermal properties of the radiation leading to HBAR thermodynamics.

3. Quantum states and density matrix: from open quantum systems and quantum optics to HBAR radiation

The standard description of the time evolution of physical states in quantum dynamics, in the form of the Schrödinger Equation (1) only applies to isolated systems described by a pure quantum state $|\Psi\rangle$. In that case, the unitary time evolution operator $\hat{U}(t, t_0) = T \exp\left[-(i/\hbar)\int_{t_0}^{t} \mathrm{d}t' \hat{H}(t')\right]$ (where T is the time-ordering operator giving the Dyson series [5,131]), governs the fundamental dynamics of the state $|\Psi(t)\rangle$ at a any given time t through the Hamiltonian, in such a way that $|\Psi(t)\rangle = \hat{U}(t, t_0)|\Psi(t_0)\rangle$.

However, a more general treatment is needed for any system that is not closed, but interacting with an environment, or part of a larger system to which it may entangled. In their most general form, this defines the larger class of *open quantum systems* [132], whose description requires a density matrix (density operator).

We briefly outline next the definition and main concepts associated with the density matrix, and summarise the particular form of this operator that has been developed for the theory of lasers in quantum optics. We further consider analog systems, including HBAR radiation and its reduced density matrix.

3.1. Density matrix in quantum physics: basic definitions and properties

The necessity to extend the standard pure-state approach based on the Schrödinger Equation (1) became apparent as soon as formal quantum mechanics was born. In 1927, the density matrix – also called density operator – was introduced as a more general characterisation of a physical state in quantum physics and its associated dynamic evolution. This is a remarkable extension, due to von Neumann [19] and Landau [21], that brings to completion the quantum dynamics programme of Equations (1) and (3). Over the following decades, this approach has been gradually applied to a variety of problems in fundamental quantum physics and statistical mechanics.

One of the earliest findings was the realisation that the density matrix is needed even in simple cases where one looks at subsystems of larger system [21]. This concept has developed into a central tool in the description of quantum entanglement and quantum information more generally [22]. In addition, attempts to understand the role played by the environment in quantum systems have stressed the need to use states consisting of statistical mixtures. This has led to a systematic development of the theory of open quantum systems as a more recent quantum development that requires a density matrix as a conceptually distinct description of their states [132].

3.1.1. Probabilistic definition of the density matrix

The quantum dynamics programme of the Schrödinger and Heisenberg pictures, implemented via Equations (1) and (3), involves *pure states*. These are states described by normalised vectors in Hilbert space, which can be prepared when one has maximal amount of information about the given physical system. A natural extension is to consider states about which only partial information is available. These *mixed states* can be described as statistical mixtures of pure states properly weighted with a probability distribution associated with an incomplete knowledge of the system. Such extensions encompass the types of states used in statistical-mechanical and thermodynamic treatments of systems, and in physical situations where subsystems need to be analysed independently from the environment or in the presence of quantum entanglement: see the examples discussed below.

With these ideas in mind, the density matrix can be defined as the mathematical description of a general quantum state that exists as *a statistical mixture of an ensemble of normalised pure states* $\{|\psi_i\rangle\}$. If this general state has a probability p_i of being state $|\psi_i\rangle$, the general definition of the density matrix is [5,132],

$$\rho = \sum_i p_i |\psi_i\rangle\langle\psi_i| \tag{37}$$

where the real nonnegative probabilities p_i (i.e. $0 \leq p_i \leq 1$) are subject to the normalisation condition

$$\sum_i p_i = 1. \tag{38}$$

Several qualifying remarks are in order regarding this definition.

- First, the states $\{|\psi_i\rangle\}$ are normalised but otherwise arbitrary: they do not need to be orthogonal.
- Second, a pure state $|\psi\rangle$ can be represented by only one term in the sum (37), as a projection operator $|\psi\rangle\langle\psi|$.
- Third, the definition of the density matrix (37), with Equation (38), is a convex weighted sum of the projection operators of the constituent pure states $\{|\psi_i\rangle\}$.
- Fourth, the decomposition of a mixed state into a mixture of pure states of the form (37) is not unique.

The general definition of a quantum state (37) gives a rigorous representation of the two types of probabilities that can enter in quantum mechanical systems:

(i) the intrinsic probabilistic nature of the quantum state vectors (quantum uncertainty);
(ii) the incomplete nature of the information about the initial state of the system, as described by the weighted sum (37).

3.1.2. Properties and operator definition of the density matrix

The explicit probabilistic definition of a general quantum state via Equation (37) can be replaced by an equivalent operator statement that defines the density matrix ρ as a self-adjoint positive semidefinite operator of trace one [5,132]. Specifically, the density operator ρ is characterised by the following three properties.

(1) Self-adjointness: $\rho = \rho^\dagger$.
(2) Positive semi-definiteness: all of the eigenvalues of ρ are non-negative (≥ 0).
[This is required by the probabilities p_i in Equation (37) being nonnegative.]
(3) $\mathrm{Tr}(\rho) = 1$.
[This trace normalisation is equivalent to the probability normalisation condition (38).]

Moreover, the eigenvalues and corresponding operator trace of ρ can be used to characterise the nature of the quantum state, as follows.

- *Pure State*. A quantum pure is a state with no classical uncertainty. This amounts to all the eigenvalues being zero, except for a single eigenvalue equal to unity. It is characterised by the idempotent condition $\rho = \rho^2$. As an operator trace relation, this is equivalent to a purity $\mathrm{Tr}(\rho^2) = 1$.
- *Mixed State*. A proper quantum mixed state is a state that is not pure. As such, it is represented by a nontrivial statistical ensemble, as in Equation (37) with more than one nonzero probability. This implies it has multiple nonzero eigenvalues. As an operator trace relation, this is equivalent to a purity $0 < \mathrm{Tr}(\rho^2) < 1$.

As a result, the operator trace gives an invariant definition of probabilistic statements, including:

- the primary definition of expectation value of an operator A as $\langle A\rangle_\rho = \mathrm{Tr}(\rho A)$;

- the density matrix of subsystems of larger system in terms of partial traces: see Equation (43) in Section 3.2.

In addition, the time evolution is given by the von Neumann equation, as shown in Section 3.2.

3.1.3. Density matrix: examples

- *System in thermodynamic equilibrium with a thermal reservoir.*
  A familiar example of a mixed state is that of a system in thermal equilibrium. This is critical for our discussion of the remainder of this review article.
  In what is called the canonical ensemble, a system exchanges energy with an environment or heat bath at temperature T; thus, it is not in a pure state. We can then write the mixed state in the form of Equation (37), in terms of the eigenstates $|n\rangle$ of the system Hamiltonian H^S, i.e. $\rho = \sum_n p_n |n\rangle\langle n|$, with normalised probabilities
  $$p_n = Z^{-1} e^{-\beta E_n}, \quad \text{where } \beta = 1/(k_B T) \tag{39}$$
  is the inverse temperature parameter, $Z \equiv Z(\beta) = \sum_n e^{-\beta E_n} = \mathrm{Tr}(e^{-\beta H^S})$, and E_n is the energy of the state $|n\rangle$. Then, thermal-equilibrium density matrix given by
  $$\rho = Z^{-1} e^{-\beta H^S}. \tag{40}$$
  It should be noted that the operator H^S is associated with the given system S (and not with the combined system Hamiltonian that includes the environment).
- *Spin 1/2 examples.*
  Spin 1/2 systems provide simple examples of density matrices, with beams of particles having different polarisations. In the examples below, with a slight abuse of notation, we use both the Dirac notation and matrix representations; for the latter, the usual standard Pauli-matrix representation is used [5].

  (i) A completely polarised beam with a given orientation of spin. For example, the z component of spin: $S_z = -\hbar/2$ gives
  $$\rho = |+\rangle\langle+| = \begin{pmatrix} 0 & 0 \\ 0 & 1 \end{pmatrix}.$$
  And the x component of spin: $S_x = \pm\hbar/2$ gives
  $$\rho = |\pm\rangle_x\langle\pm|_x = \frac{1}{2}\begin{pmatrix} 1 & \pm 1 \\ \pm 1 & 1 \end{pmatrix},$$
  as $|\pm\rangle_x = (1/\sqrt{2})(|+\rangle \pm |-\rangle)$ For both examples, as these are pure states, the density matrices satisfy $\rho = \rho^2$ and $\mathrm{Tr}(\rho^2) = 1$.

  (ii) An unpolarised beam, which is maximally mixed, i.e. an incoherent mixture or statistical ensemble with the same proportions of spin up and spin down; thus, $p_+ = p_- = 1/2$ in the definition of Equation (37)]:
  $$\rho = \frac{1}{2}(|+\rangle\langle+|) + \frac{1}{2}(|-\rangle\langle-|) = \frac{1}{2}\begin{pmatrix} 1 & 0 \\ 0 & 1 \end{pmatrix} = \frac{1}{2}\mathbb{1}_2.$$

As this is a mixed state, $\rho \neq \rho^2 = (1/4)\mathbb{1}_2$ and Tr $(\rho^2) = 1/2 < 1$. This is the purity characterisation of a maximally mixed state. And as the state is completely unpolarised, all spin components have zero expectation values: $\langle S_j \rangle = \mathrm{Tr}(\rho S_j) = 0$ (with $j = x, y, z$), as $\rho \propto \mathbb{1}_2$ and the spin-matrix traces are zero. Moreover, ρ can be trivially rewritten as the incoherent sum (with equal weights) in terms of spin plus and minus for arbitrary orientations of the quantisation axis.

(iii) Finally, partially polarised beams representing arbitrary mixed states can represented as $\rho = p_1\rho_1 + p_2\rho_2$, as in Equation (37), with $p_1 + p_2 = 1$ and ρ_j (with $j =$ 1, 2) being a generic density matrix of a pure state with arbitrary choice of spin orientation.]

3.2. Density matrix in quantum physics: open quantum systems

In this section, as in the introductory Section 1, we are using H to denote a generic global Hamiltonian of a possibly combined system.

3.2.1. Quantum dynamics: von Neumann equation

The quantum dynamics in the density-matrix generalised framework is governed by the von Neumann Equation (4), i.e.

$$\frac{\mathrm{d}\rho}{\mathrm{d}t} = \frac{1}{i\hbar}[H, \rho]. \tag{41}$$

Equation (41) is also referred to as the Liouville-von Neumann or quantum Liouville equation, as it can be viewed as generalising the classical Liouville equation for the phase-space distribution function [132]: according to the formal classical-quantum correspondence principle [133], the classical Poisson brackets are promoted to quantum-mechanical commutators [5]. Constructively, Equation (41) can be established from the Schrödinger Equation (1) and the definition (38); but, in its final form, it captures the more general evolution of quantum-mechanical systems, with the qualifications discussed in the next two paragraphs.

It should be noted that the von Neumann Equation (41) describes the evolution for the whole system, including the environment, and can be used as the starting point for approximation schemes leading to master equations that extend the Schrödinger Equation (1) as a predictive tool for the evolution of all states. In this sense, Equation (41) serves as the generator of a variety of derived master equations tailored to specific physical applications, as discussed below. An example of a master equation originally used in quantum optics is given in the next section.

3.2.2. Open quantum systems

The dynamics described by the von Neumann equation is especially insightful in open quantum systems, when applied along with the separation of a system S within a larger, combined system. In this case, the global Hamiltonian is

$$H = H^S + H^E + H^{SE} \tag{42}$$

where H^S is the given system Hamiltonian, H^E is the Hamiltonian of the complementary system or 'environment' (whose specific state is typically unknown), and H^{SE} describes their interaction.

In this formalism, the system S is in a state given by a reduced form of the density matrix, via the partial trace

$$\rho^S(t) = \mathrm{Tr}_E\left[\rho^{SE}(t)\right]. \tag{43}$$

The partial trace effectively sums over the degrees of freedom of the environment, leaving only the relevant degrees of freedom of the system S by itself. This is a reduction process, usually described as 'averaging out' the states of the complementary system; then, the reduced dynamics involves an effective treatment of the system subject to a quantum master equation. The corresponding time evolution, unlike that for the original von Neumann Equation (41), becomes nonunitary. The loss of unitarity is associated with the physical exchange of information of the given system S with the environment E; see Figure 5. It is this physical exchange that is formally implemented by the mathematical prescription (43). As a result of the response to the external conditions to which the given system S is subject to, there exist a variety of master equations [132]. In this sense, *a quantum master equation is the most general equation for time evolution of an open quantum system*, extending the applicability of quantum dynamics beyond the original Schrödinger Equation (1). Our primary example of this reduction process and use of a practical master equation, which we will address in the next section, is a quantum-optics master equation that has a broad range of applications, including for HBAR radiation.

3.2.3. Perturbation theory of density matrix

As a final step, the density matrix can be evaluated using perturbation theory provided that the coupling is sufficiently weak. This is an important approximation needed to get practical results as the combined system presents a formidable problem.

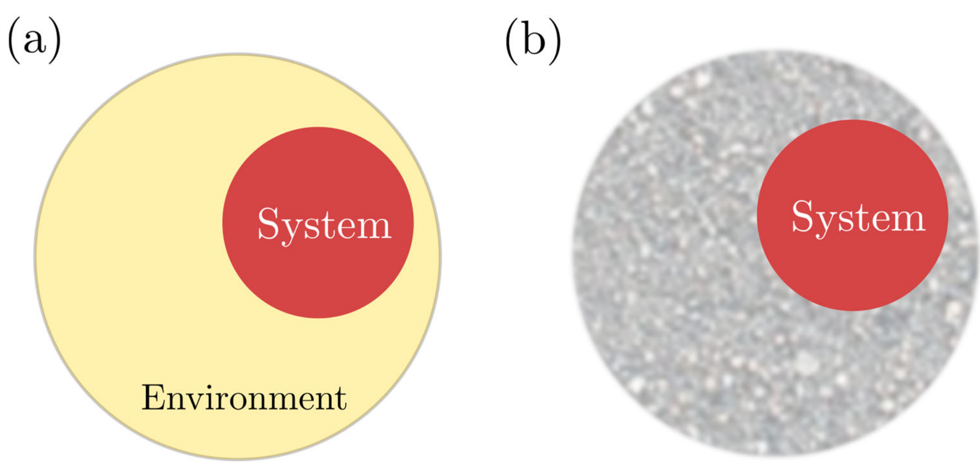

Figure 5. Schematic representation of the exchange of physical information of the system (S) with the environment (E). The corresponding mathematical procedure is that of the partial trace, Equation (43).

The successive orders are given by repeated commutator iterations with the Hamiltonian, leading to a sequence of terms that can be evaluated explicitly, and for which additional approximations and averages are available.

Using this approach to second-order perturbation theory within the interaction picture (i.e. with $H_{\text{int}} = H_{\text{int},I}$), the perturbative expansion is

$$\begin{aligned} \rho(t) =& \rho(0) - (i/\hbar)\int_0^t \mathrm{d}t' \; [H_{\text{int}}, \rho(0)] \\ &+ (-i/\hbar)^2 \int_0^t \mathrm{d}t' \int_0^{t'} \mathrm{d}t'' \left[H_{\text{int}}, [H_{\text{int}}, \rho(0)]\right] + \ldots, \end{aligned} \tag{44}$$

and this pattern continues to all orders. This is the density-matrix generalisation for mixed states of the Dyson series of pure states [131] mentioned above, and the generalisation of the well-known perturbation theory approach within canonical quantum field theory [6].

In essence, the derivation of useful master equations follows a two-step reduction procedure:

$$\begin{pmatrix} \text{Perturbation theory} \\ \text{Equation (44)} \end{pmatrix} \Longrightarrow \begin{pmatrix} \text{Reduction to system } S \\ \text{Partial trace, Equation (43)} \end{pmatrix}$$

Next, we will show how these general results, including the two-step reduction process, Equations (43) and (44), are used for a particular quantum-optics form of the reduced density matrix.

3.3. Reduced density matrix in quantum optics: from lasers to curved spacetime

The quantum optics approach to the density matrix was developed in the 1960s for an improved understanding of the operation of lasers and masers [47,48]. This practical field evolved from Einstein's original work on the stimulated emission of electromagnetic radiation [134], allowing for the possibility of population inversion and subsequent invention of lasers and masers [135,136].

3.3.1. Scully-Lamb master equation

Initially, for the laser-related applications, a semiclassical approach was used: a quantum treatment of the atoms combined with a classical picture for the laser field, along the lines of the simple model described in Section 2. But in the early 1960s, Glauber [137] pointed out that only a fully quantum-mechanical description would be reliable, requiring the development of a density matrix for the laser electromagnetic field. In a sequence of seminal papers [138,139], this problem was solved for the reduced density matrix of the single-mode laser field under a specific set of assumptions (see below), leading to the first laser master equation, whose diagonal elements are given by

$$\dot{\rho}_{n,n} = \underbrace{-\left\{[\alpha - \beta(n+1)](n+1)\,\rho_{n,n} - (\alpha - \beta n)n\,\rho_{n-1,n-1}\right\}}_{\text{pumping}} - \underbrace{\gamma\left[n\,\rho_{n,n} - (n+1)\,\rho_{n+1,n+1}\right]}_{\text{damping}}, \tag{45}$$

in terms of the optical parameters α, β, and γ, known as the linear gain, saturation, and loss respectively. In the Scully-Lamb master equation, while the most interesting elements are the diagonal ones, $\rho_{n,n}$, its more general form also includes off-diagonal elements [138,139]. This equation relies on several assumptions that make it useful and versatile even beyond lasers, but not universal. More generally, the master equations for laser systems comprise a vast topic in quantum optics [47,48]. Among the assumptions leading to the master Equation (45) are:

- the two-level atom model and electromagnetic coupling of Section 2, with interaction Hamiltonian (34) and associated probabilities;
- the injection of atoms at a specific rate;
- the particular use of the optical parameters α, β, and γ;
- and a Markovian approximation (memoryless property): the future evolution is solely determined by its current state.

This master equation is further described in the next section, where it is generalised to be used in specific spacetime backgrounds in the presence of black holes.

The Scully-Lamb laser model, with Equation (45), in addition to leading to a deeper understanding of this technology, has generated a vast literature of research in: quantum optics and open quantum systems (for example [140–143], and references therein); Bose-Einstein condensates (BEC) as 'atom laser' analogs [144–147]; and black hole physics (as further discussed in this review article) [55]. The terms in Equation (45) describe probability flows between the photon occupation number n and the adjacent numbers $(n-1)$ and $(n+1)$, having a structural form

$$\dot{\rho}_{n,n} = \underbrace{-\left[R_{\mathrm{e},n}\,(n+1)\,\rho_{n,n} - R_{\mathrm{e},n-1}\,n\,\rho_{n-1,n-1}\right]}_{\text{emission}} - \underbrace{\left[R_{\mathrm{a},n}\,n\,\rho_{n,n} - R_{\mathrm{a},n+1}\,(n+1)\,\rho_{n+1,n+1}\right]}_{\text{absorption}}, \tag{46}$$

in which $R_{\mathrm{e},n}$ and $R_{\mathrm{a},n}$ are emission and absorption probabilities associated with pumping and damping in the laser model – in effect, the pumping terms are primarily governed by stimulated emission via the excitation rate of atoms in the cavity, mode frequency, and dipole matrix element, while the damping is due to cavity losses described by a quality factor [47]. However, written in the form of Equation (46), the master equation leads to a broader class of applications for analog systems, including the ones mentioned above. This general form is shown in part (a) of Figure 6. (The complete figure will be discussed further below; the parts labelled (b) and the notation are specific to the HBAR radiation analog system of the next section.)

3.3.2. Analog systems

For the BEC analog system, one typically has a dilute system forming a gas of N ideal bosons, which are realised experimentally with atoms; and the N particles are confined in three-dimensional harmonic trap [144]. In addition, these are in equilibrium at temperature $T \ll T_c$ (with T_c being the BEC transition temperature). Under these conditions, the master equation for the diagonal elements, with $n \equiv n_0$ being the number of bosons in the ground state, has the same form as Equation (45), with the following analog

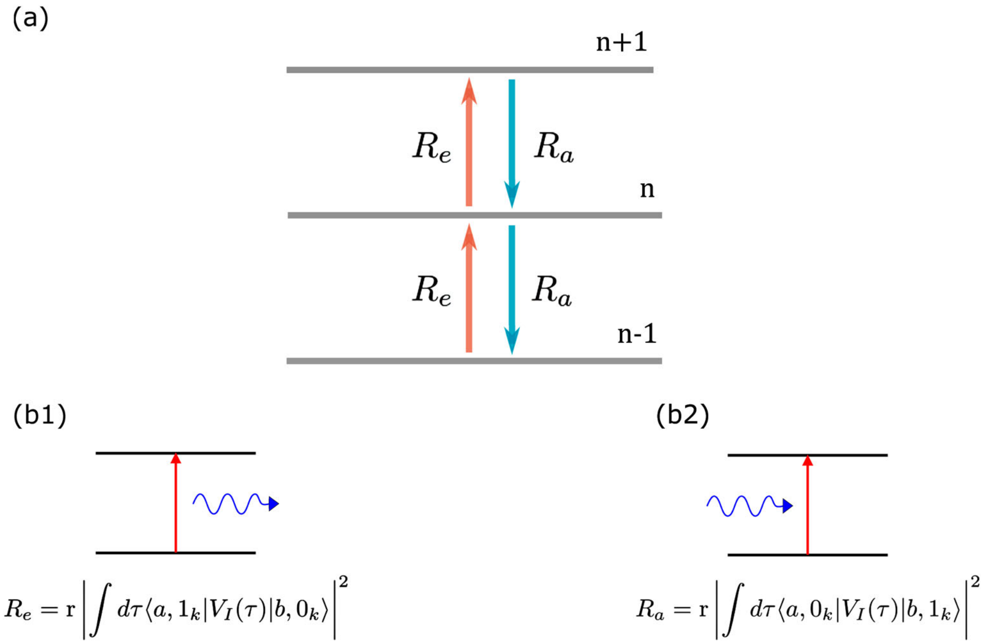

Figure 6. Probability flows governed by the generalised Scully-Lamb master Equation (51). Part (a) describes the flows between the three relevant levels of the field mode, with specific transition rates R. The modes are labelled with $k \equiv \mathbf{s}$. Parts (b1) and (b2) display the two relevant transition processes, for the given initial condition starting from the atomic ground state.

replacements [145]: $\alpha \to \kappa(N+1)$, $\beta \to \kappa$, and $\alpha \to \kappa N(T/T_c)^3$ (and κ a rate constant); and R_e and R_a represent cooling and heating rates. This master equation has been generalised for arbitrary temperatures T in Ref. [146] (see the review and additional results in Ref. [147]).

The laser in cavity, and the analog systems described by Equation (46) require the use of a density matrix because part of the system has an element of randomness that is treated as a reservoir. In the laser, the model involves excited atoms emit photons in a cavity at a given mode; a density matrix is needed for the electromagnetic laser field as the atoms are injected into the cavity, and their degrees of freedom are averaged out. This averaging process leading to a reduced density matrix is described in the next section for the analog system of atoms falling into the black hole: HBAR radiation [55], where the resulting master equation is described by a particular important case of Equation (46).

3.4. Reduced density matrix for HBAR field

We are now ready to review the results on the analog density matrix of the HBAR radiation emitted by a cloud of atoms falling into a black hole [55]. A complete derivation of these results can be seen in Ref [83]. In short, the properties of the density matrix derived in this way are essential to the analysis of the state and thermal properties of the HBAR radiation field.

3.4.1. Composite system and reduction procedure

In what follows, we will refer to the field as the photon system (labelled with $\mathcal{P}$), where the choice of a scalar field yields a simple model of emission of scalar photons. This is the result of its interaction with an atom (labelled with $\mathcal{A}$). Then, the quantum master equation has indeed the form outlined in Equation (46) and applies to the reduced density matrix ($\rho^{\mathcal{P}}$) of the field, due to the random injection of atoms. This density matrix can be obtained by the general reduction procedure: via partial tracing (over the atomic degrees of freedom) from the density matrix of the composite system,

$$\rho^{\mathcal{P}} = \mathrm{Tr}_{\mathcal{A}}\left(\rho^{\mathcal{P}\mathcal{A}}\right). \tag{47}$$

The time evolution of the combined atom-field system is governed by the von Neumann equation for the density matrix $\rho^{\mathcal{P}\mathcal{A}}$. As in Equation (44), in second-order perturbation theory within the interaction picture,

$$\begin{aligned}\rho^{\mathcal{P}\mathcal{A}}(\tau) = \rho^{\mathcal{P}\mathcal{A}}(\tau_0) - \frac{i}{\hbar}\int_{\tau_0}^{\tau} \mathrm{d}\tau'[V_I(\tau'), \rho^{\mathcal{P}\mathcal{A}}(\tau_0)] \\ + \left(-\frac{i}{\hbar}\right)^2 \int_{\tau_0}^{\tau} \mathrm{d}\tau' \int_{\tau_0}^{\tau'} \mathrm{d}\tau''[V_I(\tau'), [V_I(\tau''), \rho^{\mathcal{P}\mathcal{A}}(\tau_0)]],\end{aligned} \tag{48}$$

where $V_I = H_{\mathrm{int},I}$ is the interaction potential or Hamiltonian in the interaction picture. For the initial state of the combined system, one can consider the tensor product $\rho^{\mathcal{P}\mathcal{A}}(\tau_0) = \rho^{\mathcal{P}}(\tau_0) \otimes \rho^{\mathcal{A}}(\tau_0)$, where the atoms and field are initially uncorrelated. The required time parameter τ in Equation (48) is the proper time of free-fall trajectories.

3.4.2. Experimental procedure and injection averaging

The standard experimental setup in quantum optics involves an optical cavity. A cloud of atoms acts as a reservoir within the cavity. The cavity can be defined with appropriate mirrors in a given spacetime geometry. This setup, with the averaging procedure, as depicted in Figures 2 and 3, is the black-hole analog of a standard quantum engineering approach that is useful for experimental studies of quantum information [148,149]. In such studies of 'reservoir computing' [150], atomic quantum reservoirs are physical systems used to process information in a similar way to how neural networks work – they are often composed of atoms in a cavity, in designs that have also been modelled with the QRM of Section 2.2. For the HBAR problem, the atoms are injected in their ground state, the initial atomic density matrix (at time τ_0) is $\rho^{\mathcal{A}} = |b\rangle\langle b|$. The evolution of the radiation field is averaged over a distribution of injection times. In this model, which generalises the original Scully-Lamb model of a laboratory laser cavity, a Markovian property is assumed. As an operational procedure, the effective evolution of the field is obtained by: (i) tracing over the atomic degrees of freedom (with $\mathrm{Tr}_{\mathcal{A}}$), leading to the reduced field density matrix $\rho^{\mathcal{P}} = \mathrm{Tr}_{\mathcal{A}}\,(\rho^{\mathcal{P}\mathcal{A}})$; and (ii) implementing an averaging procedure with a time scale larger than the reservoir's memory time (time scale for a representative distribution of injection times). As a result, a master equation of the form (47) is obtained: this is the equation for an approximate coarse-grained reduced density matrix $\rho^{\mathcal{P}}$.

The cavity analog for a spacetime geometry corresponds to a spatial region bounded by constant values of coordinates adapted to stationary configurations. (As mentioned in the introductory part of Section 2, the 'optical cavity model' is a useful device to simulate the Boulware vacuum – see Figure 3 – but caution should be exercised in its interpretation.) For example, for the Schwarzschild geometry, the spatial coordinates are adapted to a set of static observers, with the coordinate time t being a convenient parameter to label the 'cavity time' (experienced at given, fixed locations of an optical cavity) – the actual cavity time, which is a static proper time, experiences gravitational time dilation with a factor $\sqrt{-g_{tt}(r)} = \sqrt{f(r)}$. If an atom is injected at an initial coordinate time $t_0 = t_{i,a}$, the subsequent geodesic motion is given by the equations in Section 4. As $\tau = \tau(t)$, the time parameter τ can be replaced by t, and the corresponding 'microscopic' change in the field density matrix is $\delta\rho_a^{\mathcal{P}} \equiv \delta\rho^{\mathcal{P}}(t;\, t_{i,a}) = \rho^{\mathcal{P}}(t) - \rho^{\mathcal{P}}(t_{i,a})$. Thus, the corresponding course-grained or 'macroscopic' change is

$$\dot{\rho}^{\mathcal{P}} \equiv \frac{\Delta\rho^{\mathcal{P}}}{\Delta t} = \mathfrak{r}\,\frac{1}{\Delta N}\sum_a \delta\rho^{\mathcal{P}}(t;\, t_{i,a}) = \mathfrak{r}\,\overline{\delta\rho^{\mathcal{P}}}, \tag{49}$$

where the overdot notation gives the rate of change [47] with respect to the cavity time t, $\mathfrak{r} = \Delta N/\Delta t$ is the injection rate, and $\overline{\delta\rho^{\mathcal{P}}}$ is the average microscopic change with respect to particle injection. The statistical average is defined starting with a number of atoms ΔN during a time interval T, in the form $(1/\Delta N)\sum_a X^{\mathcal{P}} = \int dt_{i,a} f(t_{i,a}) X^{\mathcal{P}}$ (when applied to a field quantity $X^{\mathcal{P}}$), where $f(\xi)$ is the probability distribution of the random variable. Then,

$$\overline{\delta\rho^{\mathcal{P}}} = \int \mathrm{d}t_i\, f(t_i)\, \delta\rho^{\mathcal{P}}(t;\, t_i). \tag{50}$$

For a completely random distribution of injection times, a uniform distribution $f(t_i) = 1/T$ can be chosen. The resulting coarse-grained field density matrix satisfies the multimode form of the generalised Scully-Lamb master equation [83]

$$\begin{aligned}\dot{\rho}_{\mathrm{diag}}(\{n\}) = -\sum_j \Big\{ & R_{\mathrm{e},j}\big[(n_j+1)\,\rho_{\mathrm{diag}}(\{n\}) - n_j\,\rho_{\mathrm{diag}}(\{n\}_{n_j-1})\big] \\ & + R_{\mathrm{a},j}\big[n_j\,\rho_{\mathrm{diag}}(\{n\}) - (n_j+1)\,\rho_{\mathrm{diag}}(\{n\}_{n_j+1})\big]\Big\},\end{aligned} \tag{51}$$

which is valid under the assumption that only the diagonal elements are relevant; this is the case for *random injection times*. In Equation (51), the emission and absorption rate coefficients are $R_{e,j} = \mathfrak{r}\,P_{e,j}$ and $R_{a,j} = \mathfrak{r}\,P_{a,j}$, with $\mathfrak{r}$ being the atom injection rate; and the index j is shorthand for a given mode $\boldsymbol{s}_j$, with the single-mode quantum numbers $\boldsymbol{s}$ chosen in an ordered sequence. In addition, the diagonal elements of the density matrix are denoted by $\rho_{\mathrm{diag}}(\{n\}) \equiv \rho_{n_1,n_2,\ldots;n_1,n_2,\ldots}$, where we further developed the notation of Section 2.1: $\{n\} \equiv \{n_1,\, n_2,\, \ldots,\, n_j,\, \ldots\}$ for the occupation number representation, along with $\{n\}_{n_j+q} \equiv \{n_1,\, n_2,\, \ldots,\, n_j+q,\, \ldots\}$ (with q an integer-number shift). In Section 5.3, we will use Equation (51) to establish the thermal nature of the HBAR radiation field.

4. Quantum aspects of spacetime: black holes, horizons, and conformal quantum mechanics (CQM)

This is a mainly self-contained section where we address the essential geometric features of the spacetime background. It serves as an introduction to spacetime properties related to black holes, as well as to the near-horizon approximation and conformal quantum mechanics. In the main text of this article, we will consider a generalisation of Schwarzschild spacetime geometries; further generalisation to include black hole rotation is discussed in Appendix 2.

However, one should also keep in mind that this background is of direct relevance for the computation of the probabilities (35) and (36) for HBAR radiation, which requires geometry-specific field modes and spacetime worldlines. These probabilities will be computed in the next section, where we will derive the emission of radiation fields due to the fall of particles through the event horizon, as well the associated black hole thermodynamics.

For the remainder of this article, with the exception of the first paragraph of the next Section 4.1 or unless stated otherwise, we will use Planck natural units ($\hbar = 1$, $c = 1$, $k_B = 1$, $G = 1$).

4.1. Black hole geometry and horizons

We first introduce a general class of static spacetime geometries with black holes, defined via the metric

$$ds^2 = -f(r)\,dt^2 + \left[\,f(r)\right]^{-1} dr^2 + r^2\, d\Omega^2_{(D-2)} \tag{52}$$

in D spacetime dimensions. Inspection of Equation (52) reveals a spherically symmetric metric written in coordinates (t, r, Ω), where the time and radial metric elements are $-g_{tt} = g^{rr} = f(r)$, and Ω describes the usual angular spherical coordinates of the unit $(D-2)$-sphere with metric $d\Omega^2_{(D-2)}$. The prime example is the ordinary four-dimensional ($D = 4$) Schwarzschild metric [38,85,90], which is due to a black hole of mass M, for which $f(r) = 1 - 2GM/r$, where Newton's gravitational constant G is restored. By extension, a metric of the form (53) describing a spacetime gravitational background with an event horizon, may be called a 'generalised Schwarzschild geometry'. One such generalisation is the Reissner-Nordström (RN) black hole [38,85,90], with mass M and electric charge Q, for which $f(r) = 1 - 2GM/r + K_e GQ^2/r^2$ (withn K_e being Coulomb's constant). More general spacetime realisations include extensions to any number of dimensions $D \geq 4$ [151]. Specifically, for the particular case of an RN black hole of mass M and electric charge Q, the factor $f(r)$ in Equation (53) becomes $f(r) = 1 - (R_M/r)^{D-3} + (R_Q/r)^{2(D-3)}$ with the characteristic length scales R_M and R_Q given similarly in terms of M and Q^2. These extensions also allow for combinations of Schwarzschild, Reissner-Nordström, and de Sitter geometries with a cosmological constant Λ, and black hole solutions with additional quantum charges [152]; for example, the inclusion of a cosmological constant is achieved with an extra term $-2\Lambda r^2/[(D-1)(D-2)]$ in $f(r)$. Further extensions with angular momentum, for rotating black holes, can be treated similarly, as addressed in Appendix 2.

The generalised Schwarzschild geometries of Equation (52) are static and spherically symmetric, i.e. the metric has invariance under time translations and spatial rotations. Metric invariance is an example of an isometry: a transformation that preserves distances between points in a metric space. A Killing vector field is an infinitesimal generator of an isometry; distances between points on the manifold remain unchanged when following the flow of the Killing vector. For the generalised Schwarzschild metric, time and rotational invariance are described by the corresponding Killing vectors [38,85,90]

$$\boldsymbol{\xi}_{(t)} = \partial_t, \quad \boldsymbol{\xi}_{(\phi)} = \partial_\phi, \tag{53}$$

where ϕ is a rotational angle around a generic plane. For a particular coordinate choice in Equation (52), spherical symmetry refers to the symmetries of the sphere with metric $d\Omega^2_{(D-2)}$; these involve a complete set of angular Killing vectors, e.g. with respect to the standard azimuthal angle ϕ and 2 additional orientations in 4-dimensional spacetime [38,85,90]). Generally, one can use the norms and inner products of Killing vectors to set up geometrical interpretations in coordinate-free forms. In particular, for questions related to time evolution, the product $g_{tt} = \boldsymbol{\xi}_{(t)} \cdot \boldsymbol{\xi}_{(t)}$ plays an important role because the flow of the time-translation Killing vector $\boldsymbol{\xi}_{(t)}$ generates time evolution. (For example, in a Schwarzschild background, $\boldsymbol{\xi}_{(t)}$ is proportional to the spacetime velocity of a static observer, i.e. one that remains at a fixed position with constant spatial coordinates.)

For our discussion of acceleration radiation, the most relevant features of the geometries defined by Equation (52) are related to the existence of an event horizon $\mathcal{H}$. This is a hypersurface that is the interior boundary of the region in spacetime from which a light ray can travel to infinity. For a static spacetime [as described by Equation (52)], it can be identified via the polynomial roots of the metric component

$$g_{tt} = \boldsymbol{\xi}_{(t)} \cdot \boldsymbol{\xi}_{(t)} = f(r) = 0. \tag{54}$$

Thus, at every point on the hypersurface $\mathcal{H}$, the norm of the time-translation Killing vector $\boldsymbol{\xi}_{(t)}$ becomes null, defining a null tangent direction, while the Killing vectors associated with the other (angular) directions remain spacelike. By definition, this makes $\mathcal{H}$ a null hypersurface. Now, the light cones built at every point on a null hypersurface are tangent to it and confined to one side: thus, the geodesics cross the surface in only one direction (inward). Therefore, the null condition (54) signals the presence of an event horizon as a boundary where all timelike or null geodesics are ingoing and cannot go back to infinity. The event horizon itself is generated by light rays that cannot escape the black hole. Moreover, this a general result for stationary spacetimes that can be further confirmed by a detailed analysis of the geodesics and spacetime causal structure [38,85,90]. Stationary geometries that are not static: they are typically associated with a black hole with angular momentum or rotation and exhibit additional subtleties; see Appendix 2.

Given the existence of an event horizon for the generalised Schwarzschild geometries of Equation (52), a near-horizon analysis can be carried out, centred on the functional dependence of the external nongravitational fields in the neighbourhood of the outer event horizon ($r = r_+$). As we show in the next two sections, the near-horizon behaviour gives crucial insights into the emergence of conformal symmetries and black-hole thermodynamics.

Two important quantities related to the event horizon are closely linked with the black hole's thermodynamic and quantum features: the surface gravity and the black hole horizon area. First, the surface gravity is defined from the timelike Killing vector $\boldsymbol{\xi} \equiv \boldsymbol{\xi}_{(t)}$ in Equation (53) as the horizon value κ from

$$\kappa^2 = -\frac{1}{2}\left(\nabla_\mu \xi_\nu\right)(\nabla^\mu \xi^\nu)\bigg|_{r=r_+}, \tag{55}$$

for a normalised vector $\boldsymbol{\xi}$ that conforms to an operationally defined notion of gravitational acceleration [38,90,153]. A normalisation is required due to the multiplicative ambiguity in the definition of the Killing vector. In asymptotically flat and static spacetimes, including the ones described the generalised Schwarzschild metrics (52), this can be enforced with a unit normalisation via the inner product,

$$\boldsymbol{\xi} \cdot \boldsymbol{\xi}\big|_{r\to\infty} = -1. \tag{56}$$

In such spacetimes, the acceleration κ defined via Equations (55) and (56) can be shown to be constant over the entire event horizon, and agrees with an operational value needed to keep a test particle in the near-horizon region as measured from infinity. Appendix 2 shows how to generalise this definition centred on Equation (55). For the generalised Schwarzschild black holes from Equation (52) (with $r = r_+$), it takes the form

$$\kappa = \frac{f'_+}{2}, \tag{57}$$

where $f'_+ = f'(r_+) \neq 0$ for nonextremal geometries. This geometrical quantity (55)–(57) is proportional to the Hawking temperature, as given in Equation (8). Second, the horizon area, generally defined via integration with the metric of the angular coordinates (on the unit sphere), takes the D-dimensional form [77,151]

$$A = \Omega_{(D-2)}\, r_+^{D-2}, \tag{58}$$

in terms of the solid angle $\Omega_{(D-2)}$ in D dimensions; in 4D, this reduces to the familiar area $A = 4\pi r_+^2$. This geometrical area (58) is, in all cases, proportional to the Bekenstein-Hawking entropy (9). In particular, this implies that the area changes are governed by

$$\delta A = 8\pi\,\frac{\delta M}{\kappa} \tag{59}$$

in the pure Schwarzschild case (mass M only), and similar expressions where δM is replaced by a subtracted energy associated with electric fields or rotation in the RN and Kerr geometries respectively, suggesting a thermodynamic analogy (see Appendix 2). In Section 6, we show that these are not just analogies but represent a genuine quantum thermodynamic framework both for the intrinsic properties of black holes and the related properties of horizon-brightened acceleration.

4.2. Scalar field: quantisation and near-horizon analysis

The Euler-Lagrange equation for a scalar field in a generic gravitational background $g_{\mu\nu}$ is given by the classical curved-spacetime Klein-Gordon Equation (12). Thus, this determines the functional form of the field modes $\phi_{\mathbf{s}}$ in the field expansion of Equation (6), as needed for its canonical quantisation. For the class of metrics (52), with the set of quantum numbers $\mathbf{s} = (nl\mathbf{m})$, the modes take the separable form

$$\phi_{\mathbf{s}}(t, r, \Omega) = R_{nl}(r) Y_{l\mathbf{m}}(\Omega) e^{-i\omega_{nl} t}, \tag{60}$$

where $Y_{l\mathbf{m}}(\Omega)$ are ultra-spherical harmonics, the solutions to the angular part of the Laplacian. Then, the Klein-Gordon equation can be further reduced to its normal form with the Liouville transformation [154] $R(r) = \chi(r)u(r)$, where $\chi(r) = [f(r)]^{-1/2}\, r^{-(D-2)/2}$, such that its radial part becomes

$$u''_{nl}(r) + I_{(D)}(r; \omega_{nl}, \alpha_{l,D})\, u_{nl}(r) = 0, \tag{61}$$

where $I_{(D)}$ is an effective potential; e.g. an explicit form is given in Refs. [77,81].

In principle, the physics of quantum fields in the gravitational background of a black hole can be studied directly from Equation (61). But the intrinsic properties generated by the black hole are essentially driven by the presence of the event horizon. Thus, it is plausible that some of the most essential features of the relevant physics, including quantum properties, are captured by the near-horizon behaviour. The possible relevance of the near-horizon physics for black-hole thermodynamics was highlighted in several studies starting in the late 1990s [155–162]. These efforts uncovered a form of scale symmetry associated with conformal symmetries, which appeared to be an important ingredient related to the thermal and quantum properties. More direct evidence for the role played by this symmetry in black-hole thermodynamics was shown in Refs. [77,78], and the same approach was later used to display the related properties of horizon-brightened acceleration radiation [81–84]. This is the near-horizon CQM approach that we will highlight for the derivation of thermodynamic behaviour in most of the remainder of this article. With this purpose in mind, we first begin by defining the near-horizon approximation, with details and associated symmetry to be discussed in the next section.

The near-horizon scheme involves an approximation near the outer horizon $\mathcal{H}$, $r \sim r_+$, with $r = r_+$ being the largest root of the scale-factor equation $f(r) = 0$. Thus, with the shifted variable $x = r - r_+$, the Taylor series for the scale factor $f(r)$ starts at first or higher orders. The notation $\overset{(\mathcal{H})}{\sim}$ will be used to represent this hierarchical expansion. Considering the physically relevant *nonextremal* metrics, which satisfy the condition $f'_+ \equiv f'(r_+) \neq 0$, the function $f(r)$ and its derivatives to second order are given by

$$f(r) \overset{(\mathcal{H})}{\sim} f'_+\, x[1 + O(x)], \quad f'(r) \overset{(\mathcal{H})}{\sim} f'_+[1 + O(x)], \quad f''(r) \overset{(\mathcal{H})}{\sim} f''_+[1 + O(x)], \tag{62}$$

where $f''_+ \equiv f''(r_+)$. This near-horizon approximation can be applied to the original Klein-Gordon Equation (12), leading to

$$\left[\frac{1}{x}\frac{d}{dx}\left(x\frac{d}{dx}\right) + \left(\frac{\omega}{f'_+}\right)^2 \frac{1}{x^2}\right] R(x) \overset{(\mathcal{H})}{\sim} 0, \tag{63}$$

followed by the corresponding Liouville transformation $R(x) \propto x^{-1/2}u(x)$; or directly to the reduced form of Equation (61). Thus, the final result, up to leading-order with respect to x, is a Schrödinger-like equation

$$u''(x) + \frac{\lambda}{x^2}[1 + O(x)]u(x) = 0 \tag{64}$$

[with the replacement of $u(r)$ by $u(x)$], where the dominant near-horizon physics is driven by the effective Hamiltonian

$$\mathscr{H} = p_x^2 - \frac{\lambda}{x^2}, \tag{65}$$

with an inverse square potential of coupling

$$\lambda = \frac{1}{4} + \Theta^2, \quad \Theta = \frac{\omega}{f'_+} \equiv \frac{\omega}{2\kappa}. \tag{66}$$

In Equation (66), $\kappa = f'_+/2$ is the surface gravity of the black hole, from Equations (55)–(57).

Remarkably, even though Equations (63)–(66) involve the near-horizon approximation, this simplification does not limit their scope. Basically, the near-horizon regime emerges as an effective theory that captures the essence of black-hole thermodynamics and the HBAR physics of particles falling into a black hole. In this view, specifically, the one-dimensional effective Hamiltonian $\mathscr{H}$ associated with Equation (66) is a realisation of the inverse square potential of conformal quantum mechanics [76]. The conclusion is that the near-horizon physics exhibits an *asymptotic conformal symmetry*. The near-horizon expansion and emergence of conformal quantum mechanics are as depicted in Figure 7.

4.3. Conformal symmetry: the unreasonable effectiveness of conformal quantum mechanics (CQM)

Symmetries play a crucial role in most aspects of foundational quantum physics – this has been another fundamental recurrent theme throughout the first hundred years of quantum mechanics [5].

A remarkable example that has attracted considerable attention in recent decades is conformal symmetry [163]. One particular form of this invariance is the framework known as conformal quantum mechanics (CQM), as it was called in the comprehensive presentation of Ref. [71].

4.3.1. Conformal symmetry and CQM

The CQM framework is based on the inverse-square-potential Hamiltonian $\mathscr{H}$ of Equation (65) and is manifestly scale invariant at the classical level as it is homogeneous of degree -2 [164,165]. In addition, this operator is part of an enlarged SO(2,1) symmetry group which can be interpreted as describing a lower-dimensional conformal field theory [71,166–168]. The algebra of this SO(2,1) group consists of three operators: $\mathscr{H}$, which is the generator of time displacements (with respect to a specified time t

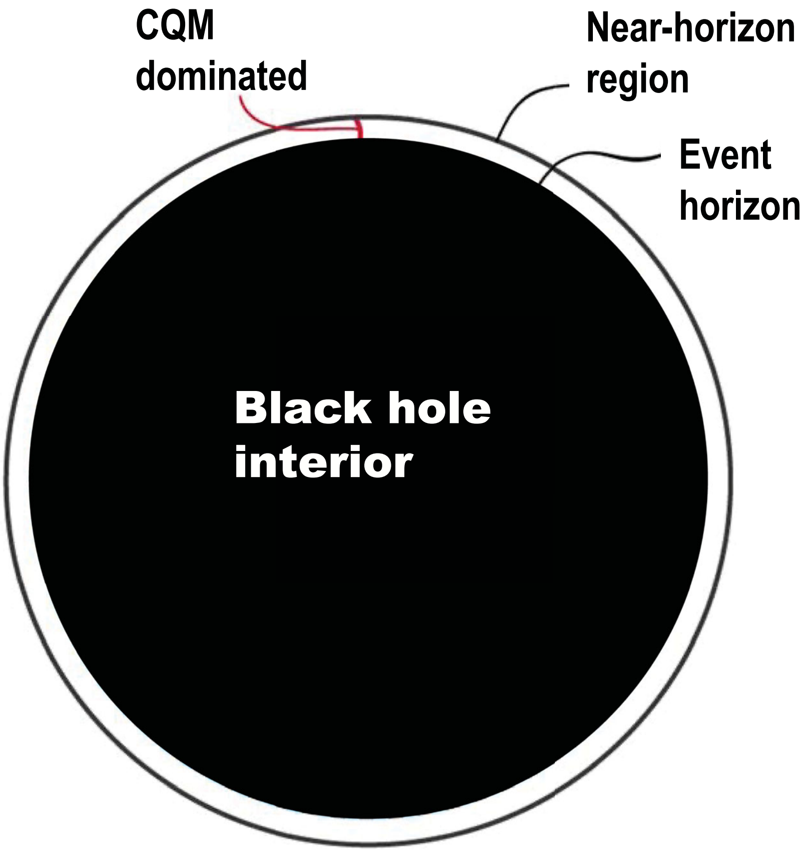

Figure 7. The near-horizon approximation can reveal properties of the black hole near the event horizon, including the emergence of conformal quantum mechanics (CQM), and the interpretation of quantum fields as providing a thermal atmosphere.

conjugate to $\mathscr{H}$), together with the dilation operator

$$D = tH - \frac{xp + px}{4} \tag{67}$$

(where p is the conjugate momentum), which performs scale transformations, e.g. as illustrated in Figure 8); and the special conformal operator

$$K = t^2 H - \frac{t(px + xp)}{2} + \frac{mx^2}{2}. \tag{68}$$

which is the generator of inverse time displacements. These operators generate the SO(2,1) *conformal algebra*

$$[D, H] = -i\hbar H, \quad [K, H] = -2i\hbar D, \quad [D, K] = i\hbar K. \tag{69}$$

This symmetry algebra has been recently studied in its most general setting using path integral methods [169], extending earlier results on path integrals of the inverse square potential [170,171].

Figure 8. The near-horizon conformal modes $\phi(r, t)$ can be pictured with their wavefronts. The event horizon is represented by the dotted line. A geometric sequence $x_{(n)} \propto \eta^n$ with ratio $\eta = e^{-2\pi/\Theta}$, and Θ defined via Equation (66), shows the piling up of the modes with an accumulation line at the horizon. This manifests scale invariance under arbitrary magnifications, with a geometric scaling depicted via the Russian-doll analogy. In this graph, $\eta^{-1} = 1.4$. For the HBAR analysis, the phase of the probability amplitudes, as shown in Equations (76)–(78), has a similar geometric scaling: $\eta = e^{-2\pi/\sigma} = e^{-\pi/\Theta}$, but the frequency scale is twice as big.

4.3.2. Physical realisations of CQM

Paraphrasing Wigner [172], the unreasonable effectiveness of CQM is manifested in its broad range of physical applications. This versatility was first recognised in the pioneering work of Jackiw [166–168], and led to the discovery of physical realisations in molecular physics [74–76], nanophysics [72], nuclear and particle physics [72], and the black-hole thermodynamics and HBAR properties discussed herein. In this sense, CQM can be regarded both as a theoretical tool for fundamental physics and as a practical tool for physical systems.

Many of these realisations involve the emergence of quantum symmetry breaking, i.e. a quantum anomaly [173,174]. This is one of the three main classes of symmetry breaking in physical systems, in addition to explicit and spontaneous symmetry breaking. Specifically, an anomaly is the breaking of a classical invariance upon quantisation. The relevance of this phenomenon has been recognised in high-energy physics since the introduction of the Adler-Bell-Jackiw anomaly [175–177]. The CQM anomaly, when its presence is allowed by the relevant physics, is based on the fact that the conformal theory is singular and ill-defined for a sufficiently *strong coupling*: any bound state energy could be rescaled to arbitrarily negative energies via the dilation operator D of Equation (67). Thus, the Hamiltonian is unbounded from below due to the scale symmetry. While this naively appears to be an intractable problem, an alternative viewpoint is available: the singular behaviour of the conformal interaction reveals the existence of additional *ultraviolet physics*. This is similar to the divergences familiar from quantum field theory and leads to a low-energy version of quantum-mechanical symmetry breaking associated with the renormalised theory. Moreover, the anomalous regime of the theory has a well-defined extension of the symmetry algebra [76,178,179].

Using an effective-field-theory approach, the renormalised theory typically generates a conformal tower of bound states [72] $E_n = E_0\, e^{-2\pi n/\Theta}$ $(n = 0, 1, \ldots)$, where Θ is the conformal parameter associated with the strength of the inverse square potential – this is defined in a manner similar to Equation (66) for near-horizon black-hole physics. Even though the symmetry is broken, and an energy scale arises associated with a ground state, the spectrum still exhibits a residual discrete version of the scale symmetry: E_n is a geometric sequence with ratio $\eta = e^{-2\pi/\Theta}$. Thus, the spectrum looks identical from any 'vantage point' via proportional rescalings. In energy space, this *geometric scaling* is identical to the Russian-doll symmetry shown in Figure 8 for the black-hole near-horizon physics of quantum field modes. A limitation is typically imposed by additional physics, making the conformal tower be a 'window' limited between two characteristic ultraviolet and infrared length scales L_{UV} and L_{IR}, with a total number of states $N_{\mathrm{conf}} \sim (\Theta/\pi) \ln (L_{\mathrm{IR}}/L_{\mathrm{UV}})$. This general framework [72] can also give additional predictions; for example, giving corrections associated with the existence of an infrared cutoff, as shown in Ref. [75], where these techniques give a modified values for critical dipole moments in the formation of molecular dipole-bound anions [74].

4.3.3. CQM in black hole physics

The relevance of conformal symmetry for the quantum and thermal properties black holes has been a recurrent theme in fundamental physics, using a variety of approaches, e.g.Refs. [155–157,180–185]. More specifically, conformal quantum mechanics (CQM) [71], as a model based upon the Hamiltonian $\mathscr{H}$ of Equation (65), *can be used as a probe of black hole thermodynamics* and related phenomena. Indeed, the CQM approach to black holes provides a universal model of black hole entropy from near-horizon physics [77–80], and can be used for the framework of HBAR radiation we are reviewing in this article [81–84]. In the current context, this conformal symmetry is revealed by the disappearance of all characteristic field scales; in particular, the field parameters μ_Φ and ξ in Equations (11) and (12) play no role in the near-horizon physics. Moreover, this invariance, as represented in Figure 8, can be pictured as arising from a gravitational blueshift that grows infinitely, with an accumulation point towards the event horizon; as a result, any other physical scales are asymptotically erased [186].

For near-horizon CQM, the leading form of the field modes can be obtained from a pair of independent solutions of the CQM Equation (64),

$$u_{\pm}(x) = x^{\frac{1}{2}\pm\sqrt{\frac{1}{4}-\lambda}} = \sqrt{x}\,x^{\pm i\Theta} \tag{70}$$

where $\Theta = \omega/f'_{+}$ as defined in Equation (67). These are outgoing/ingoing CQM modes that are normalised as asymptotically exact WKB local waves [78] and display a logarithmic-phase singular behaviour associated with scale invariance, as $x^{i\Theta} = e^{i\Theta \ln x}$. The logarithm $\ln x$ itself corresponds to the familiar tortoise coordinate of generalised Schwarzschild geometries [38,85]; but writing it in the form of the solution (70) to the corresponding near-horizon, Schrödinger-like Equation (64), makes the CQM scale invariance more manifest, as displayed in Figure 8. In addition, when their time dependence is made explicit, these solutions, in the form of Equation (60), give the outgoing and ingoing CQM modes

$$\phi_{\boldsymbol{s}}(r, \Omega, t) \overset{(\mathcal{H})}{\sim} \Phi_{\boldsymbol{s}}^{\pm\,(\mathrm{CQM})} \overset{(\mathcal{H})}{\propto} x^{\pm i\Theta} Y_{l\mathbf{m}}(\Omega) e^{-i\omega t}, \tag{71}$$

where $\overset{(\mathcal{H})}{\propto}$ denotes the hierarchical near-horizon expansion.

A closely related conformal ingredient revealed by the gravitational background consists of the near-horizon geodesic equations [81]; see generalisations in Appendix 2. The symmetries generated by the Killing vectors (53) lead to geodesic planar orbits with: (i) spacetime velocity $\mathbf{u}$, which is normalised (as all spacetime trajectories) with

$$\mathbf{u} \cdot \mathbf{u} = -1 \tag{72}$$

and (ii) conserved energy and angular momentum components (per unit mass)

$$e = -\boldsymbol{\xi}_{(t)} \cdot \mathbf{u} = f(r)\frac{\mathrm{d}t}{\mathrm{d}\tau}, \quad \ell = \boldsymbol{\xi}_{(\phi)} \cdot \mathbf{u} = r^2 \frac{\mathrm{d}\phi}{\mathrm{d}\tau}, \tag{73}$$

choosing the azimuthal angle ϕ of the orbital plane. Use of Equation (72) amounts to the assignment of an invariant particle mass μ in addition to the conserved quantities of Equation (73).

Straightforward application of the expressions in Equations (72) and (73) gives an integrated form of the geodesic equations, leading directly to the near-horizon geodesics as functional relationships $\tau = \tau(x)$ and $t = t(x)$, with the explicit dependence

$$\tau \overset{(\mathcal{H})}{\sim} -kx + \text{ const.} + O(x^2)\,, \tag{74}$$

$$t \overset{(\mathcal{H})}{\sim} -\frac{1}{2\kappa}\ln x - Cx + \text{ const.} + O(x^2). \tag{75}$$

As displayed in Equations (74), and (75), there are two constants, $k = 1/e$ and C, that govern the linear terms in x; while k only depends on the specific energy e, the constant C depends on both e and the specific angular momentum ℓ of the atom, as well as the black hole parameters (see details in Ref. [81]). However, these constants, as shown in Section 5, do not play a direct role in the dominant part of the HBAR acceleration radiation formula; in effect, unlike the governing scale symmetry of CQM, the metric spacetime symmetries only act to simplify the geodesic initial value problem but do not drive the underlying physics of HBAR. The final results of Equations (75) are the geodesic equivalent of the hierarchical near-horizon expansion of the metric shown in Equation (62). The logarithmic term is obviously the dominant near-horizon part as $x \to 0$, revealing the existence of scale invariance, which corresponds to the familiar gravitational frequency shift [186] and is a direct manifestation of the same conformal invariance that yields the logarithmic phase of the field modes.

This concludes the basic near-horizon analysis, which shows that both the field modes and the geodesics are controlled by the scale-invariant features of CQM.

5. Quantum and thermal nature of horizon-brightened acceleration radiation (HBAR)

With the results of the analysis of the effects of the gravitational field from the previous section, the HBAR radiation can be thoroughly computed with the aid of the transition probabilities (35) and (36). These results apply to the the HBAR thought experiment of Figure 2, where atoms are freely falling into the black hole. With these probabilities, we will derive the emission of radiation fields due to the fall of particles through the event horizon, as well the associated black hole thermodynamics. To highlight the role played by conformal quantum mechanics, Figure 9 displays the near-horizon region as

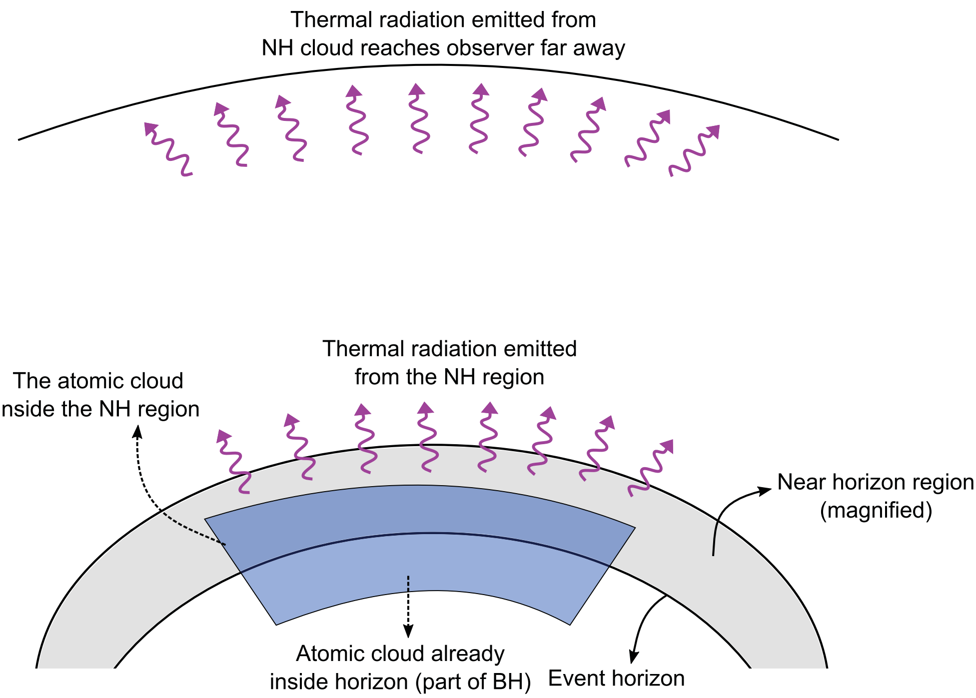

Figure 9. The thought experiment for the HBAR model displays the relevance of the near-horizon analysis leading to conformal quantum mechanics (CQM).

generating the relevant physics. Once this near-horizon analysis is enforced for the HBAR field, a remarkable set of properties and similarities with black hole thermodynamics emerge, as we will discuss in this section.

5.1. HBAR transition probabilities

The two direct consequences of the gravitational field needed for the calculations of the HBAR radiation field are the functional forms of the scalar field modes and the geodesic equations. In their near-horizon CQM forms, these are Equations (71) and (74)–(75). These results can be applied to atoms freely falling into the black hole, in the HBAR thought experiment of Figures 2 and 9. where the possible emission of outgoing radiation corresponds to the purely outgoing CQM modes of Equation (71). Then, the emission and absorption rates under free fall, using Equations (35) and (36), become

$$P_{\mathrm{e},s} \overset{(\mathcal{H})}{\sim} g^2 k^2 \left| \int_0^{x_f} \mathrm{d}x x^{-i\Theta} e^{i\omega t(x)} e^{i\nu\tau(x)} \right|^2 \tag{76}$$

and

$$P_{\mathrm{a},s} \overset{(\mathcal{H})}{\sim} g^2 k^2 \left| \int_0^{x_f} \mathrm{d}x\, x^{i\Theta} e^{-i\omega t(x)} e^{i\nu\tau(x)} \right|^2, \tag{77}$$

where $k = 1/e$ and x_f is an approximate scale setting the upper boundary of the region of dominance of the near-horizon CQM behaviour. In addition, from Equations (74) and (75), the emission rate becomes

$$R_{\mathrm{e},s} = \mathfrak{r}\, g^2 k^2 \left| \int_0^{x_f} \mathrm{d}x\, x^{-i\omega/\kappa} e^{-isx} \right|^2, \tag{78}$$

where $s = C\omega + \nu/e$. The integral of Equation (78) is essentially the probability amplitude, where the field-mode and atom contributions yield phases leading to a combined competition of two oscillatory factors: $x^{-i\omega/\kappa}$ and e^{-isx}. Clearly, the factor $x^{-i\omega/\kappa} = x^{-2i\Theta}$ is the one that governs the final outcome, with the CQM scale invariance and a conformal parameter $\omega/\kappa = 2\Theta$. Notice that this parameter includes two contributions of Θ: one from the near-horizon field modes and the one from the geodesic motion of the atom (relative to the fields). This is the factor that exhibits the Russian-doll behaviour depicted in Figure 8). On the other hand, the e^{isx} factor makes the integral average out to essentially zero away from the horizon because of its highly oscillatory nature in the limit $\nu \gg \omega$. Consequently, this behaviour generates the leading value of the integral almost exclusively from the near-horizon region. Therefore, the upper limit x_f appears as effectively infinite: it can displaced to infinity as a result of scale invariance and cancellations, leading to

$$R_{\mathrm{e},s} = \mathfrak{r}\, g^2 k^2 \left| \int_0^{\infty} \mathrm{d}x\, x^{-i\omega/\kappa} e^{-isx} \right|^2 = \frac{2\pi \mathfrak{r}\, g^2 \omega}{\kappa \nu^2} \frac{1}{e^{2\pi\omega/\kappa} - 1}. \tag{79}$$

Interestingly, as anticipated in the previous section, the probability is independent of the constants k and C; thus, it is independent of the initial conditions.

In conclusion, Equation (79) shows the existence of acceleration radiation with a Planckian distribution, provided we use the Boulware state $|B\rangle$ (with the field modes associated with stationary, generalised Schwarzschild coordinates). This points to the thermal nature of the emission rate. However, this result needs to be examined in greater detail to show it is fully endowed with all the properties of a thermal state.

5.2. Thermal behaviour: detailed balance via the Boltzmann factor

We can start by exploring the thermal behaviour through the ratio of the emission and absorption rates. These rates could be computed separately, but direct inspection of Equation (77) shows that the absorption rate follows from the emission rate via the replacement $\omega \to -\omega$. Then,

$$R_{\mathrm{a},s} = \frac{2\pi r g^2 \omega}{\kappa \nu^2} \frac{1}{1 - e^{-2\pi\omega/\kappa}} , \tag{80}$$

leading to the probability ratio

$$\frac{R_{\mathrm{e},s}}{R_{\mathrm{a},s}} = e^{-2\pi\omega/\kappa}. \tag{81}$$

This ratio has a straightforward interpretation: it corresponds to a thermal state with an effective temperature $T = \beta^{-1}$ by detailed-balance, governed by the Boltzmann factor

$$\frac{R_{\mathrm{e},s}}{R_{\mathrm{a},s}} = e^{-\beta\omega}. \tag{82}$$

Compatibility of Equations (82) and (83) implies that the field is a thermal state with temperature

$$T = (k_B\beta)^{-1} = \frac{\hbar\kappa}{2\pi k_B c} \equiv (k_B\beta_H)^{-1} = T_H, \tag{83}$$

which is identical to the black-hole Hawking temperature (8), when all the units are restored by dimensional analysis. In addition, this temperature coincides with that of the Planck distribution (80).

It should be noted that Equations (82)–(84) do show the existence of a *unique temperature* T *defined by detailed balance for all the field modes*. In the absence of such unique-temperature condition, the 'temperature' would not satisfy all the features of thermality, but would instead be an effective, mode-dependent parameter. This shows that $T = T_H$ is a candidate for a *genuine thermodynamic temperature associated with a thermal state.*

In conclusion, this proof also shows the governing role of near-horizon CQM, through the logarithmic singular nature of its modes and geodesics. This leads directly to the Boltzmann factor in the ratio of the probabilities $P_{\mathrm{e},s}$ and $P_{\mathrm{a},s}$, Equation (82). A more thorough thermal characterisation of the state of the field can be obtained via the steady-state field density matrix, as discussed in the next section.

5.3. Thermal behaviour: generalisations and steady-state field density matrix

We now extend the results of the previous section to a complete derivation of thermality under the most general conditions. For this discussion, we will use relevant parts of Appendix 2 to accommodate a black hole rotational degree of freedom via its angular momentum J and angular velocity Ω_H.

The basic framework described so far remains formally identical, and the results do apply without further changes provided that the frequency ω is replaced by the 'corotating frequency' $\tilde{\omega} = \omega - \Omega_H m$, which involves the energy ω (measured by an asymptotic observer) and the axial component m of the field angular momentum. Thus, Equations (81) and (82) generalise to the form

$$\frac{R_{e,s}}{R_{a,s}} = e^{-2\pi\tilde{\omega}/\kappa} = e^{-\beta\tilde{\omega}}. \tag{84}$$

The final conclusion remains the same:

> The value of the effective temperature defined by this procedure in Equation (84) is the same as the Hawking temperature of the black hole.

A more detailed analysis of the thermal nature of the state of the HBAR radiation field can be fully established with the master equation for the field density matrix: For a cloud of freely falling atoms, with random injection times, the diagonal part of the equation has the form (51). Thus, the properties are essentially geometry-independent and apply equally well to the generalised Schwarzschild and Kerr geometries. The steady-state density matrix $\rho^{(SS)}_{\text{diag}}(\{n\})$ is obtained when the time derivative is zero: $\dot{\rho}_{\text{diag}} = 0$, and using Equation (82); the equation is easily solved for each mode, and the combined operator is a product of independent single-mode pieces, as follows:

$$\rho^{(SS)}_{\text{diag}}(\{n\}) = N \prod_j \left(\frac{R_{e,j}}{R_{a,j}}\right)^{n_j} = \frac{1}{Z}\prod_j e^{-n_j\beta\tilde{\omega}_j}, \tag{85}$$

where $Z = N^{-1} = \prod_j Z_j = \prod_j [1 - e^{-\beta\tilde{\omega}_j}]^{-1}$ is the partition function. Finally, along with Equation (82), this verifies that: (i) it is a thermal distribution at the Hawking temperature; (ii) the steady-state average occupation numbers are $\langle n_j\rangle^{(SS)} = (e^{\beta\tilde{\omega}_j} - 1)^{-1}$.

In conclusion, the density matrix of Equation (85) defines a steady-state thermal state for HBAR radiation, which includes the primary thermal properties of Equations (82) and (83): the Boltzmann factor and the Hawking temperature. Moreover, these results apply to a large class of black holes, both of generalised Schwarzschild and Kerr types. Remarkably, these properties emerge from near-horizon CQM for all field modes. Finally, the outcome of this problem is closely related to the intrinsic thermodynamics of the black hole [54]. Indeed, in the next section, we turn our attention to this general thermodynamic problem, with fundamental origins in quantum physics: a comprehensive analysis of HBAR thermodynamics.

6. Quantum information and quantum thermodynamics: HBAR-black hole correspondence

In this section, we probe deeper into various quantum aspects of spacetime by extending the results from the density matrix via its quantum-information measure given by the von Neumann entropy (5): $S = -\mathrm{Tr}[\rho \ln \rho]$. To simplify the analysis of structural analogies between HBAR thermodynamics and black hole thermodynamics, we will continue using Planck natural units ($\hbar = 1$, $c = 1$, $k_B = 1$, $G = 1$) throughout the remainder of the paper.

Our prime example of HBAR radiation displays several features of the questions being formulated within one of the most recent outgrowths of quantum theory: *quantum thermodynamics* [187,188]. This is an interdisciplinary field that focuses on the relations between quantum physics and thermodynamics, using tools from information theory and open quantum systems. The emergence of thermodynamic behaviour from quantum principles, and the description of systems out of equilibrium are some of the signatures of this novel emphasis, bridging the gap with nonequilibrium statistical mechanics [189]. For our purposes, starting from the density matrix (86), which we have derived within an open systems approach with standard quantum-optics techniques, a complete thermodynamic analysis can be carried out, including the time evolution of the thermodynamic states using entropy flux. In that sense, HBAR thermodynamics provides a thought experiment that illustrates techniques from open quantum systems theory and quantum thermodynamics.

An important comparative remark on vacuum states in gravitational fields is relevant to the correspondence between HBAR and ordinary black hole thermodynamics. The final outcome is governed by the properties of the stationary configuration achieved by the black hole, according to the no-hair theorem [153]: this is the ultimate reason for the remarkable correspondence. However, the thermodynamics and the radiation fields of these two systems are of very different origin in terms of the initial setup. Hawking radiation assumes that the outgoing state of the field is the Unruh vacuum rather than the Boulware vacuum of the HBAR field. The Boulware vacuum is defined with normal modes of positive frequency with respect to the Killing vector ∂_t. Instead, the Unruh vacuum is defined with modes incoming from past infinity to be of positive frequency with respect to ∂_t; and those that emerge from the past horizon of positive frequency with respect to the coordinate U. The coordinate U is the affine parameter along the past horizon, and is associated with the temporal (T) and radial (R) Kruskal-Szekeres coordinates [38,85,90,153]: $U = T - R$, i.e. the Kruskal-Szekeres outgoing null coordinate. From the way it is set up, the Unruh vacuum is expected to approximate the field configuration associated with a real gravitational collapse leading to the final formation of a black hole. Evidently, this corresponds to a configuration where the black hole did not exist in the distant past and has achieved a final stationary configuration in the future. By contrast, the Boulware state fails to model this expected physical outcome – this is the reason why it has only been proposed via a thought experiment for HBAR radiation.

6.1. Radiation field entropy: HBAR entropy flux

One of the straightforward consequences of the von Neumann entropy definition (5) is its rate of change, known as the entropy flux, which is given by

$$\dot{S} = -\mathrm{Tr}\left[\dot{\rho} \ln \rho\right]. \tag{86}$$

This rate allows the extension of steady-state properties to nonequilibrium states, and their information-theoretical measures. Specifically, Equation (86) directly applies to our case study: particles falling into a black hole, and their concomitant HBAR field, i.e. it gives the entropy flux of their 'photons' or field quanta. As in Section 5.3, a thermal steady-state density matrix can be directly obtained from near-horizon CQM, under the most general initial conditions and types of black holes. This is the horizon brightened acceleration radiation (HBAR) entropy in Ref. [55].

The HBAR entropy flux, from the general von Neumann expression of Equation (86), can be computed by evaluating the operator trace via

$$\dot{S}_{\mathcal{P}} = -\sum_{\{n\}} \dot{\rho}_{\text{diag}}(\{n\}) \ln\Big[\rho_{\text{diag}}(\{n\})\Big] = -\sum_{n_1,n_2,\dots} \dot{\rho}_{n_1,n_2,\dots;n_1,n_2,\dots} \ln \rho_{n_1,n_2,\dots;n_1,n_2,\dots}, \tag{87}$$

which is a diagonal sum over all the states $\{n\}$ for all the field modes. If, in addition, the system is near a steady-state configuration, the leading order of Equation (87) is given by approximating the logarithm of the density matrix, with the value $\rho^{(SS)}_{\text{diag}}$ from Equation (85):

$$\dot{S}_{\mathcal{P}} \approx -\sum_{\{n\}} \dot{\rho}_{\text{diag}}(\{n\}) \ln\Big[\rho^{(SS)}_{\text{diag}}(\{n\})\Big] = -\sum_{j}\sum_{\{n\}} \dot{\rho}_{\text{diag}}(\{n\}) \ln \rho^{(SS)}_{n_j,n_j}, \tag{88}$$

which involves a reversal in the order of the sums and the explicitly factorised form of the HBAR density matrix (85). Then, the thermal nature of the steady-state density matrix $\rho^{(SS)}_{\text{diag}}$ converts Equation (88) into

$$\dot{S}_{\mathcal{P}} \approx \sum_{j}\sum_{\{n\}} \dot{\rho}_{\text{diag}}(\{n\})\big[n_j\beta\tilde{\omega}_j - \ln\left(1 - e^{-\beta\tilde{\omega}_j}\right)\big]. \tag{89}$$

The sums are constrained by two conditions: the trace normalisation $\text{Tr}[\rho] = 1$ and the dynamic generalisation of the occupation-number averages

$$\langle n_j\rangle \equiv \sum_{\{n\}} n_j\, \rho_{\text{diag}}(\{n\}), \tag{90}$$

where these quantities $\langle n_j\rangle \equiv \langle n_{\boldsymbol{s}}\rangle$ are defined for each set of field-mode numbers $\boldsymbol{s} = \{\tilde{\omega}, l, m\}$. In Equation (90), the averages $\langle n_j\rangle$ are not simply given by the steady-state average occupation numbers $\langle n_j\rangle^{(SS)} = (e^{\beta\tilde{\omega}_j} - 1)^{-1}$ or the exact Planck distribution, but they include a modification that guarantees a nonzero flux through $\dot{\langle n_{\boldsymbol{s}}\rangle} \neq 0$. In addition, to the same order, the constant trace normalisation yields the vanishing of the second-term in Equation (89). Thus, the entropy flux is given by

$$\dot{S}_{\mathcal{P}} \approx \beta_H \sum_{\boldsymbol{s}=\{\tilde{\omega},l,m\}} \dot{\langle n_{\boldsymbol{s}}\rangle}\, \tilde{\omega} = \frac{2\pi}{\kappa} \sum_{\boldsymbol{s}=\{\tilde{\omega},l,m\}} \dot{\langle n_{\boldsymbol{s}}\rangle}\, \tilde{\omega}, \tag{91}$$

which can be written in terms of the unique Hawking temperature (83) as geometrical surface gravity; in geometrised units

$$T_H = \beta_H^{-1} = \frac{\kappa}{2\pi}. \tag{92}$$

Equation (91) can be interpreted physically in terms of the photons of the acceleration radiation: the product $\dot{\langle n_{\boldsymbol{s}}\rangle}\, \tilde{\omega}$ is the energy flux of the field quanta at a given frequency. In the more general type of black holes with rotation (Kerr geometry), the photon energies in Equation (91) are measured in the corotating frame: $\tilde{\omega} = \omega - \Omega_H m$, which involve the energy ω (measured by an asymptotic observer) and the axial component m of the field angular momentum (along the black hole's rotational axis) coupled to the black hole's angular momentum Ω_H. Thus, the net corotating energy flux is

$$\dot{\tilde{E}}_{\mathcal{P}} = \sum_{s=\{\tilde{\omega},l,m\}} \langle \dot{n_s} \rangle \, \tilde{\omega} = \sum_{s=\{\tilde{\omega},l,m\}} \langle \dot{n_s} \rangle \, (\omega - \Omega_H m) = \dot{E}_{\mathcal{P}} - \Omega_H \dot{J}_{\mathcal{P},z}, \tag{93}$$

which consists of a combination of the change in the total energy $E_{\mathcal{P}}$ and axial angular momentum $J_{\mathcal{P},z}$ of the photons. This sequence of quantum conditions leads to a compact formula for the HBAR von Neumann entropy flux,

$$\dot{S}_{\mathcal{P}} = \beta_H(\dot{E}_{\mathcal{P}} - \Omega_H \dot{J}_{\mathcal{P},z}) = \beta_H \dot{\tilde{E}}_{\mathcal{P}}. \tag{94}$$

Or, in terms of thermodynamic changes,

$$\delta S_{\mathcal{P}} = \beta_H(\delta E_{\mathcal{P}} - \Omega_H \, \delta J_{\mathcal{P},z}) \equiv \delta S_{\mathcal{P}}^{(\mathrm{th})}, \tag{95}$$

which is identical to the changes in the usual thermodynamic entropy $S_{\mathcal{P}}^{(\mathrm{th})}$.

In conclusion, fluxes and changes in the HBAR von Neumann and thermodynamic entropies of the radiation field coincide, governed by Equation (95). Incidentally, the same conclusions can be derived directly from the von Neumann entropy, $S = -\mathrm{Tr}[\rho \ln \rho]$, with the replacement of $\dot{\rho}_{\mathrm{diag}}(\{n\})$ by $\rho_{\mathrm{diag}}(\{n\})$ in Equations (88)–(90), leading to $S_{\mathcal{P}} = \beta(E_{\mathcal{P}} - F_{\mathcal{P}})$, in terms of the Helmholtz free energy $F_{\mathcal{P}}$ that satisfies $\beta F_{\mathcal{P}} = -\ln Z = \sum_j \ln(1 - e^{-\beta \tilde{\omega}_j})$ from Equation (85). The equivalence of entropies and entropy changes described by Equation (95) is ultimately due to the universal behaviour of the black hole as a temperature reservoir that has a *unique Hawking temperature* (92).

6.2. HBAR-black-hole thermodynamic correspondence

The HBAR entropy flux described by Equations (94) and (95) has a form structurally identical to the thermodynamic changes of the black hole itself,

$$\delta S_{\mathrm{BH}} = \beta_H(\delta M - \Omega_H \delta J), \tag{96}$$

which are expressed in terms of the black hole entropy S_{BH}, its mass M and its angular momentum J. Equation (96) relates the entropy and energy changes with the black hole rotational work as required by general relativistic and thermodynamic arguments only; in particular, the combination

$$\delta \tilde{M} = \delta M - \Omega_H \delta J \tag{97}$$

is the black hole corotating energy change.

On the other hand, the celebrated black-hole Bekenstein-Hawking entropy (9), as mentioned in Section 1, involves the geometrical area of the event horizon [39,40]; in Planck units, it takes the form

$$S_{\mathrm{BH}} = \frac{1}{4} A, \tag{98}$$

so that

$$\delta S_{\text{BH}} = \frac{1}{4}\,\delta A. \tag{99}$$

It is noteworthy that, while various thermodynamic and quantum calculations indicate that there exists a proportionality between entropy and area, the correct value 1/4 of the proportionality constant cannot be obtained by simple arguments. However, the specific value of the Hawking temperature (83): $T_H = \beta_H^{-1} = \kappa/2\pi$, driven by quantum-mechanical radiation effects, does uniquely fix the proportionality prefactor [36,37]. Moreover, these results are known to be valid for all black holes, including their angular momentum. As summarised in Appendix 2, the black-hole area changes, accounting for the Hawking temperature (83), are geometrically determined to be [153]

$$\delta A = 4\beta_H(\delta M - \Omega_H \delta J). \tag{100}$$

In effect, Equation (100) follows from the geometric area change of Equation (A27) combined with the Hawking temperature (83), and the substitution (97). Therefore, the required generic black hole entropy changes (96) are indeed enforced with the Bekenstein-Hawking entropy (98) with a numerical factor 1/4.

These remarkable results reveal an *HBAR-black-hole correspondence* that extends the familiar *universal thermodynamic relations* inherent to the black hole: the Hawking temperature and the Bekenstein-Hawking entropy. The following properties capture the essence of this correspondence, including the rationale for its existence.

- First, the intrinsic thermodynamic nature of the temperature and its role in thermal equilibrium lead to the *unique Hawking temperature* (92), which is both geometrical and quantum-mechanical, and is common to both the black hole itself and the HBAR radiation field.
- Second, for the entropy, energy, and angular momentum variables, the *analog fundamental thermodynamic relations*, Equations (95) and (96), provide a rigorous thermodynamic correspondence

$$\left(S_{\mathcal{P}}, E_{\mathcal{P}}, J_{\mathcal{P},z}\right) \overset{\beta=\beta_H}{\longleftrightarrow} (S_{\text{BH}}, M, J). \tag{101}$$

  Moreover, this correspondence can be generalised to subsume any other relevant degrees of freedom consistent with no-hair theorems [153]; in particular, this includes charged black holes (Kerr-Newman geometry in 4D), with an additional charge variable.
- Third, the HBAR-field and the black hole entropies are governed by the common *near-horizon conformal symmetry of CQM*, which determines the characteristic temperature, as seen in the steps leading to Equation (83). This is the ultimate reason why the quantum field appears to mirror the black hole degrees of freedom in thermal equilibrium.
- Fourth, the HBAR-black-hole thermodynamic correspondence (101) and the Bekenstein-Hawking entropy-area relation of Equation (99) imply the existence of an analog

entropy-area relation for the HBAR entropy,

$$\dot{S}_{\mathcal{P}} = \frac{1}{4}|\dot{A}_{\mathcal{P}}|, \tag{102}$$

where $|\dot{A}_{\mathcal{P}}|$ is the absolute value of the change in the event-horizon area due to the emission of acceleration radiation.

This shows, *inter alia*, that, once the temperature is fixed, there is a unique entropy-area relation, with a proportionality prefactor equal to 1/4.

- Finally, even though the HBAR field is not the better known Hawking radiation, as seen far from the black hole, they both have identical properties: thermal nature and characterised by the same Hawking temperature $T_H = \kappa/2\pi$. As a result, the HBAR-black-hole correspondence enlarges Equation (101) with the additional mapping

$$(\text{HBAR field}) \overset{\beta=\beta_H}{\longleftrightarrow} (\text{Hawking radiation}). \tag{103}$$

Some final remarks are in order for context. Regarding the proof of the HBAR area-entropy-flux relation (102), first proposed in Ref. [55], it is structurally mandated by the HBAR-black-hole thermodynamic correspondence (101) and the Bekenstein-Hawking relation (99). However, a more direct proof follows by evaluating the area changes (100) leading to Equation (100), which have an absolute value

$$|\dot{A}| = 4\beta_H|\dot{\tilde{M}}|, \tag{104}$$

with the corotating energy change $\dot{\tilde{M}} = \dot{M} - \Omega_H \dot{J}$ as in Equation (97). Now, the contribution to $|\dot{\tilde{M}}|$ due to photon emission is the corotating energy flux (93): $|\dot{\tilde{M}}| = \dot{\tilde{E}}_{\mathcal{P}}$, which leads to the change associated with acceleration radiation:

$$|\dot{A}_{\mathcal{P}}| = 4\beta_H \dot{\tilde{E}}_{\mathcal{P}} = 4\dot{S}_{\mathcal{P}}, \tag{105}$$

where Equation (94) is used as a last step. Equation (105) amounts to the area-entropy-flux relation (103).

One important qualification of the statements above is that the HBAR radiation is mediated by the interaction of the field with the atoms. The energy and angular momentum transfers between the black hole, atoms, and field satisfy conservation laws, which can be expressed as a single energy conservation statement

$$(\delta M - \Omega_H \delta J) + \delta\tilde{E}_{\mathcal{P}} + \delta\tilde{E}_{\mathcal{A}} = 0, \tag{106}$$

where $\delta\tilde{E}_{\mathcal{P}}$ and $\delta\tilde{E}_{\mathcal{A}}$ are the field and atom corotating energy changes, i.e. their values in the frame corotating with the black hole. Thus, the black hole area change can be regarded as arising from two distinct contributions,

$$\dot{A} = \dot{A}_{\mathcal{P}} + \dot{A}_{\mathcal{A}}, \tag{107}$$

including one part associated with the atoms, $\dot{A}_{\mathcal{A}} = -4\beta_H \dot{\tilde{E}}_{\mathcal{A}}$. As a result, the area change $\dot{A}_{\mathcal{P}}$ associated with the HBAR radiation field in the area-entropy-flux relation (103): (i) is only a fraction of the total change in the black hole area; (ii) has a sign reversal (a positive corotating energy corresponds to a decrease in the area of the black hole). The corresponding increase in the HBAR entropy is still consistent with the generalised second law of thermodynamics (GSL), which involves the total sum of the entropies and not to the entropy of the black hole or of the radiation field alone. The atoms falling into the black hole have $\delta\tilde{E}_{\mathcal{A}} < 0$ with a corresponding area increase $\delta A_{\mathcal{A}} > 0$. For nonrelativistic atoms the overall area of the black hole does increase. Finally, the generalised second law of thermodynamics, $\delta S_{\text{total}} = \delta S_{\text{BH}} + \delta S_{\mathcal{A}} + \delta S_{\mathcal{P}} \geq 0$, leads to

$$\delta S_{\mathcal{A}} \geq \beta_H(\delta E_{\mathcal{A}} - \Omega_H\, \delta J_{\mathcal{A},z}), \tag{108}$$

and all the previous statements are compatible with this condition.

In short, the HBAR and Hawking radiation fields have many properties of quantum nature in common. In some sense, they are analogue systems that require a black hole, even though their origin is different, with HBAR being fed by an atomic cloud mediating the radiation process. For fairly generic random-injection conditions, both phenomena, when probed far from the black hole, have formally identical properties. Finally, the HBAR area-entropy-flux relation (103), along with the broader HBAR-black hole correspondence defined by Equations (102) and (104) are insightful result results that point to a *deep connection between the radiation field and the black hole itself*, and they both appear to be *governed by near-horizon conformal symmetry.*

7. Conclusions: frontiers of quantum knowledge and HBAR proposals

The emergence of a quantum-thermodynamic framework for black holes is a remarkable development that has made explicit the subtle interplay between quantum physics and relativistic spacetime following the seminal discoveries of Refs. [34,36,37,39–41], and with similar results for accelerated systems [42–45]. As a result, one cannot overstate the central role played by black hole thermodynamics and the Hawking effect in the frontiers of contemporary theoretical physics. The fact that quantum physics is compatible with gravity in a semiclassical limit is a nontrivial test of robustness that points to a possible theory of quantum gravity. Most importantly, the paradoxes involved by the standard Hawking effect and the black hole information paradox are topics of current interest [190–193] that suggest further compatibility via quantum information theory – but this still remains an open problem.

7.1. Network of quantum connections

In this review article, we offered a comprehensive overview of various aspects of such framework of *quantum thermodynamics* [187,188] and *quantum information* [22,23,32,33], in connection with the acceleration radiation emitted by particles in a near-horizon black hole background. Some of the highlights of this review article involve the following conceptual points.

- There exists a tight network of connections between quantum field theory, spacetime physics, and quantum optics.
- The complete framework involves thermodynamic and quantum-information features that generalise the more familiar flat-spacetime relations. Thus, this is an ideal

laboratory to explore subtle conceptual and technical features of quantum physics – making this a suitable topic to highlight a century of stunning achievements of quantum mechanics.

- In this relational setting, we reviewed a variety of successful techniques that have provided conceptual and computational tools for the physics of accelerated systems and gravitational backgrounds, including black holes. These techniques include both standard quantum field theory tools and an arsenal of related methods developed in the context of quantum optics.
- The theory of open quantum systems, with the density matrix as central object, plays a dominant role in describing the ensuing thermodynamic and information-theoretic framework.
- Specifically, the acceleration radiation due to the fall of particles in a Boulware vacuum can be studied as a thought experiment with a field vacuum configuration enforced by boundary setups similar to laser cavities around the black hole. Such Boulware-vacuum configurations amount to a cavity that is accelerated in a relativistic sense near the event horizon of black hole, generating a relative acceleration between the field and falling particles. The ensuing radiation is known as horizon-brightened acceleration radiation (HBAR).
- The HBAR field leads to a full-fledged form of HBAR thermodynamics that is in one-to-one correspondence with black hole thermodynamics.
- Specifically, HBAR thermodynamics includes a characterisation of both temperature and entropy, as well as the creation of radiation with formal analogies with Hawking radiation. The conclusion of this analysis is that the black hole acts as a reservoir with the same manifestations as in its development of standard black hole thermodynamics.

7.2. Experimental realisations

It should be stressed that the relevant experiment realising an HBAR field with astronomical black holes involves mirrors and cavities in black hole backgrounds. This may not be experimentally feasible in the foreseeable future. However, *in the best tradition of a gedanken experiment*, it does provide deep insights into and theoretical tests of black hole thermodynamics. On the other hand, one may evaluate possible experimental realisations of this thought experiment. Such realisations can be classified into two categories.

- *Black-hole analog systems.* As the study of black-hole analog systems in the lab continues to evolve [194,195], it might be possible to test some of these ideas in Earth-based labs with such black-hole analogs in the not-too-distant future. However, at present, no specific realisations of this kind, i.e. simulating a black hole, have been offered.
- *Equivalent systems that simulate relative acceleration.* As discussed in the introduction, there is vast literature dealing with mirrors and cavities involving various forms of acceleration [56–62]. A specific proposal is discussed below, in which accelerated mirrors can simulate physics equivalent to the HBAR field emission.

The most basic equivalent system that simulates relative acceleration was proposed in the original seminal paper of Ref. [55]. This is illustrated by the comparison of three configurations in Figure 10. The uniformly accelerated mirror (configuration B) produces an equivalent radiation spectrum to that of standard HBAR (configuration C); and these are distinctly different from a system where the atoms are accelerated and the field is stationary (configuration A). This equivalence is an example of the so-called relative equivalence principle discussed in [61,62]. As pointed out in Ref. [196], there is a specific laboratory dynamical-Casimir setup that can ideally reproduce the radiation field of HBAR: a superconducting transmission line microwave cavity terminated by a SQUID and coupled to an ensemble of polar molecules. This is a third equivalent system that would simulate the physics of an accelerating mirror [197–199] and a two-level atom [200]. Effectively, the SQUID simulates the same boundary condition as the moving mirror [199], with a large effective acceleration $a \gg c\omega$, where ω is the microwave-photon frequency. In this setup, a two-level atom can be replaced by a large ensemble of polar molecules trapped closed to the transmission line surface; the end result is an excitation probability of the order of $P \sim 10^{-2}$ under a reasonable choice of parameters. It is conceivable that similar proposals may lead to empirical verifications of the main physics associated with horizon-brightened acceleration radiation.

7.3. Further developments

It is also noteworthy that progress has been made in the study of acceleration radiation and HBAR entropy in a variety of black hole backgrounds. This includes an early study of HBAR radiation for detectors moving along null geodesics [201]; and a variety of extensions to other stringy and braneworld black holes [202,203], in quantum-corrected black hole geometries [204–206], and with a derivative coupling [207].

Finally, the techniques discussed in this review, from the generic quantum optics tools to the specific applications of HBAR, can be used in various extensions of the theory for a variety of gravitational backgrounds and arbitrary distributions of detectors and mirrors,

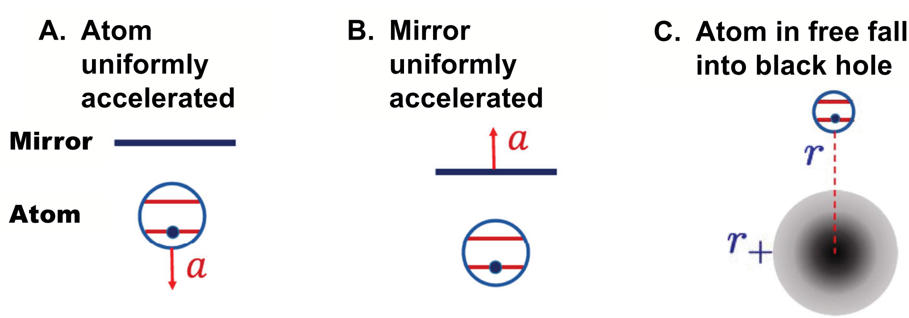

Figure 10. In the relative equivalence principle, configurations B and C are equivalent as they both involve an accelerated background field and a stationary atom. Configuration C is the standard HBAR setup, where these are relativistic covariant concepts and the field is arranged as a Boulware vacuum.

as well as other possible applications. As in some of the recent references [67–70], these analyses help clarify deep conceptual problems and point to the resolution of apparent paradoxes in relativistic systems and relativistic quantum information.

Acknowledgments

H.E.C. thanks Prof. C. A. García Canal for insightful comments.

Disclosure statement

No potential conflict of interest was reported by the author(s).

Funding

This material is based upon work supported by the Air Force Officeof Scientific Research under Grant No. FA9550-21-1-0017 (C.R.O. and A.C.).C.R.O. was partially supported by the Army Research Office (ARO), grantW911NF-23-1-0202. H.E.C. acknowledges support by the University of SanFrancisco Faculty Development Fund. M.S. work was supported by U.S. Departmentof Energy (DE-SC-0023103, FWP-ERW7011, DE-SC0024882); Welch Foundation(A-1261); National Science Foundation (PHY-2013771); Air Force Office ofScientific Research (FA9550-20-1-0366). W.U. thanks the Natural Sciences andEngineering Research Council of Canada (NSERC) (Grant No. 5 80441), and the TAMUHagler Institute for Advanced Studies for their support.

ORCID

C. R. Ordóñez http://orcid.org/0009-0003-2867-6037
A. Chakraborty https://orcid.org/0000-0001-7487-9925
H. E. Camblong https://orcid.org/0000-0001-5148-6782

References

[1] M. Jammer, *The Conceptual Development of Quantum Mechanics*, McGraw-Hill, New York, 1966.
[2] J. Mehra and H. Rechenberg, *The Historical Development of Quantum Theory*, Springer, New York, 1982.
[3] B.L. van der Waerden (ed.), *Sources of Quantum Mechanics*, Dover, New York, 1967.
[4] E. Schrödinger, *Collected Papers on Wave Mechanics*, translated from the second German edition by J.F. Shearer and W.M. Deans, eds., Blackie and Son, London, 1928.
[5] S. Weinberg, *Lectures on Quantum Mechanics*, Cambridge University Press, Cambridge, UK, 2015.
[6] S. Weinberg, *The Quantum Theory of Fields, Vol. 1: Foundations*, Cambridge University Press, Cambridge, UK, 2005.
[7] W. Heisenberg, *Über quantentheoretische Umdeutung kinematischer und mechanischer Beziehungen*, Z. Phys 33 (1925), pp. 879–893. [English translation: *On the quantum-theoretical reinterpretation of kinematical and mechanical relationship* in Ref. [3].]
[8] M. Born and P. Jordan, *Zur quantenmechanik*, Z. Phys. 34 (1925), pp. 858–888. [English translation: *On quantum mechanics*, in Ref. [3].]
[9] M. Born, W. Heisenberg, and P. Jordan, *Zur quantenmechanik II*, Z. Phys. 35 (1925), pp. 557–615. [English translation: *On quantum mechanics II*, in Ref. [3].]

[10] E. Schrödinger, *Quantisierung als Eigenwertproblem (Erste Mitteilung)*, Ann. Phys. (Leipzig) 384 (1926), pp. 361–376. Zweite Mitteilung. 384 (1926), p. 489; Dritte Mitteilung, 385 (1926), p. 437; Vierte Mitteilung, 386 (1926), p. 109. [English translation: *Quantization as an eigenvalue problem (first, second, third, and fourth communications)*, in Ref. [4].]
[11] E. Schrödinger, *An undulatory theory of the mechanics of atoms and molecules*, Phys. Rev. 28 (1926), pp. 1049–1070.
[12] P.A.M. Dirac, *The Principles of Quantum Mechanics*, Oxford University Press, Oxford, England, 1930.
[13] P.A.M. Dirac, *A new notation for quantum mechanics*, Math. Proc. Camb. Philos. Soc. 35 (1939), pp. 416–418.
[14] W. Heisenberg, *Über den anschaulichen Inhalt der quantentheoretischen Kinematik und Mechanik*, Z. Phys. 43 (1927), pp. 172–198. [English translation: *On the perceptual content of quantum theoretical kinematics and mechanics* in Ref. [3].]
[15] E. Schrödinger, *Über das Verhältnis der Heisenberg-Born-Jordanschen Quantenmechanik zu der meinen*, Ann. Phys. (Leipzig) 384 (1926), pp. 734–756. [English translation: *On the relation between the quantum mechanics of Heisenberg, Born and Jordan and that of Schrödinger*, in Ref. [4].]
[16] P.A.M. Dirac, *The physical interpretation of the quantum dynamics*, Proc. Roy. Soc. London A 113 (1927), pp. 621–641.
[17] J. von Neumann, *Mathematische Grundlagen der Quantenmechanik*, Springer, Berlin, 1932. [English Translation: R.T. Beyer, *Mathematical Foundations of Quantum Mechanics*, Princeton University Press, Princeton, 1955.]
[18] J. von Neumann, Mathematische Begründung der Quantenmechanik ["Mathematical Foundation of Quantum Mechanics"]. Gött. Nachr. Math. Phys. Klass. 1927 (1927), pp. 1–57.
[19] J. von Neumann, Wahrscheinlichkeitstheoretischer Aufbau der Quantenmechanik ["Probabilistic theory of quantum mechanics"]. Gött. Nachr. Math. Phys. Klass. 1927 (1927), pp. 245–272.
[20] J. von Neumann, Thermodynamik quantenmechanischer Gesamtheiten ["Thermodynamics of Quantum Mechanical Quantities"]. Gött. Nachr. Math. Phys. Klass. 1927 (1927), pp. 273–291.
[21] L. Landau, *Das Dämpfungsproblem in der Wellenmechanik*, Z. Phys. 45 (1927), pp. 430–441. [English translation: *The damping problem in wave mechanics* in *Collected Papers of L. D. Landau*, Pergamon Press, Oxford, England, 1965, pp. 8–18.]
[22] M.A. Nielsen and I.L. Chuang, *Quantum Computation and Quantum Information*, Cambridge University Press, Cambridge, 2000.
[23] R.J. Lewis-Swan, A. Safavi-Naini, A.M. Kaufman, and A.M. Rey, *Dynamics of quantum information*, Nat. Rev. Phys. 1 (2019), pp. 627–634.
[24] P.A.M. Dirac, *The quantum theory of the emission and absorption of radiation*, Proc. R. Soc. Lond. A 114 (1927), pp. 243–265.
[25] N.D. Birrell and P.C.W. Davies, *Quantum Fields in Curved Space*, Cambridge University Press, Cambridge, 1984.
[26] T.Y. Cao, *Conceptual Developments of 20th Century Field Theories*, Cambridge University Press, Cambridge, 1998.
[27] S. Weinberg, *The making of the standard model*, Eur. Phys. J. C 34 (2004), pp. 5–13.
[28] P.A.M. Dirac, The Lagrangian in quantum mechanics. Phys. Z. Sowjetunion 3 (1933), pp. 64–72.
[29] R.P. Feynman, *Space-time approach to non-relativistic quantum mechanics*, Rev. Mod. Phys. 20 (1948), pp. 367–387.
[30] H. Kleinert, *Path Integrals in Quantum Mechanics, Statistics, Polymer Physics, and Financial Markets*, 5th ed., World Scientific, Singapore, 2009. and references therein.
[31] C. Grosche and F. Steiner, *Handbook of Feynman Path Integrals*, Springer-Verlag, Berlin, 1998. and references therein.

[32] A. Peres and D.R. Terno, *Quantum information and relativity theory*, Rev. Mod. Phys. 76 (2004), pp. 93–123.
[33] R.B. Mann and T.C. Ralph, *Relativistic quantum information*, Class. Quantum Gravity 29 (2012), p. 220301.
[34] S.W. Hawking, *Black holes and thermodynamics*, Phys. Rev. D 13 (1976), pp. 191–197.
[35] R.M. Wald, The thermodynamics of black holes. Living Rev. Rel. 4 (2001), p. 6.
[36] S.W. Hawking, *Black hole explosions?* Nature 248 (1974), pp. 30–31.
[37] S.W. Hawking, *Particle creation by black holes*, Commun. Math. Phys. 43 (1975), pp. 199–220.
[38] S. Carroll, *Spacetime and Geometry: An Introduction to General Relativity*, Addison-Wesley, San Francisco, CA, 2003.
[39] J.D. Bekenstein, *Black holes and the second law*, Lett. Nuovo Cimento 4 (1972), pp. 737–740.
[40] J.D. Bekenstein, *Black holes and entropy*, Phys. Rev. D 7 (1973), pp. 2333–2346.
[41] J.M. Bardeen, B. Carter, and S.W. Hawking, *The four laws of black hole mechanics*, Commun. Math. Phys. 31 (1973), pp. 161–170.
[42] S.A. Fulling, *Nonuniqueness of canonical field quantization in Riemannian space-time*, Phys. Rev. D 7 (1973), pp. 2850–2862.
[43] P.C.W. Davies, *Scalar production in Schwarzschild and Rindler metrics*, J. Phys. A 8 (1975), pp. 609–616.
[44] W.G. Unruh, *Notes on black-hole evaporation*, Phys. Rev. D 14 (1976), pp. 870–892.
[45] P.C.W. Davies, S.A. Fulling, and W.G. Unruh, *Energy-momentum tensor near an evaporating black hole*, Phys. Rev. D 13 (1976), pp. 2720–2723.
[46] C. Kiefer, *Quantum Gravity*, 3rd ed., Oxford University Press, Oxford, UK, 2012.
[47] M.O. Scully and M.S. Zubairy, *Quantum Optics*, Cambridge University Press, New York, 1997.
[48] P. Meystre and M. Sargent III, *Elements of Quantum Optics*,. 4th ed., Springer, Berlin, 2007.
[49] E.R. Pike and S. Sarkar, *The Quantum Theory of Radiation*, Oxford University Press, Oxford, UK, 1996.
[50] G. Compagno, R. Passante, and F. Persico, *Atom-Field Interactions and Dressed Atoms*, Cambridge Studies in Modern Optics, Cambridge University Press, Cambridge, UK, 1995.
[51] M.O. Scully, V.V. Kocharovsky, A. Belyanin, E. Fry, and F. Capasso, *Enhancing acceleration radiation from ground state-atoms via cavity quantum electrodynamics*, Phys. Rev. Lett. 91 (2003), p. 243004.
[52] A. Belyanin, V.V. Kocharovsky, F. Capasso, E. Fry, M.S. Zubairy, and M.O. Scully, *Quantum electrodynamics of accelerated atoms in free space and in cavities*, Phys. Rev. A 74 (2006), p. 023807.
[53] M.O. Scully, V.V. Kocharovsky, A. Belyanin, E. Fry, and F. Capasso, *Reply to comment on "Enhancing acceleration radiation from ground-state atoms via cavity quantum electrodynamics" B. L. Hu and Albert Roura*, Phys. Rev. Lett. 93 (2004), p. 129302. [Phys. Rev. Lett. **93**, 129301 (2004)]
[54] J. Audretsch and R. Müller, *Localized discussion of stimulated processes for Rindler observers and accelerated detectors*, Phys. Rev. D 49 (1994), pp. 4056–4065.
[55] M.O. Scully, S. Fulling, D.M. Lee, D.N. Page, W.P. Schleich, and A.A. Svidzinsky, *Quantum optics approach to radiation from atoms falling into a black hole*, Proc. Natl. Acad. Sci. U.S.A. 115 (2018), pp. 8131–8136.
[56] S.A. Fulling and P.C.W. Davies, *Radiation from a moving mirror in two dimensional space-time: Conformal anomaly*, Proc. R. Soc. Lond. A 348 (1976), pp. 393–414.
[57] P.C.W. Davies and S.A. Fulling, *Quantum vacuum energy in two dimensional space-times*, Proc. R. Soc. Lond. A 354 (1977), pp. 59–77.
[58] P.R. Anderson, M.R.R. Good, and C.R. Evans, *Black hole – moving mirror I: An exact correspondence*, in *14th Marcel Grossmann Meeting on Recent Developments in Theoretical and Experimental General Relativity, Astrophysics, and Relativistic Field Theories (MG14): Rome, Italy*, Vol. 2, 2017, pp. 1701–1704.

[59] M.R.R. Good, P.R. Anderson, and C.R. Evans, *Black hole – moving mirror II: Particle creation*, in *14th Marcel Grossmann Meeting on Recent Developments in Theoretical and Experimental General Relativity, Astrophysics, and Relativistic Field Theories (MG14): Rome, Italy*, Vol. 2, 2017, pp. 1705–1708.
[60] M.P.E. Lock and I. Fuentes, *Dynamical Casimir effect in curved spacetime*, New J. Phys. 19 (2017), p. 073005.
[61] S.A. Fulling and J.H. Wilson, *The equivalence principle at work in radiation from unaccelerated atoms and mirrors*, Phys. Scr. 94 (2018), p. 014004.
[62] J.S. Ben-Benjamin, M.O. Scully, S.A. Fulling, D.M. Lee, D.N. Page, A.A. Svidzinsky, M.S. Zubairy, M.J. Duff, R. Glauber, W.P. Schleich, and W.G. Unruh, *Unruh acceleration radiation revisited*, Int. J. Mod. Phys. A 34 (2019), p. 1941005.
[63] M.O. Scully, *Laser entropy: From lasers and masers to Bose condensates and black holes*, Phys. Scr.95 (2020), p. 024002.
[64] H.B.G. Casimir, On the attraction between two perfectly conducting plates. Indag. Math. 10 (1948), pp. 261–263.
[65] M. Bordag, G.L. Klimchitskaya, U. Mohideen, and V.M. Mostepanenko, *Advances in the Casimir Effect*, Vol. 145, Oxford University Press, Oxford, UK, 2009.
[66] G.T. Moore, *Quantum theory of the electromagnetic field in a variable-length one-dimensional cavity*, J. Math. Phys. 11 (1970), pp. 2679–2691.
[67] V.V. Dodonov, *Fifty years of the dynamical Casimir effect*, MDPI Phys. 2 (2020), pp. 67–104.
[68] L.C.B. Crispino, A. Higuchi, and G.E.A. Matsas, *The Unruh effect and its applications*, Rev. Mod. Phys. 80 (2008), pp. 787–838.
[69] R. Passante, Dispersion interactions between neutral atoms and the quantum electrodynamical vacuum. Symmetry (Basel) 10 (2018), p. 735.
[70] S. Masood, A.S. Bukhari, and L.-G. Wang, *Atom-field dynamics in curved spacetime*, Front. Phys. 19 (2024), p. 54203.
[71] V. de Alfaro, S. Fubini, and G. Furlan, *Conformal invariance in quantum mechanics*, Nuovo Cimento A 34 (1976), pp. 569–612.
[72] H.E. Camblong and C.R. Ordóñez, *Renormalization in conformal quantum mechanics*, Phys. Lett. A 345 (2005), pp. 22–30.
[73] H.E. Camblong, L.N. Epele, H. Fanchiotti, and C.A. García Canal, *Renormalization of the inverse square potential*, Phys. Rev. Lett. 5 (2000), pp. 1590–1593.
[74] H.E. Camblong, L.N. Epele, H. Fanchiotti, and C.A. García Canal, *Quantum anomaly in molecular physics*, Phys. Rev. Lett. 87 (2001), p. 220402.
[75] H.E. Camblong, L.N. Epele, H. Fanchiotti, C.A. García Canal, and C.R. Ordóñez, *Effective field theory program for conformal quantum anomalies*, Phys. Rev. A 72 (2005), p. 032107.
[76] H.E. Camblong and C.R. Ordóñez, *Anomaly in conformal quantum mechanics: From molecular physics to black holes*, Phys. Rev. D 68 (2003), p. 125013.
[77] H.E. Camblong and C.R. Ordóñez, *Black hole thermodynamics from near-horizon conformal quantum mechanics*, Phys. Rev. D 71 (2005), p. 104029.
[78] H.E. Camblong and C.R. Ordóñez, *Semiclassical methods in curved spacetime and black hole thermodynamics*, Phys. Rev. D 71 (2005), p. 124040.
[79] H.E. Camblong and C.R. Ordóñez, Conformal enhancement of holographic scaling in black hole thermodynamics: A near-horizon heat-kernel framework. J. High Energy Phys. 12 (2007), p. 099.
[80] H.E. Camblong and C.R. Ordóñez, *Conformal tightness of holographic scaling in black hole thermodynamics*, Classical Quantum Gravity 30 (2013), p. 175007.
[81] H.E. Camblong, A. Chakraborty, and C.R. Ordóñez, *Near-horizon aspects of acceleration radiation by free fall of an atom into a black hole*, Phys. Rev. D 102 (2020), p. 085010.
[82] A. Azizi, H.E. Camblong, A. Chakraborty, C.R. Ordóñez, and M.O. Scully, *Acceleration radiation of an atom freely falling into a Kerr black hole and near-horizon conformal quantum mechanics*, Phys. Rev. D 104 (2021), p. 065006.

[83] A. Azizi, H.E. Camblong, A. Chakraborty, C.R. Ordóñez, and M.O. Scully, *Quantum optics meets black hole thermodynamics via conformal quantum mechanics. I. Master equation for acceleration radiation*, Phys. Rev. D 104 (2021), p. 084086.
[84] A. Azizi, H.E. Camblong, A. Chakraborty, C.R. Ordóñez, and M.O. Scully, *Quantum optics meets black hole thermodynamics via conformal quantum mechanics: II. Thermodynamics of acceleration radiation*, Phys. Rev. D 104 (2021), p. 084085.
[85] C.W. Misner, K.S. Thorne, and J.A. Wheeler, *Gravitation*, W. H. Freeman and Co., San Francisco, CA, 1973.
[86] D.G. Boulware, *Quantum field theory in Schwarzschild and Rindler spaces*, Phys. Rev. D 11 (1975), pp. 1404–1423.
[87] R. Brout, S. Massar, R. Parentani, and Ph. Spindel, *A primer for black hole quantum physics*, Phys. Rep. 260 (1995), pp. 329–446.
[88] A. Fabbri and J. Navarro-Salas, *Modeling Black Hole Evaporation*, World Scientific, Singapore, 2005.
[89] S. Takagi, *Vacuum noise and stress induced by uniform acceleration: Hawking-Unruh effect in Rindler manifold of arbitrary dimension*, Progr. Theor. Phys, Suppl. 88 (1986), pp. 1–142.
[90] R.M. Wald, *General Relativity*, University of Chicago Press, Chicago, 1984.
[91] G.D. Mahan, *Many-Particle Physics, Physics of Solids and Liquids*, 3rd ed., Springer, New York, 2000.
[92] P. Jordan and E. Wigner, *Über das Paulische Äquivalenzverbot ["On the Pauli Exclusion Principle"]*, Z. Phys. 47 (1928), pp. 631–651.
[93] V.A. Fock, *Konfigurationsraum und zweite Quantelung*, Z. Phys. 75 (1932), pp. 622–647. [English translation: *Configuration space and second quantization*, in *V.A. Fock – Selected Works: Quantum Mechanics and Quantum Field Theory*, L.D. Faddeev, L.A. Khalfin, and I.V. Komarov, eds., CRC Press, 2004, p. 191.]
[94] I.I. Rabi, *On the process of space quantization*, Phys. Rev. 49 (1936), pp. 324–328.
[95] I.I. Rabi, *Space quantization in a gyrating magnetic field*, Phys. Rev. 51 (1937), pp. 652–654.
[96] T. Jaynes and F.W. Cummings, *Comparison of quantum and semiclassical radiation theories with application to the beam maser*, Proc. IEEE 51 (1963), pp. 89–109.
[97] B.W. Shore and P.L. Knight, *The Jaynes-Cummings Model*, J. Mod. Opt. 40 (1993), pp. 1195–1238.
[98] A.D. Greentree, J. Koch, and J. Larson, *Fifty years of Jaynes–Cummings physics*, J. Phys. B: At. Mol. Opt. Phys. 46 (2013), p. 220201.
[99] J. Larson, T. Mavrogordatos, S. Parkins, and A. Vidiella-Barranco, The Jaynes–Cummings model: 60 years and still counting. J. Opt. Soc. Am. B 41 (2024), pp. JCM1–JCM4.
[100] D. Braak, Q.H. Chen, M.T. Batchelor, and E. Solano, *Semi-classical and quantum Rabi models: In celebration of 80 years*, J. Phys. A 49 (2016), p. 300301.
[101] D. Braak, *Integrability of the Rabi model*, Phys. Rev. Lett. 107 (2011), p. 100401.
[102] Q.-H. Chen, C. Wang, S. He, T. Liu, and K.-L. Wang, *Exact solvability of the quantum Rabi model using Bogoliubov operators*, Phys. Rev. A 86 (2012), p. 023822.
[103] H. Zhong, Q. Xie, M.T. Batchelor, and C. Lee, *Analytical eigenstates for the quantum Rabi model*, J. Phys. A: Math. Theor. 46 (2013), p. 415302.
[104] A.J. Maciejewski, M. Przybylska, and T. Stachowiak, *Full spectrum of the Rabi model*, Phys. Lett. A 378 (2014), pp. 16–20.
[105] Q. Xie, H. Zhong, M.T. Batchelor, and C. Lee, *The quantum Rabi model: Solution and dynamics*, J. Phys. A: Math. Theor. 50 (2017), p. 113001.
[106] R.F. Bishop, N.J. Davidson, R.M. Quick, and D.M. van der Walt, *Application of the coupled cluster method to the Jaynes-Cummings model without the rotating-wave approximation*, Phys. Rev. A 54 (1996), pp. R4657–R4660.
[107] R.F. Bishop, N.J. Davidson, R.M. Quick, and D.M. van der Walt, *Variational results for the Rabi Hamiltonian*, Phys. Lett. A 254 (1999), pp. 215–224.
[108] R.F. Bishop and C. Emary, *Time evolution of the Rabi Hamiltonian from the unexcited vacuum*, J. Phys. A 34 (2001), pp. 5635–5651.

[109] V. Fessatidis, J.D. Mancini, and S.P. Bowen, *Moments expansion study of the Rabi Hamiltonian*, Phys. Lett. A 297 (2002), pp. 100–104.
[110] C. Emary, *Coupled cluster techniques and the Rabi Hamiltonian*, Int. J. Mod. Phys. B 17 (2003), pp. 5477–5481.
[111] A. Pereverzev and E.R. Bittner, Exactly solvable approximating models for Rabi Hamiltonian dynamics. Phys. Chem. Chem. Phys. 8 (2006), pp. 1378–1384.
[112] N. Debergh and A.B. Klimov, *Quasi-exactly solvable approach to the Jaynes-Cummings model without rotation wave approximation*, Int. J. Mod. Phys. A 16 (2001), pp. 4057–4068.
[113] E.K. Twyeffort Irish, *Generalized rotating-wave approximation for arbitrarily large coupling*, Phys. Rev. Lett. 99 (2207), p. 173601.
[114] T. Holstein, *Studies of polaron motion: Part I. The molecular-crystal model*, Ann. Phys. (N.Y.) 8 (1959), pp. 325–342.
[115] I. Chiorescu, P. Bertet, K. Semba, Y. Nakamura, C.J.P.M. Harmans, and J.E. Mooij, *Coherent dynamics of a flux qubit coupled to a harmonic oscillator*, Nature 431 (2004), pp. 159–162.
[116] A. Wallraff, D.I. Schuster, A. Blais, L. Frunzio, R.- S. Huang, J. Majer, S. Kumar, S.M. Girvin, and R.J. Schoelkopf, *Strong coupling of a single photon to a superconducting qubit using circuit quantum electrodynamics*, Nature 431 (2004), pp. 162–167.
[117] J. Johansson, S. Saito, T. Meno, H. Nakano, M. Ueda, K. Semba, and H. Takayanagi, *Vacuum Rabi oscillations in a macroscopic superconducting qubit* LC *oscillator system*, Phys. Rev. Lett. 96 (2006), p. 127006.
[118] D.I. Schuster, A.A. Houck, J.A. Schreier, A. Wallraff, J.M. Gambetta, A. Blais, L. Frunzio, J. Majer, B. Johnson, M.H. Devoret, S.M. Girvin, and R.J. Schoelkopf, *Resolving photon number states in a superconducting circuit*, Nature 445 (2007), pp. 515–518.
[119] K. Hennessy, A. Badolato, M. Winger, D. Gerace, M. Atatüre, S. Gulde, S. Fält, E.L. Hu, and A. Imamoğlu, *Quantum nature of a strongly coupled single quantum dot-cavity system*, Nature445 (2007), pp. 896–899.
[120] E.K. Twyeffort Irish and K. Schwab, *Quantum measurement of a coupled nanomechanical resonator–Cooper-pair box system*, Phys. Rev. B 68 (2003), p. 155311.
[121] A. Blais, A.L. Grimsmo, S.M. Girvin, and A. Wallraff, *Circuit quantum electrodynamics*, Rev. Mod. Phys. 93 (2021), p. 25005.
[122] R.J. Glauber, *The quantum theory of optical coherence*, Phys. Rev. 130 (1963), pp. 2529–2539.
[123] B.S. DeWitt, *Quantum gravity: The new synthesis*, in *General Relativity: An Einstein Centenary Survey*, S.W. Hawking and W. Israel, eds., Cambridge Press, Cambridge, UK, 1979.
[124] W.G. Unruh and R.M. Wald, *What happens when an accelerating observer detects a Rindler particle*, Phys. Rev. D 29 (1984), pp. 1047–1056.
[125] P.G. Grove and A.C. Ottewill, *Notes on 'particle detectors'*, J. Phys. A: Math. Gen. 16 (1983), pp. 3905–3920.
[126] S.-Y. Lin and B.L. Hu, *Backreaction and the Unruh effect: New insights from exact solutions of uniformly accelerated detectors*, Phys. Rev. D 76 (2007), p. 064008.
[127] E.G. Brown, E. Martín-Martínez, N.C. Menicucci, and R.B. Mann, *Detectors for probing relativistic quantum physics beyond perturbation theory*, Phys. Rev. D 87 (2013), p. 084062.
[128] D.E. Bruschi, A.R. Lee, and I. Fuentes, *Time evolution techniques for detectors in relativistic quantum information*, J. Phys. A: Math. Theor. 46 (2013), p. 165303.
[129] B.L. Hu, S.-Y. Lin, and J. Louko, *Relativistic quantum information in detectors–field interactions*, Classical Quantum Gravity 29 (2012), p. 224005.
[130] J. Foo, S. Onoe, and M. Zych, *Unruh-deWitt detectors in quantum superpositions of trajectories*, Phys. Rev. D 102 (2020), p. 085013.
[131] J.J. Sakurai and J. Napolitano, *Modern Quantum Mechanics*, 3rd ed., Cambridge University Press, Cambridge, England, 2020.
[132] H.-P. Breuer and F. Petruccione, *The Theory of Open Quantum Systems*, Oxford University Press, Oxford, England, 2002.

[133] P.A.M. Dirac, *The fundamental equations of quantum mechanics*, Proc. Roy. Soc. London A 109 (1925), pp. 642–653.
[134] A. Einstein, *Zur Quantentheorie der Strahlung*, Phys. Z. 18 (1917), pp. 121–128. [English translation: *On the quantum theory of radiation* in D. ter Haar, *The Old Quantum Theory*, Pergamon Press, Oxford, England, 1967, pp. 167–183.]
[135] T.H. Maiman, *Stimulated optical radiation in ruby*, Nature 187 (1960), pp. 493–494.
[136] M. Bertolotti, *Masers and Lasers: An Historical Approach*, 2nd ed., CRC Press, Boca Raton, 2015.
[137] R.J. Glauber, in *Quantum Optics and Electronics*, Les Houches, 1964, C. De Witt, A. Blandin, and C. Cohen Tannoudji, eds., Gordon and Breach, New York, 1965, p. 63.
[138] M.O. Scully and W.E. Lamb Jr., *Quantum theory of an optical maser*, Phys. Rev. Lett. 16 (1966), pp. 853–855.
[139] M.O. Scully and W.E. Lamb Jr., *Quantum theory of an optical maser. I. General theory*, Phys. Rev.159 (1967), pp. 208–226.
[140] H.J. Carmichael and D.F. Walls, *Modifications to the Scully-Lamb laser master equation*, Phys. Rev. A 9 (1974), pp. 2686–2697.
[141] J. Gea-Banacloche, *Emergence of classical radiation fields through decoherence in the Scully-Lamb laser model*, Found. Phys. 28 (1997), pp. 531–548.
[142] I.I. Arkhipov, A. Miranowicz, O.D. Stefano, R. Stassi, S. Savasta, F. Nori, and S.K. Özdemir, *Scully-Lamb quantum laser model for parity-time-symmetric whispering-gallery microcavities: Gain saturation effects and nonreciprocity*, Phys. Rev. A 99 (2019), p. 053806.
[143] F. Minganti, I.I. Arkhipov, A. Miranowicz, and F. Nori, *Liouvillian spectral collapse in the Scully-Lamb laser model*, Phys. Rev. Res. 3 (2021), p. 043197.
[144] V. DeGiorgio and M.O. Scully, Analogy between the laser threshold region and a second-order phase transition. Phys. Rev. A 2 (1970), pp. 1170–1177.
[145] M.O. Scully, *Condensation of N bosons and the laser phase transition analogy*, Phys. Rev. Lett. 82 (1999), pp. 3927–3931.
[146] V.V. Kocharovsky, M.O. Scully, S.Y. Zhu, and M.S. Zubairy, Condensation of N bosons. II. Nonequilibrium analysis of an ideal Bose gas and the laser phase-transition analogy. Phys. Rev. A 61 (2000), p. 023609..
[147] On Bose–Einstein condensation and Unruh–Hawking radiation from a quantum optical perspective: M.O. Scully, A. Svidzinsky, and W. Unruh, J. Low Temp. Phys. 208 (2022), p. 160; and references therein.
[148] S. Pielawa, G. Morigi, D. Vitali, and L. Davidovich, *Generation of Einstein-Podolsky-Rosen-entangled radiation through an atomic reservoir*, Phys. Rev. Lett. 98 (2007), p. 240401.
[149] S. Pielawa, L. Davidovich, D. Vitali, and G. Morigi, *Engineering atomic quantum reservoirs for photons*, Phys. Re. A 81 (2010), p. 043802.
[150] C. Zhu,1, P.J. Ehlers, H.I. Nurdin, and D. Soh, *Practical few-atom quantum reservoir computing*, Phys. Rev. Res. 7 (2025), p. 023290.
[151] R. Myers and M.J. Perry, *Black holes in higher dimensional space-times*, Ann. Phys. (N.Y.) 172 (1986), pp. 304–347.
[152] T. Ortín, *Gravity and Strings*, Cambridge University Press, Cambridge, UK, 2004.
[153] V. Frolov and I. Novikov, *Black Hole Physics: Basic Concepts and New Developments,* Vol. 96, Springer Science & Business Media, Berlin, 1998.
[154] A.R. Forsyth, *A Treatise on Differential Equations*, 6th ed., Macmillan, London, 1929.
[155] A. Strominger, *Black hole entropy from near-horizon microstates*, J. High Energy Phys. 1998(02) (1998), pp. 009–009.
[156] S. Carlip, *Black hole entropy from conformal field theory in any dimension*, Phys. Rev. Lett. 82 (1999), pp. 2828–2831.
[157] S. Carlip, *Symmetries, horizons, and black hole entropy*, Gen. Relativ. Gravit. 39 (2007), pp. 1519–1523.
[158] S.N. Solodukhin, *Conformal description of horizon's states*, Phys. Lett. B 454 (1999), pp. 213–222.

[159] T.R. Govindarajan, V. Suneeta, and S. Vaidya, *Horizon states for AdS black holes*, Nucl. Phys. B583 (2000), pp. 291–303.
[160] D. Birmingham, K.S. Gupta, and S. Sen, *Near-horizon conformal structure of black holes*, Phys. Lett. B 505 (2001), pp. 191–196.
[161] K.S. Gupta and S. Sen, *Further evidence for the conformal structure of a Schwarzschild black hole in an algebraic approach*, Phys. Lett. B 526 (2002), pp. 121–126.
[162] G.W. Gibbons and P.K. Townsend, *Black holes and Calogero models*, Phys. Lett. B 454 (1999), pp. 187–192.
[163] P. Di Francesco, P. Mathieu, and D. Sénéchal, *Conformal Field Theory*, Springer, New York, 1997.
[164] H.E. Camblong, L.N. Epele, H. Fanchiotti, and C.A. García Canal, *Dimensional transmutation and dimensional regularization in quantum mechanics: I. General theory*, Ann. Phys. (N.Y.) 287 (2001), pp. 14–56.
[165] H.E. Camblong, L.N. Epele, H. Fanchiotti, and C.A. García Canal, *Dimensional transmutation and dimensional regularization in quantum mechanics: II. Rotational invariance*, Ann. Phys. (N.Y.)287 (2001), pp. 57–100.
[166] R. Jackiw, *Introducing scale symmetry*, Phys. Today 25 (1972), pp. 23–27.
[167] R. Jackiw, *Dynamical symmetry of the magnetic monopole*, Ann. Phys. (N.Y.) 129 (1980), pp. 183–200.
[168] R. Jackiw, *Dynamical symmetry of the magnetic vortex*, Ann. Phys. (N.Y.) 201 (1990), pp. 83–116.
[169] H.E. Camblong, A. Chakraborty, P. Lopez Duque, and C.R. Ordóñez, *Spectral properties of the symmetry generators of conformal quantum mechanics: A path-integral approach*, J. Math. Phys.64 (2023), p. 092302.
[170] H.E. Camblong and C.R. Ordóñez, *Regularized Green's function for the inverse square potential*, Mod. Phys. Lett. A 17 (2002), pp. 817–826.
[171] H.E. Camblong and C.R. Ordóñez, *Path integral treatment of singular problems and bound states*, Int. J. Mod. Phys. A 19 (2004), pp. 1413–1439.
[172] E.P. Wigner, *The unreasonable effectiveness of mathematics in the natural sciences*, Commun. Pure Appl. Math. 13 (1960), pp. 1–14.
[173] S.B. Treiman, R. Jackiw, B. Zumino, and E. Witten, *Current Algebras and Anomalies*, World Scientific, Singapore, 1985.
[174] J.F. Donoghue, E. Golowich, and B.R. Holstein, *Dynamics of the Standard Model*, Cambridge University Press, Cambridge, UK, 1992.
[175] J.S. Bell and R. Jackiw, *A PCAC puzzle: $\Pi^0 \to \gamma\gamma$ in the σ-model*, Nuovo Cimento A 60 (1969), pp. 47–61.
[176] S. Adler, *Axial-vector vertex in spinor electrodynamics*, Phys. Rev. 177 (1969), pp. 2426–2438.
[177] S. Adler and W.A. Bardeen, *Absence of higher-order corrections in the anomalous axial-vector divergence equation*, Phys. Rev. 182 (1969), pp. 1517–1536.
[178] G.N.J. Añaños, H.E. Camblong, C. Gorrichátegui, E. Hernández, and C.R. Ordóñez, *Anomalous commutator algebra for conformal quantum mechanics*, Phy. Rev. D 67 (2003), p. 045018.
[179] G.N.J. Añaños, H.E. Camblong, and C.R. Ordóñez, *SO(2,1) conformal anomaly: Beyond contact interactions*, Phys. Rev. D 68 (2003), p. 025006.
[180] A. Strominger and C. Vafa, *Microscopic origin of the Bekenstein-Hawking entropy*, Phys. Lett. B379 (1996), pp. 99–104.
[181] S. Ryu and T. Takayanagi, *Holographic derivation of entanglement entropy from the anti–de sitter space/conformal field theory correspondence*, Phys. Rev. Lett. 96 (2006), p. 181602.
[182] M. Guica, T. Hartman, W. Song, and A. Strominger, *The Kerr/CFT correspondence*, Phys. Rev. D80 (2009), p. 124008.
[183] A. Castro, A. Maloney, and A. Strominger, *Hidden conformal symmetry of the Kerr black hole*, Phys. Rev. D 82 (2010), p. 024008.

[184] A. Castro and F. Larsen, *Near-extremal Kerr entropy from AdS2 quantum gravity*, J. High Energy Phys. 12 (2009), pp. 037–037.
[185] T. Hartman, W. Song, and A. Strominger, *Holographic derivation of Kerr-Newman scattering amplitudes for general charge and spin*. J. High Energy Phys. 03 (2010) 118.
[186] I. Agullo, J. Navarro-Salas, G.J. Olmo, and L. Parker, *Hawking radiation by Kerr black holes and conformal symmetry*, Phys. Rev. Lett. 105 (2010), p. 211305.
[187] J. Gemmer, M. Michel, and G. Mahler, *Quantum Thermodynamics: Emergence of Thermodynamic Behavior Within Composite Quantum Systems*, 2nd ed., Springer, Berlin, 2009.
[188] S. Deffner and S. Campbell, *Quantum Thermodynamics: An Introduction to the Thermodynamics of Quantum Information*, Morgan & Claypool Publishers, San Rafael, 2019.
[189] R. Zwanzig, *Nonequilibrium Statistical Mechanics*, Oxford University Press, Oxford, 2001.
[190] S.D. Mathur, *The information paradox: A pedagogical introduction*, Class. Quantum Gravity 26 (2009), p. 224001.
[191] A. Perez, *Black holes in loop quantum gravity*, Rep. Progr. Phys. 80 (2017), p. 126901.
[192] A. Almheiri, T. Hartman, J. Maldacena, E. Shaghoulian, and A. Tajdini, *The entropy of Hawking radiation*, Rev. Mod. Phys. 93 (2021), p. 035002.
[193] S. Raju, *Lessons from the information paradox*, Phys. Rep. 943 (2021), pp. 1–80.
[194] C.R. Almeida and M.J. Jacquet, Analogue gravity and the Hawking effect: Historical perspective and literature review. Eur. Phys. J. H 48 (2023), p. 15.
[195] S.L. Braunstein, M. Faizal, L.M. Krauss, and N.A. Sha, *Analogue simulations of quantum gravity with fluids*, Nat. Rev. Phys. 5 (2023), pp. 612–622.
[196] A.A. Svidzinsky, J.S. Ben-Benjamin, S.A. Fulling, and D.N. Page, *Excitation of an atom by a uniformly accelerated mirror through virtual transitions*, Phys. Rev. Lett. 121 (2018), p. 071301.
[197] C.M. Wilson, G. Johansson, A. Pourkabirian, M. Simoen, J.R. Johansson, T. Duty, F. Nori, and P. Delsing, *Observation of the dynamical Casimir effect in a superconducting circuit*, Nature (London)479 (2011), pp. 376–379.
[198] P. Lahteenmaki, G.S. Paraoanu, J. Hassel, and P.J. Hakonen, *Dynamical Casimir effect in a Josephson metamaterial*, Proc. Natl. Acad. Sci. U.S.A. 110 (2013), pp. 4234–4238.
[199] J.R. Johansson, G. Johansson, C.M. Wilson, and F. Nori, *Dynamical Casimir effect in a superconducting Coplanar Waveguide*, Phys. Rev. Lett. 103 (2009), p. 147003.
[200] M. Wallquist, K. Hammerer, P. Rabl, M. Lukin, and P. Zoller, *Hybrid quantum devices and quantum engineering*, Phys. Scr. T137 (2009), p. 014001.
[201] K. Chakraborty and B.R. Majhi, *Detector response along null geodesics in black hole spacetimes and in a Friedmann-Lemaitre-Robertson-Walker universe*, Phys. Rev. D 100 (2019), p. 045004.
[202] S. Sen, R. Mandal, and S. Gangopadhyay, *Near horizon aspects of acceleration radiation of an atom falling into a class of static spherically symmetric black hole geometries*, Phys. Rev. D 106 (2022), p. 025004.
[203] A. Das, S. Sen, and S. Gangopadhyay, *Horizon brightened accelerated radiation in the background of braneworld black holes*, Phys. Rev. D 109 (2024), p. 064087.
[204] S. Sen, R. Mandal, and S. Gangopadhyay, *Equivalence principle and HBAR entropy of an atom falling into a quantum corrected black hole*, Phys. Rev. D 105 (2022), p. 085007.
[205] A. Jana, S. Sen, and S. Gangopadhyay, *Atom falling into a quantum corrected charged black hole and HBAR entropy*, Phys. Rev. D 110 (2024), p. 026029.
[206] A. Jana, S. Sen, and S. Gangopadhyay, *Inverse logarithmic correction in the horizon brightened acceleration radiation entropy of an atom falling into a renormalization group improved charged black hole*, Phys. Rev. D 111 (2025), p. 085017.
[207] A. Das, S. Sen, and S. Gangopadhyay, *Derivative coupling in horizon brightened acceleration radiation: A quantum optics approach*, Phys. Rev. D 112 (2025), p. 065006.
[208] C. Bambi, *Astrophysical black holes: A compact pedagogical review*, Ann. Phys. (Berlin) 530 (2018), p. 1700430.

[209] S.A. Teukolsky, *The Kerr metric*, Class. Quantum Gravity 32 (2015), p. 124006.
[210] L. Landau and E.M. Lifshitz, *The Classical Theory of Fields*, 4th ed., Pergamon Press, Oxford, 1975.
[211] C. Flammer, *Spheroidal Wave Functions*, Stanford University Press, Stanford, 1957.
[212] M. Abramowitz and I.A. Stegun, *Handbook of Mathematical Functions*, eds. Dover Publications, New York, 1972. Chap. 21.
[213] A.A. Starobinsky, Amplification of waves during reflection from a rotating "black hole". Sov. Phys. JETP 37 (1973), pp. 28–32.
[214] W.G. Unruh, *Second quantization in the Kerr metric*, Phys. Rev. D 10 (1974), pp. 3194–3205.

Appendices

Appendix 1. Basic elements of quantum optics

In this appendix, we review the basic foundational elements of quantum optics needed for the main body of this article. These ingredients involve interacting atomic systems and electromagnetic fields, as described below and in Section 2. Throughout the article, we have used a scalar field to describe the relevant physics; instead, here we show how these elements are defined with the full-fledged electromagnetic field.

Quantum optics, by itself, is a huge interdisciplinary field. It is also the underlying theory that led to the discovery and further development of the laser [135,136], which is used in a variety of setups in experiments in physics, biology, chemistry, and other fields of science and engineering. This broad field was originally introduced to model the interaction between electromagnetic fields as photons and ordinary matter. For our purposes, we provide an outline of the quantisation of the electromagnetic fields and the atom-field dipole interaction. The atom-field interaction in quantum optics is of widespread use in a variety of applications; in particular, for systems involving spacetime backgrounds (gravitational fields and noninertial systems), it leads to a definition of the Unruh-DeWitt detector, which is a standard probe of nontrivial spacetime effects, as seen in Sections 2.2 and 2.3. More detailed descriptions and derivations of various theoretical and experimental aspects of quantum optics can be found in the standard Refs. [47,48].

A.1. Quantisation of the electromagnetic fields

From the free Maxwell's equations in classical electrodynamics, the electric field $\mathbf{E}$ is shown to obey the wave equation

$$\nabla^2 \mathbf{E} - \frac{\partial^2 \mathbf{E}}{\partial t^2} = 0 \tag{A1}$$

(with the speed of light $c = 1$). Now, plane waves constitute a basis set for the solutions of the wave equation in flat spacetime. Thus, for ordinary laboratory experiments where quantum electrodynamics and quantum optics were developed, one can expand the electric fields in terms of this set of plane waves

$$\mathbf{E}(\mathbf{r}, t) = \sum_{\mathbf{k}} \boldsymbol{\varepsilon}_{\mathbf{k}} \mathcal{E}_{\mathbf{k}} \alpha_{\mathbf{k}} e^{i\mathbf{k}\cdot\mathbf{r} - i\omega_k t} + \mathrm{H.c.}, \tag{A2}$$

as a particular case of the general expansion of the form (6), in which the labelling $\mathbf{s}$ of the states is in terms of the wave number $\mathbf{k}$. In this standard treatment, the field is confined in a large but finite cubic cavity of length L and volume $V = L^3$, so that the field momentum is discrete instead of continuous. To change the distribution from discrete to continuous, one has to replace the sum over momentum with an integral:

$$\sum_{\mathbf{k}} \longrightarrow 2\left(\frac{L}{2\pi}\right)^3 \int d^3k.$$

In Equation (A2), $\boldsymbol{\varepsilon}_k$ is the electric field polarisation unit vector, $\mathbf{k}$ is the momentum of the field, $\omega_{\mathbf{k}} = |\mathbf{k}|$ is the frequency of the field, $\alpha_{\mathbf{k}}$ is the dimensionless amplitude of each mode, $\mathcal{E}_{\mathbf{k}}$ is the electric field strength

$$\mathcal{E}_{\mathbf{k}} = \left(\frac{\omega_{\mathbf{k}}}{2\epsilon_0 V}\right)^{1/2}, \tag{A3}$$

in naturalised SI units. Due to the periodic boundary conditions, the momentum components take the values $k_i = 2\pi n_i/L$, where are non-negative integers. Hence, the set of numbers (n_x, n_y, n_z) defines a mode of the field. Following Maxwell's equations, the momentum vector and the polarisation vector obey the constraint

$$\mathbf{k} \cdot \boldsymbol{\varepsilon}_{\mathbf{k}} = 0, \tag{A4}$$

which means that the fields are transverse (orthogonal to the propagation direction), and the polarisation vector only has two independent directions. In the summary that follows, we consider the electric field polarised in a certain direction (for example, the x axis).

The canonical quantisation of the electric field is implemented as in Equations (6) and (7) by promoting the mode amplitudes $\alpha_{\mathbf{k}}$ to quantum annihilation operators. Thus, the quantised electric field takes the form

$$\hat{\mathbf{E}}(\mathbf{r}, t) = \sum_{\mathbf{k}} \boldsymbol{\varepsilon}_{\mathbf{k}} \mathcal{E}_{\mathbf{k}} \hat{a}_{\mathbf{k}} e^{i\mathbf{k}\cdot\mathbf{r} - i\omega_k t} + \text{H.c.}, \tag{A5}$$

where $\hat{a}_{\mathbf{k}}$ is the corresponding annihilation operator, and its Hermitian adjoint is the creation operator $\hat{a}^\dagger_{\mathbf{k}}$. The creation and annihilation operators satisfy a particular form of the general canonical commutation relations (7) that are a consequence of the basic canonical commutators of conjugate field variables, e.g.$[\hat{a}_{\mathbf{k}}, \hat{a}^\dagger_{\mathbf{k}'}] = \delta_{\mathbf{k}\mathbf{k}'}$, with the other commutators being zero. Then, the Hamiltonian of the electromagnetic fields can be cast in the form

$$\mathcal{H} = \sum_k \omega_{\mathbf{k}} \left(\hat{a}^\dagger_{\mathbf{k}} \hat{a}_{\mathbf{k}} + \frac{1}{2}\right), \tag{A6}$$

which, with the removal of the zero-point energy as in Equation (25b), yields

$$\mathcal{H} = \sum_k \omega_{\mathbf{k}} \hat{a}^\dagger_{\mathbf{k}} \hat{a}_{\mathbf{k}}. \tag{A7}$$

The energy eigenstates build up the Fock space, where the states of the system have any number of particles, with $|0\rangle$ being the vacuum state and $\left|n_1, n_2, \ldots, n_j, \ldots\right\rangle$ being an excited state with the occupation number n_i referring to the number of photons with momentum $\mathbf{k}_i$. The action of the creation and annihilation operator in Fock space is given by

$$\hat{a}_{k_j}\left|n_1, n_2, \ldots, n_j, \ldots\right\rangle = \sqrt{n_j}\left|n_1, n_2, \ldots, n_j - 1, \ldots\right\rangle, \tag{A8}$$

$$\hat{a}^\dagger_{k_j}\left|n_1, n_2, \ldots, n_j, \ldots\right\rangle = \sqrt{n_j + 1}\left|n_1, n_2, \ldots, n_j + 1, \ldots\right\rangle. \tag{A9}$$

Additional details of this field-theory construction are given in Section 2.1.

A common model in quantum optics involves the use of single field mode inside a cavity interacting with a two-state atom. In that case, the sum over the momentum modes in Equation (A7) is not enforced and the system is described in a Hilbert space corresponding to one photon.

A.2. Atom-field interaction

A typical setup consists of an uncharged two-state atom interacting with the electromagnetic field. The Hilbert space of the two-state atom is the same as a spin-1/2 particle, and hence the Hamiltonian can be written as the spin-1/2 Hamiltonian with the spin oriented along the z-direction without any loss of generality. The interaction between the atom and the field is modelled by a dipole interaction. Therefore, the total Hamiltonian of the field-atom system can be written as in Equation (30): $H = H_{\rm at} + H_{\rm em} + H_{\rm int}$, where we more generally have

$$H_{\rm at} = E_a|a\rangle\langle a| + E_b|b\rangle\langle b|, \tag{A10}$$

$$H_{\rm em} = \sum_k \omega_{\mathbf{k}}\, \hat{a}^\dagger_{\mathbf{k}}\hat{a}_{\mathbf{k}}, \tag{A11}$$

$$H_{\rm int} = \hat{\mathbf{P}}(t)\cdot\hat{\mathbf{E}}(t,\mathbf{r}). \tag{A12}$$

Here, $|a\rangle$ and $|b\rangle$ are the excited and ground state of the atom with energies E_a and E_b. The frequency of transition of the atom is then defined as $\nu = E_a - E_b$. The dipole moment operator $\mathbf{P}$ can be written as

$$\mathbf{P}(t) = \sum_{i,j}|i\rangle\langle i|\hat{\mathbf{P}}(t)\big|j\rangle\langle j| = \sum_{i,j}\hat{\sigma}_{ij}\boldsymbol{\mathcal{P}}_{ij}\, e^{i(E_i-E_j)t}, \tag{A13}$$

where $\hat{\sigma}_{ij} = |i\rangle\langle j|$ with $i,j\in\{a,b\}$ and $\boldsymbol{\mathcal{P}}_{ij} = \langle i|\hat{\mathbf{P}}(0)\big|j\rangle$ are the dipole moment matrix elements in the atomic basis. Now, the dipole moment matrix has zero diagonal and non-zero off-diagonal terms due to the parity of the dipole moment operator:

$$\boldsymbol{\mathcal{P}}_{ij} = e\langle i|\mathbf{r}\big|j\rangle = \begin{cases} 0 & \text{if } i=j \\ \boldsymbol{\mathcal{P}}_{ab} & \text{if } i\neq j \end{cases}, \tag{A14}$$

where $\boldsymbol{\mathcal{P}}_{ab}$ is considered real and $\boldsymbol{\mathcal{P}}_{ab} = \boldsymbol{\mathcal{P}}_{ba}$.

This is the standard setup that justifies the use of a model with a scalar field and an analogue monopole coupling, as in Section 2.

Appendix 2. Spacetime physics and black holes

Given their observational and theoretical relevance, this appendix summarises the main definitions and properties of the geometry of nonextremal Kerr black holes [38,85,90,153]. As this overview shows, leaving aside some technicalities, the basic properties of the near-horizon region, black hole thermodynamics, HBAR physics, and related CQM are the same as for generalised Schwarzschild black holes of Section 4.

A.3. Kerr metric in Boyer-Lindquist coordinates

Kerr black holes are the four-dimensional rotating black holes that are of current interest in astronomical realisations [208]; see Figure A1. They are described by the Kerr metric [209] as the unique vacuum solution of the Einstein field equations in 4D in the presence of a black hole of mass M and angular momentum J. In Boyer-Lindquist coordinates (t, r, θ, ϕ), the Kerr metric can be written in a variety of forms. Using geometrised natural units with $c = 1$ and $G = 1$, in terms of its coordinate components, it reads

$$ds^2 = -\frac{(\Delta - a^2\sin^2\theta)}{\rho^2}\,dt^2 - \frac{4Mr}{\rho^2}a\sin^2\theta\,dt\,d\phi + \frac{\rho^2}{\Delta}\,dr^2 + \rho^2\,d\theta^2 + \frac{\Sigma^2}{\rho^2}\sin^2\theta\,d\phi^2 \tag{A15}$$

where $a = J/M$, called the rotational Kerr parameter, is the angular momentum per unit mass.

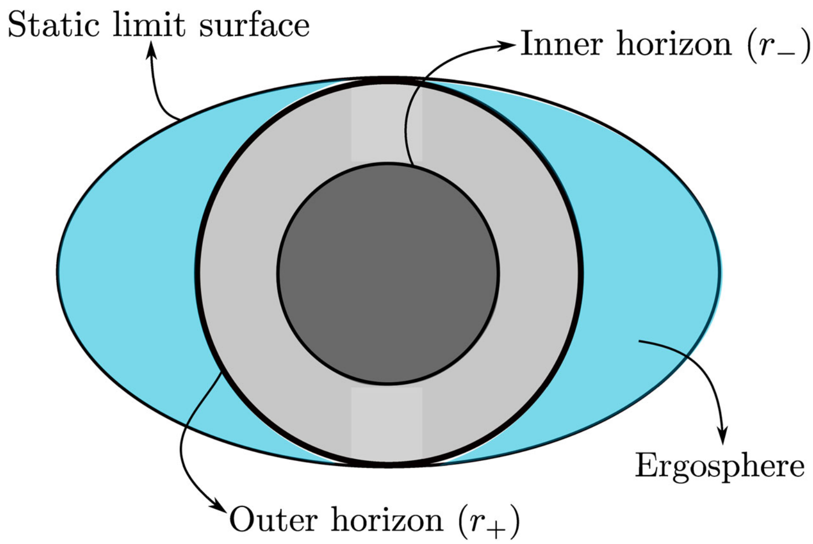

Figure A1. A rotating black hole represented by the Kerr metric (A15). The horizons (outer and innner) and the static limit hypersurfaces are characterised by the conditions $g_{\tilde{t}\tilde{t}} \propto \Delta = 0$, i.e. Equation (A20); and $g_{tt} \propto \Delta - a^2 \sin^2\theta = 0$, respectively. In the diagram, we are not displaying the structure inside the inner horizon (including the inner static limit), which is thought to be unrealisable for astrophysical black holes.

In Equation (A15), the auxiliary quantities Δ, ρ, and Σ are given as

$$\begin{aligned}\Delta &= r^2 - 2Mr + a^2, \quad \rho^2 = r^2 + a^2\cos^2\theta,\\ \Sigma^2 &= \left(r^2 + a^2\right)\rho^2 + 2Mra^2\sin^2\theta = (r^2 + a^2)^2 - \Delta a^2 \sin^2\theta.\end{aligned} \tag{A16}$$

It should be noted that all the results and implications of this appendix and in the main text, including the HBAR results, are similarly valid with the addition of a black hole electric charge Q, if the replacement $2Mr \longrightarrow 2Mr - Q^2$ is made (which amounts to $a^2 \to a^2 + Q^2$ within the function Δ, when all the terms involving M are rewritten in terms of Δ).

A second form of the Kerr metric uses a shift of the angular coordinate ϕ to remove the off-diagonal metric term $g_{t\phi}$, by completing the square in Equation (A15). With the auxiliary quantity

$$\varpi = -\frac{g_{t\phi}}{g_{\phi\phi}}, \tag{A17}$$

this insightful form of the metric reads

$$\mathrm{d}s^2 = -\frac{\Delta\rho^2}{\Sigma^2}\,\mathrm{d}t^2 + \frac{\rho^2}{\Delta}dr^2 + \rho^2\,\mathrm{d}\theta^2 + \frac{\Sigma^2}{\rho^2}\sin^2\theta\left(\mathrm{d}\phi - \varpi\,\mathrm{d}t\right)^2, \tag{A18}$$

showing that ϖ can be interpreted as a position-dependent angular velocity [210] for the frame dragging of spacetime around the black hole. This is a form of the metric that is ideally suited for the near-horizon analysis, as it displays a structure similar to the generalised Schwarzschild metrics (52), leading directly to the CQM dominance and ensuing thermodynamic implications.

A.4. Kerr spacetime symmetries and structure

The symmetries of Kerr spacetime can be analysed in a manner similar to the Schwarzschild geometry (53), with the Killing vectors of Equation (53). These are associated with independence with respect to time t and azimuthal angle ϕ, as arising from the stationary and axisymmetric invariances of the geometry. In addition, similar techniques (as in Section 4.1), can be used for the analysis of the structure of Kerr spacetime, including the horizons and details implied by the black hole's rotation. Here, two sets of hypersurfaces can be identified as critical boundaries, as follows.

- *Static (stationary) limit hypersurfaces or ergosurfaces* $\mathcal{S}^{\pm}$. These boundaries are identified by the radii $r_{e,\pm} = r_{e,\pm}(\theta)$ that are roots of the equation

$$g_{tt} = \boldsymbol{\xi}_{(t)} \cdot \boldsymbol{\xi}_{(t)} = 0 \Longrightarrow r_{e,\pm} = M \pm \sqrt{M^2 - a^2 \cos^2 \theta} \tag{A19}$$

(see Figure A1). On these hypersurfaces $\mathcal{S}^{\pm}$, the norm of $\boldsymbol{\xi}_{(t)}$ becomes null: thus, they are infinite-redshift hypersurfaces, by comparison of time t measurements near $r_{e,\pm}$ with asymptotic infinity.

In addition, $\boldsymbol{\xi}_{(t)}$ becomes spacelike for $r_{e,-} < r < r_{e,+}$ (being timelike near asymptotic infinity, and generally for $r > r_{e,+}$ or $r < r_{e,-}$). Then, a simple analysis shows that timelike geodesics of static observers do not exist within these boundaries ($r_{e,-} < r < r_{e,+}$) and all paths are dragged along in the direction of the black hole's rotation. (Thus, the hypersurfaces $\mathcal{S}^{\pm}$ are '*static or stationary limits*'.)

Finally, these hypersurfaces are not horizons. This can be proved in two ways: (i) they are not null because they include a timelike direction corresponding to the diagonal form of the metric (A18); (ii) the geodesic analysis also shows that outgoing timelike or null geodesics do cross the outer static limit $r_{e,+} = M + \sqrt{M^2 - a^2 \cos^2 \theta}$. In essence, the condition $g_{tt} = 0$ does not characterise the horizon because it fails to account for the effect on geodesics of the black hole's rotational degree of freedom.
- *Outer and Inner Horizons* $\mathcal{H}^{\pm}$. Effectively, these hypersurfaces are identified by the radii $r_{\pm}$ that give the locations of the outer (r_+) and inner (r_-) horizons, via the roots of the equation

$$\Delta = 0 \Longrightarrow r_{\pm} = M \pm (M^2 - a^2)^{1/2} \tag{A20}$$

(see Figure A1). For the outer horizon: outgoing timelike or null geodesics do not exist crossing this surface (they are all ingoing), when the value $r = r_+$ is reached; this is indeed the characterisation of a stationary event horizon (see below).

The structure (A20) with two horizons is also found for the Reissner-Nordström (RN) case with electric charge, within the class of generalised Schwarzschild metrics (53). However, for Kerr spacetimes, new features emerge due to the rotation that breaks spherical symmetry and generates the additional static limit hypersurfaces. Specifically, the Kerr-spacetime structure includes the regions known as ergospheres (outer: $r_+ < r < r_{e,+}$ and inner: $r_{-,e} < r < r_-$). See Figure A1; the outer ergosphere is most often discussed in the literature, as it lies outside the event horizon, and has many surprising features associated with frame dragging, including the Penrose process [38,85,90] and astrophysical implications [208,209]. For the analysis of interest in most practical applications, including acceleration radiation (as in this review article), the non-extremal geometry is considered, as defined by the physical condition $M>a$, which amounts to $\Delta'_+ \equiv \Delta'(r_+) = r_+ - r_- \neq 0$, and where the prime stands for the radial derivative; this excludes naked singularities ($M<a$) [38,90].

Most importantly, the horizon condition (A20) can be understood by considering the black hole's rotational degree of freedom. A useful derived parameter is the black hole's angular velocity Ω_H, which is the horizon limit of the frame-dragging angular velocity (A17):

$$\Omega_H = \lim_{r \to r_+} \varpi = \frac{a}{r_+^2 + a^2} = \frac{a}{2Mr_+}. \tag{A21}$$

This parameter is proportional to the black hole's angular momentum J and appears in other important physical quantities. Moreover, Ω_H can be given an operational physical meaning by considering a particle approaching the event horizon along a geodesic: its angular velocity $\Omega = \mathrm{d}\phi/\mathrm{d}t$ is restricted to an increasingly narrow range and is forced to become Ω_H as $r \to r_+$. Further insight into horizon and near-horizon properties is gained by considering the corotating Boyer-Lindquist coordinates [186],

$$\tilde{t} = t, \quad \tilde{\phi} = \phi - \Omega_H t, \tag{A22}$$

associated with fiducial stationary observers corotating with the black hole itself. The coordinates (A22) make the metric (A18) diagonal to leading order in the near-horizon region and exactly diagonal at $\mathcal{H}$. In addition, these coordinates naturally select a corotating Killing vector relevant for the spinning event horizon as the well-known linear combination [38,85,90]

$$\boldsymbol{\xi} \equiv \boldsymbol{\xi}_{(\tilde{t})} = \partial_{\tilde{t}} = \boldsymbol{\xi}_{(t)} + \Omega_H \boldsymbol{\xi}_{(\phi)}. \tag{A23}$$

The Killing vector $\boldsymbol{\xi}$ of Equation (A23) is timelike outside the event horizon and becomes null at the event horizon $\mathcal{H} \equiv \mathcal{H}^+$, where

$$g_{\tilde{t}\tilde{t}} = \boldsymbol{\xi}_{(\tilde{t})} \cdot \boldsymbol{\xi}_{(\tilde{t})} = -\frac{\Delta\rho^2}{\Sigma^2} = 0. \tag{A24}$$

This explains the criterion of Equation (A20) for the selection of Kerr horizons. Furthermore, Equations (A20) and (A24) select a hypersurface $\mathcal{H}^\pm$, with a null tangent direction along $\boldsymbol{\xi}$, and two angular directions that are spacelike – this can be deduced from the diagonal form of the metric (A18). By definition, this makes $\mathcal{H}^\pm$ a null hypersurface generated by light rays. Incidentally, this finding implies that the null direction is also normal to $\mathcal{H}^\pm$; in the chosen Boyer-Lindquist coordinates, the normal corresponds to the radial coordinate, and the vanishing of its norm is fixed by the following condition on the metric component: $g^{rr} \propto \Delta = 0$. As for the case of generalised Schwarzschild black holes, such null hypersurface is a horizon. For the outer hypersurface at $r = r_+$, this is an event horizon, where all timelike or null geodesics are ingoing and cannot go back to infinity; the inner hypersurface at $r = r_-$ is classified as a Cauchy horizon [38]. Finally, this simple set of arguments indicates that $\boldsymbol{\xi}$ describes a spacetime evolution in a corotating frame with the same basic characteristics found in the neighbourhood of a generalised Schwarzschild black hole. Therefore, one can predict that the near-horizon physics will exhibit an analog behaviour, as in Section 4.2, governed by scale symmetry in the form of CQM – this is verified in this appendix for a scalar field.

As in Section 4, the two most relevant geometrical quantities for quantum thermodynamics are the surface gravity and the black hole horizon area. From Equation (55), with $r = r_+$, the surface gravity of a Kerr black hole takes the form

$$\kappa = \frac{\Delta'_+}{2(r_+^2 + a^2)}, \tag{A25}$$

which is again proportional to the Hawking temperature (8). And the horizon area, generally defined via

$$A = \int \sqrt{g_{\theta\theta} g_{\phi\phi}}\, \mathrm{d}\theta\, \mathrm{d}\phi = 4\pi(r_+^2 + a^2), \tag{A26}$$

is also proportional to the Bekenstein-Hawking entropy (9). In particular, from Equations (A20) and (A25), this implies that the area changes are

$$\delta A = 8\pi \frac{\delta \tilde{M}}{\kappa}, \tag{A27}$$

where $\delta\tilde{M}$ is the corotating energy change of Equation (97). Equation (A27) extends Equation (59) and its RN generalisations to incorporate the black hole's angular momentum.

A.5. Field theory and near-horizon approximation on Kerr spacetime

For a quantum field theory on Kerr spacetime, we consider a real scalar field Φ as the simplest representative of the relevant behaviour of acceleration radiation. This mirrors our treatment in the main text of this article; see Section 2.1.

The Klein-Gordon Equation (12) with mass μ_Φ and possibly nonminimal coupling ξ, i.e. i.e.

$$\frac{1}{\sqrt{-g}}\partial_\mu\left(\sqrt{-g}\,g^{\mu\nu}\,\partial_\nu\Phi\right) - (\mu_\Phi^2 + \xi R)\Phi = 0,$$

in the geometric background of a Kerr spacetime metric (A15), takes the form

$$\begin{aligned} &-\frac{\Sigma^2}{\Delta}\frac{\partial^2\Phi}{\partial t^2} - \frac{4Mra}{\Delta}\frac{\partial^2\Phi}{\partial t\,\partial\phi} + \left(\frac{1}{\sin^2\theta} - \frac{a^2}{\Delta}\right)\frac{\partial^2\Phi}{\partial\phi^2} \\ &+\frac{\partial}{\partial r}\left(\Delta\frac{\partial\Phi}{\partial r}\right) + \frac{1}{\sin\theta}\frac{\partial}{\partial\theta}\left(\sin\theta\frac{\partial\Phi}{\partial\theta}\right) - \mu_\Phi^2\rho^2\Phi = 0. \end{aligned} \tag{A28}$$

The general solution of Equation (A28) can be written in terms of a set of modes $\phi_{\tilde{\omega}lm}(t,\boldsymbol{r})$ in separable form,

$$\phi_{\omega lm}(t,\boldsymbol{r}) \equiv \phi_{\boldsymbol{s}}(t,r,\Omega) = R_{\boldsymbol{s}}(r)S_{lm}(\theta)e^{im\phi}e^{-i\omega t}, \tag{A29}$$

where $\boldsymbol{r} = (r,\theta,\phi)$, and $S_{lm}(\theta)$ are oblate spheroidal wave functions of the first kind [153,211,212], which satisfy the angular equation

$$\frac{1}{\sin\theta}\frac{\mathrm{d}}{\mathrm{d}\theta}\left(\sin\theta\frac{\mathrm{d}S}{\mathrm{d}\theta}\right) + \left[a^2\omega^2\cos^2\theta - \frac{m^2}{\sin^2\theta} + \Lambda_{\boldsymbol{s}} - a^2\mu_\Phi^2\cos^2\theta\right]S = 0. \tag{A30}$$

The normalised combination $Z_{lm}(\Omega) = (2\pi)^{-1/2}S_{lm}(\theta)e^{im\phi}$ is usually called a spheroidal harmonic. Equation (A30) is a Sturm-Liouville problem where the separation constant $\Lambda_{\boldsymbol{s}}$ is an eigenvalue of a self-adjoint operator – thus, the regular solutions form a complete orthogonal set labelled by a discrete 'spheroidal' number l. In addition, $\Lambda_{\boldsymbol{s}}$ and the associated solutions depend on the discrete quantum numbers l and m as well the continuous parameters μ_Φ and ω that appear in the dimensionless combinations $a\mu_\Phi$ and $a\omega$. Then, the separation of variables of Equation (A29) gives the corresponding radial function $R(r)$ subject to the equation

$$\frac{\mathrm{d}}{\mathrm{d}r}\left(\Delta\frac{\mathrm{d}R}{\mathrm{d}r}\right) + \left[\frac{(r^2+a^2)^2\omega^2 - 4Mram\omega + a^2m^2}{\Delta} - \Lambda_{\boldsymbol{s}} - a^2\omega^2 - \mu_\Phi^2 r^2\right]R = 0. \tag{A31}$$

The near-horizon approximation can be implemented with $x \equiv r - r_+ \ll r_+$, using the expansions $\Delta(r)\overset{(\mathcal{H})}{\sim}\Delta'_+\,x[1+O(x)]$, and $\Delta'(r)\overset{(\mathcal{H})}{\sim}\Delta'_+[1+O(x)]$, where $\Delta'_+ = r_+ - r_-$. The derivation can proceed in either one of two ways. In the first approach, the radial Equation (A31) is the starting point for the near-horizon expansion; then, the leading terms as $r \to r_+$ are the one with radial derivatives and the ones with an inverse Δ factor, where square completion can be used, along with the black hole angular velocity Ω_H of Equation (A21,) to get a shifted frequency

$$\tilde{\omega} = \omega - \Omega_H m. \tag{A32}$$

The resulting leading-order near-horizon radial equation becomes

$$\left[\frac{1}{x}\frac{\mathrm{d}}{\mathrm{d}x}\left(x\frac{\mathrm{d}}{\mathrm{d}x}\right) + \left(\frac{\tilde{\omega}}{f'_+}\right)^2\frac{1}{x^2}\right]R(x)\overset{(\mathcal{H})}{\sim}0, \quad \text{with } f'_+ = \frac{\Delta'_+}{(r_+^2+a^2)} \tag{A33}$$

and, via a Liouville transformation $R(x) \propto x^{-1/2}u(x)$,

$$u''(x) + \frac{\lambda}{x^2}[1 + O(x)]u(x) = 0, \quad \lambda = \frac{1}{4} + \Theta^2, \quad \Theta = \frac{\tilde{\omega}}{f'_+} \equiv \frac{\tilde{\omega}}{2\kappa}, \tag{A34}$$

with the Kerr surface gravity κ of Equation (A25). Equations (A33) and (A34) are the CQM expressions for a Kerr black hole, which can be viewed as the analogues of the Schwarzschild-like metric Equations (64)–(67), with ω replaced by $\tilde{\omega}$.

In the second approach, the alternative expression for the Kerr metric of Equation (A18) gives additional insight into the conformal nature of the near-horizon equations. Indeed, the covariant metric (A18) describes the physics in a corotating frame with angular velocity ϖ. In this interpretation, a shifted azimuthal coordinate is implicitly given by $d\phi - \varpi\, dt$. As the near-horizon region is approached with $r \to r_+$, this frame becomes the black hole's corotating frame, with an angular velocity $\varpi \to \Omega_H$, and with the coordinate transformation to the corotating Boyer-Lindquist coordinates (A22), i.e. $\tilde{t} = t$ and $\tilde{\phi} = \phi - \Omega_H t$. This transformation converts Equation (A29) (exactly, and not just in the near-horizon region) into

$$\phi_{\tilde{\omega}lm}(\boldsymbol{r}, t) = R(r)S(\theta)e^{im\tilde{\phi}}e^{-i\tilde{\omega}\tilde{t}}, \quad \tilde{\omega} = \omega - m\Omega_H. \tag{A35}$$

Here, the timelike behaviour of the associated Killing vector $\boldsymbol{\xi}_{(\tilde{t})} = \boldsymbol{\xi}$ allows for positive frequency modes of the Klein-Gordon Equation (12) within the ergosphere and near the horizon, via the condition

$$\boldsymbol{\xi}_{(\tilde{t})}\phi_s = -i\tilde{\omega}\phi_s. \tag{A36}$$

Then, inversion of the metric gives the contravariant components needed for the Klein-Gordon Equation (12); moreover, making the transition to the near-horizon region, instead of Equation (A28) or Equation (A31), one can directly write

$$\left[-\frac{\Sigma^2}{\rho^2\Delta}\frac{\partial}{\partial\tilde{t}^2} + \frac{\rho^2}{\Sigma^2\sin^2\theta}\frac{\partial}{\partial\tilde{\phi}^2} + \frac{1}{\rho^2}\frac{\partial}{\partial r}\left(\Delta\frac{\partial}{\partial r}\right) + \frac{1}{\rho^2}\frac{\partial}{\partial\theta^2}\right]\Phi \tag{A37}$$

$$\stackrel{(\mathcal{H})}{\sim}\left[-\frac{(r^2+a^2)^2}{\rho^2\Delta}\frac{\partial}{\partial\tilde{t}^2} + \frac{1}{\rho^2}\frac{\partial}{\partial r}\left(\Delta\frac{\partial}{\partial r}\right)\right]\Phi \stackrel{(\mathcal{H})}{\sim} 0, \tag{A38}$$

due to the leading behaviour $\Delta(r) \stackrel{(\mathcal{H})}{\sim} \Delta'_+ x$, which selects the radial-time sector of the metric. Equation (A38) reproduces again the asymptotically exact Equation (A33). It should be noted that the first three terms of Equation (A28), involving derivatives with respect to t and ϕ, actually combine to the diagonal form of the metric exhibited in Equation (A18), i.e. they correspond to $[g^{tt}(\partial_t + \varpi\partial_\phi)^2 + (1/g_{\phi\phi})\partial_\phi^2]\Phi$ (after removal of an overall factor $1/\rho^2$); this provides a direct link between the two approaches (fixed vs corotating frames, and their near-horizon limits).

The assignments leading to CQM, via Equations (A33) and (A34), show that one can define an equivalent scale factor

$$f(r) \equiv \frac{\Delta}{(r^2 + a^2)}, \tag{A39}$$

for comparison with the analogue Schwarzschild-like metrics. [For example, Equation (A25) conforms to this replacement for $\kappa = f'_+/2$.] In essence, this argument shows that,

> with the factor $f(r)$ of Equation (A39), *the near-horizon Kerr metric is a generalised Schwarzschild metric (53) in the corotating frame.*

Finally, as in Section 4.2, and applying Equation (A35), a pair of linearly independent solutions is given by $u(x) \propto x^{1/2 \pm i\Theta}$, so that

$$\Phi^{\pm(\text{CQM})}_{\omega lm} \propto x^{\pm i\Theta} e^{im\tilde{\phi}} S_{lm}(\theta) e^{-i\tilde{\omega}\tilde{t}}, \tag{A40}$$

thus generalising Equation (71). In addition, a crucially important property of this analysis is noteworthy. The radial Equation (A33) is the particular scalar case (for spin $s = 0$) of the Teukolsky equation [153] valid for arbitrary field spin with the same structural form. As a result, the conformal behaviour displayed in the near-horizon approximation (see below) is universal: it is exhibited by all fields, with arbitrary spin, in the background of generic black holes.

The geodesic equations are also obtained by a similar analysis as in Section 4.3, in terms of the specific energy and axial component of angular momentum, defined via Equations (73), in addition to the invariant mass μ and the Carter constant $\mathcal{Q}$ [85]. In this case, if the second-order geodesics are written explicitly, a near-horizon limiting procedure yields the same for of Equations (74) and (75). The coordinate ϕ also needs to be specified, and has an expansion with another logarithmic term; but the relevant corotating coordinate has a simple linear expression $\tilde{\phi}^{(\mathcal{H})} \sim \alpha x + O(x^2)$. The coefficients k, C, and α, which are expressed in terms of the conserved quantities and a limiting value of the coordinate θ, do not play a direct role in the radiation formulas. Instead, as in Section 4.3, it is the logarithmic term in the coordinate time expansion (75), combined with a similar term of the radial part of the mode, that completely determines the final Planck form of the radiation equations.

In closing, there is one final remark on the Kerr metric that involves a technicality related to the vacuum. The choice of vacuum states is a subtle and important physical criterion in curved spacetime [25]. The definition of a Boulware-like vacuum needed for the HBAR thought experiment is subtle because of the superradiant modes [153,213,214]. This issue, along with the resolution, are discussed in Refs. [82,84]. This difficulty can be bypassed via the introduction of a boundary that excludes the regions of asymptotic infinity, e.g. using a mirror. Any such properly controlled field mode would qualify as Boulware-like and is suitable for the generation of HBAR radiation.

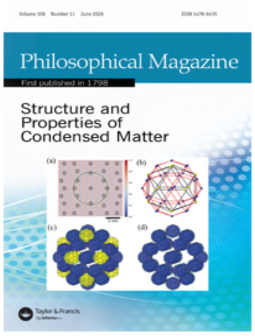

Philosophical Magazine

ISSN: 1478-6435 (Print) 1478-6443 (Online) Journal homepage: www.tandfonline.com/journals/tphm20

A solution of the quantum time of arrival problem via mathematical probability theory

Maik Reddiger

PHILOSOPHICAL MAGAZINE
https://doi.org/10.1080/14786435.2026.2627725

Taylor & Francis
Taylor & Francis Group

OPEN ACCESS Check for updates

A solution of the quantum time of arrival problem via mathematical probability theory

Maik Reddiger

Center for Research, Transfer, and Entrepreneurship, Anhalt University of Applied Sciences, Köthen (Anhalt), Germany

ABSTRACT

Time of arrival refers to the time a particle takes after emission to impinge upon a suitably idealised detector surface. Within quantum theory, no generally accepted solution exists so far for the corresponding probability distribution of arrival times. In this work we derive a general solution for a single body without spin impacting on a so called ideal detector in the absence of any other forces or obstacles. A solution of the so called screen problem for this case is also given. After discussing the shortcomings of the so called 'absorbing boundary condition', which is arguably the natural approach within quantum mechanics, we construct the ideal detector model via mathematical probability theory. This detector model assures that the probability flux through the detector surface is always positive, so that the corresponding distributions can be derived via an approach originally suggested by Daumer, Dürr, Goldstein, and Zanghì. The resulting dynamical model is based on an adaption of the Madelung equations and is, strictly speaking, not compatible with quantum mechanics. Still, it is well-described within geometric quantum theory. Geometric quantum theory is a novel adaption of quantum mechanics, which makes the latter consistent with mathematical probability theory. Implications to the general theory of measurement and avenues for future research are also provided. Future mathematical work should focus on finding an appropriate distributional formulation of the evolution equations and studying the well-posedness of the corresponding Cauchy problem.

ARTICLE HISTORY
Received 15 August 2025
Accepted 31 January 2026

KEYWORDS
Time of arrival; time of flight; quantum measurement; ideal detector; geometric quantum theory; projection postulate

MATHEMATICS SUBJECT CLASSIFICATION 2020
81P15; 81P05; 81S99; 82D99

1. Introduction

In simple terms, the time of arrival problem concerns the question of how long it takes a quantum particle after emission to reach a suitably idealised detector surface.

The status of the problem within contemporary physics is a paradox in the following sense: on the one hand, it appears intuitively simple. On the other hand, common quantum-mechanical concepts do not seem to suffice to adequately address it:

CONTACT Maik Reddiger maik.reddiger@hs-anhalt.de Center for Research, Transfer, and Entrepreneurship, Anhalt University of Applied Sciences, Hubertus 1a, Köthen (Anhalt) 06366, Germany

This article has been corrected with minor changes. These changes do not impact the academic content of the article.

famously, time is not an 'observable' in the theory (cf. Sec. A.8 in [1–3]). Accordingly, a large variety of conceptually different approaches have been suggested so far (see e.g. [4–14]) and no scientific consensus on the resolution of the problem has been attained. Reviews on the subject are given in [15] and Section 2 of [16].

Of course, the indeterminateness of quantum phenomena requires a restatement of the problem: what is asked for is the corresponding probability distribution. It is the task of quantum theory to predict this distribution for any given setup.

The purpose of this work is to provide a systematic, yet at this point not mathematically rigorous solution to the problem through the use of mathematical probability theory [17–19] and a systems of equations discovered by Madelung in 1926 [20–22]. Though the approach can in principle be generalised, we restrict ourselves to the non-relativistic regime and the case of a single body 'without spin' impacting on a so called ideal detector in the absence of any other forces or obstacles.

While the question of the (first) arrival time distribution on a non-interacting surface in space might be within the reach of scientific inquiry, this situation is not of empirical concern – with the single exception of the asymptotic case treated in quantum scattering theory [23–25]. Only the latter can be reasonably linked to experiment. It is therefore more appropriate to refer to 'times of impact' rather than 'times of arrival'. The construction of a detector model is therefore imperative [1,13], at least for the purpose of making empirical predictions 'in the near field' (cf. [23]).

Accordingly, we qualitatively define an *ideal detector* as a surface, which captures the body upon impact and holds it fixed, but does otherwise not interact with it. That in any actual experiment the body will not stay fixed on the surface shall not be of any greater concern, since for modelling purposes we are only interested in where the body impacts and when. It is a choice of convenience that the body is modelled to stay on the surface after impact. In personal conversations with experimental physicists it was confirmed that contemporary detectors are highly efficient and that such an idealised detector model may indeed be of empirical use.

An overview of this work as well as its main results is given hereafter.

Section 2 provides a refined problem statement. The problem is then discussed in the context of the so called 'absorbing boundary condition' [13,14,23]. We find that that approach is rather natural within the theory of quantum mechanics and nonetheless objectionable on physical grounds. In Section 3, we employ mathematical probability theory to motivate the introduction of a probability surface density σ on the detector surface $\mathcal{D}$ and construct the aforementioned ideal detector model.

In Section 4, we show how this model leads to an adapted form of Madelung's equations: the *(free) 1-body Madelung equations in the presence of an ideal detector*. This is a constrained system of nonlinear partial differential evolution equations in the (volume) probability density ρ in the region Ω, the probability surface density σ on the detector surface $\mathcal{D} = \partial\Omega$, as well as the probability current velocity $\vec{v}$ (see Equations (6) and (12) below for definitions in terms of a given wave function). To state the equations, we recall the definition of the stochastic velocity [26–28]:

$$\vec{u} = \frac{\hbar}{2m}\frac{\nabla\rho}{\rho}. \tag{1}$$

We further denote the outward-pointing unit normal vector field on $\mathcal{D}$ by $\vec{n}$, the

Heaviside step function by θ, the Dirac distribution on $\mathcal{D}$ by $\delta_{\mathcal{D}}$ and the restriction of a field to $\mathcal{D}$ by $\restriction_{\mathcal{D}}$. The system of equations is then given by

$$m\left(\frac{\partial \vec{v}}{\partial t} + (\vec{v}\cdot\nabla)\vec{v}\right) = m(\vec{u}\cdot\nabla)\vec{u} + \frac{\hbar}{2}\Delta\vec{u} \tag{2a}$$

$$\frac{\partial \rho}{\partial t} + \nabla\cdot\left(\rho\vec{v}\right) = \vec{n}\cdot\left(\rho\vec{v}\right)\restriction_{\mathcal{D}}\ \theta\left(-\vec{n}\cdot\left(\rho\vec{v}\right)\restriction_{\mathcal{D}}\right)\ \delta_{\mathcal{D}} \tag{2b}$$

$$\frac{\partial \sigma}{\partial t} = \vec{n}\cdot\left(\rho\vec{v}\right)\restriction_{\mathcal{D}}\ \theta\left(\vec{n}\cdot\left(\rho\vec{v}\right)\restriction_{\mathcal{D}}\right), \tag{2c}$$

subject to the constraints

$$\nabla\times\vec{v} = 0 \tag{2d}$$

$$\int_{\Omega}\rho\,\mathrm{d}^3r + \int_{\mathcal{D}}\sigma\,\mathrm{dS} = 1. \tag{2e}$$

We also derive a formal Schrödinger equation, Equation (33) below. A proposal for a corresponding weak formulation is given in the appendix.

This dynamical part of the solution to the time of arrival problem is heuristic in the sense that at this point Equation (2a) are only formal. That is, a rigorous solution requires the formulation of a corresponding system of distributional PDEs and a well-posedness result under suitable conditions on the initial data (cf. [29]). Since the aim of this work is to focus on the main ideas and such mathematical questions are beyond its scope, at this point the proposed solution only meets the standards of theoretical physics in terms of rigour, not those of mathematical physics.

In Section 5, we derive the impact time distribution $\mathbb{T}$ in terms of the normal component of the (time-dependent) probability current density

$$\vec{j} = \rho\vec{v} \tag{3}$$

with respect to $\mathcal{D}$. The probability that the body impinges on $\mathcal{D}$ between time $t \geq 0$ and $t+\Delta t$ for $\Delta t > 0$ is given by

$$\mathbb{T}([t, t+\Delta t]) = \int_{t}^{t+\Delta t}\mathrm{d}t'\int_{\mathcal{D}}\mathrm{dS}\ \vec{n}\cdot\vec{j}_{t'}\restriction_{\mathcal{D}}\ \theta\left(\vec{n}\cdot\vec{j}_{t'}\restriction_{\mathcal{D}}\right). \tag{4}$$

From this expression, a solution of the so called 'screen problem' [23,30] is also inferred.

Section 6 concludes with a discussion of the model in the context of the theory of measurement and the encompassing theoretical framework, as well as potential avenues for further research.

2. Problem description

We consider a connected, closed subset Ω of $\mathbb{R}^3$ such that its interior Ω is nonempty and its topological boundary $\partial\Omega$ is a smooth surface. We interpret the latter as an ideal detector surface $\mathcal{D} = \partial\Omega$. For instance, Ω may be the half-space $(0, \infty)\times\mathbb{R}^2$ or a closed ball of some given radius.

The initial position probability density $\rho_0 \in L^1(\Omega, \mathbb{R})$ of the body we require to be compactly supported in Ω. Furthermore, the support of ρ_0, denoted by $\operatorname{supp}\rho_0$, ought to be connected (cf. Remark 3.4 in [29]). Figure 1 provides a graphical depiction. Physically, the body is emitted from a particle gun at time $t = 0$ within the region $\operatorname{supp}\rho_0$ in Ω. The body then evolves freely, up until it impinges on the detector $\mathcal{D}$. The function $\rho : t \mapsto \rho_t$ describes the time evolution of that position probability density in space.

A more refined physical interpretation of ρ may be obtained on the basis of the concept of a statistical ensemble [31–33]. For an elaboration thereof in the context of this work, see Section 5.1 in [34], Section 2.1 in [35], as well as Section 3 in [28]).

The choice of the detector model is crucial for the physical description, since it has a direct impact on the evolution of $\rho : t \mapsto \rho_t$ (see also [1]). Corresponding evolution laws for the whole system need to be determined before one can address more advanced physical questions such as arrival time distributions. Proposals for the latter, which do not account for this point, may serve as approximations in some instances, but they do not fully solve the problem. Hence, we seek to implement the ideal detector model in terms of dynamical equations for the body.

A seemingly natural approach was given by Werner in the 1980s [14] (see also [36]). Therein the detector model is motivated from abstract considerations within the theory of quantum mechanics. It is not based on given physical properties of the detector.

While this work advocates for a different approach, it is nonetheless illustrative to see explicitly how the two approaches differ and why.

To recapitulate the results of [14], we consider a normalised, scalar wave function Ψ_0 on Ω. For $t \geq 0$ we let it evolve according to the free Schrödinger equation

$$\mathrm{i}\hbar \frac{\partial}{\partial t}\Psi_t = -\frac{\hbar^2}{2m}\Delta\Psi_t. \tag{5}$$

The Born rule for position now states that the probability density for the position of the body is

$$\rho = |\Psi|^2. \tag{6}$$

The aforementioned physical condition is then implemented by imposing a suitable boundary condition on Ψ_t at $\mathcal{D}$ for every $t \geq 0$ (cf. [13,14]).

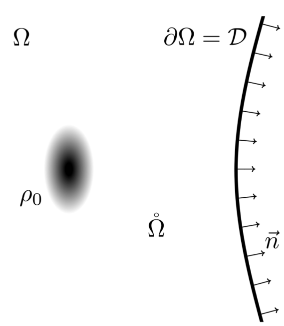

Figure 1. Sketch of the physical setup. An initial probability density ρ_0 is placed in a region $\Omega \subseteq \mathbb{R}^3$ with interior $\mathring{\Omega}$ in front of a detector screen $\partial\Omega = \mathcal{D}$ with unit normal vector field $\vec{n}$. The task is to determine the time evolution of the density ρ and predict the impact time distribution on $\mathcal{D}$.

Denote by $\vec{n}$ the unit normal vector field of $\mathcal{D}$ pointing away from Ω, denote restrictions of functions in Ω to $\mathcal{D}$ (if defined) by $\restriction_{\mathcal{D}}$, and let β be some (suitably regular) complex-valued function on $\mathcal{D}$. Then the boundary condition is

$$\vec{n} \cdot (\nabla\Psi) \restriction_{\mathcal{D}} = \beta \Psi \restriction_{\mathcal{D}} \tag{7}$$

with $\mathrm{Im}(\beta) \geq 0$ and a further technical requirement on β, which is only of minor interest here (cf. Secs. II and IV in [14]). For constant β this constitutes a homogeneous Robin boundary condition [37,38].

Again, if we argue on the basis of quantum-mechanical concepts, Equation (5) in conjunction with the condition (7) is rather natural. First, it does not modify the basic dynamical equation, Equation (5). Second, condition (7) may be formulated purely in terms of the wave function Ψ and its derivatives. And third, condition (7) is linear in Ψ.

Still, Cavendish and Das [23] argue that for constant β this approach yields qualitatively incorrect predictions for a variety of setups. The case of constant β appears to be the one most studied [13,23,36,39–44].

To continue the analysis of Equation (7), we consider the probability current density vector field

$$\vec{j} = \frac{\hbar}{m} \mathrm{Im}\left(\Psi^* \nabla \Psi\right) \tag{8}$$

(cf. Equation (3) above). Multiple authors have acknowledged its crucial role in the evolution problem [9,13,45–47].

We shall employ $\vec{j}$ to show that the boundary condition (7) indeed assures that $\mathcal{D}$ is 'absorbing' in a natural sense.

From Equation (7) and the definition of $\vec{j}$, Equation (8), it directly follows that

$$\vec{n} \cdot \vec{j} \restriction_{\mathcal{D}} = \frac{\hbar}{m} \mathrm{Im}\beta \; \rho \restriction_{\mathcal{D}} . \tag{9}$$

Since $\mathrm{Im}(\beta) \geq 0$, the above expression is positive. In the next step, we consider the implications of Equation (9) for the evolution of the total probability contained in Ω. By multiplying Equation (5) with Ψ^* and taking the imaginary part, we derive the so called *continuity equation*:

$$\frac{\partial \rho}{\partial t} + \nabla \cdot \vec{j} = 0. \tag{10}$$

Denote now the surface area element on $\mathcal{D}$ by dS. The rate of change of probability contained in Ω, as implied by Equation (10), is then given as follows:

$$\frac{\mathrm{d}}{\mathrm{d}t} \int_{\Omega} \rho_t \, \mathrm{d}^3 r = -\int_{\Omega} \nabla \cdot \vec{j}_t \, \mathrm{d}^3 r = -\int_{\mathcal{D}} \vec{n} \cdot \vec{j}_t \restriction_{\mathcal{D}} \mathrm{dS} = -\frac{\hbar}{m} \int_{\mathcal{D}} \mathrm{Im}\beta \; \rho_t \restriction_{\mathcal{D}} \mathrm{dS}. \tag{11}$$

This rate is negative. Accordingly and as claimed, the boundary condition (7) indeed assures that probability flows out of Ω and into $\mathcal{D}$. In this sense, the detector is absorbing.

Still, there are three general reasons to hold Equation (9) as physically unsatisfactory, irrespective of the results of [23].

First, it is arguably ad hoc. Surely, in [14] it was motivated from more general quantum-mechanical considerations. Nevertheless, the condition introduces the complex function β on $\mathcal{D}$ without specifying how it is physically determined. In order to solve the evolution problem, a particular choice of β is required.

For the second objection, we recall the definition of $\vec{v}$. This was implicitly given in terms of $\vec{j}$ via Equations (3) and (8):

$$\rho \vec{v} = \frac{\hbar}{m} \mathrm{Im}\big(\Psi^* \nabla \Psi\big). \tag{12}$$

Through a fluid dynamical analogy, $\vec{v}$ may be understood as the velocity at which an 'infinitesimal' amount of probability flows at the respective point in space and time (cf. Section 5.1 in [34]). The boundary condition (7) then implies that

$$\vec{n} \cdot \vec{v} \restriction_{\mathcal{D}} = \frac{\hbar}{m} \mathrm{Im}\beta \geq 0. \tag{13}$$

Accordingly, Equation (7) fixates the normal component of $\vec{v}$ on $\mathcal{D}$ to a priori given values. Yet such a condition is arguably unphysical: the boundary condition for an absorbing ideal detector should not fixate (components of) the probability current velocity. Instead it ought to state directly how well the detector absorbs the probability current.

The last objection is closely related to the former one. For this we recall the stochastic velocity $\vec{u}$ from Equation (1). In terms of Ψ it is given via

$$\rho \vec{u} = \frac{\hbar}{m} \mathrm{Re}\big(\Psi^* \nabla \Psi\big). \tag{14}$$

In full analogy to Equation (13), the boundary condition (7) implies the following constraint on $\vec{u}$

$$\vec{n} \cdot \vec{u} \restriction_{\mathcal{D}} = \frac{\hbar}{m} \mathrm{Re}\beta. \tag{15}$$

Thus, Equation (7) also fixates the normal component of $\vec{u}$ on $\mathcal{D}$ to a priori given values. Again, it is physically questionable, why such a constraint ought to hold for an ideal detector.

The alternative approach in the next section reproduces the successes of the boundary condition (7), while also alleviating its drawbacks.

3. The ideal detector model

In this section we construct a novel ideal detector model on the basis of mathematical probability theory and physical requirements imposed on the detector.

We recall that in Equation (11) we related the change of probability in Ω to the amount of probability flowing into the detector. In the approach pursued in [14], the boundary condition (7) at $\mathcal{D}$ assured that the relevant quantity $\vec{n} \cdot \vec{j} \restriction_{\mathcal{D}}$ was positive, so that this probability could only enter the detector and not leave. In the literature, this is sometimes and incorrectly [48,49] called the 'no (quantum) backflow condition' and it is the origin of many of the conceptual problems arising in the context of the time of arrival problem [11,16,46,50]. Here we also aim to impose dynamical equations, which assure that the detector is absorbing in this sense.

Mathematical probability theory [17] shall be employed as a heuristic tool for constructing the ideal detector model. Mathematical probability theory was axiomatized by Kolmogorov in 1933 [18,19]. The theory in conjunction with its descendant, mathematical statistics [51], has enjoyed enormous success across the empirical sciences – so far with the exception of (fundamental) quantum physics. In a prior work [28] it was argued that the historical development of quantum theory – rather than empirical evidence – is plausibly the reason for this state of affairs (cf. Section 2 of [28] in particular). Mathematical probability theory is a standard topic in the mathematical literature. An introduction may be found, for instance, in [17].

In mathematical probability theory the notion of a probability space is fundamental (cf. Def. 1.38(iii) and Section 1.5 in [17]). By definition, a *probability space* is a tuple $(\Omega, \mathcal{A}, \mathbb{P})$ such that Ω is a nonempty set, $\mathcal{A}$ is a suitably chosen σ-algebra on Ω and $\mathbb{P}: \mathcal{A} \to [0, 1]$ is a measure with the property that $\mathbb{P}(\Omega) = 1$. Ω is called the *sample space*. $\mathcal{A}$ may be viewed as the collection of all (random) events. Hence, a *(random) event* is a subset A of Ω, which is also an element of $\mathcal{A}$. The number $\mathbb{P}(A)$ is then the *probability of* A. The measure $\mathbb{P}$ is called a *probability measure* or a *probability distribution* (if it is associated to a random variable, see Section 1.5 in [17]).

In quantum theory, the probability measure is usually time-dependent. We write $\mathbb{P}_t$ for the probability measure at time $t \in \mathbb{R}$ (cf. Section 4 in [28]). Accordingly, the main goal of this section is to construct a suitable time-dependent probability space for the problem at hand.

At any given time t, the body is either in the space Ω or on the detector $\mathcal{D}$. The (volume) probability density ρ determines the probability for finding the body in a given region of space by integrating it over that region. Yet we should also be able to compute the probability of finding the body in a given area on the detector. This motivates the introduction of a *(time-dependent) surface probability density* σ on $\mathcal{D}$. In order to assure that ρ and σ indeed determine probabilities, we must impose that

$$1 = \int_{\Omega} \rho_t \, \mathrm{d}^3 r + \int_{\mathcal{D}} \sigma_t \, \mathrm{dS} \tag{16}$$

holds for all $t \geq 0$.

Equation (16) indeed enables us to construct a (time-dependent) probability space on the set Ω. It is given by Ω together with the Lebesgue sets $\mathcal{B}^*(\Omega)$ and the probability measure

$$\mathbb{P}_t : \mathcal{B}^*(\Omega) \to [0, 1] \; , \qquad U \mapsto \mathbb{P}_t(U). \tag{17}$$

For any $U \in \mathcal{B}^*(\Omega)$ and all $t \geq 0$, the measure $\mathbb{P}_t$ is defined via

$$\mathbb{P}_t(U) = \int_{U \cap \Omega} \rho_t \, \mathrm{d}^3 r + \int_{U \cap \mathcal{D}} \sigma_t \, \mathrm{dS}. \tag{18}$$

Equation (16) is then equivalent to

$$\mathbb{P}_t(\Omega) = 1. \tag{19}$$

Hence, $\mathbb{P}_t$ is indeed a probability measure. $\mathbb{P}_t(U)$ gives the probability that the body is either in space in the region $U \cap \Omega$ or on the detector surface in the region $U \cap \mathcal{D}$.

In general and unless $\sigma_t = 0$, $\mathbb{P}_t$ is singular with respect to the Lebesgue measure on Ω (cf. Section 7.4 in [17]): for any $U \in \mathcal{B}^*(\Omega)$ the set $U \cap \mathcal{D}$ always has Lebesgue measure zero and yet the probability to find the body there may be nonzero.

From a dynamical point of view, we find that Equation (16) constitutes a time-dependent constraint on ρ and σ. This constraint needs to be satisfied by the initial data. For later times it will be enforced by the dynamical equations. On the initial data we simply impose the condition: commonly, we choose $\sigma_0 = 0$, so that the body is initially situated in Ω and ρ_0 is taken to be a probability density in the mathematical sense of the word. For $t>0$, we satisfy Equation (16) by guaranteeing that

$$\frac{\mathrm{d}}{\mathrm{d}t}\,\mathbb{P}_t(\Omega) = \int_\Omega \frac{\partial \rho_t}{\partial t}\,\mathrm{d}^3 r + \int_{\mathcal{D}} \frac{\partial \sigma_t}{\partial t}\,\mathrm{dS} = 0. \tag{20}$$

If the continuity Equation (10) is assumed to hold, we may insert it into Equation (20). We then find that

$$\frac{\partial \sigma}{\partial t} = \vec{n}\cdot\vec{j}\restriction_{\mathcal{D}} \tag{21}$$

suffices to satisfy Equation (16) for $t > 0$, provided it is satisfied for $t = 0$. Equation (21) then implies that the time evolution of σ is given via

$$\sigma_t = \int_0^t \vec{n}\cdot\vec{j}_{t'}\restriction_{\mathcal{D}}\,\mathrm{d}t' + \sigma_0. \tag{22}$$

We define the detector to be absorbing, if at every point $\vec{x}$ on $\mathcal{D}$ the function $t \mapsto \sigma_t(\vec{x})$ is increasing. This is consistent with our prior usage of the term in Section 2.

A natural means to obtain this property is to impose other conditions at the boundary, so that $\partial\sigma/\partial t > 0$. An example would be condition (9) from Section 2. Yet, it appears that the problems of condition (9) generalise to this context in the following sense: such a boundary condition will involve the ad hoc introduction of new functions on $\mathcal{D}$ or the ad hoc coupling of $\vec{j}$ to other quantities already given. That is, a different detector model is needed.

In the approach pursued here, we instead *modify the continuity Equation* (10). Specifically, we use a Dirac distribution $\delta_{\mathcal{D}}$ on $\mathcal{D}$ to introduce a source/sink term on the detector surface:

$$\frac{\partial \rho}{\partial t} + \nabla\cdot\vec{j} = R\,\delta_{\mathcal{D}}. \tag{23}$$

The function R is defined on $\mathcal{D}$ and formally $\delta_{\mathcal{D}}$ is chosen such that for any sufficiently regular function $\phi : \Omega \to \mathbb{R}$ it holds that

$$\int_\Omega \phi\,\delta_{\mathcal{D}}\,\mathrm{d}^3 r = \int_{\mathcal{D}} \phi\restriction_{\mathcal{D}}\mathrm{dS}. \tag{24}$$

Equation (20) constitutes a necessary condition on R. It is satisfied, whenever

$$R = \vec{n}\cdot\vec{j}\restriction_{\mathcal{D}} - \frac{\partial \sigma}{\partial t}. \tag{25}$$

It follows from the definition that the detector is absorbing, if and only if the rate $\partial\sigma/\partial t$ is positive. How this is assured, depends on the particular detector model.

From Section 1 we recall the physical requirement on an ideal detector, that, once the body impinges on the detector surface $\mathcal{D}$, it stays thereon and is thus permanently removed from the interior Ω. We call this property *perfect absorption*, so that ideal detectors are, by definition, *perfectly absorbing*. Mathematically, we implement this property by introducing the Heaviside function θ and simply setting

$$\frac{\partial\sigma}{\partial t} = \vec{n}\cdot\vec{j}\restriction_{\mathcal{D}}\ \theta\big(\vec{n}\cdot\vec{j}\restriction_{\mathcal{D}}\big). \tag{26}$$

Equation (22) is then replaced by

$$\sigma_t = \int_0^t \vec{n}\cdot\vec{j}_{t'}\restriction_{\mathcal{D}}\ \theta\big(\vec{n}\cdot\vec{j}_{t'}\restriction_{\mathcal{D}}\big)\mathrm{d}t' + \sigma_0. \tag{27}$$

By construction, perfectly absorbing detectors are absorbing.

Of course, if $\vec{n}\cdot\vec{j}\restriction_{\mathcal{D}}$ were to take on negative values, then it may seem like the choice of Equation (26) would amount to ignoring the probability flowing out of the detector surface. However, Equation (25) in conjunction with Equation (26) yields the following expression:

$$R = \vec{n}\cdot\vec{j}\restriction_{\mathcal{D}}\ \theta\big(-\vec{n}\cdot\vec{j}\restriction_{\mathcal{D}}\big). \tag{28}$$

We shall show that Equation (28) implies that there is no probability flowing from $\mathcal{D}$ into Ω. To this end, we consider an arbitrary (sufficiently regular) $U \in \mathcal{B}^*(\Omega)$ and the corresponding (outward pointing) surface normal $\vec{n}'$ on ∂U with differential surface element $\mathrm{d}S'$. By decomposing

$$\partial U = \big(\partial U \setminus \mathcal{D}\big) \cup (\partial U \cap \mathcal{D}) \tag{29}$$

and using Equation (28) for the integral over $\partial U \cap \mathcal{D}$, we find that

$$\frac{\mathrm{d}}{\mathrm{d}t}\int_U \rho_t\, \mathrm{d}^3 r = -\int_{\partial U\setminus\mathcal{D}} \vec{n}'\cdot\vec{j}\restriction_{\partial\mathcal{U}}\ \mathrm{d}S' - \int_{\partial U\cap\mathcal{D}} \vec{n}\cdot\vec{j}\restriction_{\mathcal{D}}\ \theta\big(\vec{n}\cdot\vec{j}\restriction_{\mathcal{D}}\big)\mathrm{d}S. \tag{30}$$

The first summand gives the amount of probability flowing into the other spatial region $\Omega \setminus U$, while the second summand gives the amount of probability flowing into the relevant part of the detector surface, $\partial U \cap \mathcal{D}$. That the latter is negative for arbitrary choices of U means that probability can only flow into the detector surface $\mathcal{D}$; it can never flow out.

In summary, it was shown that the modified continuity Equation (23) in conjunction with the source/sink function R, as given via Equation (28), assures that the detector is absorbing. Conversely, if this is assumed, then probability conservation yields that the rate of change for the surface probability density σ is given via Equation (26).

Since this was achieved without the introduction of any restrictive boundary condition, Equations (23), (28), and (26) may be understood as a general detector model. To set some terminology, we say that those equations model an *ideal detector (with surface probability density* σ*).*

4. Dynamics in the presence of an ideal detector

In Section 3 above, we have seen that one can model a perfectly absorbing ideal detector by adding an appropriate sink term to the continuity equation. However, the Schrödinger equation implies the continuity Equation (10) (cf. Section 2). The Schrödinger equation is therefore incompatible with the derived, modified continuity Equation (23) for $R \neq 0$.

In this section we argue that the modified continuity Equation (23) may still be used to set up physically sensible dynamical equations. This is achieved by taking a broader view on quantum dynamics, which is based on a system of partial differential equations discovered by Madelung in the 1920s [20–22,27,34]. While the resulting, adapted system of dynamical equations is incompatible with the quantum-mechanical formalism, it may be regarded as a typical model within *geometric quantum theory*. Geometric quantum theory is a novel adaption of quantum mechanics, which makes the latter consistent with mathematical probability theory (cf. [28,34]). After motivating the dynamical equations of interest here, we provide a brief review of the theory and show how the results of Section 3 are naturally embedded within this novel formalism.

In 1926 Madelung derived a reformulation of Schrödinger's equation [20–22]. His system of PDEs is closely reminiscent of dynamical equations commonly encountered in Newtonian continuum mechanics. A sizable amount of literature on the Madelung equations may be found under the somewhat deceiving heading of 'quantum hydrodynamics' (see e.g. [52–63]). Upon defining ρ, $\vec{v}$ and $\vec{u}$ as in Equations (6), (12), and (14) above and using a formulation due to Nelson [27], the Madelung equations are the system of PDEs consisting of the Madelung force equation (for some given potential V)

$$m\left(\frac{\partial \vec{v}}{\partial t} + (\vec{v} \cdot \nabla)\vec{v}\right) = -\nabla V + m(\vec{u} \cdot \nabla)\vec{u} + \frac{\hbar}{2}\Delta\vec{u}, \tag{31}$$

the continuity Equation (10), as well as the irrotationality condition

$$\nabla \times \vec{v} = 0. \tag{32}$$

The Madelung equations are a nonlinear system of constrained evolution equations in terms of the (time-dependent) probability density ρ and the (time-dependent) vector field $\vec{v}$. It is a subject of contemporary mathematical research, whether there exists a distributional formulation for suitably chosen initial data such that the corresponding initial value problem is well-posed. In particular, the status of Equation (32) has been a source of much debate. The interested reader is referred to [29,52,53,55,64–66].

The Madelung equations are of interest to the discussion here, since they decouple what is arguably the dynamical part of the Schrödinger equation, Equation (31), from the part ensuring probability conservation, Equation (10).

The central idea for defining the dynamics for a single (not necessarily free) body in the presence of an ideal detector is therefore to replace Equation (10) by Equation (23) (together with Equation (28)), while keeping Equations (31) and (32). For $V = 0$, the full system of equations is then indeed given by Equation (2a). In either case, σ may be obtained from Equation (27).

One may ask, whether this new system of PDEs gives rise to a modified Schrödinger equation. For non-distributional source terms and under stronger conditions of regularity, a corresponding modified Schrödinger equation was indeed given in Proposition 6.1 of [34].

By carrying this equation over in a purely formal manner, we obtain

$$\mathrm{i}\hbar\frac{\partial}{\partial t}\Psi = -\frac{\hbar^2}{2m}\Delta\Psi + V\Psi + \mathrm{i}\frac{\hbar^2}{2m}\,\vec{n}\cdot\mathrm{Im}\left(\frac{\nabla\Psi}{\Psi}\bigg|_{\mathcal{D}}\right)\theta\big(-\vec{n}\cdot\mathrm{Im}\big(\Psi^*\nabla\Psi\big)\restriction_{\mathcal{D}}\big)\delta_{\mathcal{D}}\Psi\restriction_{\mathcal{D}}. \quad (33)$$

Whether and how Equation (33) may be recast into a mathematically meaningful expression is an open question. The interested reader may find an arguably natural approach to this question in the appendix.

Quantum mechanics requires that the infinitesimal generator of time evolution, the Hamiltonian, is a linear and even (unbounded) self-adjoint operator on the respective L^2-space (cf. Sec. VIII.4 in [67] and Section 1.2.1 in [68]). Equation (33) is nonlinear in Ψ and the corresponding Hamiltonian fails to be even symmetric. Therefore, at least within the theory of quantum mechanics, this detector model leads to unacceptable dynamics.

Still, Equations (23), (28), (31), (32), and (26) (respective Equation (2a) for $V = 0$) in principle define a sensible system of PDEs for the quantities ρ, $\vec{v}$, and σ. We shall call this system of equations the *(1-body) Madelung equations in the presence of an ideal detector*. Of course, mathematically one still requires an appropriate weak formulation and a proof of well-posedness for suitably chosen initial data [29], yet such questions are beyond the scope of this work. Rather, we shall ask whether the system is acceptable from a physical point of view, in spite of the overt incompatibility with the theory of quantum mechanics.

It was already argued that this dynamical model is physically natural. Yet if it is not embedded within a physically justified theoretical framework, it may still seem ad hoc. This theoretical framework exists and is known as *geometric quantum theory*. Indeed, the solution of the time of arrival problem presented in this work ought to be considered an application of geometric quantum theory – one in which the conceptual differences to the theory of quantum mechanics exhibit themselves on a dynamical level. In Section 7 of [28], the existence of such models was already anticipated.

Geometric quantum theory is a research program in both non-relativistic and relativistic quantum theory, which is based on two core hypotheses:

(I) Fundamental equations of quantum theory admit a Madelung formulation (i.e. a formulation akin to the Madelung equations).
(II) Quantum phenomena are described via mathematical probability theory.

Originally, geometric quantum theory was born out of the observation that the Madelung equations suggest a physically natural solution to the problem of (first) quantisation under holonomic constraints (cf. Section 1.1 and Remark 3.5 in [34]). Instead of providing yet another ad hoc quantisation scheme, however, geometric quantum theory traces the common quantum-mechanical operators back to physically natural random variables. That is, at each time ‘observables’ are modelled by real scalar or real vector-valued functions on the probability space. Those random variables are motivated from the close analogy of the Madelung equations to the theory of diffusion (cf. Section 4 in [34] and Section 5 in [28]). For the many-body Schrödinger theory with time-independent scalar potential, it was found that central quantum-mechanical predictions are reproduced in this manner. Moreover, for this class of models a mathematically rigorous formulation has been attained and the ability of the theory to make novel predictions in certain instances has been ascertained [28]. Geometric quantum theory provides a natural approach to the classical limit, which is asymptotically given by the case that $\hbar$ is small in comparison to the characteristic length and time scales in the particular model (cf. [34,55] and Rem. 3.1 in [29]). Roughly, this is the limit in which the latter two summands on the right hand side of Equation (31) vanish. Thus, in geometric quantum theory there is no 'Heisenberg cut' and in passing to the classical limit no need arises to change the underlying probability theory. Furthermore, an approach to (general-)relativistic geometric quantum theory has already been developed in [69].

Geometric quantum theory is connected to de Broglie-Bohm theory [70–74] and Nelson's theory of stochastic mechanics [27,75–78] through the incorporation of the Madelung equations into the basic formulation of the theory. Still, the latter two theories are mostly depicted as reinterpretations or extensions of quantum mechanics, while geometric quantum theory is a distinct theory. Of course, if the current velocity vector field is sufficiently regular, the Picard-Lindelöf theorem makes it possible to consider 'Bohm trajectories' within geometric quantum theory. Furthermore, in Section 2.2 of [35] it was argued that, for reasons of internal consistency, stochastic mechanics requires mathematical probability theory to hold. If this view is taken, geometric quantum theory constitutes a generalisation of stochastic mechanics, which does not rely on any particular model of particle trajectories (see also [79,80]).

In practical applications of geometric quantum theory, one carries over the respective Schrödinger equation from quantum mechanics and one then considers its Madelung formulation. By Postulate (I), geometric quantum theory requires that such a formulation exists. For the N-body Schrödinger equation [35,74], the Pauli equation [54,61] and the Dirac equation [81–83] such formulations have indeed been discovered. In the next step, one replaces the quantum-mechanical operators by respective physical random variables, as motivated from the Madelung formulation. In accordance with Postulate (II), this allows one to employ mathematical probability theory for making specific predictions in relation to the probability distributions of those random variables (cf. Section 7 in [28]).

We shall discuss the implications of geometric quantum theory for the class of models considered in this work. Following [28], a physical model in geometric quantum theory consists of three basic ingredients:

(1) A time-dependent probability space, which gives the probability that the bodies are in particular configurations (Born rule for position).
(2) A collection of time-dependent physical random variables, such as position, energy, etc.
(3) A time evolution law for those quantities.

For the problem at hand, the probability space has already been described in Section 3. Through the use of differential equations and initial conditions for ρ and σ, we were able to guarantee that condition (16) is met for all times.

As random variables, we have introduced the probability current velocity $\vec{v}$ and the stochastic velocity $\vec{u}$ (via ρ in Equation (1)). The position random variable $\vec{r}$, the probability current momentum $\vec{p} = m\vec{v}$ as well as the angular momentum of the probability current $\vec{r} \times \vec{p}$ (around the origin) were implicit in the description. The energy random variable can be directly obtained from the Madelung force equation:

$$E = \frac{m}{2}\vec{v}^2 + V - \frac{m}{2}\vec{u}^2 - \frac{\hbar}{2}\nabla \cdot \vec{u}. \tag{34}$$

Note that the latter two summands are responsible for quantum tunnelling.

In the case of interest, $V = 0$ and thus the time evolution of ρ, σ and $\vec{v}$ is given via the free Madelung equations in the presence of an ideal detector, Equation (2a). From those three quantities all other physically relevant random variables can be computed.

We conclude this section with the note that, if $\mathbb{P}_t(\mathcal{D}) \neq 0$ for some t, we may compute the conditional probability measure given $\mathcal{D}$ (at time t). It is denoted by $\mathbb{P}_t(\,.\,|\mathcal{D})$ and for any $U \in \mathcal{B}^*(\Omega)$ it is given via

$$\mathbb{P}_t(U|\mathcal{D}) = \frac{\mathbb{P}_t(U \cap \mathcal{D})}{\mathbb{P}_t(\mathcal{D})} = \frac{1}{\mathbb{P}_t(\mathcal{D})}\int_{U\cap\mathcal{D}} \sigma_t \, \mathrm{dS} \tag{35}$$

(cf. Definition 8.2 in [17]). $\mathbb{P}_t(\,.\,|\mathcal{D})$ is of interest, because it allows us to compute probabilities, probability distributions and expectation values of random variables under the condition that the body is on the detector screen. This may be considered an 'after/during measurement' condition.

For instance, the expectation of the probability current momentum at time t with respect to $\mathbb{P}_t(\,.\,|\mathcal{D})$ is given via

$$\mathbb{E}_t(\vec{p}_t|\mathcal{D}) = \frac{1}{\mathbb{P}_t(\mathcal{D})}\int_{\mathcal{D}} \vec{p}_t \restriction_{\mathcal{D}} \sigma_t \, \mathrm{dS} \tag{36}$$

(cf. Definition 8.9 in [17]). It may be understood as a measure of how 'hard' the body hits the detector on average at time t.

5. Time of arrival probability

In order to solve the time of arrival problem, we now ask for the probability that the body impacts on the detector surface between t and $t + \Delta t$ with $t \geq 0$ and $\Delta t > 0$. We shall assume that initially $\mathbb{P}_0(\mathcal{D}) = 0$, which is equivalent to $\sigma_0 = 0$ (Lebesgue almost everywhere).

To begin, it is imperative to know that neither quantum mechanics nor geometric quantum theory in its current state of development are able to make specific predictions for individual bodies: they are concerned with the ensemble [31–33] as a whole, not the individual samples constituting the ensemble (cf. Section 2.1 in [35] and Section 3 in [28]). They are phenomenological theories in the sense that only probabilities for the ensemble can be computed. For instance, they can predict the probability that the body is in a certain region of space at time t; yet they can generally not predict that the body is in a certain region of space at time $t + \Delta t$, given that *the same body* was in some other region at time t. In other words, there is generally no 'resolution' on the level of the individual sample, as so called 'hidden variable theories' such as de Broglie-Bohm theory [12,45] or stochastic mechanics [11] aim to achieve (see also [84] for the related concept of 'first hit time' in the theory of stochastic processes).

That the context at hand provides us with a different situation is due to the fact that the detector model was constructed in such a manner, that after impact the individual body stays at its impact location.

Thus, we can infer that for an ideal detector the probability that the body hits the detector surface up until (and including) any time $t' \geq 0$ is given by the quantity

$$\mathbb{T}\big([0, t']\big) = \mathbb{P}_{t'}(\mathcal{D}). \tag{37}$$

Accordingly, Equation (37) does not hold, when the detector is not absorbing, i.e. when there is so called 'quantum reentry' [11,48,49]: in general, $\mathbb{P}_{t'}(\mathcal{D})$ gives the probability that at time t' a given body in the ensemble is on the detector surface. Hence, if that body can leave its location of impact, $\mathbb{P}_{t'}(\mathcal{D})$ does not contain any information about prior impacts. It is only through the ideal detector model that we can use $\mathbb{P}$ to determine the impact time distribution. In this instance, this distribution is the same as the distribution for the 'time of flight', defined as the time the body stays in the interior Ω after emission at $t = 0$.

To determine the arrival probability for an interval, we formally require $\mathbb{T}$ to be a probability measure. The function $t' \mapsto \mathbb{T}([0, t'])$ on $[0, \infty)$, as given by Equation (37), may then be formally viewed as cumulative probability distribution function. Hence, we find

$$\mathbb{T}((t, t + \Delta t]) = \mathbb{T}([0, t + \Delta t]) - \mathbb{T}([0, t]) \tag{38}$$

$$= \mathbb{P}_{t+\Delta t}(\mathcal{D}) - \mathbb{P}_t(\mathcal{D}). \tag{39}$$

While cumulative distribution functions may be discontinuous in general, the formula for the rate $\partial\sigma/\partial t$, Equation (26), suggests that $t' \mapsto \mathbb{T}([0, t'])$ is continuous. Therefore, $\mathbb{T}(\{t'\}) = 0$ for any $t' \geq 0$ and thus

$$\mathbb{T}([t, t + \Delta t]) = \mathbb{T}((t, t + \Delta t]) = \mathbb{P}_{t+\Delta t}(\mathcal{D}) - \mathbb{P}_t(\mathcal{D}). \tag{40}$$

Equation (40) provides the answer to the stated problem. An analogous expression was given by Daumer et al. [45], though using the different rate (21).

We shall also construct the respective probability space $(\Lambda, \mathcal{A}', \mathbb{T})$. First, we recall that the function $t \mapsto \mathbb{P}_t(\mathcal{D})$ is monotonously increasing and bounded from above by 1. The limit

$$p_\infty = \lim_{t \to \infty} \mathbb{P}_t(\mathcal{D}) \tag{41}$$

therefore exists, yet it need not equal 1. By definition, p_∞ is the probability that the body impacts on the detector surface at an any time:

$$\mathbb{T}([0, \infty)) = p_\infty. \tag{42}$$

Conversely, the quantity $1 - p_\infty$ gives the probability that the body never reaches the detector surface. Unless $p_\infty = 1$, one needs to account for this particular event in defining $\mathbb{T}$ (cf. [1,5]). We shall choose the convention to symbolically represent the event by the singleton $\{\emptyset\}$. We therefore obtain the following

$$\Lambda = [0, \infty) \cup \{\emptyset\} \tag{43}$$

with

$$\mathbb{T}(\{\emptyset\}) = 1 - p_\infty \quad \text{and} \quad \mathbb{T}(\Lambda) = 1. \tag{44}$$

Accordingly, the σ-algebra $\mathcal{A}'$ is the one generated from the union of the Lebesgue sets $\mathcal{B}^*([0,\infty))$ and the set $\{\emptyset\}$ (cf. Theorem 1.16 in [17]). We shall write this as follows:

$$\mathcal{A}' = \Sigma\big(\mathcal{B}^*([0,\infty)) \cup \{\emptyset\}\big). \tag{45}$$

Equation (40) then suggests the following general formula for the probability measure $\mathbb{T}$ for an arbitrary $J \in \mathcal{A}'$:

$$\mathbb{T}(J) = \int_{J\setminus\{\emptyset\}} \mathrm{d}t \int_{\mathcal{D}} \mathrm{dS}\ \frac{\partial\sigma}{\partial t} + \mathbb{T}(J \cap \{\emptyset\}). \tag{46}$$

Formula (46) in conjunction with Equation (26) (along with the respective probability space) is indeed what is suggested here as a general solution to the time of arrival problem for a single body and an ideal detector. $\mathbb{T}$ is the probability distribution for the impact time of the body, which also accounts for the event of no impact. For $J \in \mathcal{B}^*([0,\infty))$ the quantity $\mathbb{T}(J)$ is the probability that the body impacts on the detector at any time t with $t \in J$. For $J = \{\emptyset\}$ the quantity $\mathbb{T}(J) = \mathbb{T}(\{\emptyset\})$ is the probability that the body never impacts on the detector.

To close this section, we shall introduce a closely related probability space, which allows one to compute the probability that the body impinges on the surface in a given interval of time and a given region on the detector surface. Determining this probability is called the *screen problem* [23,30].

The respective probability measure $\mathbb{D}$ can be defined on the measurable space

$$\big(([0,\infty) \times \mathcal{D}) \cup \{\emptyset\}, \Sigma\big(\mathcal{B}^*([0,\infty) \times \mathcal{D}) \cup \{\emptyset\}\big)\big). \tag{47}$$

For the event of no impact we again have

$$\mathbb{D}(\{\emptyset\}) = 1 - p_\infty. \tag{48}$$

For an event $U \in \mathcal{B}^*(\mathcal{D} \times [0,\infty))$ the measure is given via

$$\mathbb{D}(U) = \int_U \mathrm{d}t\mathrm{dS}\ \frac{\partial\sigma}{\partial t}. \tag{49}$$

In analogy to Equation (46), we may therefore write down the general formula

$$\mathbb{D}(J) = \int_{J\setminus\{\emptyset\}} \mathrm{d}t\mathrm{dS}\ \frac{\partial\sigma}{\partial t} + \mathbb{D}(J \cap \{\emptyset\}) \tag{50}$$

for any $J \in \Sigma(\mathcal{B}^*([0,\infty) \times \mathcal{D}) \cup \{\emptyset\})$.

We call $\mathbb{D}$ the *(ideal) detector distribution*. $\mathbb{D}$ is the joint probability distribution for the impact location and the impact time of the body, which also accounts for the event of no impact. For J as above with $J \cap \{\emptyset\} = \emptyset$, the quantity $\mathbb{D}(J)$ is the probability that the body impacts on the detector at any time t and location $\vec{r}$ with $(t, \vec{r}) \in J$. For $J = \{\emptyset\}$ the quantity $\mathbb{D}(J) = \mathbb{D}(\{\emptyset\}) = \mathbb{T}(\{\emptyset\})$ is the probability that the body never impacts on the detector. As noted by Cavendish and Das [23], $\mathbb{T}$ may be viewed as a marginal distribution of $\mathbb{D}$.

This solution of the screen problem via Equation (50) is, of course, provided in the context of the dynamics determined by Equation (2a). Otherwise, the solution is not wholly original, for, again, Daumer et al. [45] have implicitly suggested Equation (49) to hold and a more explicit formula was given by Tumulka in [13] – though both works used Equation (21) instead of Equation (26) for the rate.

6. Conclusion

In the context of the time of arrival problem, we have addressed the question of measurement by explicitly including the ideal detector model in the equations for the dynamical evolution of the system. In the context of the larger, foundational debate on measurement within quantum theory, it shall be remarked that measurement always requires a probe, such as a detector, another particle or radiation. That contemporary theory, at least in part, replaces this physical process by an abstract projection instead of modelling it directly (cf. [31,85] and Remark 4.55(a) in [68]) is arguably one of the reasons why a resolution of the time of arrival problem has proven so difficult: therein lies the motivation for the numerous attempts to construct a 'time operator'. Arguably, such approaches did not succeed, because they pursued abstraction on the grounds of weak physical arguments over concrete physical models [1,30]. In this sense, the aforementioned, paradoxical status of the time of arrival problem in contemporary quantum theory points at the limitations of the projection postulate in our contemporary theory of measurement. Addressing these limitations will require, on the one hand, a justification for the empirical success of the projection postulate in certain instances, and, on the other hand, a theoretical framework, which does not rely on it for describing the physical process of measurement.

This work constitutes a step in this direction. Here it was possible to forego the use of the projection postulate by modelling the measurement outcomes directly via the probability surface density σ Section 3. The respective detector model, however, necessitates a broader view on quantum dynamics than what the theory of quantum mechanics can supply. Far from being ad hoc, it was shown in Section 4 how this broader view on quantum dynamics is embedded within the theoretical framework of geometric quantum theory [28,34,35]. Geometric quantum theory is a novel adaption of quantum mechanics, which makes the latter consistent with mathematical probability theory (cf. [28,34]). In the theory, predictions of measurement outcomes are obtained by including the interaction of the probe with the system of interest in the dynamical model, rather than relying on the Dirac-von Neumann axioms. Since geometric quantum theory generally uses the same evolution equations for modelling this process as quantum mechanics, differences in prediction tend to be quantitative in nature, seldom qualitative.

At the end of Section 4, it was also shown how geometric quantum theory is able to make statements about the system 'after measurement': for this purpose, mathematical probability theory supplies the tools of conditional probability measures and conditional expectation values. It is to be expected that a general treatment, which addresses the aforementioned limitations of the projection postulate, will also make use of these tools.

In this respect, it is also worthwhile to recall the limitations of both quantum mechanics and geometric quantum theory in its current form with regards to making predictions for individual samples in the ensemble Section 5: only in isolated instances, it is possible to make such predictions. In this instance, it was the ideal detector model that ultimately enabled the prediction of the time of impact distribution. For the related tunnelling time problem [86–89], however, nothing can be said about the position of the individual body shortly after it reaches or has traversed the barrier. That is, without any further physical assumptions, this problem is beyond the limitations of contemporary theory.

We shall also address further developments of the model presented in this work. Among those, finding an appropriate distributional formulation of the system of Equation (2a) appears to be most pressing. A contribution towards the resolution of this question for the original Madelung equations may be found in [29], though even for that system the question remains unresolved and a proof of well-posedness for an appropriate formulation with suitably chosen initial data $(\rho_0, \vec{v}_0)$ currently seems to be beyond reach. Well-posedness results for non-linear systems of equations in Newtonian continuum mechanics are, however, known to be difficult to obtain, so that a more pragmatic approach seems appropriate. Numerical solutions to a given distributional formulation of Equation (2a) may be possible without a rigorous result of well-posedness. In lower-dimensional analogue models, closed-form solutions may be within reach. Furthermore and as done in the appendix, one may consider a suitable weak formulation of the modified Schrödinger equation (33) instead. Such pragmatic approaches may also open up the path to empirical tests.

An obvious further refinement of the presented model is to include particle spin and its interaction with electromagnetic radiation [54,61,89–94]. Works that aim to solve the time of arrival problem for multiple bodies already exist [42,95–97], so it is natural to ask how to generalise Equation (2a) to the many-body case. The latter is also of potential, independent concern, since the ability to enclose a finite domain with a perfectly absorbing boundary may have applications to numerical quantum chemistry (see e.g. [98] on the so called 'curse of dimensionality' in this context). Another possible extension of the model is the inclusion of interactions of the body with the detector surface: for instance, one may charge the detector and consider electromagnetic interactions or even include stochastic interactions with the detector surface, thus creating a potential link to the theory of open quantum systems [99,100]. Of course, it is also natural to consider generalisations to the relativistic domain [69,97,101,102].

On a final note, one may extend the model to contexts, which are of central importance to the foundations of quantum theory. For instance, one may consider the ideal detector model in the context of Bell test experiments [93,103,104]. It may also be used to obtain a probabilistic 'near field' model of the double slit experiment [39,40,105–107] by modelling the screen with the slits via a homogeneous Dirichlet boundary condition. Such a model may indeed provide an illustrative example for how geometric quantum theory, which is based on mathematical probability theory and a point mass model of particles, is able to predict the correct wave-like statistics.

Acknowledgments

The author would like to thank Valter Moretti for drawing his attention to the problem as well as Pascal Naidon, Siddhant Das, Ángel Sanz, Sophya Garashchuk, Vitaly Rassolov, Lev Vaidman, and Alisson Tezzin for helpful discussion.

Disclosure statement

No potential conflict of interest was reported by the author(s).

ORCID

Maik Reddiger http://orcid.org/0000-0002-0485-5044

References

[1] G.R. Allcock, *The time of arrival in quantum mechanics I. Formal considerations*, Ann. Phys. 53 (1969), pp. 253–285. https://doi.org/10.1016/0003-4916(69)90251-6.
[2] W. Pauli, *Die allgemeinen prinzipien der wellenmechanik*, in *Prinzipien der Quantentheorie I*, S. Flügge, ed., Springer, Vol. 5, 1958, pp. 1–160.
[3] W. Pauli, *Die allgemeinen Prinzipien der Wellenmechanik: Neu heraus gegeben und mit historischen Anmerkungen versehen von Norbert Straumann*, Springer, Berlin, 1990.
[4] R. Brunetti and K. Fredenhagen, *Time of occurrence observable in quantum mechanics*, Phys. Rev. A 66 (2002), pp. 044101. https://doi.org/10.1103/PhysRevA.66.044101.
[5] S. Das and W. Struyve, *Questioning the adequacy of certain quantum arrival-time distributions*, Phys. Rev. A 104 (2021), pp. 042214. https://doi.org/10.1103/PhysRevA.104.042214.
[6] V. Delgado and J.G. Muga, *Arrival time in quantum mechanics*, Phys. Rev. A 56 (1997), pp. 3425–3435. https://doi.org/10.1103/PhysRevA.56.3425.
[7] S. Goldstein, R. Tumulka, and N. Zanghì, Arrival times versus detection times. Found. Phys. 54 (2024), article number 63. https://doi.org/10.1007/s10701-024-00798-y.
[8] N. Grot, C. Rovelli, and R.S. Tate, *Time of arrival in quantum mechanics*, Phys. Rev. A 54 (1996), pp. 4676–4690. https://doi.org/10.1103/PhysRevA.54.4676.
[9] T. Jurić and H. Nikolić, *Arrival time from Hamiltonian with non-Hermitian boundary term*, Universe 10 (2024), article number 35. https://doi.org/10.3390/universe10010035.
[10] J. Kijowski, *On the time operator in quantum mechanics and the heisenberg uncertainty relation for energy and time*, Rep. Math. Phys. 6 (1974), pp. 361–386. https://doi.org/10.1016/S0034-4877(74)80004-2.
[11] P. Naidon, *Inequivalence of stochastic and Bohmian arrival times in time-of-flight experiments*, Phys. Rev. A 109 (2024), pp. 063312. https://doi.org/10.1103/PhysRevA.109.063312.
[12] M.V. Scherer, A.D. Ribeiro, and R.M. Angelo, *Testing trajectory-based determinism via probability distributions*. Chin. J. Phys 97 (2025), pp. 1199–1212. https://doi.org/10.1016/j.cjph.2025.08.020.
[13] R. Tumulka, *Distribution of the time at which an ideal detector clicks*, Ann. Phys. 442 (2022), pp. 168910. https://doi.org/10.1016/j.aop.2022.168910.
[14] R. Werner, *Arrival time observables in quantum mechanics*, Ann. Inst. Henri Poincaré 47 (1987), pp. 429–449.
[15] J.G. Muga and C.R. Leavens, *Arrival time in quantum mechanics*, Phys. Rep. 338 (2000), pp. 353–438. https://doi.org/10.1016/S0370-1573(00)00047-8.
[16] S. Das, *Arrival-time distributions and spin in quantum mechanics*, PhD thesis, Ludwig-Maximilians-University of Munich, Munich, 2023.
[17] A. Klenke, Probability Theory: A Comprehensive Course, 3rd ed., Springer, Berlin, 2020. https://doi.org/10.1007/978-3-030-56402-5.
[18] A. Kolmogoroff, Grundbegriffe der Wahrscheinlichkeitsrechnung, Springer, Berlin, 1933. https://doi.org/10.1007/978-3-642-49888-6.
[19] A. Kolmogorov, Foundations of the Theory of Probability, 2nd ed., Chelsea Publishing, New York, 1956. Trans. by N. Morrison.
[20] E. Madelung, *Eine anschauliche deutung der gleichung von Schrödinger*, Naturwissenschaften 14 (1926), pp. 1004–1004. https://doi.org/10.1007/BF01504657.

[21] E. Madelung, *Quantentheorie in hydrodynamischer form*, Z. Physik 40 (1927), pp. 322–326. https://doi.org/10.1007/BF01400372.
[22] E. Madelung, *Quantum theory in hydrodynamical form*. Trans. by D. Delphenich, 2015. Available at http://www.neo-classical-physics.info/uploads/3/4/3/6/34363841/madelung_-_hydrodynamical_interp..pdf.
[23] W. Cavendish and S. Das, *Absorbing detectors meet scattering theory*, Phys. Rev. A 112 (2025), pp. 062217. https://doi.org/10.48550/arXiv.2509.07518.
[24] M. Reed and B. Simon, Methods of Modern Mathematical Physics: Scattering Theory, Vol. III, Academic Press, New York, 1979.
[25] J.R. Taylor, Scattering Theory: The Quantum Theory on Nonrelativistic Collisions, Wiley, New York, 1972.
[26] E.A. Carlen, *Conservative diffusions*, Commun. Math. Phys. 94 (1984), pp. 293–315. https://doi.org/10.1007/BF01224827.
[27] E. Nelson, *Derivation of the Schrödinger equation from Newtonian mechanics*, Phys. Rev. 150 (1966), pp. 1079–1085. https://doi.org/10.1103/PhysRev.150.1079.
[28] M. Reddiger, *On the applicability of Kolmogorov's theory of probability to the description of quantum phenomena. Part I: Foundations*, Quantum Stud.: Math. Found. 13 (2026), article number 1. https://doi.org/10.1007/s40509-025-00375-6.
[29] M. Reddiger and B. Poirier, *Towards a mathematical theory of the Madelung equations: Takabayasi's quantization condition, quantum quasi-irrotationality, weak formulations, and the Wallstrom phenomenon*, J. Phys. A: Math. Theor. 56 (2023), pp. 193001. https://doi.org/10.1088/1751-8121/acc7db.
[30] B. Mielnik, *The screen problem*, Found. Phys. 24 (1994), pp. 1113–1129. https://doi.org/10.1007/BF02057859.
[31] L.E. Ballentine, *The statistical interpretation of quantum mechanics*, Rev. Mod. Phys. 42 (1970), pp. 358–381. https://doi.org/10.1103/RevModPhys.42.358.
[32] A. Pechenkin, *The statistical (ensemble) interpretation of quantum mechanics*, in *The Oxford Handbook of the History of Quantum Interpretations*, O. Freire Junior, G. Bacciagaluppi, O. Darrigol, T. Hartz, C. Joas, A. Kojevnikov and O. Pessoa Junior, eds., Oxford University Press, Oxford, 2022, pp. 1247–1264.
[33] R. von Mises, Probability, Statistics, and Truth, 2nd ed., Dover Publications, New York, 1957.
[34] M. Reddiger, *The Madelung picture as a foundation of geometric quantum theory*, Found. Phys. 47 (2017), pp. 1317–1367. https://doi.org/10.1007/s10701-017-0112-5.
[35] M. Reddiger, *Towards a probabilistic foundation for non-relativistic and relativistic quantum theory*, PhD thesis, Lubbock: Texas Tech University, 2022. url: https://hdl.handle.net/2346/91876
[36] T. Fevens and H. Jiang, *Absorbing boundary conditions for the Schrödinger equation*, SIAM J. Sci. Comput. 21 (1999), pp. 255–282. https://doi.org/10.1137/S1064827594277053.
[37] P.C. Bressloff, *Diffusion-mediated absorption by partially-reactive targets: Brownian functionals and generalized propagators*, J. Phys. A: Math. Theor. 55 (2022), pp. 205001. https://doi.org/10.1088/1751-8121/ac5e75.
[38] L. Frolov, *Detecting screens modeled by Schrödinger operators that generate C0 contraction semigroups*, Rev. Math. Phys. 11 (2025), article number 2550036. https://doi.org/10.1142/S0129055X25500369.
[39] A. Ayatollah Rafsanjani, M. Kazemi, A. Bahrampour, and M. Golshani, *Can the double-slit experiment distinguish between quantum interpretations?* Commun. Phys. 6 (2023), article number 195. https://doi.org/10.1038/s42005-023-01315-9.
[40] A. Ayatollah Rafsanjani, M. Kazemi, V. Hosseinzadeh, and M. Golshani, *Non-local temporal interference*, Sci. Rep. 14 (2024), article number 3615. https://doi.org/10.1038/s41598-024-54018-8.
[41] L. Frolov, S. Teufel, and R. Tumulka, *Existence of Schrödinger evolution with absorbing boundary condition*, Math. Phys. Anal. Geom. 28 (2025), pp. 27. https://doi.org/10.1007/s11040-025-09521-3.

[42] R. Tumulka, *Detection-time distribution for several quantum particles*, Phys. Rev. A 106 (2022), pp. 042220. https://doi.org/10.1103/PhysRevA.106.042220.
[43] R. Tumulka, *Absorbing boundary condition as limiting case of imaginary potentials*, Commun. Theor. Phys. 75 (2022), pp. 015103. https://doi.org/10.1088/1572-9494/ac9bea.
[44] R. Tumulka, *On a derivation of the absorbing boundary rule*, Phys. Lett. A 494 (2024), pp. 129286. https://doi.org/10.1016/j.physleta.2023.129286.
[45] M. Daumer, D. Dürr, S. Goldstein, and N. Zanghì, *On the quantum probability flux through surfaces*, J. Stat. Phys. 88 (1997), pp. 967–977. https://doi.org/10.1023/B:JOSS.0000015181.86864.fb.
[46] N. Vona and D. Dürr, *The role of the probability current for time measurements*, in *The Message of Quantum Science: Attempts Towards a Synthesis*, P. Blanchard and J. Fröhlich, eds., Springer, Heidelberg, 2015, pp. 95–112.
[47] N. Vona, G. Hinrichs, and D. Dürr, *What does one measure when one measures the arrival time of a quantum particle?* Phys. Rev. Lett. 111 (2013), pp. 220404. https://doi.org/10.1103/PhysRevLett.111.220404.
[48] A. Goussev, *Equivalence between quantum backflow and classically forbidden probability flow in a diffraction-in-time problem*, Phys. Rev. A 99 (2019), pp. 043626. https://doi.org/10.1103/PhysRevA.99.043626.
[49] A. Goussev, *Probability backflow for correlated quantum states*, Phys. Rev. Res. 2 (2020), pp. 033206. https://doi.org/10.1103/PhysRevResearch.2.033206.
[50] G.R. Allcock, *The time of arrival in quantum mechanics III. The measurement ensemble*, Ann. Phys. 53 (1969), pp. 311–348. https://doi.org/10.1016/0003-4916(69)90253-X.
[51] M.J. Schervish, Theory of Statistics, 2nd ed., Springer, New York, 1997.
[52] P. Antonelli, L.E. Hientzsch, and P. Marcati, *On some results for quantum hydrodynamical models (Mathematical analysis in fluid and gas dynamics)*, in 数理解析研究所講究録 2070, 2018, pp. 107–129. Available at http://hdl.handle.net/2433/241991.
[53] P. Antonelli and P. Marcati, *On the finite energy weak solutions to a system in quantum fluid dynamics*, Commun. Math. Phys. 287 (2009), pp. 657–686. https://doi.org/10.1007/s00220-008-0632-0.
[54] I. Bialynicki-Birula, M. Cieplak, and J. Kaminski, Theory of Quanta, Oxford University Press, New York, 1992. Trans. by A. M. Furdyna.
[55] I. Gasser and P.A. Markowich, *Quantum hydrodynamics, Wigner transforms and the classical limit*, Asymptot. Anal. 14 (1997), pp. 97–116. https://doi.org/10.3233/ASY-1997-14201.
[56] P. Holland, *Symmetries and conservation laws in the Lagrangian picture of quantum hydrodynamics*, in *Concepts and Methods in Modern Theoretical Chemistry: Statistical Mechanics*, S. Ghosh and P. Chattaraj, eds., Taylor & Francis, Boca Raton, 2012.
[57] L. Jánossy, *Zum hydrodynamischen modell der quantenmechanik*, Z. Physik 169 (1962), pp. 79–89. https://doi.org/10.1007/BF01378286.
[58] L. Jánossy, *The hydrodynamical model of wave mechanics: The many-body problem*, Acta Physica 27 (1969), pp. 35–46. https://doi.org/10.1007/BF03156734.
[59] L. Jánossy and M. Ziegler, *The hydrodynamical model of wave mechanics I: The motion of a single particle in a potential field*, Acta Phys. Hung. 16 (1963), pp. 37–48. https://doi.org/10.1007/BF03157004.
[60] L. Jánossy and M. Ziegler-Náray, *The hydrodynamical model of wave mechanics II: The motion of a single particle in an external electromagnetic field*, Acta Phys. Hung. 16 (1964), pp. 345–353. https://doi.org/10.1007/BF03157974.
[61] L. Jánossy and M. Ziegler-Náray, *The hydrodynamical model of wave mechanics III: Electron spin*, Acta Phys. Hung. 20 (1966), pp. 233–251. https://doi.org/10.1007/BF03158167.
[62] A. Jángel, M.C. Mariani, and D. Rial, *Local existence of solutions to the transient quantum hydrodynamic equations*, Math. Mod. Meth. Appl. S 12 (2002), pp. 485–495. https://doi.org/10.1142/S0218202502001751.
[63] L.M. Morato, *Formation of singularities in madelung fluid: A nonconventional application of itô calculus to foundations of quantum mechanics*, in *Stochastic Analysis and Applications: The Abel Symposium 2005*, Springer, 2007, pp. 527–540.

[64] T.C. Wallstrom, *On the derivation of the Schrödinger equation from stochastic mechanics*, Found. Phys. Lett. 2 (1989), pp. 113–126. https://doi.org/10.1007/BF00696108.

[65] T.C. Wallstrom, *On the initial-value problem for the Madelung hydrodynamic equations*, Phys. Lett. A 184 (1994), pp. 229–233. https://doi.org/10.1016/0375-9601(94)90380-8.

[66] T.C. Wallstrom, *Inequivalence between the Schrödinger equation and the Madelung hydrodynamic equations*, Phys. Rev. A 49 (1994), pp. 1613–1617. https://doi.org/10.1103/PhysRevA.49.1613.

[67] M. Reed and B. Simon, Methods of Modern Mathematical Physics: Functional Analysis, Vol. I, Academic Press, New York, 1972.

[68] V. Moretti, Fundamental Mathematical Structures of Quantum Theory: Spectral Theory, Foundational Issues, Algebraic Formulation, Springer, Cham, 2019.

[69] M. Reddiger and B. Poirier, *Towards a probabilistic foundation of relativistic quantum theory: The one-body Born rule in curved spacetime*, Quantum Stud.: Math. Found. 12 (2024), article number 5. https://doi.org/10.1007/s40509-024-00349-0.

[70] D. Bohm, *A suggested interpretation of the quantum theory in terms of hidden variables. I*, Phys. Rev. 85 (1952), pp. 166–179. https://doi.org/10.1103/PhysRev.85.166.

[71] D. Bohm, *A suggested interpretation of the quantum theory in terms of hidden variables. II*, Phys. Rev. 85 (1952), pp. 180–193. https://doi.org/10.1103/PhysRev.85.180.

[72] D. Dürr, S. Goldstein, and N. Zanghì, *On a realistic theory for quantum physics*, in *Stochastic Process, Physics and Geometry*, S. Albeverio, G. Casati, U. Cattaneo, D. Merlini, and R. Moresi, eds., World Scientific, Singapore, 1992, pp. 374–391.

[73] D. Dürr, S. Goldstein, and N. Zanghì, Quantum Physics without Quantum Philosophy, Springer, Berlin, 2013.

[74] P.R. Holland, The Quantum Theory of Motion: An Account of the de Broglie-Bohm Causal Interpretation of Quantum Mechanics, Cambridge University Press, Cambridge, 1993.

[75] G. Bacciagaluppi, *A conceptual introduction to Nelson's mechanics*, in *Endophysics, Time, Quantum and the Subjective*, World Scientific, 2005, pp. 367–388. https://doi.org/10.1142/9789812701596_0020.

[76] I. Fényes, *Eine wahrscheinlichkeitstheoretische begründung und interpretation der quantenmechanik*, Z. Physik 132 (1952), pp. 81–106. https://doi.org/10.1007/BF01338578.

[77] E. Nelson, Quantum Fluctuations, Princeton University Press, Princeton, 1985.

[78] E. Santos, *Stochastic interpretations of quantum mechanics*, in *The Oxford Handbook of the History of Quantum Interpretations*, O. Freire Junior, G. Bacciagaluppi, O. Darrigol, T. Hartz, C. Joas, A. Kojevnikov and O. Pessoa Junior, eds., Oxford University Press, Oxford, 2022, pp. 1247–1263.

[79] E.A. Carlen, *Stochastic mechanics: A look back and a look ahead*, in *Diffusion, Quantum Theory, and Radically Elementary Mathematics*, W. G. Faris, ed., Princeton University Press, Princeton, pp. 117–139. https://doi.org/10.1515/9781400865253.117.

[80] E. Nelson, *Review of stochastic mechanics*, J. Phys. Conf. Ser. 361 (2012), article number 012011. https://doi.org/10.1088/1742-6596/361/1/012011.

[81] L. Fabbri, *De Broglie–Bohm formulation of dirac fields*, Found. Phys. 52 (2022), article number 116. https://doi.org/10.1007/s10701-022-00641-2.

[82] L. Fabbri, *Dirac theory in hydrodynamic form*, Found. Phys. 53 (2023), pp. 54. https://doi.org/10.1007/s10701-023-00695-w.

[83] L. Fabbri, *Madelung structure of the Dirac equation*, J. Phys. A: Math. Theor. 58 (2025), pp. 195301. https://doi.org/10.1088/1751-8121/add2b0.

[84] R. Bass, The measurability of hitting times. Electron. Commun. Probab. 15 (2010), pp. 99–105. https://doi.org/10.1214/ECP.v15-1535.

[85] L.E. Ballentine, *Limitations of the projection postulate*, Found. Phys. 20 (1990), pp. 1329–1343. https://doi.org/10.1007/BF01883489.

[86] V. Delgado, S. Brouard, and J. Muga, *Does positive flux provide a valid definition of tunnelling times?* Solid State Commun. 94 (1995), pp. 979–982. https://doi.org/10.1016/0038-1098(95)00162-X.

[87] E.H. Hauge and J.A. Støvneng, *Tunneling times: A critical review*, Rev. Mod. Phys. 61 (1989), pp. 917–936. https://doi.org/10.1103/RevModPhys.61.917.
[88] R. Landauer and T. Martin, *Barrier interaction time in tunneling*, Rev. Mod. Phys. 66 (1994), pp. 217–228. https://doi.org/10.1103/RevModPhys.66.217.
[89] B. Poirier and R. Lombardini, *Dwell times, wavepacket dynamics, and quantum trajectories for particles with spin 1/2*, Entropy 26 (2024), article number 336. https://doi.org/10.3390/e26040336.
[90] S. Das and S. Aristarhov, *Comment on 'the spin dependence of detection times and the non-measurability of arrival times'*, 2023. https://doi.org/10.48550/arXiv.2312.01802.
[91] S. Das and D. Dürr, *Arrival time distributions of spin-1/2 particles*, Sci. Rep. 9 (2019), article number 2242. https://doi.org/10.1038/s41598-018-38261-4.
[92] S. Das, M. Nöth, and D. Dürr, *Exotic Bohmian arrival times of spin-1/2 particles: An analytical treatment*, Phys. Rev. A 99 (2019), article number 052124. https://doi.org/10.1103/PhysRevA.99.052124.
[93] A. Drezet, *Arrival time and Bohmian mechanics: It is the theory which decides what we can measure*, Symmetry 16 (2024), article number 1325. https://doi.org/10.3390/sym16101325.
[94] S. Goldstein, R. Tumulka, and N. Zanghì, *On the spin dependence of detection times and the nonmeasurability of arrival times*, Sci. Rep. 14 (2024), pp. 3775. https://doi.org/10.1038/s41598-024-53777-8.
[95] S. Selstø, *Absorption and analysis of unbound quantum particles one by one*, Phys. Rev. A 103 (2021), pp.012812. https://doi.org/10.1103/PhysRevA.103.012812.
[96] S. Selstø and S. Kvaal, *Absorbing boundary conditions for dynamical many-body quantum systems*, J. Phys. B: At. Mol. Opt. Phys. 43 (2010), pp. 065004. https://doi.org/10.1088/0953-4075/43/6/065004.
[97] A.S. Tahvildar-Zadeh and S. Zhou, *Detection time of dirac particles in one space dimension*, in *Physics and the Nature of Reality: Essays in Memory of Detlef Dürr*, A. Bassi, S. Goldstein, R. Tumulka, N. Zanghì, eds., Springer International Publishing, Cham, 2024, pp. 187–201. https://doi.org/10.1007/978-3-031-45434-9_14.
[98] V.A. Rassolov and S. Garashchuk, *Computational complexity in quantum chemistry*, Chem. Phys. Lett. 464 (2008), pp. 262–264. https://doi.org/10.1016/j.cplett.2008.09.026.
[99] H.-P. Breuer and F. Petruccione, The Theory of Open Quantum Systems, Oxford University Press, Oxford, 2002, 648 pp.
[100] A.N. Jordan and I.A. Siddiqi, Quantum Measurement: Theory and Practice, Cambridge University Press, Cambridge, 2024.
[101] S. Das, *Relativistic electron wave packets featuring persistent quantum backflow*, 2021. https://doi.org/10.48550/arXiv.2112.13180.
[102] R. Tumulka, *Detection time distribution for dirac particles*, 2016. https://doi.org/10.48550/arXiv.1601.04571.
[103] A. Aloy, T.D. Galley, C.L. Jones, S.L. Ludescher, and M.P. Mueller, *Spin-bounded correlations: Rotation boxes within and beyond quantum theory*, 2023. https://doi.org/10.48550/arXiv.2312.09278.
[104] A. Tezzin, *Violating the KCBS inequality with a toy mechanism*, Found. Sci. 30 (2025), pp. 73–87. https://doi.org/10.1007/s10699-023-09928-7.
[105] S. Das, D.-A. Deckert, L. Kellers, S. Krekels, and W. Struyve, *Double-slit experiment revisited*, Ann. Phys. 479 (2025), pp.170054. https://doi.org/10.1016/j.aop.2025.170054.
[106] G. Kälbermann, Single- and double-slit scattering of wavepackets. J. Phys. A: Math. Gen. 35 (2002), pp. 4599–4616. https://doi.org/10.1088/0305-4470/35/21/309.
[107] A.S. Sanz and S. Miret-Artés, A trajectory-based understanding of quantum interference. J. Phys. A: Math. Theor. 41 (2008), pp. 435303. https://doi.org/10.1088/1751-8113/41/43/435303.
[108] L.C. Evans, Partial Differential Equations, 2nd ed., American Mathematical Society, Providence, 2010.

Appendix

The purpose of this appendix is to present a proposal for a weak formulation of the modified Schrödinger Equation (33). As such, it is meant to enable a rigorous study thereof and also pave the path to numerical implementations.

For an introduction to the topic of weak formulations of PDEs, the reader may consult e.g. [108], in particular Section 1.3.2. A discussion of weak formulations of the Madelung equations is given in [29].

The basic idea is to first acknowledge that Equation (33) is non-linear, hence a weak formulation of a non-linear PDE is sought. Multiplying by Ψ^* is then natural for two reasons: first, division by Ψ is circumvented and, second, one would also take this step in deriving the Madelung equations. One then follows the usual procedure of finding a weak formulation for a complex evolution PDE.

Accordingly, we formally multiply Equation (33) with Ψ^* and rearrange:

$$\begin{aligned} 0 = {} & \mathrm{i}\hbar\Psi^*\frac{\partial\Psi}{\partial t} + \frac{\hbar^2}{2m}\Psi^*\Delta\Psi - V\Psi^*\Psi \\ & - \mathrm{i}\frac{\hbar^2}{2m}\,\vec{n}\cdot\mathrm{Im}(\Psi^*\nabla\Psi)\restriction_{\mathcal{D}}\,\theta\big(-\vec{n}\cdot\mathrm{Im}\big(\Psi^*\nabla\Psi\big)\restriction_{\mathcal{D}}\big)\delta_{\mathcal{D}} \end{aligned} \tag{A1}$$

The usual procedure is now to multiply Equation (A1) by a general, suitable 'test function', integrate over all variables of the test function and use integral theorems to 'shift' as many derivatives to the test function as possible. Since Equation (A1) is an evolution equation, we may choose one of two options: either use time-independent test functions and ask for the resulting equation to hold for almost all times or use time-dependent test functions in a 'fully variational formulation'. We make the former choice by requiring the test function ϕ to be in $C_0^\infty(\Omega, \mathbb{C})$, the space of (time-independent) complex-valued, compactly supported, smooth functions on Ω.

In this manner, the following weak formulation is obtained: For all $\phi \in C_0^\infty(\Omega, \mathbb{C})$

$$\begin{aligned} 0 = {} & \int_\Omega \mathrm{d}^3r\left(\mathrm{i}\hbar\Psi^*\frac{\partial\Psi}{\partial t} - \frac{\hbar^2}{2m}|\nabla\Psi|^2 - V|\Psi|^2 - \frac{\hbar^2}{2m}(\Psi^*\nabla\Psi)\cdot\nabla\right)\phi \\ & + \int_{\mathcal{D}} \mathrm{dS}\,\frac{\hbar^2}{2m}\big(\vec{n}\cdot\mathrm{Re}(\Psi^*\nabla\Psi)\restriction_{\mathcal{D}} + \mathrm{i}\,\vec{n}\cdot\mathrm{Im}(\Psi^*\nabla\Psi)\restriction_{\mathcal{D}}\,\theta\big(+\vec{n}\cdot\mathrm{Im}(\Psi^*\nabla\Psi)\restriction_{\mathcal{D}}\big)\big)\phi\restriction_{\mathcal{D}} \end{aligned} \tag{A2}$$

holds almost everywhere on $[0, \infty)$.

It is apparent from Equation (A2) that Ψ needs to be weakly differentiable at least once both in space and time. Accordingly, whenever the singular term in Equation (A1) is non-zero, it must result out of second-order distributional derivatives of Ψ in space. It is also noteworthy that Equations (16) and (27) need to hold for almost all $t \in [0, \infty)$, so that the probability measure $\mathbb{P}_t$ is well-defined. Those two equations impose stronger integrability conditions on Ψ and $\mathrm{Im}(\Psi^*\nabla\Psi)$ than Equation (A2) alone.

There also exists a natural approach to separating the complex Equation (A2) into two real ones. This yields a coupled system of two PDEs instead, namely an equation encoding the physical dynamics as well as a weak formulation of the continuity equation with the respective source term (2b). They are obtained by separating the real and imaginary parts of Equation (A2) for purely real (or purely imaginary) test functions. For all $\phi, \xi \in C_0^\infty(\Omega, \mathbb{R})$ we then require that the two equations

$$\begin{aligned} 0 = {} & \int_\Omega \mathrm{d}^3r\left(\hbar\mathrm{Im}\left(\Psi^*\frac{\partial\Psi}{\partial t}\right) + \frac{\hbar^2}{2m}|\nabla\Psi|^2 + V|\Psi|^2 + \frac{\hbar^2}{2m}\mathrm{Re}\big(\Psi^*\nabla\Psi\big)\cdot\nabla\right)\phi \\ & - \int_{\mathcal{D}} \mathrm{dS}\,\frac{\hbar^2}{2m}\,\vec{n}\cdot\mathrm{Re}\big(\Psi^*\nabla\Psi\big)\restriction_{\mathcal{D}}\,\phi\restriction_{\mathcal{D}}, \end{aligned} \tag{A3a}$$

$$
\begin{aligned}
0 = &\int_\Omega \mathrm{d}^3 r \left(\frac{\partial |\Psi|^2}{\partial t} - \frac{\hbar}{m} \mathrm{Im}\big(\Psi^* \nabla \Psi\big) \cdot \nabla \right) \xi \\
&+ \int_{\mathcal{D}} \mathrm{d}S \, \frac{\hbar}{m} \, \vec{n} \cdot \mathrm{Im}\big(\Psi^* \nabla \Psi\big) \restriction_{\mathcal{D}} \, \theta\big(+\vec{n} \cdot \mathrm{Im}(\Psi^* \nabla \Psi) \restriction_{\mathcal{D}}\big) \xi \restriction_{\mathcal{D}}
\end{aligned}
\tag{A3b}
$$

hold almost everywhere on $[0, \infty)$.

Philosophical Magazine

ISSN: 1478-6435 (Print) 1478-6443 (Online) Journal homepage: www.tandfonline.com/journals/tphm20

Revisiting de Broglie's famous paper of 1924

Edward A. Davis

To cite this article: Edward A. Davis (06 Apr 2026): Revisiting de Broglie's famous paper of 1924, Philosophical Magazine, DOI: 10.1080/14786435.2026.2633792

To link to this article: https://doi.org/10.1080/14786435.2026.2633792

PHILOSOPHICAL MAGAZINE
https://doi.org/10.1080/14786435.2026.2633792

Taylor & Francis
Taylor & Francis Group

OPEN ACCESS Check for updates

Revisiting de Broglie's famous paper of 1924

Edward A. Davis

Department of Materials Science and Metallurgy, University of Cambridge, Cambridge, UK

ABSTRACT

Louis-Victor de Broglie secured his place in the history of quantum physics by proposing the existence of *matter waves*. Following the concept accepted early in the twentieth century that light waves could display properties characteristic of particles (photons), de Broglie suggested the complementary principle that particles could display properties characteristic of waves. Within a few years, this far-reaching proposal was experimentally verified. The well-known formula for the wavelength λ of the wave associated with a particle of momentum p, namely $\lambda = h/p$, does not appear in de Broglie's original paper, which was published in this journal in 1924. What is derived from the starting assumption that the frequency of the wave is the rest energy of the particle divided by Planck's constant h, is the wave's velocity, which turns out to be c^2/v, where v is the particle's velocity. This velocity, being superluminal, means that the wave cannot transport energy. De Broglie called it a *phase* wave and postulated a *group* of such waves having virtually, but not exactly, the same velocity and wavelength. The *group velocity* of such a large number of almost identical phase waves is then shown, very satisfactorily, to be equal to the velocity of the particle. The proposal by de Broglie inspired Schrödinger to develop the mathematical foundations of wave mechanics. Whereas in conventional quantum theory, phase waves are considered fictional, de Broglie considered them to have a certain physical reality, renaming them *pilot* or guiding waves – a concept developed later by Bohm in 1952.

ARTICLE HISTORY
Received 8 October 2025
Accepted 14 February 2026

KEYWORDS
de Broglie relation; phase waves; group velocity

1. Introduction

The concept of matter waves was proposed by de Broglie (Figure 1) in his PhD thesis, which he submitted to the University of Paris in 1923 [1]. His first paper on the subject was published in the *Philosophical Magazine* [2] one year later. The title of this paper, 'A Tentative Theory of Light Quanta', encapsulates the main topics covered in its nine sections, with his revolutionary concept being developed in one of these sections. This has the subtitle 'An important Theorem on the Motion of Bodies' and takes up less than two pages of the journal.

CONTACT Edward A. Davis ead34@cam.ac.uk Department of Materials Science and Metallurgy, University of Cambridge, Cambridge, CB3 OFS, UK

Figure 1. Louis-Victor Pierre Raymond de Broglie (1892–1987).

Many textbooks distil de Broglie's principal ideas into a single equation relating the wavelength λ of the wave associated with a body to its momentum p, namely $\lambda = h/p$, where h is Planck's constant. Surprisingly, this equation, which is normally stated as being a postulate by de Broglie, does not appear at all in the paper, although a non-relativistic form of it is briefly referred to in his thesis. It is, however, given importance in the Nobel Prize lecture he delivered five years later in 1929.

In the present article, de Broglie's theoretical proposals will be outlined and the wavelength-momentum relation derived from these. Consideration will be given to the content of his thesis as well as his 1924 paper.

2. The de Broglie hypothesis

The starting point of de Broglie was to assign a frequency of vibration ν_0 to a body of rest mass m_0. He obtained a relation between these two quantities by equating the expressions for the energy of a quantum (as found for light) and the internal rest energy of a body, both proposed by Einstein, as follows

$$E = h\nu_0 = m_0c^2$$

where h is Planck's constant and c is the velocity of light.

The above equation is a *hypothesis* by de Broglie, with the nature of the vibration being described in his thesis as follows:

> *"Must we suppose that this periodic phenomenon occurs in the interior of energy packets? This is not at all necessary; the results … will show that it is spread out over an extended space. Moreover, what must we understand by the interior of a parcel of energy? An electron is for us the archetype of an isolated parcel of energy, which we believe, perhaps incorrectly, to*

know well; but, by received wisdom, the energy of an electron is spread over all space with a strong concentration in a very small region, but otherwise whose properties are very poorly known. That which makes an electron an atom of energy is not its small volume that it occupies in space, I repeat: it occupies all space, but the fact that it is undividable, (means) that it constitutes a unit."

Here, de Broglie anticipates the result of his analysis, namely that the oscillation to be associated with the particle is spatially extensive, although concentrated in a small region. He also specifically refers here to an *electron* as the particle, although his analysis is not restricted to a particular particle.

3. Phase and group waves

De Broglie's theory is developed from the above starting point as follows.

If the body (hereafter referred to in this article as a particle) is moving with a velocity v with respect to a fixed observer, then the frequency of vibration as perceived by the observer is raised as a consequence of the mass of the particle being seen to be increased from m_0 to $m_0/\sqrt{1-\beta^2}$ where $\beta = \mathrm{v}/c$. The frequency, according to the fixed observer, is therefore:

$$\nu_p = \frac{1}{h}\frac{m_0c^2}{\sqrt{1-\beta^2}} = \frac{\nu_0}{\sqrt{1-\beta^2}}$$

[N.B. Some of the symbols used in this article for various quantities differ from those used by de Broglie. The reason for the subscript *p* will become evident shortly. The lower-case symbol for velocity has not been italicised to avoid confusion with the symbol for frequency.]

Since $\sqrt{1-\beta^2} \le 1$, it follows that $\nu_p > \nu_0$. However, according to a Lorentz relativistic transformation, the frequency ought to be lowered, not raised! Indeed, the frequency seen by the fixed observer should be

$$\nu_L = \nu_0\sqrt{1-\beta^2}$$

with the $\sqrt{1-\beta^2}$ factor in the numerator, not the denominator. How did de Broglie resolve this apparent dilemma?

Quoting from his thesis: '*The two frequencies are fundamentally different. This is a difficulty that has intrigued me for a long time. It has brought me to the following conception, which I denote "the theorem of phase harmony"*'.

De Broglie then proposes that the moving body coincides in space with a wave whose frequency is the higher of the above two frequencies and, quoting from his paper, '*If, at the beginning the internal phenomenon of the moving body is in phase with the wave, this harmony of phase will always persist*'.

How is it possible for a periodic phenomenon connected to a body moving with velocity v, whose frequency of vibration is, for the fixed observer, equal to $\nu_L = \nu_0\sqrt{1-\beta^2}$, to appear to him/her to be constantly in phase with a wave of (higher) frequency $\nu_p = \frac{\nu_0}{\sqrt{1-\beta^2}}$? The answer is that this is possible if the latter has a velocity equal to c^2/v

De Broglie provides two ways of showing this.

Method 1.

The Lorentz spatial (x) and time (t) coordinate transformations for the same event in two frames S and S' when S' moves with a velocity v relative to S along the x-axis are

$$x' = \frac{1}{\sqrt{1-\beta^2}}(x - \mathrm{v}t) \qquad t' = \frac{1}{\sqrt{1-\beta^2}}\left(t - \frac{\mathrm{v}x}{c^2}\right)$$

If the oscillatory motion in the reference frame of the particle is described by $\sin 2\pi\nu_0 t$ then, in the reference frame of the fixed observer, the motion can be described by

$$\sin[2\pi\nu_0 \frac{1}{\sqrt{1-\beta^2}}\left(t - \frac{\mathrm{v}x}{c^2}\right)]$$

which is the equation of a wave having a frequency $\frac{\nu_0}{\sqrt{1-\beta^2}}$ and a velocity c^2/v.

[Note: A wave of the form $\sin(\omega t - kx)$ has a frequency $\omega/2\pi$ and travels with a velocity ω/k.]

Method 2.

Suppose that the body moves a distance x in time t. Its internal vibration, as viewed by a fixed observer, can be expressed as sin $2\pi\nu_L t$ =sin $2\pi\nu_L(x/\mathrm{v})$. At the same place, the wave is given by sin $2\pi\nu_p(t - x/V_p)$, where V_p is its velocity. The internal vibration and the wave will be in phase if these two expressions are equal, which, it can be shown by inserting the values of ν_L and ν_p, is satisfied when $V_p = c^2/\mathrm{v} = c/\beta$.

Since $\beta < 1$, the velocity of the wave accompanying the particle is greater than the speed of light, and hence the wave cannot transport energy. De Broglie called it a *phase wave*. Then, without offering any clarifying explanation, he considers a *group* of such waves having virtually, but not exactly, the same *phase* velocity. Referring to (but not referencing) the work of Lord Rayleigh on the superposition of waves having different velocities or wavelengths, de Broglie uses this treatment from classical wave theory to infer that such a group of phase waves combine to form a wave having a *group* velocity.

A general equation [3] relating the group velocity V_g associated with a large number of almost identical phase waves having an average frequency ν and an average velocity V_p, is

$$1/V_g = \mathrm{d}(\nu/V_p)/\mathrm{d}\nu$$

[In textbooks, the group velocity is normally expressed as $V_g = d\omega/dk$ where $\omega = 2\pi\nu$ and $k = 2\pi/\lambda$. Writing $1/\lambda = \nu_p/V_p$ the equivalence of the two expressions is evident.]

Using $\nu_p = \frac{1}{h}\frac{m_0c^2}{\sqrt{1-\beta^2}}$, namely the frequency of the phase wave, and the value for $V_p = c/\beta$, it can be shown (see Appendix for the derivation) that the group velocity is $V_g = \beta c = \mathrm{v}$, namely the velocity of the particle.

Therefore, the group velocity equals the velocity of the particle itself and hence is the velocity at which energy is transported. In the words of de Broglie, '*The velocity of the moving body is the energy velocity of a group of waves .... corresponding to very slightly different values of β.*

Note that the product of the group velocity and the phase velocity $V_gV_p = c^2$.

Table 1. Velocity and frequency of the particle (in its rest frame), and of the associated phase and group waves.

	VELOCITY	FREQUENCY
PARTICLE	$\rightarrow$ v	$\nu_0 = m_0 c^2/h$
PHASE WAVE(S)	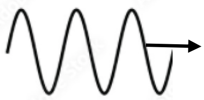 $V_p = c/\beta = c^2/\mathrm{v}$	$\nu_p = \dfrac{\nu_0}{\sqrt{1-\beta^2}}$
GROUP WAVE	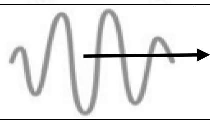 $V_g = \beta c = \mathrm{v}$	

To summarise the situation at this juncture, the Table 1 lists the velocity and frequency associated with the particle and the two types of wave. (Note: the group wave is not a plane wave and has no meaningful frequency.)

4. The wavelength—momentum relation

The wavelength associated with the phase waves – the so-named de Broglie wavelength – can be derived from their velocity and frequency as follows:

$$\lambda = V_p/\nu_p = (c^2/\mathrm{v})\sqrt{1-\beta^2}\Big/\nu_0$$

Inserting $\nu_0 = m_0 c^2/h$

we have $\lambda = h\sqrt{1-\beta^2}\big/m_0\mathrm{v}$

Now, the momentum of the particle as seen by a fixed observer is

$$p = m_0\mathrm{v}\Big/\sqrt{1-\beta^2}$$

Hence

$$\lambda = h/p$$

This is the de Broglie wavelength-momentum relationship and holds for relativistic as well as for non-relativistic particles.

5. Comments

It might be considered surprising that the de Broglie formula is obtained when using the parameters of the phase waves, particularly as these waves (1) are something of a fabrication in the sense that their main purpose is to form the group wave, (2) are essentially infinite in number and in spatial extent, (3) are superluminal, and (4) are unable individually to carry energy but postulated to do so when superimposed.

Although Fourier decomposition of waves containing these features is now quite a familiar technique, the reasoning in de Broglie's paper would have seemed quite extraordinary at the time. Nevertheless, the significance of his work was recognised fairly quickly. Within a few years of publication of the paper, experimental proof of the wave nature of electrons was obtained by the diffraction experiments undertaken by Davisson and Germer [4] in 1927 and by G P Thomson [5] in the same year. The results of both experiments confirmed quantitatively the de Broglie relation between momentum and wavelength.

6. Bohr orbits

Ten years before de Broglie put forward his revolutionary idea of matter waves, Niels Bohr wrote a trilogy of papers [6–8] that built on Rutherford's nuclear model of atoms by proposing that electrons moved in circular orbits around a central nucleus, with the Coulomb attractive force being balanced by the centrifugal force. Furthermore, Bohr recognised that the allowed stable orbits were those for which the angular momentum is an integral multiple of Planck's constant divided by 2π.

The latter condition can be expressed by the equation

$$mvr = nh/2\pi \text{ with } n = 1,\ 2,\ 3\ldots$$

where m and v are the mass and velocity of the orbiting electron, and r is the radius of its orbit.

In his thesis and the subsequent paper, de Broglie shows that the Bohr condition for stable orbits follows straightforwardly from his concept of matter waves. He writes that for stability, the length of the orbit 'must be resonant with the wave; in other words, the points of a wave located at whole multiples of the wavelength must be in phase'. This resonance condition is $2\pi r = n\lambda$, that is to say, the length of the orbit contains a whole number of wavelengths.

Substituting $\lambda = h/p = h/m\text{v}$, in the above equation, one finds $2\pi r = nh/m\text{v}$, which is the same as the Bohr stability condition.

(N.B. In textbooks, the reasoning is normally reversed; namely, insertion of $\lambda = h/p = h/m\text{v}$ in the Bohr equation leads to the conclusion that the orbits must contain a whole number of wavelengths.)

One might ask what the nature of the phase waves is in the context of Bohr orbits? In this case they are standing waves with nodes fixed in space, in contrast to the faster-than-light waves postulated for unbound electrons.

Figure 2 illustrates one such wave corresponding to an orbit with $n = 3$.

Group waves do not play a role; there is no wave packet accompanying the electron in its path. Instead, the uncertainty in the location of the electron – which can be anywhere along the orbit – is an obvious feature of this representation.

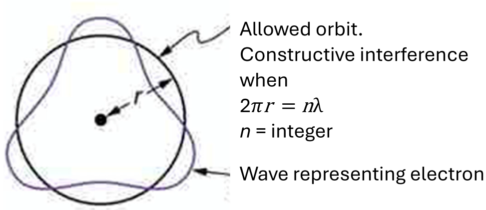

Figure 2. Schematic of a wave associated with an electron in orbit around a nucleus.

7. Heisenberg and Schrödinger

The superposition of multiple plane waves having different wavelengths to form a wave packet (see Figure 3) is not confined to quantum phenomena but is associated with wave motions in general. However, to attain an isolated and relatively localised wave packet, such as is required to represent, say, a free electron, requires the superposition of an essentially infinite number of plane waves with amplitudes having a continuous distribution. The larger the range of wavelengths $\Delta\lambda$ associated with the multiple waves, the smaller the spatial spread Δx of the resulting wave packet. Here, Δ could be the width at half-maximum of a distribution of values or the standard deviation of a Gaussian distribution.

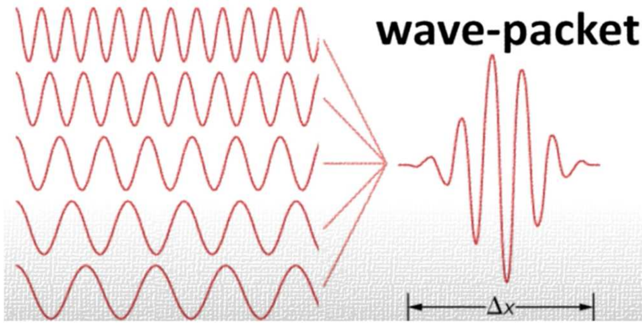

Figure 3. Superposition of a large number of waves with different wavelength to form a wave packet.

For a group of phase waves with central wavelength λ, the relation between the three quantities can be written as

$$\frac{\Delta x \Delta \lambda}{\lambda^2} \geq \frac{1}{4\pi}$$

with the value of the constant on the right-hand side being associated with a Gaussian distribution of the amplitudes of the component waves. Other distributions lead to larger values of the constant.

From the de Broglie relation $\lambda = h/p$, one obtains $\Delta\lambda = h\Delta p/p^2 = \Delta p\lambda^2/h$.

Hence, the above equation becomes

$$\Delta x \Delta p \geq h/4\pi$$

This is Heisenberg's Uncertainty Principle. It follows directly from wave theory and the de Broglie relation. Although Heisenberg did not derive the above equation using wave theory, of which he was in general critical, he recognised that it was an alternative way of demonstrating it [9].

There is no doubt that the concept of matter waves initiated the development of wave mechanics, as formulated by Schrödinger a few years later. Although Schrödinger accepted the de Broglie relation between wavelength and momentum, his views on the phase waves differed. Although the Schrödinger equation rests on the concept that a particle's motion is governed by the propagation of its associated phase waves, he did not consider these to be superluminal. This is not because his theory was non-relativistic, but because he chose to take the total energy of a particle as the sum of its kinetic and potential energies, rather than its rest energy m_0c^2 as de Broglie had postulated.

So, rather than de Broglie's starting assumption, namely $E = h\nu_0 = m_0c^2$, Schrödinger took, for a free particle with kinetic energy $m\text{v}^2/2 = p^2/2m$,

$$E = h\nu_p = p^2/2m$$

which provides an expression for the frequency of the phase wave. [Note: in the non-relativistic limit, $\nu_p = \nu_0$ – see Table 1.]

The frequency of Schrödinger's phase waves, therefore, differs markedly from that deduced by de Broglie. This could mean a difference either in their wavelength or in their velocity. Clearly, one would not wish it to be in the wavelength, as the de Broglie relation was known to be confirmed experimentally. So, Schrödinger's phase wave velocity is reduced from that of de Broglie by the factor

$$mc^2/(m\text{v}^2/2) = 2c^2/\text{v}^2$$

Recalling that the de Broglie phase velocity is c^2/v, the Schrödinger phase velocity is therefore v/2, i.e. half the particle velocity.

Despite this vast difference in phase velocities, it is reassuring to find that the group velocity is unchanged and equals the particle velocity, just as in de Broglie's analysis – see Appendix.

8. Envoi

One of the examiners of de Broglie's thesis was Paul Langevin. He must have considered the proposal of matter waves to be somewhat of a wild idea because he sent the thesis to Einstein for his opinion prior to making his own decision on it. Einstein replied 'I believe it is a first feeble ray of light on the worst of our physics enigmas'. The examining committee wisely awarded de Broglie his doctorate!

The experimental evidence for the wave nature of particles and the validity of the de Broglie relation between wavelength and momentum was soon forthcoming. Following early confirmatory results for electrons, the relation was later verified for protons, neutrons and atoms. As described in this article, the wavelength associated with such particles is that of the phase waves. Somewhat disturbing is that the velocities of the phase waves are superluminal according to de Broglie but equal to half the particle velocity according to Schrödinger. Fortunately, the group velocity is equal to the particle velocity in both theories.

Although the concept of a wave packet formed from an infinite set of phase waves is a useful one in visualising a particle's motion and behaviour, in current conventional quantum theory the component phase waves have no physical significance and the magnitude of their velocities would appear to be of no consequence at all. In Schrödinger's equation, the *wavefunction* associated with a particle is an imaginary quantity. However, as proposed by Born in 1926, the wavefunction, when multiplied by its complex conjugate, provides a measure of the probability of finding the particle in a particular region of space, which in many cases bears a strong resemblance to the profile of a wave packet.

In 1927, de Broglie introduced his ‘two-solution’ theory, which distinguished his phase waves from the wavefunction of Schrödinger’s equation, regarding ‘the phase wave as physically real and the wavefunction as fictional but of statistical significance [10]. At the 5th Solvay Congress held in 1927, he proposed a simpler version of this concept, referring to the phase waves as *pilot waves*, implying they control the motion of the particle. However, following criticism from Bohr, Pauli and others, de Broglie abandoned the idea, returning to develop it only much later in his life; see the review by Colin et al. [11].

In 1952, Bohm independently proposed a model [12] along similar lines to that of de Broglie suggesting that the particle’s position, momentum and trajectory, whilst being related to the wavefunction, are well defined at all times, in contrast to the so-called Copenhagen interpretation, which considers these quantities as becoming definite only after a physical measurement, the consequence of which is a collapse of the wavefunction. Bohm’s approach, which was subsequently termed the de Broglie-Bohm theory, attracted little interest for a decade or so. However, it has subsequently been considerably developed [13], particularly after Philippidis et al [14] published a graphic illustration of the trajectories taken by particles in the double-slit experiment using the concept of the *quantum potential* – a major feature of Bohm’s theory. The support and work of J.S. Bell was also very influential; see, for example, [15]. Versions of Bohmian mechanics have been developed for particles with spin [16] and for relativistic quantum fields [17]. Other examples are presented or referred to in papers in the Article Collection (*Bohm in Brazil: Reflections on 100 years of Quantum*) published in this journal.

Disclosure statement

No potential conflict of interest was reported by the author.

References

[1] L. de Broglie, Recherches sur la théorie des quanta, PhD thesis, University of Paris, Ann. de Physique (10) 3, 22 (1925). Translated by A.F. Kracklauer, https://fondationlouisdebroglie.org/LDBoeuvres/De Broglie Kracklauer.pdf (1923).

[2] L. de Broglie, *A tentative theory of light quanta*. Philos. Mag. 35 (1924), pp. 446458.

[3] J.W. Strutt, *The Theory of Sound, Volume 1*, Dover Publications, New York, 1894. pp 301-302.

[4] C. Davisson and L.H. Germer, *Diffraction of electrons by a crystal of nickel*. Phys. Rev. 30 (1927), pp. 705740. doi:10.1103/PhysRev.30.705

[5] G.P. Thomson, *Diffraction of cathode rays by a thin film*. Nature 119 (1927), pp. 890. doi:10.1038/119890a0

[6] N. Bohr, *On the constitution of atoms and molecules Part I*. Philos. Mag. 26 (1913), pp. 125.

[7] N. Bohr, *On the constitution of atoms and molecules Part II*. Philos. Mag. 26 (1913), pp. 476562.

[8] N. Bohr, *On the constitution of atoms and molecules Part III*. Philos. Mag. 26 (1913), pp. 857875.

[9] W. Heisenberg, *The Physical Principles of the Quantum Theory*, The University of Chicago Press, Chicago, 1930. pp 1415.

[10] L. de Broglie, *The double solution theory: A new interpretation of wave mechanics*. J. Phys. 5 (1927), pp. 225.
[11] S. Colin, T. Durt, and R. Willox. de Broglie's double solution program: 90 years later, arXiv:1703.06158v1 quantum-ph 17 March 2017.
[12] D. Bohm, *A suggested interpretation of the quantum theory in terms of 'hidden' variables*. Phys. Rev. 85 (1952), pp. 166–705193. doi:10.1103/PhysRev.85.166
[13] P. Holland, *The quantum Theory of Motion*, Cambridge University Press, Cambridge, 1993.
[14] C. Philippidii, C. Dewdney, and B.C. Hiley, *Quantum interference and the quantum potential*. Nuovo Cimento 52 (1979), pp. 15–28. doi:10.1007/BF02743566
[15] A. Whitaker, *Einstein, Bohr and the Quantum Dilemma 2nd Edition.*, Cambridge University Press., Cambridge, 2006.
[16] T. Norsen. The pilot-wave perspective on spin, 82 pp 337-348, 2014.
[17] D. Durr, S. Goldstein, R. Tumulka, and N. Zanghi, *Bohmian mechanics and quantum field theory*. Phys. Rev. Lett 93 (2004), pp. 90402. doi:10.1103/PhysRevLett.93.090402

Appendix

A general equation relating a group velocity V_g to a phase velocity V_p, first proposed by Lord Rayleigh and used by de Broglie, is

$$1/V_g = \mathrm{d}(\nu_p/V_p)/\mathrm{d}\nu$$

Rearranging the expression for the frequency of the phase wave, namely $\nu_p = \frac{1}{h}\frac{m_0 c^2}{\sqrt{1-\beta^2}}$, β can be expressed as

$$\beta = (h^2\nu_p^2 - m_0^2c^4)^{1/2}/h\nu_p$$

Hence, since $V_p = c/\beta$, $\quad \nu_p/V_p = (h^2\nu_p^2 - m_0^2c^4)^{1/2}/ch$

and
$$\mathrm{d}(\nu_p/V_p)/\mathrm{d}\nu = [\tfrac{1}{2}(h^2\nu_p^2 - m_0^2c^4)^{-1/2} \times 2\nu_p h^2]/ch$$
$$= h\nu_p/c(h^2\nu_p^2 - m_0^2c^4)^{1/2}$$
$$= 1/\beta c$$

Hence $\quad V_g = \beta c = \mathrm{v}$

The same result arises in the non-relativistic limit when the frequency of the phase wave is $\nu_p = mv^2/2h$ and its velocity is $V_p = \mathrm{v}/2$ as in Schrödinger's treatment. In this case

$$1/V_g = \mathrm{d}(\nu_p/V_p)/\mathrm{d}\nu$$

becomes
$$1/V_g = \mathrm{d}(m\mathrm{v}/h)/\mathrm{d}\nu$$
$$= [\mathrm{d}(m\mathrm{v}/h)/\mathrm{d}\mathrm{v}][\mathrm{d}\mathrm{v}/\mathrm{d}\nu]$$
$$= [m/h][h/m\mathrm{v}]$$

and so $\quad V_g = \mathrm{v}$

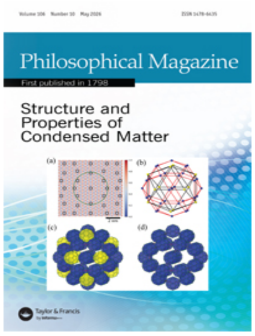

Taylor & Francis
Taylor & Francis Group

Philosophical Magazine

ISSN: 1478-6435 (Print) 1478-6443 (Online) Journal homepage: www.tandfonline.com/journals/tphm20

The quantum measurement problem: a review of recent trends

Anderson A. Tomaz, Rafael S. Mattos & Mario Barbatti

PHILOSOPHICAL MAGAZINE
https://doi.org/10.1080/14786435.2025.2601922

The quantum measurement problem: a review of recent trends

Anderson A. Tomaz[a], Rafael S. Mattos[a] and Mario Barbatti[a,b]

[a]Aix Marseille University, CNRS, ICR, Marseille, France; [b]Institut Universitaire de France, Paris, France

ABSTRACT

Left on its own, a quantum state evolves deterministically under the Schrödinger equation, forming superpositions. Upon measurement, however, a stochastic process governed by the Born rule collapses it to a single outcome. This dual evolution of quantum states – the core of the Measurement Problem – has puzzled physicists and philosophers for nearly a century. Yet, amid the cacophony of competing interpretations, the problem today is not as impenetrable as it once seemed. This paper reviews the current status of the Measurement Problem, distinguishing between what is well understood and what remains unresolved. We examine key theoretical approaches, including decoherence, many-worlds interpretation, objective collapse theories, hidden-variable theories, dualistic approaches, deterministic models, and epistemic interpretations. To make these discussions accessible to a broader audience, we also reference curated online resources that provide high-quality introductions to central concepts.

ARTICLE HISTORY
Received 8 August 2025
Accepted 1 December 2025

KEYWORDS
Decoherence; measurement problem; quantum state collapse; interpretations of quantum mechanics

1. Introduction

Quantum mechanics, as we learn in college, posits that an isolated system evolves unitarily and deterministically following the Schrödinger equation. When we measure the system, the Born rule determines the output probabilities. The quantum state collapses in a non-unitary, stochastic way, so the same outcome is obtained if the measurement is repeated. Despite its awkward double rule of evolution, this seemingly simple framework enabled comprehension of nature and technological advances to a level that our species has never seen before.

Nevertheless, let us ask what 'measure the system' means. We will not find an answer in the standard formulation of quantum mechanics. This innocent question unravels a disturbing thread of conceptual problems, which are surprisingly difficult to address experimentally and may have dramatic philosophical consequences for our conception of the world.

The Measurement Problem has been haunting physicists and philosophers of science for almost as long as the century since quantum mechanics was proposed. We can take as

CONTACT Anderson A. Tomaz anderson.alves-tomaz@univ-amu.fr; Mario Barbatti mario.barbatti@univ-amu.fr Aix Marseille University, CNRS, ICR, Av. Esc. Normandie Niemen, Marseille 13397, Cedex 20, France

an anecdotal example the World Science Festival held in the first semester of 2024, a science popularization event hosted by Brian Greene. Greene asked three quantum mechanics specialists about the Measurement Problem and got three entirely distinct answers. The entry Interpretations of Quantum Mechanics in Wikipedia contains thirteen distinct classes of theories and interpretations, and it does not even account for some recent proposals.

The cacophony of proposed solutions to the Measurement Problem – including voices from parts of the physics community that question whether the problem even exists – is disturbing. It hurts our conception of science as delivering a consistent description of reality. Why, after a century of quantum mechanics, do we still have no consensus on its most fundamental process? What do we truly understand about the Measurement Problem?

Any newcomer trying to get an answer to these questions faces a formidable challenge: the Measurement Problem research is spread throughout countless isolated sub-communities. These groups do not talk to each other, making it exceptionally difficult to build an overview of what's going on. The large number of single-author papers doesn't help either. These papers raise hypotheses and propose theories and tests. However, most don't resonate within a mature community and only add to the cacophony.

As newcomers to the field ourselves – we just published our first contribution recently [1] – we felt firsthand all these issues. We tackled this challenge with extensive reading, discussion, and consultation with specialists on specific topics. We explored all corners of the field rather than focussing on a single subfield. This review arose naturally. We aim to deliver a broad overview of the several competing research lines. We don't aim for a comprehensive survey (which would not be possible within the reasonable limits of a paper) but rather to illuminate the central questions currently being discussed, allowing curious non-specialists to start exploring the literature on their own. In doing so, we hope to show that the Measurement Problem is not as bleak as it seems, although there is still much to be uncovered.

Given the Measurement Problem's central role, it is unsurprising that several other reviews have been recently published to explore its unresolved aspects from different perspectives. Hance and Hossenfelder [2] critically assess whether the problem is fundamental or an artefact of our theoretical framework. In a synthetic review, they identify five requirements that any satisfactory solution to the problem must satisfy and analyze several proposed solutions. Müller [3] followed a different path. Instead of focussing on the proposed solutions, he approaches the Measurement Problem from a formal logic perspective. He decomposes it into six independent problems, which should be investigated separately. Meanwhile, Freire Jr. [4] delivers a historical account, linking the foundations of quantum mechanics to current scientific and technological advances.

Surveys dedicated to objective collapse theories are numerous. Bassi, Dorato, and Ulbricht [5] present an in-depth analysis of objective collapse models from theoretical, experimental, and philosophical perspectives. Carlesso et al. [6] further explore experimental tests beyond interferometric setups, while Donadi and Bassi [7] review gravity-induced collapse models. These studies update the comprehensive review by Bassi and collaborators from 2013 [8] and build on the foundational report on dynamical reduction models by Ghirardi and Bassi [9], which remains a central reference in the field.

Each of these works is worth the attention of readers interested in the status of foundational discussions of quantum mechanics. Nevertheless, none delivers a broad coverage of the Measurement Problem; that's precisely what we missed when we started our journey. Addressing this gap, our review organises the various proposed solutions into a structured overview, offering a broad reference point for both specialists and newcomers.

Our work also brings a distinct perspective by examining the Measurement Problem through the chemistry lens (since two authors, RSM and MB, are theoretical chemists). Historically, chemists have treated quantum mechanics pragmatically, using it as a tool rather than engaging with its foundational questions. However, recent advances in quantum materials [10, 11], quantum dots for imaging and drug delivery [12], ultrafast spectroscopy [13], and quantum computing [14, 15] have brought the Measurement Problem into sharper focus at the chemistry labs. These fields increasingly rely on quantum coherence, entanglement, and decoherence – concepts central to quantum measurement theory [16, 17]. As chemists push the boundaries of quantum state control, they may need to reconsider long-standing assumptions about wave function collapse, observer effects, and the role of decoherence in chemical processes.

Despite being unconventional in scientific papers, we extensively referred to non-peer-reviewed web resources, including books, essays, and videos. These resources offer a plain language introduction and analysis free from intimidating technicalities. They naturally don't replace technical literature, but should not be neglected as relevant entry points to the subject.

2. Quantum state description and evolution

This section briefly introduces basic quantum mechanics concepts, focussing on the elements most relevant to the following discussions. For in-depth treatments, we refer the reader to standard textbooks [18, 19]. Concise and accessible overviews can be found in Refs. [20, 21].

Quantum mechanics encodes all information about a physical system in the quantum state $|\psi\rangle$, a complex-valued unit vector in the Hilbert space $\mathcal{H}$. In a finite Hilbert space, all unit vectors are possible physical states of the system.

Consider, for example, the ammonia molecule NH_3 (Figure 1). Its more stable geometry resembles a pyramid, with the three hydrogen atoms forming a triangular basis and the nitrogen atom lying above or below it. Thus, ignoring molecular vibrations and rotations, the nuclear quantum state of ammonia $|\psi\rangle$ has two components,

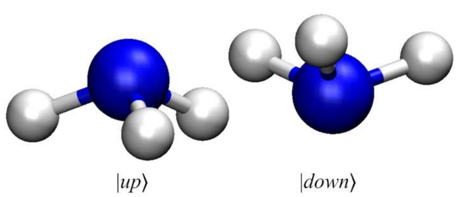

Figure 1. The ammonia (NH_3) molecule serves as an example of a two-state quantum system. Its equilibrium geometry is pyramidal, with the nitrogen atom lying above or below the hydrogen plane. These two geometric configurations, labelled $|up\rangle$ and $|down\rangle$, may form a quantum superposition.

corresponding to pyramids up and down [22, Chapters 8 & 9]. Let's name them $|up\rangle$ and $|down\rangle$ states, respectively, meaning we will treat NH_3 as a quantum bit (or a qubit).

In this example, the general quantum state $|\psi\rangle$ is a two-dimensional vector (see Figure 2(a)) written as

$$|\psi\rangle = C_u|up\rangle + C_d|down\rangle, \tag{1}$$

where C_u and C_d are complex-valued coefficients (or amplitudes) with $|C_u|^2 + |C_d|^2 = 1$. Equation (1) trivially generalises to any number of dimensions as

$$|\psi\rangle = \sum_n C_n|\phi_n\rangle. \tag{2}$$

For a continuous basis, it becomes $|\psi\rangle = \int \mathrm{d}s\phi(s)|s\rangle$, and the amplitudes are called *wave functions.*

So far, our example has been restricted to unit vectors, also known as *pure states*. Nonetheless, the usual situation is imperfect knowledge, where we only know that the system is in one of several possible pure states $|\psi_i\rangle$, each occurring with probability p_i. In this case, it is more appropriate to describe the system using a density operator

$$\rho \equiv \sum_i p_i|\psi_i\rangle\langle\psi_i|, \tag{3}$$

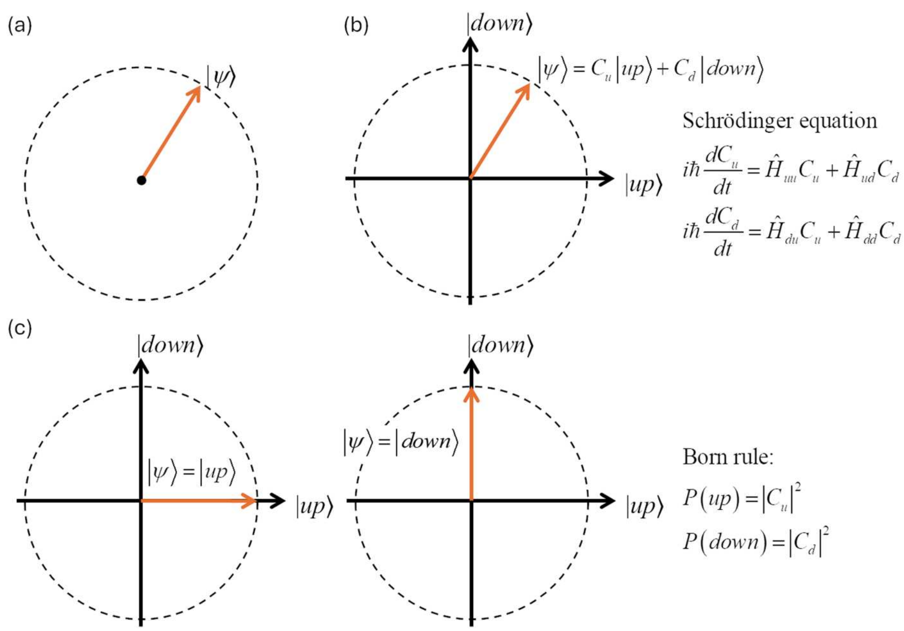

Figure 2. Schematic representation of the quantum description of a two-state system, such as the NH_3 molecule in Figure 1. (a) The quantum state $|\psi\rangle$ encapsulates all the system's information and exists as a vector in Hilbert space (illustrated here as a dashed circle plus the central dot). (b) Once a basis is selected, $|\psi\rangle$ is expressed in terms of its basis components, with complex-valued amplitudes C_i. The Hamiltonian operator $\hat{H}$ governs the state's deterministic evolution via the Schrödinger equation. (c) Upon measurement, the state $|\psi\rangle$ collapses to one of the basis vectors, with the probability of each outcome given by $|C_i|^2$ according to the Born rule.

which captures statistical uncertainty over an ensemble of pure states. Densities are operators with unit trace and satisfy $\langle a|\rho\,|a\rangle \geq 0$ for any normalised state $|a\rangle$, regardless of the chosen basis. A density operator represents a pure state if $Tr(\rho^2) = 1$; otherwise, the state is *mixed*.

For a composite system consisting of two subsystems $\mathcal{A}$ and $\mathcal{B}$ with Hilbert spaces $\mathcal{H}_A$ and $\mathcal{H}_B$, the total Hilbert space is the tensor product

$$\mathcal{H} = \mathcal{H}_A \otimes \mathcal{H}_B. \tag{4}$$

A pure state of the total system is a unit vector in $\mathcal{H}$. It is called *separable* if it can be written as

$$|\psi\rangle = |a_k\rangle \otimes |b_k\rangle; \tag{5}$$

otherwise, it is said to be *entangled*. $|a_i\rangle$ and $|b_i\rangle$ are normalised, not necessarily orthogonal, states of the two systems. A general pure state can be expressed as a superposition of product basis states:

$$|\psi\rangle = \sum_{i,j} C_{ij}|a_i\rangle \otimes |b_j\rangle. \tag{6}$$

For mixed states, a density operator ρ is said to be *separable* if it can be written as

$$\rho = \sum_k p_k \rho_k^{(A)} \otimes \rho_k^{(B)}, \tag{7}$$

where each $\rho_k^{(A)}$ and $\rho_k^{(B)}$ are density operators on $\mathcal{H}_A$ and $\mathcal{H}_B$, and $p_k \geq 0$, $\sum_k p_k = 1$. Otherwise, ρ is entangled.

The generalisation to more than two subsystems is straightforward.

The state vector is a dynamical quantity that evolves unitarily according to $|\psi(t)\rangle = U(t, t_0)\,|\psi(t_0)\rangle$, which implies it satisfies the Schrödinger equation:

$$\mathrm{i}\hbar \frac{\mathrm{d}}{\mathrm{d}t}|\psi(t)\rangle = \hat{H}|\psi(t)\rangle, \tag{8}$$

where $\hat{H}$ is the Hamiltonian operator (see Figure 2(b)). Equivalently, the density operator $\rho(t)$ evolves according to the von Neumann equation:

$$\mathrm{i}\hbar \frac{\mathrm{d}\rho(t)}{\mathrm{d}t} = \left[\hat{H}, \rho(t)\right], \tag{9}$$

where $[\hat{H}, \rho] = \hat{H}\rho - \rho\hat{H}$ denotes the commutator.

Every measurable physical quantity (observable) is represented by a self-adjoint operator $\hat{O} = \hat{O}^\dagger$ on $\mathcal{H}$. The possible outcomes of a measurement of $\hat{O}$ are its eigenvalues $o_n \in \mathbb{R}$. For a *non-degenerate spectrum*, the probability of obtaining the outcome o_n at measurement time t' is (see Figure 2(c))

$$P(o_n) = \left|\langle o_n \mid \psi(t')\rangle\right|^2, \tag{10}$$

where $|o_n\rangle$ is the corresponding eigenstate. In terms of the density operator, this probability becomes

$$P(o_n) = \mathrm{Tr}\Big[|o_n\rangle\langle o_n|\rho(t')\Big]. \tag{11}$$

This formulation corresponds to a *projective measurement* (also known as a *projection-valued measure*, or PVM), where the outcome o_n is associated with the projection operator $|o_n\rangle\langle o_n|$. For more general types of quantum measurements – such as those involving degenerate spectra or *positive operator-valued measures* (POVMs) – we refer the reader to Ref. [21] for a pedagogical overview.

According to the standard postulates of quantum mechanics, after the measurement, the system is left in the normalised eigenstate $|o_n\rangle$ if o_n was measured. This state change is referred to as *quantum state collapse*. In this discussion, we assumed that collapse is instantaneous and occurs at t'. Standard quantum theory gives no clue as to whether this is precise or not. Recent resonant inelastic X-ray scattering (RIXS) experiments have suggested that state collapse occurs gradually over a finite time [23]. However, this interpretation remains ambiguous, as the observed dynamics could also be explained by progressive decoherence rather than a fundamental modification of quantum measurement. We will return to when and how long it takes for collapse to occur in discussing Objective Collapse Theories in Section 5.3. The implications of an instantaneous collapse are explored in Section 5.7, in the context of quantum field measurements.

3. The problems with quantum measurements

To summarise the description of the quantum state evolution discussed in the previous section, standard quantum mechanics prescribes that a quantum state follows two types of time evolution: Left on its own, it evolves with the Schrödinger equation, which is unitary and deterministic [18, Ch 3, 19, Ch 1]. During a measurement, the system produces a classical outcome with probabilities given by the Born rule. In idealised cases, this is often described by a non-unitary state update (the *projection postulate*), but more generally, a measurement is any transformation that extracts classical information from a quantum system. These processes must be probabilistic and cannot allow communication between distant systems without a physical carrier.

There are different ways to scrutinise this description [3, 24, 25]. Here, we follow Schlosshauer [26, Ch 2], who decomposed it into three problems: the *problem of the preferred basis*, the *problem of the nonobservability of interference*, and the *problem of outcomes*. Each of these challenges arises naturally from the standard formulation of quantum mechanics and highlights a gap in our understanding of what happens when a quantum system is measured. Below, we define these problems in sequence.

The problem of the preferred basis. Suppose we have an apparatus to detect whether the NH_3 molecule is *up* or *down*. This apparatus is also modelled as a quantum system, initially in a 'ready' state. If it measures the molecule *up*, its pointer moves to 1; if it detects *down*, it moves to 0 (in the following, we will omit $\otimes$ for brevity):

$$\begin{aligned} |up\rangle|ready\rangle &\rightarrow |up\rangle|1\rangle, \\ |down\rangle|ready\rangle &\rightarrow |down\rangle|0\rangle. \end{aligned} \tag{12}$$

If the molecule is initially in the superposition

$$|\psi\rangle = \frac{1}{\sqrt{2}}\big(|up\rangle + |down\rangle\big), \tag{13}$$

the measurement interaction leads to an entangled state:

$$|\psi\rangle|ready\rangle \rightarrow \frac{1}{\sqrt{2}}\big(|up\rangle|1\rangle + |down\rangle|0\rangle\big). \tag{14}$$

This one-to-one correlation between system and apparatus defines the premeasurement state in the von Neumann measurement scheme [26], where a collapse (or equivalent mechanism) is needed to produce a definite outcome.

The same final state can be expressed in a different basis. Define (Figure 3):

$$\begin{aligned} |+\rangle &= \tfrac{1}{\sqrt{2}}\big(|up\rangle + |down\rangle\big), \\ |-\rangle &= \tfrac{1}{\sqrt{2}}\big(|up\rangle - |down\rangle\big), \end{aligned} \tag{15}$$

and

$$\begin{aligned} |A\rangle &= \tfrac{1}{\sqrt{2}}(|1\rangle + |0\rangle), \\ |B\rangle &= \tfrac{1}{\sqrt{2}}(|1\rangle - |0\rangle), \end{aligned} \tag{16}$$

Then the same entangled state becomes

$$|\Phi\rangle = \frac{1}{\sqrt{2}}(|+\rangle|A\rangle + |-\rangle|B\rangle). \tag{17}$$

Formally, both descriptions are equivalent. But in practise, the apparatus always produces outcomes on a specific basis – here, $\{|1\rangle, |0\rangle\}$ – not in $\{|A\rangle, |B\rangle\}$ or any other. One might argue that the apparatus, by design, selects the measurement basis. But this assumes what needs to be explained: how and why a particular basis emerges from the

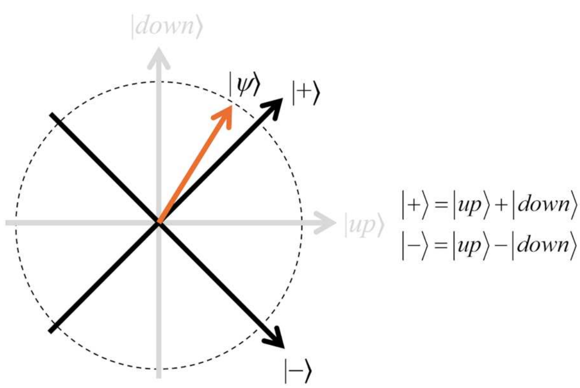

Figure 3. The choice of basis to describe the quantum system is arbitrary in principle. The quantum state $|\psi\rangle$ can be equally written in terms of the $\{|up\rangle, |down\rangle\}$ or $\{|+\rangle, |-\rangle\}$ basis. In the premeasurement entangled state, this basis ambiguity extends to the apparatus as well, although only the system's basis is illustrated here.

unitary quantum dynamics. After all, the entangled state can be expressed in many incompatible bases, and the Schrödinger equation itself does not single out any of them.

This ambiguity – why a specific set of outcomes is realised when many are in principle available – is the *problem of the preferred basis*, first formulated by Zurek [27].

The *problem of the nonobservability of interference*. Quantum mechanics predicts that systems can exist in coherent superpositions, which should produce observable interference effects. Indeed, such effects are routinely seen at microscopic scales – for instance, in electron double-slit experiments [28] or the oscillations of generalised oscillator strengths for symmetric molecules under electron impact [29]. More recently, Kanitz and coworkers demonstrated interference patterns from helium and hydrogen atoms transmitted through single-layer graphene, achieving diffraction with atoms at kiloelectronvolt energies [30].

Nevertheless, interference is never observed in macroscopic objects: tables, measurement devices, or Schrödinger's cat do not display interference fringes. One might suspect this absence is simply due to the extremely short de Broglie wavelengths of large systems, making interference effects undetectable. However, this explanation is insufficient. Under carefully controlled conditions, interference remains observable even for massive molecules with minuscule de Broglie wavelengths, as demonstrated by Talbot diffraction experiments with molecules comprising up to 2000 atoms [31]. Thus, the absence of interference in everyday situations cannot be entirely attributed to technical limitations.

The real puzzle is why coherence, though allowed in principle by the Schrödinger equation, becomes unobservable in practise beyond microscopic scales. This disconnect defines the problem of the nonobservability of interference and points toward the need for a dynamical mechanism that suppresses coherence in macroscopic systems.

The *problem of outcomes*. Even after addressing the previous two issues – identifying a preferred basis and suppressing interference – a fundamental question remains: Why do measurements yield a single, definite outcome rather than a superposition of possible results? After decoherence, the total system (including apparatus and environment) is still described by an entangled quantum state encompassing all possible outcomes (as shown in Equation (14). Yet we never observe such superpositions: each measurement yields a unique result. Indeed, what would it even mean to observe a superposition?

Standard quantum mechanics provides no mechanism for this selection. The Born rule accurately predicts the statistical distribution of outcomes over many measurements. Still, it does not explain why a particular result occurs or what selects it in an individual run.

These three problems define the core of the Measurement Problem [26, Ch 2]. The following section explores how decoherence addresses the first two problems, while a dedicated discussion on the problem of outcomes follows in Section 5.

4. Decoherence

The problem of the nonobservability of interference is addressed by decoherence. Decoherence disperses the quantum information about a system into correlations with the surrounding environment, suppressing the observable effects of superposition [26, 32]. To have a feeling of how decoherence acts, suppose that our $|up\rangle$ and $|down\rangle$ system can interact with an environment with only three states, $|e_0\rangle$, $|e_1\rangle$, and $|e_2\rangle$. We initially prepare the system in a superposition of $|up\rangle$ and $|down\rangle$ and the environment in $|e_0\rangle$, such that the initial state of the system plus environment is

$$|\Psi(t_0)\rangle = (a|up\rangle + b|down\rangle) \otimes |e_0\rangle. \tag{18}$$

Because of the interaction between the system and its environment, the joint quantum state becomes entangled:

$$|\Psi(t_1)\rangle = a|up\rangle|e_1\rangle + b|down\rangle|e_2\rangle. \tag{19}$$

We can monitor the system's evolution alone, averaging it over the environment states. This is done by computing the reduced density matrix for the system. This average is obtained by taking the trace over the environment's states of the full-density operator:

$$\begin{aligned} \rho_S &= \mathrm{Tr}_E[|\Psi\rangle\langle\Psi|] \\ &= \begin{bmatrix} |a|^2 & ab^*\langle e_2|e_1\rangle \\ ba^*\langle e_1|e_2\rangle & |b|^2 \end{bmatrix} \end{aligned} \tag{20}$$

The diagonal terms $|a|^2$ and $|b|^2$ are the $|up\rangle$ and $|down\rangle$ *populations*. The off-diagonal terms are the *coherences* and are responsible for quantum interferences.

In general, the environmental states are not orthogonal, and the coherences are non-null. However, as time passes, the environment states tend to become effectively orthogonal because their dynamics are different when the environment interacts with the system's $|up\rangle$ and $|down\rangle$ geometries. Thus, the off-diagonal terms tend to zero,

$$\rho_S = \begin{bmatrix} |a|^2 & ab^*\langle e_2|e_1\rangle \\ ba^*\langle e_1|e_2\rangle & |b|^2 \end{bmatrix} \xrightarrow{\text{Decoherence}} \begin{bmatrix} |a|^2 & 0 \\ 0 & |b|^2 \end{bmatrix}, \tag{21}$$

because $\langle e_1|e_2\rangle$ dynamically becomes null. This process is called *decoherence*.

In formal terms, decoherence arises from the time propagation of the reduced density matrix, which evolves with a *master equation* of the type [26, Ch 4].

$$\frac{\mathrm{d}\rho_S(t)}{\mathrm{d}t} = \underbrace{-i\hbar\left[\hat{H}_S, \rho_S(t)\right]}_{\text{Unitary evolution}} + \underbrace{\hat{D}\left[\rho_S(t)\right]}_{\text{Decoherence/dissipation}}, \tag{22}$$

where $\hat{H}_S$ is the system's Hamiltonian, including the environment's perturbation. $\hat{D}$ is the term responsible for decoherence to the environment.

Decoherence tends to be extremely fast when considering the environment as a multidimensional system. For example, we can employ the Joos-Zeh model [33] to estimate the decoherence time of the and $|up|down$ superposition in ammonia gas. According to this model, the coherence in Equation (21) decays exponentially,

$$\rho_S\left(up, down, t\right) = \rho_S\left(up, down, 0\right)e^{-\frac{t}{\tau_D}}, \tag{23}$$

with a decoherence time given as

$$\tau_D = \frac{1}{\frac{8}{3\hbar^2}\frac{N}{V}(2\pi M)^{\frac{1}{2}}a^2(\Delta x)^2(k_B T)^{\frac{3}{2}}}. \tag{24}$$

In this equation, N/V is the number density of the gas at temperature T. M is the molecular mass. a is the molecule's size (the molecule is assumed to be a dielectric sphere), and Δx is the displacement between the $|up\rangle$ and $|down\rangle$ geometries. Plugging these quantities in Equation (24), we find that NH_3 coherence disappears almost instantaneously within 10^{-19} s under room temperature and pressure. Although the superposition persists in the combined system *and* environment, its effects become unobservable due to dispersal in the gas.

Although decoherence often occurs in femtoseconds or even sub-femtoseconds, specific molecular systems exhibit surprisingly long-lived coherence effects. For instance, Kaufman et al. [34] demonstrated that electronic coherences could survive for hundreds of femtoseconds in molecules with near parallel potential energy surfaces due to reduced dephasing between branched wavepackets (see also Figure 4). Schultz et al. [16] comprehensively review cases where vibronic coupling and structured environments lead to long coherence lifetimes, including examples from light-harvesting complexes in photosynthesis.

Babcock et al. [35] reported superradiant effects in tryptophan networks extending over microtubule-scale architectures, which require long-lived electronic coherence. This is remarkable, since superradiance typically unfolds over hundreds of femtoseconds [36]. For isolated tryptophan in aqueous solution, electronic decoherence occurs in less than 100 fs [37], implying that the protein scaffold must be critical in preserving coherence to allow superradiant emission. Babcock's result has also attracted media attention (see here and here) because it may support Hameroff-Penrose's hypothesis on the quantum origin of consciousness (see Section 5.6.2).

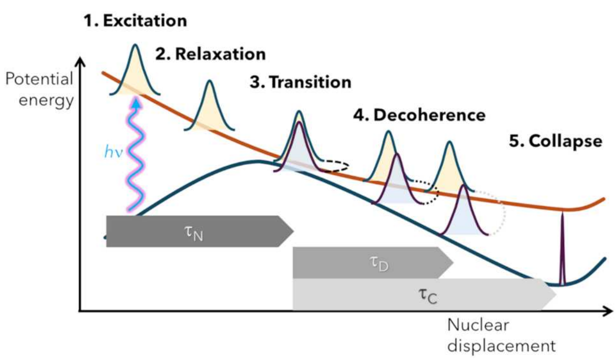

Figure 4. Schematic illustration of molecular evolution after photoexcitation. The nuclear wavepacket initially relaxes in the excited state until reaching a degeneracy region with the ground state within a time τ_N. There, coherence builds, but it is quickly counteracted by decoherence due to wavepacket dephasing, disappearing within τ_D. Up to this point, the Schrödinger equation provides an impeccable description of the phenomenon. If the molecule is measured at τ_C, it will either be in the ground (as illustrated) or in the excited state, with statistics following the Born rule.

These findings suggest that molecular architecture can sometimes counteract decoherence, challenging the assumption that coherence always vanishes rapidly. Theory, especially atomistic simulations [38], has still to catch up in this field.

In addition to suppressing quantum interferences, decoherence also addresses the problem of the preferred basis. It leads to the selection of a stable outcome basis through a process known as *einselection*, which drives the quantum state to the basis least entangled with the environment (this basis is known as the *pointer basis*) [27]. This preferred basis depends on the Hamiltonian [39]. Assuming that the position operator commutes with the system-environment interaction Hamiltonian (usually the case), decoherence tends to select the position eigenstates as the preferred basis as long as the interaction Hamiltonian is more important for the dynamics than the system's Hamiltonian. If both terms compete, the preferred basis is one close to coherent states, which minimises the uncertainty in both position and momentum. If the system's Hamiltonian dominates the dynamics, energy eigenstates are preferred as the basis.

For a molecule in a gas, Paz and Zurek's analysis [39] implies that the outcome basis of the environment selects for measuring nuclei is approximately position states. On the other hand, energy states emerge as the preferred outcome basis for measuring electrons. Thus, when we initially chose the $\{|up\rangle, |down\rangle\}$ basis for describing the quantum state of the ammonia molecule, we did it because it matched our classical intuition of nuclei corresponding to particles with defined positions. After discussing decoherence, we realise that we may have developed such a classic intuition because the environment selects the $\{|up\rangle, |down\rangle\}$ basis and suppresses superposition effects, creating a world of particles with well-defined positions.

Nevertheless, einselection may not be the last word in the preferred basis problem. Adil and co-authors have recently shown that the preferred basis is not solely dictated by the system-environment interaction, but also by the natural factorisation of the global Hilbert space [40]. Different factorizations can lead to multiple coexisting sets of pointer states, meaning classical behaviour emerges in different ways depending on the structure of the Hamiltonian. These coexisting classical realms challenge the idea that einselection always yields a single classical outcome. They may even reignite the preferred basis problem, but now at the level of Hamiltonian factorisation.

Decoherence explains why quantum superpositions become locally invisible; however, it does not explain why multiple observers consistently agree on what they observe. Zurek proposed that this consensus arises through *Quantum Darwinism* [41, 42], a process in which the environment acts not as a sink of information but as a communication channel. As the system interacts with its surroundings, information about its pointer states – those least perturbed by decoherence – is redundantly imprinted across many fragments of the environment. Different observers can then independently access these fragments to infer the same system properties without disturbing them. Objectivity, in this view, emerges as a Darwinian selection of information: only the most robust, redundantly recorded observables survive to be classically shared.

Decoherence is part of the standard quantum mechanics toolkit. It is an experimentally well-documented effect crucial for quantum mechanical applications, such as quantum information [21]. Regardless of one's preferred interpretation, the role of decoherence remains essential and cannot be ignored.

This dominant role of decoherence in the current understanding of quantum mechanical processes does not imply a consensus. Landsmann, for instance, characterises decoherence as 'an unmitigated disaster' [43, Ch 11]. His core criticism is that decoherence rigorously only occurs in an environment with infinite degrees of freedom after infinite interaction time with the system. Kastner reinforces this criticism by noticing that decoherence claims of describing irreversible processes suffer from similar conceptual problems already present in statistical mechanics when explaining the emergence of irreversibility from reversible processes [44].

5. Facing the problem of outcomes

In the previous section, we saw that decoherence clarifies a significant portion of the Measurement Problem. However, the *problem of outcomes* is still open: After the basis is chosen and quantum superpositions are suppressed, the system remains in a mixture of possible outcomes. Decoherence does not tell how and why only one of these outcomes is measured. At this point, standard interpretation of quantum mechanics postulates an additional dynamic step, the collapse:

$$\rho_S = \begin{bmatrix} |a|^2 & ab^*\langle e_2|e_1\rangle \\ ba^*\langle e_1|e_2\rangle & |b|^2 \end{bmatrix} \xrightarrow{\text{Decoherence}} \begin{bmatrix} |a|^2 & 0 \\ 0 & |b|^2 \end{bmatrix} \begin{array}{c} \xrightarrow{\text{Collapse}} \begin{bmatrix} 1 & 0 \\ 0 & 0 \end{bmatrix} \\ \text{or} \\ \xrightarrow{\text{Collapse}} \begin{bmatrix} 0 & 0 \\ 0 & 1 \end{bmatrix} \end{array} \tag{25}$$

We illustrate these different processes with an example of a photoexcited molecule undergoing internal conversion in Figure 4. Light initially promotes the molecule to an excited electronic state. The nuclear wavepacket evolves on the potential energy surface of the excited state until it reaches a region of degeneracy with the ground state potential energy surface. There, quantum coherence builds between the two states, creating a state superposition. The dephasing between the wavepacket components in each state counteracts, causing decoherence. All events up to this point, including decoherence, can be simulated by propagating the Schrödinger equation for the molecule [45]. If the molecule is measured, it will be found to be either in the ground or excited state. However, our simulation can only tell the probabilities of these outputs.

Standard quantum mechanics assumes that a wave function collapse occurred. Nevertheless, the existence of collapse is far from consensual. It is regarded as a superfluous hypothesis [46] in several quantum mechanical interpretations.

In the following subsections, we will dive into a few classes of potential solutions that represent the current debate on the Measurement Problem, with little attention to philosophical and historical aspects. More comprehensive approaches can be found in Refs. [4, 43, Introduction & Ch 11, 47, 48].

Before that, we should clarify the concepts we are dealing with. In literature, decoherence and collapse concepts are sometimes used interchangeably. We should avoid it, as these phenomena may, in principle, be completely independent and occur on different time scales.

As stated in Equation (25), decoherence acts on the off-diagonal terms of the system's reduced density matrix. Collapse, however, zeroes all diagonal terms except one in the *entire* density matrix – that is, the matrix describing the system, apparatus, and observer collectively, which Equation (25) does not represent. We can be a bit more flexible with this definition. In principle, a quantum theory including collapse could go as far as to provide a diagonal density matrix. This means we would be left in a situation of statistical uncertainty: the collapse occurred, but the theory only informed us of the probability of each outcome. We could call such a case an *epistemic* collapse. If, however, the theory zeroes the diagonal (except one) elements, then we would have an *ontic* collapse.

5.1. Many-worlds interpretation

The lack of information on the outcomes is not a problem for some interpretations. For instance, the Many-Worlds Interpretation (or Relative State Interpretation or, still, Everettian Quantum Mechanics) proposes that the remaining outcomes after decoherence correspond to independent universe branches [49]. Observers existing in each branch perceive different outcomes because their quantum state, entangled with the molecular quantum state, also branches. In one branch, the combined molecule-observer quantum state may be $|up\rangle|observer{-}sees{-}up\rangle$ and in another, $|down\rangle|observer{-}sees{-}down\rangle$. No observed branches with superpositions of both states exist because of decoherence toward the environment (surrounding the system and the observer) suppressing them [50]. Thus, the Many-Worlds Interpretation posits the existence of a single quantum universe composed of non-communicating classical branches.

For the Many-Worlds Interpretation, the quantum state $|\psi\rangle$ is a complete description of reality (no hidden variables are required), exclusively evolving according to the Schrödinger equation (collapse is only an illusion caused by the universe branching) [51, 52]. Thus, the Many-Worlds Interpretation is consistent with standard quantum mechanics and requires no modification to the theory. However, it remains an interpretation rather than a testable theory, since it currently makes no unique experimental predictions. A significant challenge is the technical infeasibility of maintaining and measuring a quantum system in a coherent superposition of orthogonal states, especially for large systems. This difficulty explains why superpositions of macroscopic states cannot be observed directly due to rapid decoherence. Susskind and Aaronson demonstrated this limitation using methods from quantum computational complexity, naming it the *quantum-hard problem* [53, 54].

A puzzling feature of the Many-Worlds Interpretation is understanding how the deterministic branching relates to the wave function amplitudes and the Born rule. Carroll and Sebens [55] propose that this relation is established after decoherence occurs but before the measurement is registered. In this period, if the observer wants to estimate which branch they are, their rational credence directly leads to the Born rule. Thus, the probabilistic character of quantum mechanics would be a subjective aspect arising from the observer's self-locating uncertainty. Carroll and Sebens' derivation of the Born rule is only strictly valid if the ratios of branch amplitudes are the square roots of rational numbers. However, they argue that the large number of branches in practical situations always allows this condition to be approximately satisfied. This approximation also enables experimental tests of their hypothesis by searching for minor deviations from the Born rule. Kent [56] sharply questioned the conceptual and mathematical soundness of Carroll and Sebens' account, arguing that their notion of self-locating uncertainty presupposes an objective and well-defined branching of the wave function – something not provided by the Everettian framework itself.

Like Carroll and Sebens, Short [57] derives the Born rule in Many-Worlds Interpretation based on estimating the probability of picking a random branch among many. However, instead of relying on self-locating uncertainty, he does it by establishing three axioms that the probability must satisfy: (1) the probability depends only on the present state (regardless of how it was generated); (2) only branches with non-zero amplitudes count as components of the many-world state; (3) probability cannot flow between uncoupled worlds. Short then shows that the Born rule uniquely satisfies these axioms.

The Many-Worlds Interpretation may seem exotic to non-specialists due to its exuberant ontology. Despite this perception, it is a serious contender among the proposed solutions to the Measurement Problem. It is a popular interpretation among physicists, with prominent supporters like Carroll [51, 52, 55], Tegmark [58], Zeh [46, 59, 60], and Deutsch – though their formulations vary in how explicitly Everettian they are and in the extent of their commitment to the metaphysics of many worlds. However, it also faces outstanding critics, like Penrose [61] and Albert. For Landsmann, the Many-Worlds Interpretation would be 'acceptable only if truly everything else has failed' [43, Ch 11].

5.2. Epistemic interpretations

Epistemic interpretations claim that a quantum state is no more than a mathematical tool to predict outcomes. This stance is shared by interpretations such as the Relational Interpretation [62–64], Quantum Information-Theoretic approaches [65], Quantum Bayesianism [66], and Indivisible Stochastic Process Theory [67], which are discussed next.

5.2.1. Relational interpretation

The *Relational Interpretation* of quantum mechanics (or *relational quantum mechanics*), proposed by Rovelli, focuses on the interaction between systems, emphasising that properties are defined only in relation to such interactions [64]. Thus, the molecular geometry may be well-defined for a nearby molecule in the environment acting as an observer while remaining in superposition for another molecule that is too distant to interact significantly.

Rovelli draws attention to the fact that this state dependence on a specific observer is not new in physics. It is analogous, for instance, to the velocity dependence on the particular reference frame in which it is measured. The novelty in quantum mechanics is that the non-commutative nature of quantum variables implies that not all properties can be sharply defined simultaneously [64], limiting the completeness of information derivable from a single interaction.

In the Relational Interpretation, the wave function is not ontologically real (see Section 6 for discussion). Instead, it serves as a tool for predicting the probabilities of interaction outcomes. Conceptual issues with measurement arise only when undue ontological weight is assigned to it. By treating the wave function purely as a predictive instrument, measurement can be reframed as an ordinary interaction, resolving these difficulties.

The Relational Interpretation is characterised by a sparse ontology [64], meaning that properties are not defined between interactions. Nevertheless, it remains a realist interpretation because it posits a physical world of interacting systems.

Giacomini, Castro-Ruiz, and Brukner have recently extended relational ideas beyond Rovelli's Relational Quantum Mechanics by incorporating *Quantum Reference Frames, QRF* [68]. In their approach, a QRF is simply a quantum system elevated to the role of a reference frame so that its degrees of freedom define the *origin* relative to which one describes other systems. By extending canonical transformations to the quantum domain, Giacomini et al. show how usual frame changes (translations, for example) remain valid even if the reference frame itself is in a superposition or entangled state. Their approach leads to the relativity of notions like superposition and entanglement. If a given particle is in a spatial superposition from the lab's viewpoint, then from the particle's viewpoint, the lab may itself appear in a corresponding superposition.

This perspective may offer new insights into the Measurement Problem, particularly in Wigner's friend scenarios, where the possibility of conflicting accounts among observers becomes natural if each observer constitutes its own QRF [68, 69]. Section 5.3.2 discusses how Giacomini and Brukner use QRFs to challenge Penrose's conjecture on gravity-induced collapse [70].

5.2.2. Information-theoretic and QBism views

Another epistemic perspective comes from quantum information theory, which treats quantum mechanics as an axiomatic framework akin to thermodynamics. Brukner and Zeilinger [65] argue that quantum theory is fundamentally about information, not underlying physical reality. Its postulates describe how information is processed, not how systems evolve in space and time.

Recent experimental results reinforce this perspective. Spegel-Lexne and co-authors demonstrated the equivalence of entropic uncertainty and wave-particle duality [71], suggesting that quantum measurement can be understood through informational constraints rather than wave function collapse.

A more radical variant of this informational approach is *Quantum Bayesianism*, or QBism [66]. QBism interprets the quantum state not as a system property but as a tool that reflects an agent's personal beliefs (or more precisely, *doxastic states*) about the outcomes of their measurements. For instance, assigning the state $|up$ to a molecule expresses an agent's expectation about what they will experience upon interacting with it, not a claim about an objective feature of the molecule. When a measurement is made, the quantum state is updated to reflect the agent's new information, akin to a Bayesian update of probabilities. From this perspective, collapse is not a physical transformation but the agent updating their beliefs in response to their own experience, which is the measurement outcome [66, 72].

Some no-go theorems are sometimes cited as challenging epistemic views, particularly the Pusey-Barrett-Rudolph (PBR) theorem [73]. It shows that, under certain assumptions, quantum states cannot be interpreted merely as statistical knowledge about underlying physical states – that is, hidden variables (see Section 5.4). Instead, the quantum state must be part of physical reality. However, this conclusion applies only to models that posit such hidden variables. Interpretations like QBism, which deny the existence of underlying ontic states altogether, fall outside the scope of the theorem [74, 75]. Rovelli has made similar clarifications for relational interpretations as well [76].

Another supposed challenge to QBism comes from Ozawa's intersubjectivity theorem [77, 78], which claims that two observers jointly measuring a system must agree on its outcome. This has been interpreted as incompatible with QBism's agent-centric framework. However, Schack has recently argued that this conclusion is mistaken and that QBism maintains consistency across observers without requiring objective outcomes in the traditional sense [79].

A common misunderstanding is to conflate QBism with older subjectivist interpretations, such as that of London and Bauer [80], who suggested that collapse results from an observer becoming aware of an outcome. However, QBism takes a different stance: the measurement outcome is not something the agent discovers; it is the agent's experience. No underlying *real* wave function remains untouched – it is a theory about actions and consequences, not objective ontologies [81].

By rejecting objective quantum states, QBism sidesteps many interpretative paradoxes, offering a consistent but radically subjective view in which quantum theory serves as a decision-making tool for agents.

5.2.3. Indivisible stochastic process theory

Barandes has recently proposed the *Indivisible Stochastic Process Theory*, where classical configurations of particles, fields, or qubits evolve via non-Markovian dynamics [67, 82]. In this type of dynamics, which recovers all results from conventional quantum mechanics, transition probabilities cannot be estimated at intermediate times. In Barandes' approach, wave functions are considered predictive tools only, and the Hilbert space of quantum mechanics is demoted to a convenient instrumentalist framework without an ontological basis.

Barandes draws a historical analogy, comparing the transition from instrumentalist frameworks in quantum mechanics to the Copernican revolution, where the instrumental Ptolemaic system of epicycles was replaced by a more fundamental description based on forces. Similarly, he advocates for a clear physical picture to supersede the abstract formalism of Hilbert space mechanics.

Unlike the Relational Interpretation (Section 5.2.1), the Indivisible Stochastic Process formulation posits a non-perspectival, objective reality: each system has a definite configuration that evolves stochastically in time. The ontology is well-defined at all times: each system has a definite configuration, even between interactions. What is sparse are the dynamical laws, since conditional probabilities connecting two moments in time are generally defined only when the earlier time is either the initial time or a special kind of interaction event (called a division event). This framework does not assume divisibility or Markovianity.

By embedding quantum systems within generalised stochastic systems, the Indivisible Stochastic Process formulation aligns with a realist philosophy, reinterpreting quantum systems as governed by dynamic interactions without requiring measurement to be treated as a distinct or special process.

5.3. Objective collapse theories

5.3.1. Agnostic objective collapse

Opposed to Many-Worlds Interpretation and epistemic interpretations, *objective collapse theories* consider that collapse is a physical process, and that standard quantum mechanics is still incomplete [5, 8]. Thus, these theories attempt to change the Schrödinger equation to account for the collapse. This subsection deals with agnostic objective collapse, that is, theories that do not attribute a cause to the collapse. In the following subsection, we will look at gravity-induced collapse.

Most objective collapse theories predict that a system in quantum superposition randomly localises in one of the outcomes given enough time [8, 83–85]. The quantum state is driven by a stochastic Schrödinger equation, such as the *quantum-state diffusion equation* [86, 87]

$$\mathrm{d}|\psi\rangle = -\frac{i}{\hbar}\hat{H}|\psi\rangle\,\mathrm{d}t + \sum_n \big(\hat{A}_n - \langle A_n\rangle\big)|\psi\rangle \mathrm{d}W_n - \frac{\eta}{2}\sum_n \big(\hat{A}_n - \langle A_n\rangle\big)^2|\psi\rangle\,\mathrm{d}t. \tag{26}$$

In addition to the usual Hamiltonian term, the right-hand side contains two additional terms that tend to localise the state in one of the eigenstates of the operators $\hat{A}_n$, as illustrated in Figure 5 for $\hat{A}_n = \hat{H}$. The collapse is stochastic and controlled by a Wiener process W_n (with $\langle \mathrm{d}W_n\rangle = 0$ and $\mathrm{d}W_m\,\mathrm{d}W_n = \delta_{mn}\eta\,\mathrm{d}t$), which, for the ensemble density, the statistical distribution of outcomes follows the Born rule. A positive real constant η sets the noise strength (diffusion rate), hence the collapse timescale. The equation is nonlinear due to the $\langle A_n\rangle = \langle\psi|\hat{A}_n|\psi\rangle/\langle\psi|\psi\rangle$ terms. However, the evolution of the ensemble density is linear thanks to the quadratic last term [88]. This linearity is required to avoid superluminal information exchange.

Different objective collapse theories have been proposed, corresponding to specific choices of operators $\hat{A}_n$, including the Hamiltonian operator [89], position operators (*GRW* after the initials of the authors [90]), density number operators (*CSL* for *Continuous Spontaneous Localization* [84]), and mass density operators [91] (which is discussed in Section 5.3.2). These specific models are thoroughly reviewed in Refs. [5, 9].

No observers or interacting systems are required in Equation (26). The localisation time depends on the size of the system. It may take billions of years for an isolated ammonia molecule in superposition to collapse to $|up\rangle$ or $|down\rangle$. In a gas, however, such localisation occurs nearly instantaneously.

5.3.2. Gravity-induced objective collapse

The highest stakes among the objective collapse theories are those proposing that gravity is the cause of the collapse. Penrose [92], for instance, claims that distinct mass distributions in superposition (μ_{up} for up or μ_{down} for down in ammonia molecule) would cause slightly different spacetime distortions. The instability associated with these superimposed distortions leads to the wave function collapse within a time

$$\tau_c = \frac{\hbar}{E_\Delta} \tag{27}$$

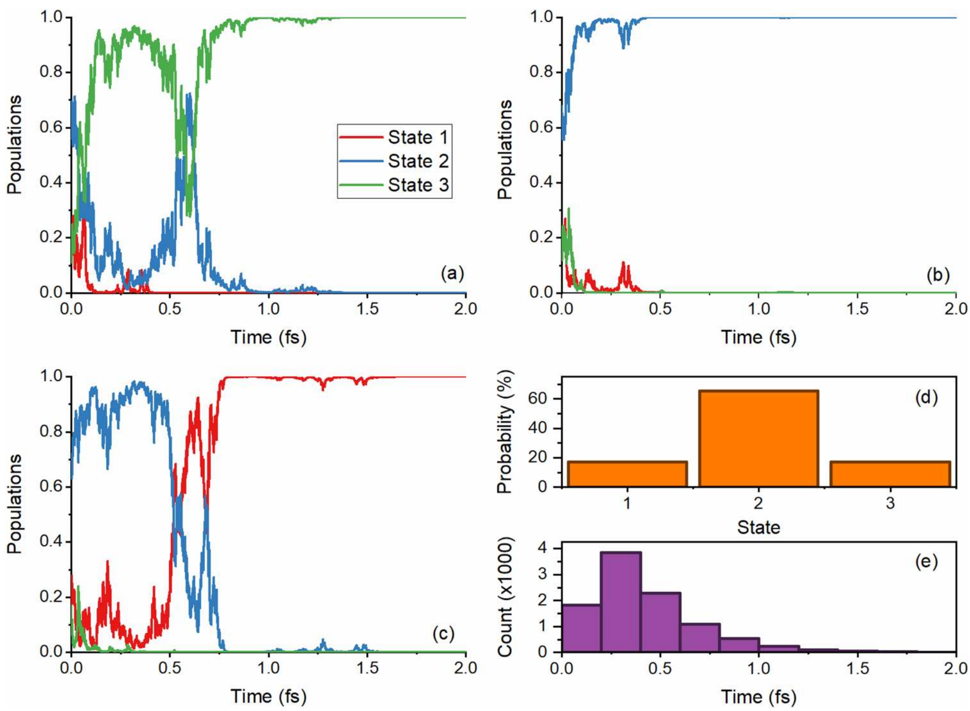

Figure 5. Example of application of the stochastic Schrödinger equation (Equation (26)) taking the Hamiltonian of the one-dimensional harmonic oscillator for the operators $\hat{A}_n$. The system is initially in a superposition $|\psi(0)\rangle = \sqrt{\frac{1}{6}}|1\rangle + \sqrt{\frac{2}{3}}|2\rangle + \sqrt{\frac{1}{6}}|3\rangle$ of the ground and first two excited states. The oscillator's mass and angular frequency are equal to one atomic unit. η was arbitrarily chosen as 0.25 au. (a)–(c) Shows the population evolution in three realizations, each collapsing to a different state. (d) The statistics over 10 thousand realizations show that the stochastic formulation recovers the Born rule with 1/6, 2/3, and 1/6 probabilities for states 1, 2, and 3, respectively. (e) For the employed parameters, the collapse occurs within a few femtoseconds. Simulations were performed using the Skitten program developed in our group.

where E_Δ is the Newtonian gravitational self-energy

$$E_\Delta = 4\pi G \int d^3\mathbf{r} d^3\mathbf{r}' \frac{\left(\mu_{up}(\mathbf{r}') - \mu_{down}(\mathbf{r}')\right)\left(\mu_{up}(\mathbf{r}) - \mu_{down}(\mathbf{r})\right)}{|\mathbf{r} - \mathbf{r}'|}, \tag{28}$$

and G is the gravitational constant. This collapse time can also be derived by computing the difference between Newtonian free-fall accelerations in the space surrounding each geometry [93]. A direct application of Equation (27) predicts it would take billions of years to collapse the wave function of an isolated molecule, but only 10^{-27} s to observe collapse in a 10 kg body (Figure 6) [1].

The same collapse time arises from the *Quantum Mechanics with Universal Density Localization* (QMUDL), the model Diósi proposed for the stochastic state evolution [91]. In QMUDL, the Schrödinger equation is modified to

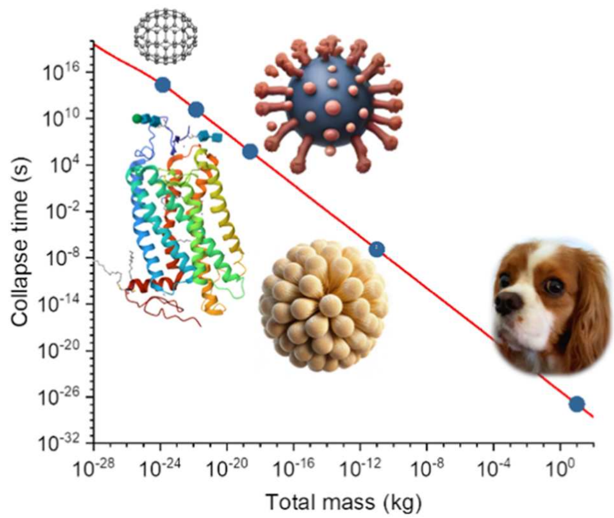

Figure 6. Diósi-Penrose collapse time as a function of the total mass. The estimate was made for a homogeneous carbon system. The collapse times for such a system with the masses of fullerene C_{70}, a protein, an adenovirus, a grain of pollen, and a small dog are indicated. Figure reproduced from Ref. [1].

$$\begin{aligned} \mathrm{d}|\psi\rangle = & -\frac{i}{h}\hat{H}|\psi\rangle\,\mathrm{d}t + \int\big(\hat{\mu}(\mathbf{r}) - \langle\hat{\mu}(\mathbf{r})\rangle\big)\,\mathrm{d}W(\mathbf{r})\,\mathrm{d}\mathbf{r}|\psi\rangle \\ & -\frac{\kappa G}{4\hbar}\int\int\frac{\big(\hat{\mu}(\mathbf{r}) - \langle\hat{\mu}(\mathbf{r})\rangle\big)\big(\hat{\mu}(\mathbf{r}') - \langle\hat{\mu}(\mathbf{r}')\rangle\big)}{|\mathbf{r}-\mathbf{r}'|}\,\mathrm{d}\mathbf{r}\,\mathrm{d}\mathbf{r}'|\psi\rangle\,\mathrm{d}t, \end{aligned} \tag{29}$$

where the scalar Wiener process is defined by $\langle \mathrm{d}W\rangle = 0$ and $\mathrm{d}W(\mathbf{r})\,\mathrm{d}W(\mathbf{r}') = \kappa G\,\mathrm{d}t/(2\hbar|\mathbf{r}-\mathbf{r}'|)$. This equation is a particular case of Equation (26) where the operators $\hat{A}_n$ are taken proportional to the mass density operator $\hat{\mu}$. The random noise is proportional to the ratio between the gravitational constant G and the reduced Planck constant —. κ is an arbitrary dimensionless constant. Despite the distinct and independent derivations, the collapse time (27) is generally called the *Diósi-Penrose Model*.

The Diósi-Penrose model has attracted criticism on multiple fronts. Gao [94] raised several issues on the Penrose conjecture. His main point is that Penrose's argument by analogy with the conventional quantum mechanical time-uncertainty principle is not rigorous enough. Moreover, he is also right to point out that although we commonly refer to the Diósi-Penrose model, Diósi and Penrose theories are fundamentally distinct, arriving at the same collapse time through independent, though conceptually related, arguments. Diósi himself [95] notes their similarities and differences and suggests that further work is needed to clarify whether the two frameworks are compatible.

Giacomini and Brukner [70] also challenged Penrose's conjecture that quantum superposition conflicts with Einstein's equivalence principle. Using the Quantum Reference Frames (QRF) formalism (see also 5.2.1), they showed that it is possible to generalise the principle (or, more precisely, always to make the metric field locally Minkowskian) even in the presence of quantum superpositions of massive bodies.

Additionally, our atomistic simulations showed that the Diósi-Penrose collapse time reaches a minimum value independent of superposition displacement and, in some instances, can be surprisingly long [1]. Figurato et al. [96] have also independently concluded that the model could have too long collapse times for macroscopic bodies. Beyond these theoretical concerns, experimental tests have also challenged the model. Donadi et al. [97] and Arnquist et al. [98] conducted underground experiments to test gravity-related collapse mechanisms. Their results placed stringent constraints on the model's parameters (see Section 5.3.3).

Although all these points must be considered when assessing the validity of the Diósi-Penrose model, none of them directly falsifies the model. And, as Thorne said, 'Penrose has a way of always being right, even when he does things in a strange way' [99].

Oppenheim has recently proposed another hypothesis that attributes wave function collapse to the influence of gravity. Indeed, his *Postquantum Theory of Classical Gravity* does not focus on the Measurement Problem and has a more ambitious goal of reconciling gravity and quantum mechanics [100]. Oppenheim's central hypothesis is that gravity is a classical field. To ensure classical gravity can interact coherently with quantum matter fields, Oppenheim and colleagues developed a *Classical Quantum (CQ) Dynamics* framework, which circumvents the usual obstacles encountered by semiclassical models, such as violation of the superposition principle due to nonlinearities in the equations of motion [100–102].

The CQ dynamics of the hybrid state $\rho(z, t)$ (where z represents the classical phase space coordinates) is expressed in terms of the general master equation [100]

$$\begin{aligned}\frac{\partial \rho}{\partial t} = &-\frac{i}{\hbar}\left[\hat{H}, \rho\right] + \sum_{\mu,\nu} \lambda^{\mu\nu}\left(\hat{L}_\mu \rho \hat{L}_\nu^\dagger - \frac{1}{2}\left\{\hat{L}_\mu^\dagger \hat{L}_\nu, \rho\right\}_+\right) \\ &+ \int \mathrm{d}z' \sum_{\mu,\nu} W^{\mu\nu}(z|z'; t)\hat{L}_\mu \rho \hat{L}_\nu^\dagger - \frac{1}{2}\sum_{\mu,\nu} W^{\mu\nu}(z; t)\left\{\hat{L}_\nu^\dagger \hat{L}_\mu, \rho\right\}_+,\end{aligned} \tag{30}$$

which can describe back reactions of quantum matter fields in classical (including gravitational) fields. This equation has completely positive dynamics (hence probabilities remain positive), preserves the trace (probabilities are conserved), and is linear in the density operator (superluminal signalling is avoided). In addition to the commutator term responsible for the unitary evolution and the Lindbladian term [20] (proportional to $\lambda^{\mu\nu}$) causing decoherence, the integral term promotes jumps in the quantum and classical subsystems. The last term preserves the norm of the quantum state.

Like in modelling open quantum systems [103], Equation (30) is not directly solved for ρ but rather through an ensemble of stochastic trajectories (*unraveling procedure*) [104, 105]. In each trajectory, the quantum degrees of freedom undergo stochastic projection onto the eigenstates of the corresponding Lindblad operators, collapsing to a definite outcome in a manner that statistically recovers the Born rule. These quantum jumps induce corresponding phase space jumps in the classical degrees of freedom, representing a backreaction of the quantum system on the classical one. In addition to collapse, this equation also describes decoherence, leading to the suppression of quantum coherence over time. Figure 7 illustrates the quantum and classical stochastic jumps in a system composed of a qubit and a classical particle discussed in Ref. [104]

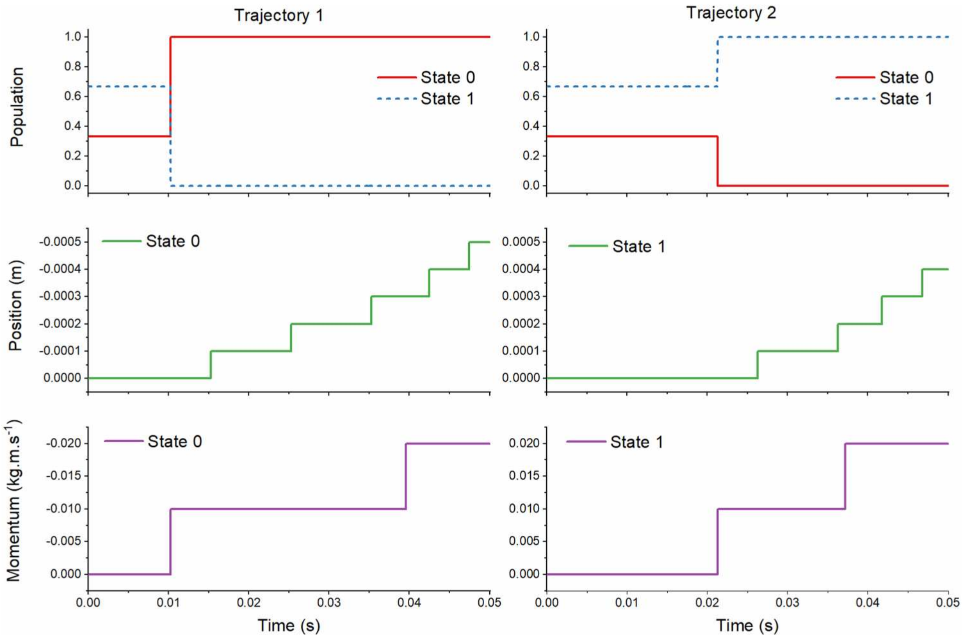

Figure 7. Evolution of the quantum state population and classical phase space coordinates (q, p) in the CQ dynamics (Equation (30) with diagonal Lindblad operators of a qubit interacting with a classical particle [104]. The initial state is $\delta(q)\delta(p)(\sqrt{\frac{1}{3}}|0\rangle + \sqrt{\frac{2}{3}}|1\rangle)$. The figure shows two stochastic trajectories. On the left, the interaction between the subsystems collapses the qubit to state 0, while on the right, it collapses to state 1. Stochastic jumps in the classical phase space are also observed due to backreaction. If many trajectories are computed, they will be distributed as 1/3 in 0 and 2/3 in 1. The trajectories were propagated for 0.05 s, with a timestep of 2.5×10^{-5} s. The jump rate was $\tau = 0.01$ s. The other parameters are $B = 1$ J·s·m^{-1}, $m = 1$ kg, and $\omega = 1$ s^{-1}. Simulations were performed with the program provided in Ref. [104].

Even though stochastic trajectories are introduced as a means to propagate the density evolution (30), Oppenheim and co-authors assign them ontological significance [104]. A stochastic trajectory represents the system collapsing to a specific state, just as it is also done in the other objective collapse theories discussed above. Their theory implies that collapse does not require measurement, as it occurs naturally due to interactions with a classical field [104].

Gravity-induced wave function collapse may have profound implications for physics. If any of these theories are confirmed, it would not only close the Measurement Problem but also imply that gravity plays a unique role in nature, different from the other fundamental interactions. Moreover, it would also impact future efforts to reconcile general gravity and quantum mechanics, moving toward what Penrose calls the gravitization of quantum mechanics [106].

5.3.3. Experimental assessment of objective collapse theories

Experimental efforts to test objective collapse models, especially CSL, have gained remarkable traction in recent years [6, 9, 98, 107, 108]. One of the most direct approaches involves matter-wave interferometry with large molecules or nanoparticles, designed to probe the persistence of quantum coherence at mesoscopic scales [1]. Gasbarri et al. argue that the microgravity environment of space, with its long free-fall times and low noise, offers a unique setting for such experiments, enabling both interferometric and non-interferometric tests with unprecedented sensitivity to collapse effects [108].

Beyond interferometry, several non-interferometric techniques have been proposed to test collapse models without requiring explicit superpositions. Carlesso et al. reviewed platforms such as optomechanical resonators, ultra-cold atoms, and solid-state systems, where collapse-induced noise may manifest as excess heating or anomalous diffusion [6]. Other proposals investigate spontaneous X-ray emission from the random motion of charged particles, a distinctive prediction of CSL. These diverse strategies have steadily improved the empirical bounds on collapse parameters, ruling out wide ranges of the originally proposed parameter space for both CSL and Diósi-Penrose models.

Recent studies have expanded the scope of experimental constraints. Altamura et al. analyzed data from the LISA Pathfinder mission and found that rotational degrees of freedom could provide tighter bounds than translational motion in some scenarios [107]. In a related direction, Howl, Penrose, and Fuentes proposed an experiment using a Bose–Einstein condensate prepared in a spatial superposition to test gravitationally induced collapse [93].

As discussed in Section 5.3.2, the Diósi-Penrose model ties collapse to gravitational self-energy. Figurato et al. investigated whether the model predicts rapid enough collapse for macroscopic systems and showed that it does not always do so across the entire parameter range [96]. Meanwhile, an underground experiment at the Gran Sasso Laboratory searched for spontaneous radiation arising from collapse-induced diffusion, placing strong limits on the spatial resolution of mass density – enough to exclude the original parameter-free version of the Diósi-Penrose proposal [97].

These efforts signal a shift in the status of objective collapse theories from speculative constructs to empirically testable frameworks. Among them, CSL stands out for its tuneable parameters and broad compatibility with experimental platforms, while the Diósi-Penrose and Oppenheim models offer more rigid, gravity-motivated alternatives. For example, Angeli et al. recently demonstrated that if gravity is both classical and local, as in Oppenheim's proposal (see Section 5.3.2), then it must induce diffusion in quantum systems, a phenomenon potentially observable with large-scale mechanical probes such as torsion pendulums [109].

Altogether, these developments underscore the increasing interconnection of collapse models with experimental physics. Whether or not they ultimately capture physical reality, they provide concrete benchmarks for testing the limits of quantum theory and may yet point toward deeper structures beyond it.

Despite the increasing experimental scrutiny of objective-collapse models, the idea that the Schrödinger equation may provide only an incomplete description of physical evolution continues to inspire new proposals. A recent one by Dick reframes the Measurement Problem as an *interaction problem* [110]. In this view, every inelastic energy exchange between systems acts as a mutual observation, interrupting the smooth Schrödinger evolution and producing definite outcomes. The wave function is interpreted as an epistemic superposition of possible ontic outcomes – elastic channels describing continuous evolution, inelastic ones involving discontinuous quantum jumps. Although this approach introduces no explicit modification of the Schrödinger equation, it assumes that the equation captures only the evolution of relative probability amplitudes, not the actual transitions that occur during energy exchange. In this sense, Dick's proposal can be regarded as a minimalist form of objective collapse, locating the breakdown of unitarity within ordinary interactions rather than in new stochastic dynamics.

5.4. Hidden-variables theories

5.4.1. Physical restrictions on hidden variables

Hidden variable theories (also known as *ontic* theories) explore the hypothesis that the quantum state $|\psi\rangle$ may not be a complete description of the system and that a set of additional (hidden) variables may contain further information (accessible or not) [111]. The hidden variables discussion is where the Measurement Problem spills the most on other fundamental questions of quantum mechanics, such as nonlocality in entangled systems, the completeness of quantum mechanics, and the existence of properties independently of measurement.

Hidden variable theories are typically framed within the limits of two no-go theorems and a few physically motivated restrictions. The theorems are the Bell and the Kochen-Specker ones. Bell's theorem states that no local hidden-variable theory can be entirely compatible with quantum mechanics [112, Ch 2, 113]. Local in this context means that 'the result of a measurement on one system be unaffected by operations on a distant system with which it has interacted in the past' [112, Ch 2].

In turn, the *Kochen-Specker theorem* [113–115] states that any hidden variable theory consistent with quantum mechanics must renounce either all observables having definite values at all times or these values being independent of how they are measured. The theorem is strictly valid for Hilbert spaces with dimension greater than two.

Finally, the physical restrictions are the non-signalling principle (imposing that non-locality cannot be harvested to exchange superluminal information) and the statistical independence (supposing that initial statistical setups can be completely uncorrelated; see also Section 5.5).

The situation seems simple from there. For instance, the experimental violations of Bell's inequalities [116] – confirming the predictions of quantum mechanics – imply that physical theories must either be non-local or not have properties defined at all times. However, no-go theorems are as strong as their underlying hypotheses, often deeply hidden in the deduction. The restrictions imposed by these theorems and physical principles have been constantly challenged [117, 118] (except for the non-signalling principle, which is likely the only consensual rule in the game). Relaxing statistical independence (sometimes loosely called the *free-will principle*) in Bell's theorem, for example, may allow for building consistent local and realist theories. We will return to this point in Section 5.5.

5.4.2. Bohmian mechanics

Most of the practical development in hidden-variable theories happens in the framework of Bohmian Mechanics, which posits the existence of corpuscles moving in a non-Newtonian way and guided by a wave function [119]. The corpuscle's velocities are determined by a velocity field (the de Broglie-Bohm Equation) dependent on the wave function, which, in turn, follows the Schrödinger evolution. This deterministic time evolution in Bohmian Mechanics automatically solves the problem of outcomes. Although Bohmian Mechanics' experimental predictions are equivalent to quantum mechanics [120], it is not discarded that they could be experimentally tested [121]. A striking example is the experiment by Sharoglazova et al. [122], who investigated the energy-speed relationship of wave-guided photons in a microcavity. They observed that for evanescent states within a potential step, lower-energy particles exhibited higher speeds. This result is in tension with standard Bohmian Mechanics, which predicts zero speed for such particles.

Poirier has proposed an alternative theory that prescribes non-Newtonian trajectories but entirely discards wave functions [123, 124]. In this case, the quantum system is described by an ensemble of interacting deterministic real-valued trajectories with well-defined positions and momenta. This type of theory inscribes itself into the tradition of hydrodynamic interpretation of quantum mechanics, inaugurated by Madelung right after Schrödinger's original work [125, 126, p. 222]. In Madelung's interpretation, quantum mechanics is modelled as a quantum fluid [127], which can be understood as *many interacting classical worlds* [128].

This picture of many interacting classical worlds has been the basis of molecular dynamics simulations, where the nuclear wave function time evolution is commonly approximated by interacting and non-interacting trajectories, depending on the approach [129, 130]. Tully, who proposed surface hopping, the most popular method for nonadiabatic molecular dynamics simulations, employed the Madelung Hydrodynamic Interpretation to justify using mixed quantum-classical approximations [131]. These molecular dynamics simulations, however, adopt the trajectory approach pragmatically without any foundational claim.

5.5. Deterministic models

Bell's theorem shows that no local hidden variable theories can reproduce all quantum mechanical predictions [112]. Thus, the experimental violation of Bell's inequalities seemed to be the end of any local deterministic model. However, Bell's theorem explicitly requires the validity of the *statistical independence assumption*, which states that the experimental settings are not influenced by any hidden factors determining the system's evolution. This section surveys two local deterministic models – Superdeterminism and Retrocausality – built on the challenge to the statistical independence assumption.

Superdeterminism posits that hidden correlations between measurement settings and system properties predetermine quantum outcomes [132]. 't Hooft proposed a concrete realization of this idea in his Cellular Automaton Interpretation (CAI) [133]. In this model, the universe is fundamentally described by a discrete, classical system evolving in time, much like a computer program updating the values of a grid according to fixed rules. These underlying configurations, called ontological states, evolve deterministically and form the actual physical reality. The familiar quantum formalism emerges only as a statistical approximation of our ignorance about the precise ontological state. In this view, superpositions are not real: they are computational tools that summarise ensembles of possible classical states. 't Hooft argues that violations of Bell inequalities do not imply nonlocality, but instead reflect our mistaken identification of such statistical templates with physical systems.

A recent proposal by Donadi and Hossenfelder [134] introduced a local, deterministic model for wave function collapse that explicitly violates statistical independence while reproducing standard quantum predictions. Their model suggests that all quantum states, except measurement eigenstates, are unstable under hidden-variable perturbations and deterministically collapse before reaching the detector. Unlike objective collapse models (see Section 5.3), the collapse dynamics in the Donadi-Hossenfelder model are entirely deterministic.

Cosmic Bell Experiments have provided stringent tests of the statistical independence assumption in Bell's theorem [116, 135]. These experiments avoid the possibility that hidden variables could influence detector settings by randomly determining measurement choices using distant astrophysical sources. By doing so, they attempt to close the *freedom-of-choice* loophole, which is crucial for evaluating the plausibility of superdeterministic explanations. In a landmark experiment, Rauch et al. [116] used high-redshift quasars – whose light originated billions of years ago – to set measurement parameters in a Bell test. Their results remained consistent with standard quantum mechanics, implying that superdeterministic correlations, if they exist, should date back to the early universe. Similarly, Handsteiner et al. [135] employed light from distant galaxies to eliminate potential local influences on detector choices. While these results do not *strictly* rule out superdeterminism, it must account for cosmological-scale correlations to remain viable, raising deep challenges for its plausibility.

Retrocausal Interpretations also challenge the statistical independence assumption, but, even bolder than Superdeterminism, it assumes influence from future events. Such interpretations propose that the Measurement Problem arises from assuming a one-way flow of time. Models such as the *Two-State Vector Formalism* [136] describe quantum systems by an initial state evolving forward in time and a final state evolving backward from the measurement outcome. The interaction of these forward- and backward-evolving states determines the probabilities of different results. The Pechukas' forces [137], which are still the primary justification used today for momentum rescaling along nonadiabatic coupling vectors in molecular dynamics [138], were derived from this same type of forward and backward propagation to determine quantum transitions in atomic collisions.

Retrocausality is still an active research field. Adlam [139] proposed that accepting nonlocality and imposing relativistic constraints (such as the nonexistence of a preferred reference frame) leads to retrocausality. Sutherland [140] derived the Born rule within a retrocausal model. This is a significant result because it changes the status of the rule from a postulate to a natural consequence of incorporating time-symmetric boundary conditions in quantum mechanics. A notable development is the *Fixed-Point Formulation* proposed by Ridley and Adlam, which presents an atemporal, all-at-once framework for retrocausality and includes a full derivation of the Born rule [141, 142]. Another recent contribution is van der Pals' *retrocausal hidden-variable model* [143], which attributes the emergence of definite outcomes to resonance conditions between advanced and retarded virtual photons. These photons arise from an underlying, time-symmetric periodic process occurring beneath the Heisenberg uncertainty threshold.

Both Superdeterminism and Retrocausality remain controversial and experimentally unverified. Nevertheless, despite their speculative nature, these models provide a striking contrast to interpretations that rely on wave function collapse, branching universes, or fundamental randomness [144], keeping the possibility of a fully local and deterministic resolution to the Measurement Problem open.

5.6. Dualist collapse hypotheses

5.6.1. Classical-apparatus inducing collapse

The core of the *Copenhagen Interpretation* of quantum mechanics, developed by Bohr and Heisenberg, is the assumption that any experiment in physics must be described in terms of classical physical concepts [43, Introduction]. When such an experiment falls within the realm of quantum mechanics, the tension between the system's quantum description and the apparatus's classical description is the crucial factor that causes statistical uncertainty and ultimately selects a single output [145]. There is no claim that the classical apparatus is not composed of quantum particles. It is just that the description of the experiment is restricted to the use of classical terminology.

This quantum-classical duality, formulated as the *Heisenberg Cut* arbitrarily separating classical from quantum systems, still plays a role in a pragmatic definition of measurement [146]. It is also at the basis of the *asymptotic emergence hypothesis* [147], which poses that collapse is a unitary physical process. Asymptotic emergence employs algebraic quantum theory to demonstrate that some phenomena forbidden in the quantum limit (like collapse) are allowed in the classical limit due to some exponential sensitivity to perturbations in the Hamiltonian [147].

In a series of works [148, 149], Schonfeld has explored cloud chambers, Geiger counters, and Stern-Gerlach experiments for empirical tests of quantum measurement, including possible deviations from the Born rule in detecting rare events. He challenges the conventional view that measurement is an axiomatic feature of quantum mechanics, proposing that measurement emerges phenomenologically from collective interactions in quantum detection systems. He analyzed the detailed microstructure of real measurement systems, using classical idealizations selectively where it seems mathematically or intuitively reasonable.

Oppenheim's Postquantum Theory provides another perspective for the classical-quantum duality [100], treating gravity as a classical entity interacting dynamically with quantum systems, causing wave function collapse (see Section 5.3.2 for a detailed discussion).

5.6.2. Mind-inducing collapse

A historically relevant but discredited hypothesis is that consciousness causes collapse. Wigner advocated for it until he learned about Zeh's work on what would come to be known as decoherence [150]. We mainly mention this mind-matter duality here to disentangle a few ideas that are sometimes mixed up.

First, there is the actual proposal that consciousness causes the collapse, which presupposes a matter-mind duality. The discomfort this hypothesis raises in our physical understanding of the world has never been better embodied than in Bell's quip [151], 'Was the wave function of the world waiting to jump for thousands of millions of years until a single-celled living creature appeared? Or did it have to wait a little longer, for some better qualified system … with a PhD?'

Then, there is an epistemic proposal where the mind does not objectively cause the collapse. Instead, the apparent collapse is an illusion arising when the observer becomes aware of the measurement outcome. We find such a perspective in London and Bauer [80, p. 251] who, in 1939, attributed the essential role played by consciousness to be 'the increase of knowledge, acquired by the observation'.

Finally, Hameroff and Penrose [152] put forward precisely the opposite hypothesis: collapse causes consciousness. (And quantum coherences in the microtubules mentioned in Section 4 would be part of this process.) They argue that if consciousness cannot be reduced to an algorithmic process, then its physical origin must be in the stochastic nature of the wave function collapse, which, for Penrose, is an objective event, as discussed in Section 5.3.

5.7. Measurement in quantum field theory

Quantum field theory (QFT) poses specific challenges to the Measurement Problem that are more daunting than in standard, non-relativistic quantum mechanics [153]. Because QFT integrates quantum mechanics and special relativity, locality is a built-in concept. This differs entirely from non-relativistic quantum mechanics, where locality is an add-on assumption, like when Bell imposed it in deriving his theorem. Sorkin showed that applying standard collapse rules to QFT can lead to *superluminal information transfer* in scenarios he termed *impossible measurements* [154]. More recently, this issue has been reframed as a violation of the broader *no-signalling* principle, which prohibits communication without a physical carrier [155].

Figure 8 illustrates a version of Sorkin's impossible measurement using our NH_3 qubit. Alice, Bob, and Charlie are ready to perform measurements on a molecule-field coupled system at times t_A (Alice), t_B (Bob), and t_C (Charlie). They are spaced to allow causal effects between Bob and Alice and between Charlie and Bob, but not between Alice and Charlie. In the relativity lingo, Alice and Charlie are *spacelike* separated.

Alice prepares a molecule in a $|down\rangle$ state and can choose whether to flip it to $|up\rangle$ at time t_A or not. The molecule is coupled to an electromagnetic field. The field state is $|f_u\rangle$

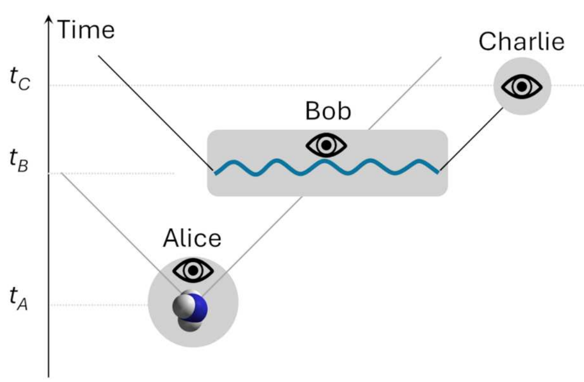

Figure 8. Impossible measurement in QFT adapted from Ref. [154] Charlie, at time t_C, cannot know if Alice flipped the molecule at t_A or not. Could an instantaneous collapse of the electromagnetic field's state in Bob's measurement at t_B enable superluminal information transfer between Alice and Charlie?.

if the molecule is $|up\rangle$ and $|f_d\rangle$ if the molecule is $|down\rangle$. The field is initially $|f_d\rangle$ and, after t_A, it is updated according to Alice's choice. At t_B, Bob measures the field projected on $(|up\rangle|f_u\rangle + |down\rangle|f_d\rangle)/\sqrt{2}$. Charlie, who, at time t_C, has no direct information about Alice's choice, attempts to indirectly discover that by measuring the field at t_C, which was updated after Bob's intervention. Sorkin argues that, in principle, Charlie's measurements on the field could reveal Alice's choice, implying superluminal exchange. Therefore, avoiding such impossible measurements would require nontrivial constraints on which observables are consistent with causality.

Such imprecision in the description of the measurement in QFT has been characterised, with a flair to the dramatic, as 'a major scandal in the foundations of quantum physics' [156]. Recently, Bostelmann, Fewster, and Ruep proposed that the situation is naturally solved within algebraic QFT as long as probes and couplings are constrained to be local [153, 157, 158].

This approach, originally developed as a general framework for describing measurement in algebraic QFT, was not tailored to solve the Sorkin problem, but rather aims to identify and localise induced system observables and to characterise state updates. The application to the Sorkin scenario, as presented in [158], thus constitutes a nontrivial test of the framework. Their analysis is valid for general fields and spacetime geometries, making it a promising step toward a rigorous measurement theory in QFT.

A complementary approach is proposed by Polo-Gómez, Garay, and Martín-Martínez, who develop a measurement theory for QFT based on spatially smeared particle detector models – such as the Unruh-DeWitt detector – that interact locally and covariantly with quantum fields [159]. Their framework, applicable to general fields and spacetime geometries, avoids problems such as Sorkin's impossible measurements and allows localised interactions without invoking instantaneous collapse. While Bostelmann et al. pursue a mathematically rigorous algebraic route, Polo-Gómez et al. adopt a more operational strategy grounded in how detectors realistically interact with quantum fields.

Other proposals inspired by quantum field theory and signal analysis take a different route, using mathematical tools to reinterpret collapse as a statistical construction. For instance, Morgan proposed a framework based on classical random fields and operator-algebraic methods to model quantum phenomena, offering an alternative strategy that remains within a classical probabilistic setting [160]. In his work, these fields – equipped with nontrivial correlation structures – are used to reproduce quantum statistics and construct joint probabilities even for noncommuting observables. His emphasis lies not on deriving definite outcomes from quantum theory, but on modelling the empirical structure of datasets generated by repeated measurements. This approach aims to preserve locality and realism, challenging standard assumptions about the necessity of wave function collapse or quantization itself.

6. The ontological status of the wave function

One fundamental question underlying the Measurement Problem is whether the wave function represents an actual physical object (Ψ-*ontic*) or is merely a mathematical tool encoding information (Ψ-*epistemic*) [161]. The Many-Worlds Interpretation (Section 5.1), Objective Collapse Theories (Section 5.3), and Hidden-Variable Theories

(Section 5.4) align with the Ψ-ontic view, while epistemic interpretations (Section 5.2) are, by definition, Ψ-epistemic.

A common argument for the Ψ-epistemic view is that the wave function evolves in an abstract, high-dimensional configuration space, making it unlikely to correspond to anything physically real [161]. However, such a criticism does not intimidate Ψ-ontic proponents, who argue that the wave function describes something fundamental about reality, even if not in three-dimensional space [162, 163]. *Wave function realism*, for example, holds that the wave function is a physical field existing in a high-dimensional configuration space [164]. Carroll and Singh take this high-dimensional Ψ-ontic stand to the extreme [52]. In an interpretation they call *Mad-Dog Everettianism*, they propose that the only fundamental elements of reality are the Hilbert space, state vectors, and hamiltonians. Everything else – including space, time, and classical variables – emerges from these.

Other Ψ-ontic interpretations have been developed to avoid the conceptual challenges of high-dimensional spaces. One approach is the *multi-field interpretation*, which states that an *N*-body wave function is a multi-field that assigns properties to sets of *N* points in the 3D space [165]. This is the view one of us adopted in an essay discussing the nature of the molecular wave function [166]. Gao [167] proposed an alternative Ψ-ontic interpretation in the 3D space that does not require multi-fields. In his view, the wave function represents a *random discontinuous motion* (RDM) of particles in real space. The wave function phase encodes momentum flow, giving it a concrete physical meaning. Moreover, RDM makes testable predictions, suggesting that collapse is an emergent effect of underlying stochastic motion rather than a fundamental postulate. Whether this model extends to relativistic quantum field theory remains an open question.

Spacetime state realism reinterprets quantum mechanics by assigning quantum states to regions of spacetime rather than treating the wave function as an object in a high-dimensional space [168]. This approach aligns more naturally with quantum field theory, which assigns quantum states to localised spacetime regions. A similar shift in emphasis to local quantities occurs in Density Functional Theory (DFT) [169], which, rather than working with the entire many-body wave function, pragmatically describes fermionic systems in terms of their density – a function of three spatial coordinates.

A different approach comes from the *Nomological Interpretation*, which suggests that the wave function is not a physical object but a law of nature governing quantum behaviour [162]. This is a common stance in interpreting Bohmian Mechanics [119, 170].

The Berry phase, which may arise during the cyclic evolution of quantum systems [171, 172], is a mathematical feature of the wave function that can be explored to assess its ontological status. Such a phase can build, for instance, when the nuclear geometry of a molecule evolves along a closed path encircling a conical intersection. (A conical intersection is a molecular geometry at which two adiabatic electronic states degenerate, forming a conical topology of the potential energy surfaces in nuclear coordinate space [173].) Unlike dynamic phases, the Berry phase is tied to the wave function's geometric properties and may, in principle, manifest in observable interference effects. Valahu et al. [174] claimed to have observed such geometric-phase interference in a trapped-ion quantum simulator mimicking conical intersection dynamics, which would strongly support the Ψ-ontic interpretation. However, it is unclear whether such effects could be observed in actual molecules since their experiment could be considered more of a controlled simulation than a molecular measurement. Moreover, Min et al. [175] and, more recently, Ibele et al. [176] have provided strong theoretical evidence that the Berry phase originates from the Born-Oppenheimer approximation and disappears in an exact electron-nuclear treatment, suggesting it may be an artefact rather than a fundamental quantum property.

Although the wave function's ontological nature remains unsettled, some recent experiments may support wave function realism. In particular, Costello et al. [177] reconstructed Bloch wave functions in GaAs semiconductors using angle-resolved photoemission data, showing that wave functions can, in some contexts, be experimentally accessed rather than only inferred. However, such reconstructions apply to quasiparticles and rely on a specific preparation context, and do not settle the deeper question of whether the wave function represents an element of reality. As Rovelli has emphasised [76], a wave function may encode the full information needed to predict measurement outcomes relative to a given observer, without implying a universally ontic status.

7. Through the forest of quantum foundations

It is easy to get lost in the Measurement Problem. The gargantuan amount of literature, the innumerable distinct theories, the endless debates, and the entanglement between physics, philosophy, and formal logic all lend anyone stepping into this field a feeling analogous to being trapped in a dense tropical forest. This review aims to offer an updated global map, which, although it cannot pinpoint the escape route, as it simply doesn't exist, will at least help us steer clear of dangerous cliffs.

Here, we provide a general overview of possible solutions to the Measurement Problem, which remains an actively discussed topic among physicists and philosophers, as well as of newly proposed theories that we consider particularly promising or disruptive. They fall into five classes of explanations: Many-Worlds Interpretations, Epistemic Interpretations, Objective Collapse Theories, Hidden-Variable Theories, and Dualistic Collapse Hypotheses.

Today, the Measurement Problem is much less puzzling than it once was. Thanks to the decoherence program, we understand how quantum interferences are suppressed and how the environment selects the outcome basis. Nevertheless, we still lack a fundamental explanation for why only a single outcome is observed in experiments, and we are still taking the first steps toward a well-defined measurement theory in quantum field theory. Indeed, given that QFT is likely the most successful physical theory ever developed, any satisfactory solution for the Measurement Problem must also be an acceptable solution for measurement in QFT. Therefore, it is worrisome to note that researchers on the Measurement Problem do not usually deal with QFT (and vice versa).

Most scientists who use quantum mechanics in their daily work focus on its practical applications rather than its interpretation. Indeed, it makes no difference whether we interpret the result of an experiment as the quantum state collapsing into a single branch or experiencing a branch that cuts off communication with all others. Such a subtle distinction belongs to defining a preferred worldview. It is even less consequential than choosing between Newtonian and Hamiltonian formulations of classical mechanics, which at least differ in their practical use. The exception concerns objective collapse theories, which propose new physics beyond conventional quantum mechanics. In any case, it makes sense to keep challenging all interpretations and theories to prune the weak and reach complete consistency on the remaining, even if we never get a single consensual description of quantum mechanics.

Acknowledgments

The authors gratefully acknowledge Stephen Adler, Jacob Barandes, Matteo Carlesso, John deBrota, Lajos Diósi, Christopher Fewster, Nicolas Gisin, Peter Morgan, Tzula Propp, Michael Ridley, Roldão da Rocha, Carlo Rovelli, Jonathan Schonfeld, Barbara Šoda, Niklas Sülzner, and Mark van der Pals for their careful reading of the first version of the manuscript and for their thoughtful and precise comments, which encouraged us and helped improve this challenging work.

Disclosure statement

No potential conflict of interest was reported by the author(s).

Funding

This work received support from the French government under the France 2030 investment plan as part of the Initiative d'Excellence d'Aix-Marseille Université (A*MIDEX AMX-22-REAB-173 and AMX-22-IN1-48) and from the European Research Council (ERC) Advanced Grant SubNano (grant agreement 832237).

References

[1] A.A. Tomaz, R.S. Mattos, and M. Barbatti, *Gravitationally-induced wave function collapse time for molecules*, Phys. Chem. Chem. Phys. 26 (2024), pp. 20785–20798.

[2] J.R. Hance and S. Hossenfelder, *What does it take to solve the measurement problem?*. J. Phys. Commun. 6 (2022), pp. 1–12.

[3] F.A. Muller, *Six measurement problems of quantum mechanics*, in *Non-Reflexive Logics, Non-Individuals, and the Philosophy of Quantum Mechanics: Essays in Honour of the Philosophy of Décio Krause*, J.R.B. Arenhart and R.W. Arroyo, eds., Springer International Publishing, Cham, 2023, pp. 225–259.

[4] O. Freire Junior, *From the interpretation of quantum mechanics to quantum technologies*, in *Oxford Research Encyclopedias, Physics*, 2024.

[5] A. Bassi, M. Dorato, and H. Ulbricht, *Collapse models: A theoretical, experimental and philosophical review*. Entropy 25 (2023), p. 645.

[6] M. Carlesso, S. Donadi, L. Ferialdi, M. Paternostro, H. Ulbricht, and A. Bassi, *Present status and future challenges of non-interferometric tests of collapse models*, Nat. Phys. 18 (2022), pp. 243–250.

[7] S. Donadi and A. Bassi, *Seven nonstandard models coupling quantum matter and gravity*. AVS Quantum Sci. 4, 025601 (2022), pp. 1–15.

[8] A. Bassi, K. Lochan, S. Satin, T.P. Singh, and H. Ulbricht, *Models of wave-function collapse, underlying theories, and experimental tests*, Rev. Mod. Phys. 85 (2013), pp. 471–527.

[9] A. Bassi and G. Ghirardi, *Dynamical reduction models*, Phys. Rep. 379 (2003), pp. 257–426.

[10] B. Keimer and J.E. Moore, *The physics of quantum materials*, Nat. Phys. 13 (2017), pp. 1045–1055.

[11] F. Campaioli, S. Gherardini, J.Q. Quach, M. Polini, and G.M. Andolina, *Colloquium: quantum batteries*. Rev. Mod. Phys. 96, 031001 (2024), pp. 1–36.

[12] M.C. Biswas, M.T. Islam, P.K. Nandy, and M.M. Hossain, *Graphene quantum dots (GQDs) for bioimaging and drug delivery applications: A review*, ACS Mater. Lett. 3 (2021), pp. 889–911.

[13] D. Zigmantas, T. Polívka, P. Persson, and V. Sundström, *Ultrafast laser spectroscopy uncovers mechanisms of light energy conversion in photosynthesis and sustainable energy materials*. Chem. Phys. Rev. 3, 041303 (2022), pp. 1–106.

[14] D. Claudino, *The basics of quantum computing for chemists*. Int. J. Quantum Chem. 122 (2022), p. e26990.

[15] S. McArdle, S. Endo, A. Aspuru-Guzik, S.C. Benjamin, and X. Yuan, *Quantum computational chemistry*, Rev. Mod. Phys. 92 (2020), p.015003.

[16] J.D. Schultz, J.L. Yuly, E.A. Arsenault, K. Parker, S.N. Chowdhury, R. Dani, S. Kundu, H. Nuomin, Z. Zhang, J. Valdiviezo, P. Zhang, K. Orcutt, S.J. Jang, G.R. Fleming, N. Makri, J.P. Ogilvie, M.J. Therien, M.R. Wasielewski, and D.N. Beratan, *Coherence in chemistry: foundations and frontiers*, Chem. Rev. 124 (2024), pp. 11641–11766.
[17] G.D. Scholes, A. Olaya-Castro, S. Mukamel, A. Kirrander, K.K. Ni, G.J. Hedley, and N.L. Frank, *The quantum information science challenge for chemistry*, J. Phys. Chem. Lett. 16 (2025), pp. 1376–1396.
[18] C. Cohen-Tannoudji, B. Diu, and F. Laloe, *Quantum Mechanics*, Vol. 1, Wiley-VCH, New York, USA, 2020.
[19] J.J. Sakurai, *Modern Quantum Mechanics*, Addison-Wesley, Massachusetts, 1994.
[20] D. Manzano, *A short introduction to the lindblad master equation*. AIP Adv. 10 (2020), pp. 025106-1– 025106-15.
[21] W. Wu and G.D. Scholes, *Foundations of quantum information for physical chemistry*, J. Phys. Chem. Lett. 15 (2024), pp. 4056–4069.
[22] R.P. Feynman, R. Leighton, and M. Sands, *The Feynman Lectures on Physics*, new millennium edition ed., Vol. III, Basic Books, USA, 2011. Available at https://www.feynmanlectures.caltech.edu/.
[23] N. Ignatova, V.V. Cruz, R.C. Couto, E. Ertan, A. Zimin, F.F. Guimarães, S. Polyutov, H. Ågren, V. Kimberg, M. Odelius, and F. Gel'mukhanov, *Gradual collapse of nuclear wave functions regulated by frequency tuned x-ray scattering*. Sci. Rep. 7: 43891 (2017), pp. 1–12.
[24] F. Laudisa, *The information-theoretic view of quantum mechanics and the measurement problem(s)*, Eur. J. Phil. Sci. 13 (2023), pp. 1–26.
[25] T. Maudlin, *Three measurement problems*, Topoi 14 (1995), pp. 7–15.
[26] M. Schlosshauer, *Decoherence and the Quantum-to-Classical Transition*, Springer-Verlag, Heidelberg, 2007.
[27] W.H. Zurek, *Pointer basis of quantum apparatus: into what mixture does the wave packet collapse?* Phys. Rev. D 24 (1981), pp. 1516–1525.
[28] A. Tonomura, J. Endo, T. Matsuda, T. Kawasaki, and H. Ezawa, *Demonstration of single-electron buildup of an interference pattern*, Am. J. Phys. 57 (1989), pp. 117–120.
[29] M. Barbatti, A.B. Rocha, and C.E. Bielschowsky, *Young-type interference pattern in molecular inner-shell excitations by electron impact*. Phys. Rev. A 72, 032711 (2005), pp. 032711-1–032711-6.
[30] C. Kanitz, J. Bühler, V. Zobač, J.J. Robinson, T. Susi, M. Debiossac, and C. Brand, *Diffraction of helium and hydrogen atoms through single-layer graphene*. Science 389 (2025), pp. 724–726. https://doi.org/doi:10.1126/science.adx5679.
[31] Y.Y. Fein, P. Geyer, P. Zwick, F. Kiałka, S. Pedalino, M. Mayor, S. Gerlich, and M. Arndt, *Quantum superposition of molecules beyond 25 kda*, Nat. Phys. 15 (2019), pp. 1242–1245.
[32] P. Ball, *Quantum common sense*, Aeon Magazine (2017), Available at https://aeon.co/essays/the-quantum-view-of-reality-might-not-be-so-weird-after-all.
[33] E. Joos and H.D. Zeh, *The emergence of classical properties through interaction with the environment*, Z. Phys. B: Conden. Matter 59 (1985), pp. 223–243.
[34] B. Kaufman, P. Marquetand, T. Rozgonyi, and T. Weinacht, *Long-lived electronic coherences in molecules*, Phys. Rev. Lett. 131 (2023), p. 263202.
[35] N.S. Babcock, G. Montes-Cabrera, K.E. Oberhofer, M. Chergui, G.L. Celardo, and P. Kurian, *Ultraviolet superradiance from mega-networks of tryptophan in biological architectures*, J. Phys. Chem. B 128 (2024), pp. 4035–4046.
[36] M. Gross and S. Haroche, *Superradiance: an essay on the theory of collective spontaneous emission*, Phys. Rep. 93 (1982), pp. 301–396.
[37] A. Ajdarzadeh, C. Consani, O. Bräm, A. Tortschanoff, A. Cannizzo, and M. Chergui, *Ultraviolet transient absorption, transient grating and photon echo studies of aqueous tryptophan*, Chem. Phys. 422 (2013), pp. 47–52.
[38] Y. Shu and D.G. Truhlar, *Decoherence and its role in electronically nonadiabatic dynamics*, J. Chem. Theory Comput. 19 (2023), pp. 380–395.

[39] J.P. Paz and W.H. Zurek, *Quantum limit of decoherence: environment induced superselection of energy eigenstates*, Phys. Rev. Lett. 82 (1999), pp. 5181–5185.
[40] A. Adil, M.S. Rudolph, A. Arrasmith, Z. Holmes, A. Albrecht, and A. Sornborger, *A search for classical subsystems in quantum worlds*, preprint (2024). Available at arXiv:2403.10895 [quant-ph].
[41] W.H. Zurek, *Quantum darwinism*, Nat. Phys. 5 (2009), pp. 181–188.
[42] W.H. Zurek, *Emergence of the classical world from within our quantum universe*, in *From Quantum to Classical: Essays in Honour of H.-Dieter Zeh*, C. Kiefer, ed., Springer International Publishing, Cham, 2022, pp. 23–44.
[43] K. Landsman, *Foundations of Quantum Theory: From Classical Concepts to Operator Algebras*, Springer Cham, Netherlands, 2017.
[44] R.E. Kastner, *'Einselection' of pointer observables: the new H-theorem?* Stud. History Phil. Sci. Part B: Stud. History Phil. Mod. Phys. 48 (2014), pp. 56–58.
[45] G.A. Worth, *Quantics: A general purpose package for quantum molecular dynamics simulations*, Comput. Phys. Commun. 248 (2020), p. 107040.
[46] H.D. Zeh, *There are no quantum jumps, nor are there particles!*, Phys. Lett. A 172 (1993), pp. 189–192.
[47] B. d'Espagnat, *Veiled Reality – An Analysis of Present-Day Quantum Mechanical Concepts*, Westview Press, USA, 2003.
[48] D.Z. Albert, *A Guess at the Riddle: Essays on the Physical Underpinnings of Quantum Mechanics*, Harvard University Press, 2023.
[49] D. Wallace, *The Emergent Multiverse: Quantum Theory According to the Everett Interpretation*, Oxford University Press, Oxford, UK, 2012.
[50] W.H. Zurek, *Probabilities from entanglement, born's rule from envariance*, Phys. Rev. A 71 (2005), p. 052105.
[51] S.M. Carroll and J. Lodman, *Energy non-conservation in quantum mechanics*. Found. Phys. 51, 83 (2021), pp. 1–11.
[52] S.M. Carroll and A. Singh, *Mad-dog everettianism: quantum mechanics at its most minimal*, in *What is Fundamental?*, A. Aguirre, B. Foster, and Z. Merali, eds., Springer International Publishing, Cham, 2019, pp. 95–104.
[53] S. Aaronson, Y. Atia, and L. Susskind, *On the hardness of detecting macroscopic superpositions*, Preprint (2020). Available at arXiv:2009.07450 [quant-ph].
[54] L. Susskind, *Computational complexity and black hole horizons*. Fortschritte der Physik 64 (2016), pp. 24–43.
[55] S.M. Carroll and C.T. Sebens, *Many worlds, the born rule, and self-locating uncertainty*, in *Quantum Theory: A Two-Time Success Story*, Springer, Milan, 2014, pp. 157–169.
[56] A. Kent, *Does it make sense to speak of self-Locating uncertainty in the universal wave function? remarks on sebens and carroll*, Found. Phys. 45 (2015), pp. 211–217.
[57] A.J. Short, *Probability in many-worlds theories*. Quantum 7, 971 (2023), pp. 1–10.
[58] M. Tegmark, *Our Mathematical Universe: My Quest for the Ultimate Nature of Reality*, Alfred A. Knopf, New York, 2014.
[59] H.D. Zeh, *On the interpretation of measurement in quantum theory*, Found. Phys. 1 (1970), pp. 69–76.
[60] P. Byrne, *Searching for dieter zeh*, in *From Quantum to Classical: Essays in Honour of H.-Dieter Zeh*, C. Kiefer, ed., Springer International Publishing, Cham, 2022, pp. 289–305.
[61] R. Penrose, *Fashion, Faith, and Fantasy in the New Physics of the Universe*, Princeton University Press, USA, 2016.
[62] C. Robson, *Relational quantum mechanics and contextuality*. Found. Phys. 54: 54 (2024), pp. 1–22.
[63] C. Rovelli, *Relational quantum mechanics*, Int. J. Theor. Phys. 35 (1996), pp. 1637–1678.
[64] C. Rovelli, *Space is blue and birds fly through it*, Phil. Trans. R. Soc. A: Math. Phys. Eng. Sci. 376 (2018), p. 20170312.

[65] V. Brukner and A. Zeilinger, *Information and fundamental elements of the structure of quantum theory*, in *Time, Quantum and Information*, L. Castell and O. Ischebeck, eds., Springer Berlin Heidelberg, Berlin, Heidelberg, 2003, pp. 323–354.

[66] C.A. Fuchs, N.D. Mermin, and R. Schack, *An introduction to QBism with an application to the locality of quantum mechanics*, Am. J. Phys. 82 (2014), pp. 749–754.

[67] J.A. Barandes, *The stochastic-quantum theorem*, preprint (2023). Available at arXiv:2309.03085 [quant-ph].

[68] F. Giacomini, E. Castro-Ruiz, and V. Brukner, *Quantum mechanics and the covariance of physical laws in quantum reference frames*. Nat. Commun. 10: 494 (2019), pp. 1–13.

[69] A. Vanrietvelde, P.A. Hoehn, F. Giacomini, and E. Castro-Ruiz, *A change of perspective: switching quantum reference frames via a perspective-neutral framework*. Quantum 4, 225 (2020), pp. 1–35.

[70] F. Giacomini and V. Brukner, *Quantum superposition of spacetimes obeys einstein's equivalence principle*. AVS Quantum Sci. 4, 015601 (2022), pp. 1–9.

[71] D. Spegel-Lexne, S. Gómez, J. Argillander, M. Pawłowski, P.R. Dieguez, A. Alarcón, and G.B. Xavier, *Experimental demonstration of the equivalence of entropic uncertainty with wave-particle duality*, Sci. Adv. 10 (2024), p. eadr2007.

[72] A. Franck, *Miding Matter*, Aeon Magazine (2017).

[73] M.F. Pusey, J. Barrett, and T. Rudolph, *On the reality of the quantum state*, Nat. Phys. 8 (2012), pp. 475–478.

[74] M.S. Leifer, *Can the quantum state be interpreted statistically?*, https://mattleifer.info/2011/11/20/can-the-quantum-state-be-interpreted-statistically/ (2011). Accessed: 2025-04-18.

[75] M.S. Leifer, *Is the quantum state real? An extended review of Ψ-ontology theorems*, Quanta 3 (2014), pp. 67–155.

[76] C. Rovelli, *Relational quantum mechanics*, in *The Stanford Encyclopedia of Philosophy*, E.N. Zalta and U. Nodelman, eds., Spring 2025 ed., Metaphysics Research Lab, Stanford University, Stanford, USA, 2025.

[77] A. Khrennikov, *Ozawa's intersubjectivity theorem as objection to QBism individual agent perspective*. Int. J. Theor. Phys. 63, 23 (2024), pp. 1–9.

[78] A. Khrennikov, *Relational quantum mechanics: Ozawa's intersubjectivity theorem as justification of the postulate on internally consistent descriptions*. Found. Phys. 54: 29 (2024), pp. 1–12.

[79] R. Schack, *When will two agents agree on a quantum measurement outcome? Intersubjective agreement in QBism*. International Journal of Theoretical Physics 63:254 (2024), pp. 1–9. https://link.springer.com/article/10.1007/s10773-024-05790-w.

[80] F. London and E. Bauer, *The theory of observation in quantum mechanics*, in *Quantum Theory and Measurement*, J.A. Wheeler and W.H. Zurek, eds., Princeton University Press, USA, 1983, pp. 217–259.

[81] J.B. DeBrota, C.A. Fuchs, and R. Schack, *Quantum dynamics happens only on paper: Qbism's account of decoherence*, preprint (2024). Available at arXiv:2312.14112.

[82] J.A. Barandes, *The stochastic-quantum correspondence*. Philosophy of Physics 3 (2025), pp. 1–32. https://doi.org/10.31389/pop.186.

[83] S.L. Adler, *Quantum theory as an emergent phenomenon: foundations and phenomenology*. J. Phys.: Conf. Ser. 361 (2012), pp. 1–8.

[84] G.C. Ghirardi, P. Pearle, and A. Rimini, *Markov processes in hilbert space and continuous spontaneous localization of systems of identical particles*, Phys. Rev. A 42 (1990), pp. 78–89.

[85] L.E.F.F. Torres and S. Roche, *A non-Hermitian loop for a quantum measurement*. Journal of Physics Communications 9 065001 (2025), pp. 1–9. https://doi.org/10.1088/2399-6528/ade19b.

[86] S.L. Adler and A. Bassi, *Collapse models with non-white noises*, J. Phys. A: Math. Theor. 40 (2007), pp. 15083–15098.

[87] N. Gisin and I.C. Percival, *The quantum-state diffusion model applied to open systems*. J. Phys. A: Math. Gen. 25 (1992), pp. 5677–5691.

[88] N. Gisin, *Stochastic quantum dynamics and relativity*, Helv. Phys. Acta 62 (1989), pp. 363–371.
[89] R. Schack, T.A. Brun, and I.C. Percival, *Quantum state diffusion, localization and computation*, J. Phys. A: Math. Gen. 28 (1995), pp. 5401–5413.
[90] G.C. Ghirardi, A. Rimini, and T. Weber, *Unified dynamics for microscopic and macroscopic systems*, Phys. Rev. D 34 (1986), pp. 470–491.
[91] L. Diósi, *Models for universal reduction of macroscopic quantum fluctuations*, Phys. Rev. A 40 (1989), pp. 1165–1174.
[92] R. Penrose, *On Gravity's role in quantum state reduction*, Gen. Relativ. Gravit. 28 (1996), pp. 581–600.
[93] R. Howl, R. Penrose, and I. Fuentes, *Exploring the unification of quantum theory and general relativity with a Bose–Einstein condensate*, New J. Phys. 21 (2019), p. 043047.
[94] S. Gao, *Does gravity induce wavefunction collapse? An examination of penrose's conjecture*, Stud. History Philos. Sci. Part B: Stud. History Philos. Mod. Phys. 44 (2013), pp. 148–151.
[95] L. Diósi, *On the conjectured gravity-related collapse rate $\Delta E/\hbar$ of massive quantum superpositions*, AVS Quantum Sci. 4 (2022), p. 015605.
[96] L. Figurato, M. Dirindin, J. Luis Gaona-Reyes, M. Carlesso, A. Bassi, and S. Donadi, *On the effectiveness of the collapse in the Diósi–Penrose model*, New J. Phys. 26 (2024), p. 113004.
[97] S. Donadi, K. Piscicchia, C. Curceanu, L. Diósi, M. Laubenstein, and A. Bassi, *Underground test of gravity-related wave function collapse*, Nat. Phys. 17 (2021), pp. 74–78.
[98] I.J. Arnquist, F.T. Avignone, A.S. Barabash, C.J. Barton, K.H. Bhimani, E. Blalock, B. Bos, M. Busch, M. Buuck, T.S. Caldwell, Y.D. Chan, C.D. Christofferson, P.H. Chu, M.L. Clark, C. Cuesta, J.A. Detwiler, Y. Efremenko, H. Ejiri, S.R. Elliott, G.K. Giovanetti, M.P. Green, J. Gruszko, I.S. Guinn, V.E. Guiseppe, C.R. Haufe, R. Henning, D. Hervas Aguilar, E.W. Hoppe, A. Hostiuc, I. Kim, R.T. Kouzes, T.E. Lannen V, A. Li, A.M. Lopez, J.M. López-Castaño, E.L. Martin, R.D. Martin, R. Massarczyk, S.J. Meijer, T.K. Oli, G. Othman, L.S. Paudel, W. Pettus, A.W.P. Poon, D.C. Radford, A.L. Reine, K. Rielage, N.W. Ruof, D. Tedeschi, R.L. Varner, S. Vasilyev, J.F. Wilkerson, C. Wiseman, W. Xu, C.H. Yu, and B.X. Zhu, *Search for spontaneous radiation from wave function collapse in the majorana demonstrator*, Phys. Rev. Lett. 129 (2022), p. 239902.
[99] K. Thorne, *Black Holes & Time Warps: Einstein's Outrageous Legacy (Commonwealth Fund Book Program)*, WW Norton & Company, New York City, USA, 1995.
[100] J. Oppenheim, *A postquantum theory of classical gravity?* Phys. Rev. X13 (2023), p. 041040.
[101] J. Oppenheim, *Is it time to rethink quantum gravity?* Int. J. Mod. Phys. D 32 (2023), p. 2342024.
[102] S. Carlip, *Is quantum gravity necessary?* Classical Quantum Grav. 25 (2008), p. 154010.
[103] T.A. Brun, *Continuous measurements, quantum trajectories, and decoherent histories*, Phys. Rev. A 61 (2000), p. 042107.
[104] J. Oppenheim, C. Sparaciari, B. Šoda, and Z. Weller-Davies, *Objective trajectories in hybrid classical-quantum dynamics*. Quantum 7, 891 (2023), pp. 1–47.
[105] J. Oppenheim, C. Sparaciari, B. Šoda, and Z. Weller-Davies, *Gravitationally induced decoherence vs space-time diffusion: testing the quantum nature of gravity*. Nat. Commun. 14: 7910 (2023), pp. 1–24.
[106] R. Penrose, *On the gravitization of quantum mechanics 1: quantum state reduction*, Found. Phys. 44 (2014), pp. 557–575.
[107] D.G.A. Altamura, A. Vinante, and M. Carlesso, *Improved bounds on collapse models from rotational noise of the laser interferometer space antenna pathfinder mission*, Phys. Rev. A 111 (2025), pp. L020203.
[108] G. Gasbarri, A. Belenchia, M. Carlesso, S. Donadi, A. Bassi, R. Kaltenbaek, M. Paternostro, and H. Ulbricht, *Testing the foundation of quantum physics in space via interferometric and non-interferometric experiments with mesoscopic nanoparticles*. Commun. Phys. 4, 155 (2021), pp. 1–13.

[109] O. Angeli, S. Donadi, G. Di Bartolomeo, J.L. Gaona-Reyes, A. Vinante, and A. Bassi, *Probing the quantum nature of gravity through classical diffusion*, preprint (2025). Available at arXiv:2501.13030.
[110] R. Dick, *Back to bohr: quantum jumps in Schrödinger's wave mechanics*, Quantum Rep. 6 (2024), pp. 401–408.
[111] G. Ghirardi and R. Romano, *Ontological models predictively inequivalent to quantum theory*, Phys. Rev. Lett. 110 (2013), p. 170404.
[112] J.S. Bell, *Speakable and Unspeakable in Quantum Mechanics*, 2nd ed., Cambridge University Press, Cambridge, UK, 2004. Available at https://www.cambridge.org/9780521523387.
[113] N.D. Mermin, *Hidden variables and the two theorems of john bell*, Rev. Mod. Phys. 65 (1993), pp. 803–815.
[114] C. Held, *The Kochen-Specker Theorem*, The Stanford Encyclopedia of Philosophy (Fall 2022 Edition) (2022), Available at https://plato.stanford.edu/archives/fall2022/entries/kochen-specker/.
[115] S. Kochen and E.P. Specker, *The problem of hidden variables in quantum mechanics*, J. Math. Mech. 17 (1967), pp. 59–87. Available at https://www.jstor.org/stable/24902153.
[116] D. Rauch, J. Handsteiner, A. Hochrainer, J. Gallicchio, A.S. Friedman, C. Leung, B. Liu, L. Bulla, S. Ecker, F. Steinlechner, R. Ursin, B. Hu, D. Leon, C. Benn, A. Ghedina, M. Cecconi, A.H. Guth, D.I. Kaiser, T. Scheidl, and A. Zeilinger, *Cosmic bell test using random measurement settings from high-redshift quasars*. Phys. Rev. Lett. 121 (2018), pp. 080403-1–080403-9.
[117] D.H. Oaknin, *Bypassing the Kochen–Specker theorem: an explicit non-Contextual statistical model for the qutrit*. Axioms 12, 90 (2023), pp. 1–11.
[118] K.W. Bong, A. Utreras-Alarcón, F. Ghafari, Y.C. Liang, N. Tischler, E.G. Cavalcanti, G.J. Pryde, and H.M. Wiseman, *A strong no-go theorem on the Wigner's friend paradox*, Nat. Phys.16 (2020), pp. 1199–1205.
[119] D. Dürr and S. Teufel, *Bohmian Mechanics, in Bohmian Mechanics: The Physics and Mathematics of Quantum Theory*, Springer Berlin Heidelberg, Berlin, Heidelberg, 2009, pp. 145–171.
[120] S. Das, *Detlef Dürr, arrival-time distributions, and spin in Bohmian mechanics: Personal recollections and state-of-the-art*, preprint (2023), Available at arXiv:2309.15815 [physics.hist-ph].
[121] A. Valentini, *Inflationary cosmology as a probe of primordial quantum mechanics*, Phys. Rev. D 82 (2010), p. 063513.
[122] V. Sharoglazova, M. Puplauskis, C. Mattschas, C. Toebes, and J. Klaers, *Energy–speed relationship of quantum particles challenges bohmian mechanics*, Nature 643 (2025), pp. 67–72. Available at https://doi.org/10.1038/s41586-025-09099-4.
[123] B. Poirier, *Bohmian mechanics without pilot waves*, Chem. Phys. 370 (2010), pp. 4–14.
[124] B. Poirier and H.M. Tsai, *Trajectory-based conservation laws for massive spin-zero relativistic quantum particles in 1 + 1 spacetime*, J. Phys.: Conf. Ser. 1612 (2020), p. 012022.
[125] E. Madelung, *Quantentheorie in hydrodynamischer form*, Z. Phys. 40 (1927), pp. 322–326.
[126] A. Messiah, Quantum Mechanics, Vol. I, North-Holland Publishing Company, Netherlands, 1961.
[127] P. Holland, *Computing the wavefunction from trajectories: particle and wave pictures in quantum mechanics and their relation*, Ann. Phys. 315 (2005), pp. 505–531.
[128] M.J.W. Hall, D.A. Deckert, and H.M. Wiseman, *Quantum phenomena modeled by interactions between many classical worlds*, Phys. Rev. X 4 (2014), p. 041013.
[129] R. Crespo-Otero and M. Barbatti, *Recent advances and perspectives on nonadiabatic mixed quantum-Classical dynamics*, Chem. Rev. 118 (2018), pp. 7026–7068.
[130] L.M. Ibele, E. Sangiogo Gil, E. Villaseco Arribas, and F. Agostini, *Simulations of photoinduced processes with the exact factorisation: state of the art and perspectives*. Phys. Chem. Chem. Phys. 26 (2024), pp. 26693–26718.
[131] J.C. Tully, *Mixed quantum-classical dynamics*, Faraday Discuss. 110 (1998), pp. 407–419.

[132] S. Hossenfelder and T. Palmer, *Rethinking superdeterminism*. Front. Phys. 8: 139 (2020), pp. 1–13.
[133] G. 'tHooft, The Cellular Automaton Interpretation of Quantum Mechanics, Springer, Cham, 2016.
[134] S. Donadi and S. Hossenfelder, *Toy model for local and deterministic wave-function collapse*, Phys. Rev. A 106 (2022), p. 022212.
[135] J. Handsteiner, A.S. Friedman, D. Rauch, J. Gallicchio, B. Liu, H. Hosp, J. Kofler, D. Bricher, M. Fink, C. Leung, A. Mark, H.T. Nguyen, I. Sanders, F. Steinlechner, R. Ursin, S. Wengerowsky, A.H. Guth, D.I. Kaiser, T. Scheidl, and A. Zeilinger, *Cosmic bell test: measurement settings from milky way stars*, Phys. Rev. Lett. 118 (2017), p. 060401.
[136] Y. Aharonov, P.G. Bergmann, and J.L. Lebowitz, *Time symmetry in the quantum process of measurement*, Phys. Rev. 134 (1964), pp. B1410–B1416.
[137] P. Pechukas, *Time-dependent semiclassical scattering theory. II. Atomic collisions*, Phys. Rev. 181 (1969), pp. 174–185.
[138] J.M. Toldo, R.S. Mattos, J. Pinheiro Max, S. Mukherjee, and M. Barbatti, *Recommendations for velocity adjustment in surface hopping*, J. Chem. Theory Comput. 20 (2024), pp. 614–624.
[139] E. Adlam, *Two roads to retrocausality*. *Synthese* 200(5) (2022), pp. 422–444. https://doi.org/10.1007/s11229-022-03919-0.
[140] R.I. Sutherland, *Probabilities and certainties within a causally symmetric model*. Found. Phys. 52: 75 (2022), pp. 1–17.
[141] M. Ridley, *Quantum probability from temporal structure*, Quantum Rep. 5 (2023), pp. 496–509.
[142] M. Ridley and E. Adlam, *Time and event symmetry in quantum mechanics*. Quantum Stud.: Math. Found. 12: 9 (2025), pp. 1–21.
[143] M.K. van der Pals, *A note on a possible solution to the measurement problem*, Int. J. Quantum Found. 10 (2024), pp. 26–55. Available at https://ijqf.org/archives/7019.
[144] N. Gisin, *Indeterminism in physics, classical Chaos and Bohmian mechanics: are real numbers really real?* Erkenntnis 86 (2021), pp. 1469–1481.
[145] G. Bacciagaluppi and E. Crull, *Heisenberg (and Schrödinger, and Pauli) on hidden variables*, Stud. History Phil. Sci. Part B: Stud. History Phil. Mod. Phys. 40 (2009), pp. 374–382.
[146] D. Grimmer, *The pragmatic QFT measurement problem and the need for a Heisenberg-like cut in QFT*. Synthese 202(4) (2023), pp. 1–45.
[147] N.P. Landsman, *Spontaneous symmetry breaking in quantum systems: emergence or reduction?* Stud. History Philos. Sci. Part B: Stud. History Philos. Mod. Phys. 44 (2013), pp. 379–394.
[148] J.F. Schonfeld, *Measured distribution of cloud chamber tracks from radioactive decay: A new empirical approach to investigating the quantum measurement problem*, Open Phys. 20 (2022), pp. 40–48.
[149] J.F. Schonfeld, *Does the Mott problem extend to Geiger counters?*, Open Phys. 21 (2023), p. 20230125.
[150] J. Mehra and A. Wightman, *The Collected Works of EP Wigner, vol. vi, p271* (1995).
[151] J. Bell, *Against 'measurement'*, Phys. World 3 (1990), pp. 33–41.
[152] S. Hameroff and R. Penrose, *Consciousness in the universe: A review of the 'Orch OR' theory*, Phys. Life Rev. 11 (2014), pp. 39–78.
[153] C.J. Fewster and R. Verch, *Measurement in quantum field theory*, perprint (2023). Available at arXiv:2304.13356 [math-ph].
[154] R.D. Sorkin, *Impossible measurements on quantum fields*, preprint (1993). Available at arXiv:gr-qc/9302018.
[155] N. Gisin and F. Del Santo, *Towards a measurement theory in QFT: "impossible" quantum measurements are possible but not ideal*. Quantum 8, 1267 (2024), pp. 1–11.
[156] J. Earman and G. Valente, *Relativistic causality in algebraic quantum field theory*, Int. Stud. Phil. Sci. 28 (2014), pp. 1–48.
[157] C.J. Fewster and R. Verch, *Quantum fields and local measurements*, Commun. Math. Phys. 378 (2020), pp. 851–889.

[158] H. Bostelmann, C.J. Fewster, and M.H. Ruep, *Impossible measurements require impossible apparatus*, Phys. Rev. D 103 (2021), p. 025017.
[159] J. Polo-Gómez, L.J. Garay, and E. Martín-Martínez, *A detector-based measurement theory for quantum field theory*, Phys. Rev. D 105 (2022), p. 065003.
[160] P. Morgan, *The collapse of a quantum state as a joint probability construction**, J. Phys. A 55 (2022), p. 254006.
[161] M. Hubert, *Is the statistical interpretation of quantum mechanics Ψ-ontic or Ψ-epistemic?*. Found. Phys. 53: 16 (2023), pp. 1–23.
[162] E.K. Chen, *Realism about the wave function*, Philos. Compass 14 (2019), p. e12611.
[163] A. Ney, *Three arguments for wave function realism*. Eur. J. Philos. Sci. 13: 50 (2023), pp. 1–18.
[164] D.Z. Albert, *Elementary quantum metaphysics*, in *Bohmian Mechanics and Quantum Theory: An Appraisal*, J.T. Cushing, A. Fine, and S. Goldstein, eds., Springer Netherlands, Dordrecht, 1996, pp. 277–284.
[165] M. Hubert and D. Romano, *The wave-function as a multi-field*, Eur. J. Philos. Sci. 8 (2018), pp. 521–537.
[166] M. Barbatti, *We are not empty*, Aeon Magazine (2023), Available at https://aeon.co/essays/why-the-empty-atom-picture-misunderstands-quantum-theory.
[167] S. Gao, *The Meaning of the Wave Function: In Search of the Ontology of Quantum Mechanics*, Cambridge University Press, Cambridge, UK, 2017.
[168] D. Wallace and C.G. Timpson, *Quantum mechanics on spacetime I: spacetime state realism*, Br. J. Philos. Sci. 61 (2010), pp. 697–727.
[169] R.O. Jones, *Density functional theory: its origins, rise to prominence, and future*, Rev. Mod. Phys. 87 (2015), pp. 897–923.
[170] S. Goldstein and S. Teufel, *Quantum spacetime without observers: Ontological clarity and the conceptual foundations of quantum gravity*, in *Physics Meets Philosophy at the Planck Scale: Contemporary Theories in Quantum Gravity*, C. Callender and N. Huggett, eds., Cambridge University Press, Cambridge, UK, 2001, pp. 275–289.
[171] M.V. Berry, *Quantal phase factors accompanying adiabatic changes*, Proc. R. Soc. Lond. A. Math. Phys. Sci. 392 (1984), pp. 45–57.
[172] D. Xiao, M.C. Chang, and Q. Niu, *Berry phase effects on electronic properties*, Rev. Mod. Phys. 82 (2010), pp. 1959–2007.
[173] W. Domcke, D.R. Yarkony, and H. Köppel, Conical Intersections – Electronic Structure, Dynamics and Spectroscopy, Advanced Series in Physical Chemistry, World Scientific, Singapore, 2004.
[174] C.H. Valahu, V.C. Olaya-Agudelo, R.J. MacDonell, T. Navickas, A.D. Rao, M.J. Millican, J.B. Pérez-Sánchez, J. Yuen-Zhou, M.J. Biercuk, C. Hempel, T.R. Tan, and I. Kassal, *Direct observation of geometric-phase interference in dynamics around a conical intersection*, Nat. Chem. 15 (2023), pp. 1503–1508.
[175] S.K. Min, A. Abedi, K.S. Kim, and E.K.U. Gross, *Is the molecular Berry phase an artifact of the Born-Oppenheimer approximation?*. Phys. Rev. Lett. 113, 263004 (2014), pp. 2127–2143..
[176] L.M. Ibele, E. Sangiogo Gil, B.F.E. Curchod, and F. Agostini, *On the nature of geometric and topological phases in the presence of conical intersections*, the Journal of Physical Chemistry Letters¡/DIFdel¿J. Phys. Chem. Lett. 14 (2023), pp. 11625–11631.
[177] J.B. Costello, S.D. O'Hara, Q. Wu, D.C. Valovcin, L.N. Pfeiffer, K.W. West, and M.S. Sherwin, *Reconstruction of bloch wavefunctions of holes in a semiconductor*, Nature 599 (2021), pp. 57–61.

PHILOSOPHICAL MAGAZINE

Contact us

Editorial Department | digitaleditor@philosophicalmagazine.com

Taylor & Francis
by informa